

Regulation of Inflammation in Cystic Fibrosis

Dušan Garić

McGill University, Montreal

Department of Human Genetics

Quebec, Canada

May, 2019

A thesis submitted to McGill University in partial fulfillment of the
requirements of the degree of Doctor of Philosophy

Copyright © 2019 by Dušan Garić

DEDICATION / POSVETA

This doctoral thesis is dedicated

*to my mother Branka, for her unwavering support at every step of my life,
and to the loving memories of my grandmothers, Stanka and Juca, each of whom in her own way
turned my childhood into the most wonderful fairytale ever told.*

Ova doktorska teza je posvećena

*mojoj majci Branki, za njenu neprikosnovenu podršku na svakom koraku mog života,
i dragim uspomenama na moje bake, Jucu i Stanku, koje su, svaka na svoj način, pretvorile moje
detinjstvo u najljepšu ikada ispričanu bajku.*

ABSTRACT

Cystic fibrosis (CF) is the most common autosomal recessive disease in Caucasians caused by mutations in the CF transmembrane regulator (CFTR) gene. Patients are usually diagnosed in infancy and are burdened with extensive medical treatments throughout their lives.

For a long time the mainstream therapies for CF were antibiotic treatments aimed at fighting bacterial infections and supportive therapies such as mucolytics and bronchodilators aimed at preserving lung function. Even though CFTR gene was cloned back in 1989, it was not until 2012 when the first small molecule aimed at correcting defects in CFTR protein was approved for the use in clinic. Since then, many additional small molecules aimed at targeting the function and the stability of mutated CFTR protein have been tested with various degree of success.

Unfortunately, none of these treatments are aimed at addressing the intrinsic pro-inflammatory phenotypes in CF that are independent of pathogens. Indeed, even though inflammation is normally a protective response of an organism aimed to eliminate pathogens, constitutively present inflammation in CF, which is a direct consequence of the lack of functional CFTR protein rather than the presence of pathogens, is weakening the ability of host to resolve the infection.

Despite the decades of intensive research, all the elements of this sterile inflammation have not been elucidated, and even for those that have been established the mechanisms are still unclear.

This thesis represents an effort to better understand some established pro-inflammatory defects of CF such as imbalance in certain lipid molecules (ceramides and polyunsaturated fatty acids) and to explore whether some effector molecules of the immune systems, such as a cytokine called B-cell Activating Factor (BAFF) contribute to the intrinsic inflammation as well.

Therefore, the following chapters are addressing these aims in the following order:

First, we discovered that BAFF cytokine is not an element of intrinsic inflammation in CF and as such cannot be targeted in order to improve the ability of host to resolve bacterial infections. Moreover, depleting levels of BAFF severely compromises immunological defense of lungs in mice, raising concerns for the lupus patients who are treated with anti-BAFF therapies.

Next, building further on the work from our own laboratory and revealing intricacies from the work of others, we discovered that a class of lipids called ceramides displays aberrant levels in CF: pro-inflammatory long-chain ceramides are increased whereas physiologically most abundant very-long-chain ceramides are depleted in CF mice, CF patients and CF cell line, therefore unambiguously establishing this pro-inflammatory imbalance of ceramides as an intrinsic defect of CF. The consequences of this defect on the stability of CFTR protein, which is known to localize in the areas of plasma membrane enriched in ceramides are also discussed. Importantly, this biochemical defect could be corrected with a small molecule called fenretinide, therefore raising prospects that the correction of aberrant membrane structure in CF in addition to the correction of protein folding could be used as a therapeutic approach in the future.

Third, we re-examined a well known defect in the imbalance of polyunsaturated fatty acids (PUFAs), namely increased levels of arachidonic acid and decreased level of docosahexanoic acid in CF. The existence of this defect in cell culture, unambiguously corroborated a hypothesis that this defect is intrinsic to CF, rather than a consequence of malnutrition or pancreatic dysfunction of CF patients. Finally, due to the known ability of fenretinide to interfere with retinoid and pro-inflammatory pathways essential for the expression of mucin genes, we tested its ability to selectively inhibit the expression of the Muc5AC gene which codes for mucins known to cause pathological plugging of the airways without interfering with the expression of Muc5b gene which codes for mucins known to be essential for anti-bacterial lung defense. Our preliminary results suggest that fenretinide holds promise to be used as a safe mucoregulatory agent in the future.

RÉSUMÉ

La fibrose kystique (FK) est la maladie autosomique récessive la plus répandue dans la population caucasienne, causée par des mutations du gène régulateur de conductance transmembranaire de la FK (CFTR). Les personnes atteintes en reçoivent souvent le diagnostic durant l'enfance et doivent se soumettre à des traitements médicaux exhaustifs durant toute leur vie. Pendant une longue période, les thérapies conventionnelles pour le traitement de la FK étaient la prise d'antibiotiques visant à prévenir les infections bactériennes et des traitements par inhalation de mucolytiques et de bronchodilatateurs aidant à faciliter la respiration et réduire les problèmes respiratoires. Malgré le fait que le clonage du gène CFTR date de 1989, ce n'est qu'en 2012 que fut approuvée l'utilisation clinique d'une première petite molécule développée dans le but de corriger les défauts de la protéine CFTR. Depuis ce temps, plusieurs nouvelles petites molécules tentant de cibler la fonction et la stabilité de la protéine CFTR mutée furent développées et testées mais avec succès mitigé. Malheureusement aucun de ces essais ne ciblait les phénotypes pro-inflammatoires intrinsèques de la FK, indépendants des pathogènes. En effet même si l'inflammation est la réponse normale du système immunitaire du corps face aux agents pathogènes, l'inflammation présente et caractéristique de la FK est due à la protéine CFTR dysfonctionnelle plutôt qu'à la présence d'agents pathogènes et diminue la capacité de l'organisme à combattre l'infection. Malgré les recherches intensives faites depuis de nombreuses années, les éléments de cette inflammation stérile ne sont pas tous identifiés et les mécanismes de régulation des éléments connus demeurent incertains.

Cette thèse est le résultat d'un travail entrepris afin de mieux comprendre certaines manifestations inflammatoires identifiées de la FK, par exemple un déséquilibre au niveau de certains lipides (céramides et acides gras polyinsaturés) et d'étudier le rôle possible de certaines molécules effectrices du système immunitaire, entre autres, la cytokine BAFF (B-cell activating factor), dans le développement de cette inflammation intrinsèque.

Ces objectifs sont définis dans les chapitres attenants selon l'ordre suivant :

En premier lieu, nous avons découvert que la cytokine BAFF n'est pas un facteur impliqué dans l'inflammation intrinsèque de la FK et ne peut donc être ciblée afin d'améliorer la réponse de l'organisme aux infections bactériennes. De plus, chez la souris, des niveaux diminués de BAFF ont sévèrement compromis la capacité de défense immunitaire de leurs poumons. Cette

observation a soulevé certaines inquiétudes face à l'utilisation de molécules anti-BAFF dans le traitement de personnes atteintes de lupus.

Deuxièmement, poursuivant les travaux déjà effectués dans notre laboratoire et révélant les complexités de travaux faits par d'autres équipes, nous avons découvert que les niveaux d'une classe de lipides, les céramides, sont anormaux en présence de FK : chez les souris et les personnes atteintes de FK ainsi que dans une lignée cellulaire de FK, les niveaux de céramides pro-inflammatoires à chaîne longue sont augmentés tandis que ceux des céramides à très longue chaîne, habituellement physiologiquement plus présents, y sont appauvris. Ce déséquilibre pro-inflammatoire des céramides démontre de façon claire leur rôle dans les troubles intrinsèques de la FK. Les conséquences de cette anomalie sur la stabilité de la protéine CFTR, présente dans les sites riches en céramides de la membrane cellulaire, sont également étudiées. Il est important de noter que cette anomalie biochimique pourrait être corrigée par l'utilisation d'une petite molécule, le fenrétinide ; la possibilité d'une correction de la structure anormale de la membrane cellulaire présente dans la FK et de la rectification du repliement de la protéine propose de futures avenues dans le traitement thérapeutique de la FK.

Troisièmement, nous avons étudié de nouveau l'anormalité reconnue du déséquilibre des acides gras polyinsaturés (PUFA) présente chez les sujets atteints de FK avec des niveaux augmentés d'acide arachidonique et des niveaux diminués d'acide docosahexaénoïque. L'existence de cette anomalie en culture cellulaire a clairement validé l'hypothèse émise que ce défaut est intrinsèque à la FK et non une conséquence d'une malnutrition ou d'un dysfonctionnement du pancréas chez les personnes atteintes.

Finalement, suite au pouvoir d'interférence reconnu du fenrétinide dans les mécanismes d'action des rétinoïdes essentiels à l'expression des gènes des mucines, nous avons analysé la capacité du fenrétinide d'inhiber de façon sélective l'expression du gène Muc5AC, gène qui code des mucines responsables de l'obstruction pathologique des voies respiratoires sans effet sur l'expression du gène qui code pour Muc5b, produisant des mucines connues pour leur rôle essentiel dans le système de défense antibactérienne des poumons. Nos résultats démontrent que le fenrétinide pourrait s'avérer être un agent prometteur et d'utilisation sécuritaire dans le contrôle de l'accumulation de mucus.

Table of Contents

ABSTRACT.....	iii
RÉSUMÉ	v
LIST OF ABBREVIATIONS.....	xi
LIST OF FIGURES AND TABLES.....	xvi
ACKNOWLEDGEMENTS.....	xviii
PREFACE AND CONTRIBUTION OF AUTHORS	xix
Chapter 1. General Introduction.....	1
1.1 Preface.....	2
1.2 Immunological Defense of Lungs.....	5
1.2.1 <i>The role of BAFF in B-cell development</i>	8
1.2.2 <i>The role of BAFF in lung immune defense</i>	13
1.3 Ceramides	16
1.3.1 <i>Metabolism of sphingolipids</i>	16
1.3.2 <i>Metabolic actions of ceramides</i>	20
1.3.3 <i>Ceramides as structural elements of biological membranes</i>	27
1.3.4 <i>Ceramides in CF</i>	33
1.3.5 <i>Ceramides and CFTR</i>	37
1.3.6 <i>Technical challenges in ceramide quantification</i>	41
1.4 Polyunsaturated fatty acids (PUFAs) and their metabolism in CF	44
1.4.1 <i>PUFAs in CF</i>	47
1.4.2 <i>Fenretinide</i>	50
Chapter 2. Depletion of BAFF cytokine exacerbates infection in <i>Pseudomonas aeruginosa</i> infected mice.....	55
2.1 Abstract.....	56
2.2 Introduction.....	56
2.3 Methods.....	58
2.3.1 <i>Mice</i>	58
2.3.2 <i>Neutralization of BAFF cytokine</i>	59
2.3.3 <i>Preparation of bacterial inoculums and lung infection</i>	59
2.3.4 <i>CFU quantification</i>	59

2.3.5 <i>ELISA tests</i>	59
2.3.6 <i>Pulmonary resistance</i>	59
2.3.7 <i>Flow Cytometry</i>	60
2.3.8 <i>Statistical Analysis</i>	60
2.4 <i>Results</i>	61
2.4.1 <i>Increased level of IL-10 and not BAFF is an inherent feature of cystic fibrosis</i>	61
2.4.2 <i>BAFF depletion does not have significant impact on Breg cells</i>	63
2.4.3 <i>Treg cells are not significantly altered in CF-KO mice but they are strongly depleted by anti-BAFF treatment</i>	63
2.4.4 <i>Reducing the level of BAFF in both wild-type and CF-KO mice increases their susceptibility to infection</i>	66
2.4.5 <i>Reducing the level of BAFF in CF-KO but not in wild-type mice increases their lung airway resistance</i>	67
2.5 <i>Discussion</i>	68
2.6 <i>Acknowledgements</i>	70
2.7 <i>Author Contributions</i>	70
2.8 <i>Conflict of Interest</i>	70
2.9 <i>Supplementary Figures</i>	71
Chapter 3. Fenretinide differentially modulates the levels of long- and very-long-chain ceramides by downregulating Cers5 enzyme: evidences from bench to bedside	72
3.1 <i>Abstract</i>	73
3.2 <i>Introduction</i>	73
3.3 <i>Methods and Materials</i>	75
3.3.1. <i>Cell culture</i>	75
3.3.2 <i>Measurement of mRNA expression by quantitative RT-PCR</i>	75
3.3.3 <i>Western Blot</i>	76
3.3.4 <i>Mice</i>	76
3.3.5 <i>Patients and Clinical Trial</i>	76
3.3.6 <i>Measurement of ceramide levels by mass spectroscopy</i>	77
3.3.7 <i>Statistical Analysis</i>	77
3.4 <i>Results</i>	79
3.4.1 <i>Mice</i>	79

3.4.1A <i>Very-Long-Chain Ceramide species are downregulated and Long-Chain Ceramide species are upregulated in CF-KO mice compared with WT controls</i>	79
3.4.1B <i>Fenretinide normalizes the levels of ceramides in CF-mice by downregulating long-chain ceramide species and upregulating very-long chain ceramide species</i>	79
3.4.2 CF Patients	80
3.4.3 Lung epithelial cell lines	82
3.5 Discussion	85
3.6 Acknowledgements	91
3.7 Author Disclosure	91
3.8 Supplementary Materials and Methods	92
3.8.1 <i>Cell culture</i>	92
3.8.2 <i>Measurement of mRNA expression by quantitative RT-PCR</i>	92
3.8.3 <i>Western Blot</i>	93
3.8.4 <i>Mice</i>	93
Chapter 4. Fenretinide mimics CFTR-induced correction of DHA/AA imbalance and blocks LPS-induced MUC5AC overexpression without affecting MUC5B	104
4.1 Abstract	105
4.2 Introduction	106
4.3 Materials and Methods	108
4.3.1 <i>Cell Culture</i>	108
4.3.2 <i>Molecular Biology</i>	109
4.3.3 <i>Analysis of lipid oxidation, fatty acid levels and protein oxidation</i>	111
4.3.4 <i>Mice</i>	112
4.3.5 <i>Histology</i>	112
4.3.6 <i>Ex vivo treatment of peripheral mononuclear blood cells (PMBCs)</i>	113
4.3.7 <i>Statistical Analysis</i>	113
4.4 Results	113
4.4.1 <i>Fenretinide prevents over-expression of MUC5AC gene in a lung goblet cell line after inflammatory stimulation</i>	113
4.4.2 <i>Fenretinide prevents accumulation of MUC5AC mucin in mice upon infection with P. aeruginosa</i>	117

4.4.3 Fenretinide treatment mimics the re-introduction of wild-type CFTR in $\Delta F508/\Delta F508$ lung epithelial cell line and corrects low DHA/AA ratio in lung epithelial cell line and PMBCs from CF patients	120
4.4.4 Fenretinide decreases the level of lipid oxidation without affecting protein oxidation in vitro	121
4.4.5 Fenretinide inhibits the activity of cytosolic phospholipases (cPLA2).....	122
4.5 Discussion	125
4.6 Supplementary Information	132
Chapter 5. Discussion, Conclusions and Future Directions	135
5.1 Discussion.....	136
5.2 Conclusions.....	139
5.3 Future Directions	140
Chapter 6. References.....	141
APPENDIX.....	179
A 1.0 Supplement	180
Table A 1.0 Fenretinide does not affect the levels of Cers1 and Cers4 mRNA	181

LIST OF ABBREVIATIONS

μM: micromolar

12(R)-HETE: 12-Hydroxyeicosatetraenoic acid

AA: arachidonic acid

ANOVA: Analysis of Variance

APRIL: A Proliferation-Inducing Ligand

BAFF: B-cell Activating Factor belonging to TNF Family

BAFF-R: BAFF Receptor

BAL: Bronchoalveolar lavage

BCA: bicinchoninic acid

B-cell receptor: B-cell receptor

BCMA: B-cell Maturation Antigen

BHA: butyl-hydroxyanisole

BM: Bone Marrow

Breg: B regulatory

C1P: Ceramide-1-Phosphate

CAMK2A: Calcium/calmodulin-dependent protein kinase type II subunit α

Cerk: Ceramide kinase

Cers: Ceramide synthases

Cert: Ceramide transfer protein

CF: Cystic Fibrosis

CF-KO: same as CFTR-KO

CFTR: Cystic Fibrosis Transmembrane Regulator

cfu: colony forming unit

cIAP: Inhibitor of Apoptosis Protein 1

CLP: Common Lymphoid Progenitor

CONSORT: Consolidated Standards of Reporting Trials

COX: cyclooxygenase

Cptp: C1P transport protein

Degs: Sphingolipid delta(4)-desaturases

DHA: docosahexanoic acid

D-PBS: Dulbecco's PBS
DRMs: Detergent Resistant Membranes
ELISA: Enzyme-Linked Immunosorbent Assay
EPA: Eicosapentaenoic acid
ER: Endoplasmic Reticulum
FABP: Fatty Acid Binding Protein
FADS: Fatty Acid DeSaturase
Fapp2: Four-phosphate adaptor protein 2
FDC: Follicular Dendritic Cells
FEV1: Forced expiratory volume in one second
fln: flincher
Gba: Glucosylceramidase
GM1, GD1a, GD1b, and GT1b: gangliosides
GPCRs: G-protein coupled receptors
HC: Healthy Control
HPLC-MS: High-performance liquid chromatography-mass spectrometry
HR: high responders
HSC: Hematopoietic Stem Cell
I2PP2A: Inhibitor-2 of PP2A
IFN- γ : Interferon- γ
IgA: Immunoglobulin A
IgE: Immunoglobulin E
IgG: Immunoglobulin G
IgM: Immunoglobulin M
Kdsr: Ketosphinganine reductase
kg: kilogram
KO: Knockout
LA: Linoleic Acid
Lag Longevity assurance gene
LCC: Long Chain Ceramide
lip3: lipase 3
LPPs: Lipid Phosphate Phosphatases

LPS: Lipopolysaccharide
mg: miligram
ml: mililiter
MPP: Multipotent Progenitors
MSD: Membrane Spanning Domain
mTOR: mammalian Target or Rapamycin
MUC5AC: Mucin 5AC
MUC5B: Mucin 5B
MUFAs: Monounsaturated fatty acids
NBD: Nucleotide Binding Domain
NFAT: Nuclear Factor of Activated T cells
NF- κ B Inducing Kinase: NF- κ B Inducing Kinase
ng: nanogram
NK: Natural Killer
NSAIDs: non-steroidal anti-inflammatory drugs
 $^{\circ}$ C: degree Celsius
PA508: Pseudomonas aeruginosa strain 508
PAGE: Polyacrylamide gel electrophoresis
PBS: Phosphate Buffered Saline
PC: Phosphatidylcholine
PCR: Polymerase Chain Reaction
PD-1: Programmed cell death protein 1
PE: Phosphatidylethanolamine
PI3K: Phosphoinositide 3-kinase
PKC: Protein Kinase C
PLA: Phospholipase
PMBCs: peripheral mononuclear blood cells
PP1: Protein Phosphatase 1
PP2A: Protein Phosphatase 2A
PPAR γ : Peroxisome proliferator-activated receptor γ
PR: partial responders
PU.1: Purine box factor 1

PUFAs: Polyunsaturated fatty acids
RA: Retinoic Acid
RAG: Recombination-Activating Genes
RAR: Retinoid Receptor
RARE: Retinoid Receptor Element
RBC: Red Blood Cell
RBP4: Retinol Binding Protein 4
RIP1: receptor-interacting protein 1
RIPA: Radioimmunoprecipitation assay
rpm: rotations per minute
RT: Room Temperature
RT-PCR: Reverse Transcription-PCR
RXR: retinoid X receptor
S1P: Sphingosine-1-Phosphate
SDS: Sodium dodecyl sulfate
SET: Su(var)3-9, Enhancer-of-zeste and Trithorax
Sgms: Sphingomyelin synthases
SLE: systemic lupus erythematosus
Smpd: Acidic sphingomyelinases
Sphk: Sphingosine kinases
SPOC-1: SPontaneously derived in Complete serum-free medium
Sptlc: Serine palmitoyltransferase
TACE: Transmembrane Activator and Calcium-modulating cyclophilin ligand interactor
TAK1: TGF- β -activated kinase 1
TBARs: 2-thiobarbituric acid-reactive substances
TCR: T Cell Receptor
Th2: Type 2 helper cell
TLC: Tram, Lag and CLN8
to: toppler
TRAF: TNF receptor-associated factor
Treg: T regulatory
TRPC6: Transient receptor potential channel 6

TSA: trypticase soy agar

Ugcg: Glucosylceramide synthase

VLCC: Very Long Chain Ceramide

WT: Wild Type

LIST OF FIGURES AND TABLES

Figure 1.1.1	Different classes of mutations in CFTR gene and their effects on CFTR protein.....	2
Figure 1.1.2	Activation of IL-1 α pro-inflammatory cascade in CF	4
Figure 1.3.1	Biochemical steps in the synthesis of ceramides and other sphingolipids	17
Figure 1.3.2	Subcellular localization of the enzymes involved in the metabolism of sphingolipids	18
Figure 1.3.3	Metabolic actions of endogenous ceramides	21
Figure 1.3.4	Tissue-specific distribution of ceramide synthases	24
Figure 1.3.5	Planar lipid rafts and caveolae.....	29
Figure 1.3.6	Effect of CerS2 ablation on the membrane morphology of microsomal vesicles ...	30
Figure 1.3.7	Structures of lipid rafts under normal and pathological conditions.....	31
Figure 1.3.8	Commercially available antibodies for ceramide detection recognize lipids other than ceramides and do not distinguish between long-chain and very-long-chain ceramides ...	42
Figure 1.4.1	Metabolism of ω -6 and ω -3 fatty acids starting with essential fatty acids obtained from food.....	45
Figure 1.4.2	Structures of fenretinide and retinoic acid.....	51
Figure 2.1	Experimental design/timeline of placebo (PBS) and Sandy-2 treatment followed by <i>P.</i> <i>aeruginosa</i> (PA508) infection.....	61
Figure 2.2	BAFF and IL-10 levels in uninfected WT and CFTR-KO mice, after <i>P. aeruginosa</i> (PA508) infection, and after Sandy-2 treatment	62
Figure 2.3	BAFF treatment efficiently depleted B-cells in both the lungs and spleen of infected and non-infected WT and CFTR-KO mice	64
Figure 2.4	BAFF depletion selectively decreased the % of Treg cells in the lungs of both WT and CFTR-KO mice, but did not have any effect in the spleen	65
Figure 2.5	BAFF depletion exacerbates pulmonary infection and in CF-KO mice contributes to the increase of lung resistance.....	66
Figure S2.1	71
Figure S2.2	71
Figure 3.1	80
Figure 3.2	82

Figure 3.3	83
Figure 3.4	87
Figure 3.5 Overview of ceramide structure, biosynthesis, and dimerization based mechanism of action.	90
Figure S3.1	96
Figure S3.2	97
Figure S3.3	98
Figure S3.4	99
Figure S3.5	100
Figure S3.6	101
Figure S3.7	102
Figure S3.8	103
Figure 4.1	114
Figure 4.2	115
Figure 4.3	118
Figure 4.4	119
Figure 4.5	120
Figure 4.6	123
Figure 4.7	124
Figures S4.1	133
Figure S4.2	134
Figure S4.3	134
Figure S4.4	134
Table 1.2.1 Phenotypes of BAFF and BAFF-R knockout mice and BAFF transgenic mice.....	11
Table 3.1 Demographic data of patients and healthy controls and response of patients to fenretinide in the third cycle of phase Ib clinical trial.....	78
Table S3.1 Sequences of primers for quantitative real-time PCR.....	94
Table S3.2 Levels of ceramides in healthy controls.....	95
Table 4.1 Conditions and treatment schedule for SPOC-1 cells.....	109
Table S4.1	132
Table A1.0 Fenretinide does not affect the levels of Cers1 and Cers4 mRNA.....	181

ACKNOWLEDGEMENTS

My graduate studies were a long and challenging journey through which I was mostly learning what a good science is *not* about. At the end of this tunnel, I was fortunate to meet my PhD mentor, Dr. Danuta Radzioch, who taught me invaluable lessons not only about science but also about life, and for these I remain indebted forever. I hope that her support and confidence in me will be justified by my accomplishments in the future.

Doctoral studies are very intense and at times an overwhelming enterprise. Therefore, I would like to extend my sincere gratitude to Miss Daciana Catalina Dumut and Miss Juhi Shah for sharing a large portion of this burden with me and for creating an unforgettably friendly atmosphere in the lab.

Furthermore, I would like to thank the following persons for their contributions to my research projects: Dr. Gabriella Wojewodka for generously sharing her preliminary data on ceramides with me, to Dr. Juan B. De Sanctis without whom none of the mass spectrometry experiments would ever be possible, to Dr. Bruce Mazer for his generous support of the BAFF project and to Dr. Cynthia Kanagaratham and Mr. Daniel Houle for their assistance in experiments with mice.

Interactions with my supervisory committee were always a most pleasant and rewarding experience. Therefore, I would like to thank Dr. Dao Nguyen, Dr. Erwin Schurr and Dr. Basil Petrof for their time, patience and constructive advice communicated during our annual meetings. Additionally, I was very fortunate to have Dr. Anne-Marie Lauzon always by my side and Dr. John Hanrahan as a very supportive and resourceful collaborator.

Very few people in our life leave a memorable trace fulfilled with kindness, generosity and compassion. Mrs. Marie Lamarche was indeed such a person and I owe most sincere debt of gratitude for all the little things that meant a big deal for me.

Finally, my love for science and the excitement of scientific discovery could only fill half of my heart while the other half belongs to my family and my beloved Chad. His genuine and unconditional love has been a major driving force for me through all the ebbs and tides ever since we met, and will certainly remain the source of inspiration for all the endeavors in the future.

PREFACE AND CONTRIBUTION OF AUTHORS

Format of the Thesis

This thesis is presented in the manuscript based format for a Doctoral Thesis, according to the Thesis Preparation Guidelines by the Department of Graduate and Postdoctoral Studies. The studies described here were performed under the supervision of Dr. Danuta Radzioch. Chapters containing experimental results are preceded by paragraphs linking the chapters together.

Chapter 1 consists of the three parts organized as Review articles that have already been published or are in preparation. The first part covers topics such as immunological defense of the lungs and BAFF cytokine. Second part covers the roles of ceramides in CF. Third part covers the role of polyunsaturated fatty acids in CF. The second part is adapted from the manuscript “Biochemistry of very-long-chain and long-chain ceramides in cystic fibrosis and other diseases: the importance of side chain” by Dušan Garić; Juan B. De Sanctis; Juhi Shah; Daciana Catalina Dumut; and Danuta Radzioch published in *Progress in Lipid Research*, 2019. Contribution of the authors: the thesis author (DG) researched and wrote the manuscript. JBS performed Western blots, JS and DCD edited the manuscript and DR wrote and edited the manuscript.

Chapter 2 is adapted from the manuscript: “Depletion of BAFF cytokine exacerbates infection in *Pseudomonas aeruginosa* infected mice” by Dušan Garić, Shao Tao, Eisha Ahmed, Mina Youssef, Cynthia Kanagaratham, Juhi Shah, Bruce Mazer and Danuta Radzioch published in *Journal of Cystic Fibrosis*, 2009. Contribution of authors: D.G. and D.R designed all experiments. D.R and B.M. supervised the study. D.G participated in all experiments and wrote the entire manuscript. S.T. and E.A. performed flow cytometry analyses. C.K. performed lung resistance measurements. J.S. performed all statistical analyses, prepared all the figures and helped with experiments. M.Y. participated in lung resistance studies.

Chapter 3 is adapted from the manuscript: “Fenretinide differentially modulates the levels of long- and very-long-chain ceramides by downregulating Cers5 enzyme: evidences from bench to bedside” by Dušan Garić; Juan B. De Sanctis; Gabriella Wojewodka; Daniel Houle; Shanon Cupri; Asmahan Abu-Arish; John W. Hanrahan; Marian Hajduch; Elias Matouk and Danuta Radzioch published in *Journal of Molecular Medicine*, 2017. Contribution of authors: the thesis author (DG) wrote the entire manuscript and performed *in vitro* sample processing, RNA analysis, Western blot, JBDS performed lipidomic sample and data analyses, manuscript editing;

GW performed clinical study coordination, processing specimens from clinical trial, data analysis, manuscript editing; DH performed animal experimentation; SC performed clinical study coordination, assessment of patients; AAA performed cell culture work and manuscript editing; JWH did manuscript corrections, editing and experimental design; MH performed analysis of lipid oxidation, discussion on the conceptual data analysis and exploration of molecular mechanism of action of the drug, manuscript editing; EM participated in the clinical trial concept, design and coordination, manuscript editing; DR supervised the study , performed data analysis, manuscript corrections and editing, and final approval of the manuscript for submission

Chapter 4 is adapted from the submitted manuscript: “Fenretinide mimics CFTR-induced correction of DHA/AA imbalance and blocks LPS-induced MUC5AC overexpression without affecting MUC5B” by Dušan Garić; Juan B. De Sanctis; Juhi Shah; Daciana Catalina Dumut; Mina Youssef and Danuta Radzioch, 2019. Contribution of the authors: the thesis author (DG) wrote the manuscript, performed qPCR, ELISA and Western blot analyses. JBS performed lipidomic analyses, JS and DCD made the figures, performed statistical analyses and edited the manuscript, MY harvested the lungs for histological analyses that were performed at the Histopathological core facility of the McGill University Health Center Research Institute (MUHC-RI) and DR supervised the study and edited the manuscript.

Chapter 5 contains a general discussion of the results and concepts presented in this thesis.

Claims to originality

- BAFF cytokine is not an intrinsic element of sterile inflammation in CF, but is strongly induced by *Pseudomonas* infection in the lungs of infected mice.
- BAFF cytokine is essential for immunological defense of the lungs as its depletion leads to the increased bacterial load and increased lung resistance.
- BAFF depletion leads to the significant decrease of Treg cells in the lungs, but not in the spleens of uninfected mice.
- Long-chain ceramides (LCCs) are increased whereas very-long-chain ceramides (VLCCs) are decreased in CFTR-KO mice, CF patients and CF patient derived cell line.

- Fenretinide increases the levels of LCCs and increases the levels of VLCCs by downregulating Cers5 enzyme.
- Fenretinide and Zn^{2+} ions cooperate in the modulation of ceramide levels.
- Commercially available antibodies for ceramide detection (polyclonal S58-9 and monoclonal 15B4) recognize lipids other than ceramides and do not distinguish between long-chain and very-long-chain ceramides.
- Fenretinide selectively blocks lipopolysaccharide-induced expression of Muc5AC gene, without significantly affecting the expression of Muc5B gene.
- Fenretinide effectively mimics reintroduction of wild-type CFTR in correcting pro-inflammatory lipid imbalance of CF by increasing the levels of VLCCs and docosahexanoic acid (DHA) and lowering the levels of LCCs and arachidonic acid (AA)
- Fenretinide lowers the total enzymatic activity of cytosolic phospholipases (cPLA2) in lung epithelial cells

Chapter 1.

General Introduction

1.1 Preface

Cystic fibrosis (CF) is the most common autosomal-recessive genetic disorder in Caucasians whose symptoms are manifested through the permanent dysfunction of the lungs and gastrointestinal system, which if left untreated inevitably leads to the death of the patient. It took more than 50 year after the first description of the disease back in 1936 by Fanconi (Fanconi et al., 1936) to elucidate the genetic basis of CF when a cystic fibrosis transmembrane conductance regulator (CFTR) gene was cloned in the laboratories of Francis Collins and Lap-Chee Tsui (Kerem et al., 1989; Riordan et al., 1989).

CFTR gene, located at the locus 7q21-31, codes for a 1480 amino acid long protein which functions as a chloride (Cl⁻) channel in the apical membrane of many different epithelial cells, including lung airways, sweat ducts in the skin and the epithelium of pancreatic acini. Currently there are 2063 mutations (<http://www.genet.sickkids.on.ca/cftr/StatisticsPage.html>) in CFTR gene and the most frequent one that causes the disease (75% of diagnosed patients) is a deletion of phenylalanine at the position 508 ($\Delta F508$) (Lemna et al., 1990). These mutations are divided into five classes based on their effects on CFTR production and the amount of residual CFTR function (O'Sullivan and Freedman, 2009; Rogan et al., 2011; Scriver, 1995) (**Figure 1.1.1**).

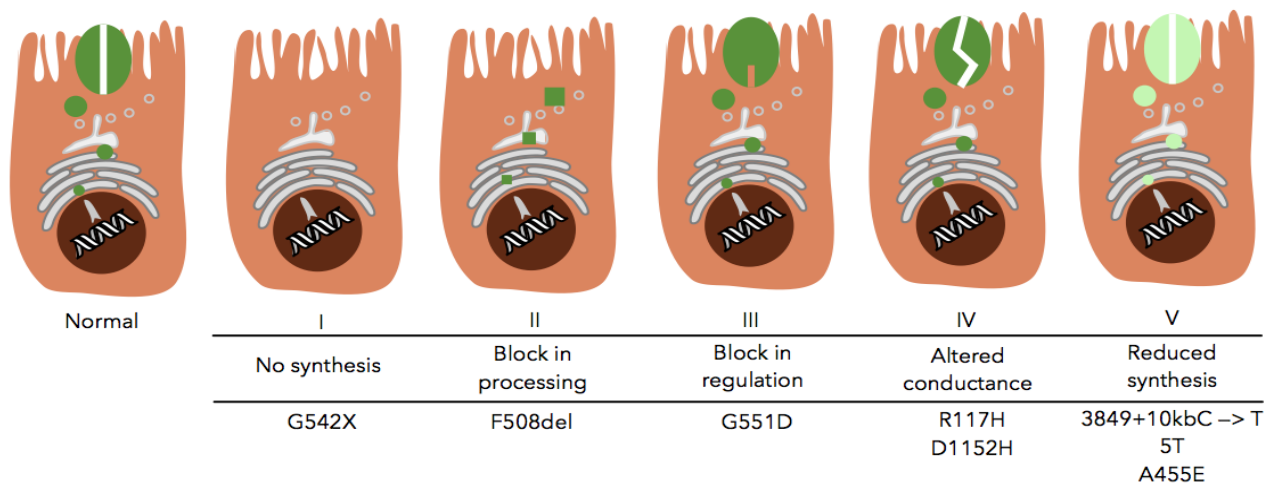


Figure 1.1.1 Different classes of mutations in CFTR gene and their effects on CFTR protein, adapted and modified from (Scriver, 1995).

Interestingly, unlike frameshift mutations or large-scale deletions which entirely annihilate the presence of CFTR protein in the cell, $\Delta F508$ mutation renders CFTR protein unstable and prone to degradation in the endoplasmic reticulum (Cheng et al., 1990; Lukacs et al., 1993). This discovery sparked the hope that pharmacological agents could be developed in order to rescue $\Delta F508$ protein from degradation. Indeed, several small molecules with this activity have been recently described (Davies et al., 2018a; Pranke et al., 2017; Van Goor et al., 2011; Veit et al., 2018b).

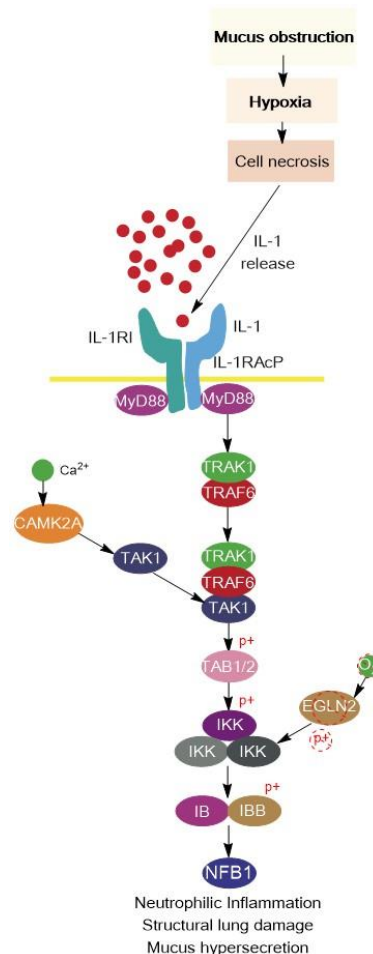
Why such a detrimental allele like $\Delta F508$ continues to linger in human population through its long evolutionary history remains a puzzle. A part of the answer seems to be in a phenomenon called *heterosis*, when heterozygous carriers of an otherwise detrimental allele experience a certain evolutionary advantage over wild-type carriers. In the case of $\Delta F508$ allele, stringent epidemiological analysis demonstrated that the evolutionary advantage might have been an increased resistance to tuberculosis that arose during the pandemic at the beginning of the 17th century in Europe (Poolman and Galvani, 2007). Importantly, these results are consistent with the recent epidemiological study done in Brazil (Bosch et al., 2017).

The epithelium of the sweat ducts and other serous ducts are normally re-absorbing salt. However, in the sweat ducts of CF patients, chloride (Cl^-) is not reabsorbed, because the function of CFTR is compromised. Therefore, excessive amounts of salt are lost in the sweat, and this elevated concentration of Cl^- in sweat (>60 mM) was used as the earliest test to confirm the diagnosis of CF (Cutting, 2013). The secretion of chloride, and secondarily of sodium and water onto the surface of the lung epithelium is a physiologic mechanism that maintains the hydration of the airways. However, in CF, this physiologic mechanism is compromised, leading to abnormally viscous mucus due to the decreased water volume and altered content of salts. This viscous mucus serves as the fertile ground for the growth of the microbes from the environment that would otherwise be cleared, leading to the downward spiral in lung function. The recurrent episodes of infection and inflammation ensue, followed by the ill-fated attempts of the body to heal the lung injury, ultimately leading to the scarring or the fibrosis of the lungs. The thickened lung tissue that accumulates over time compromises normal lung function, resulting in the progressive respiratory disease which is the primary cause of mortality and morbidity of CF patients. The acute inflammation induced by infection is normally a transient and protective

biological response aimed to eliminate the invading pathogen. However, in patients with CF, release of the large amounts of reactive oxygen species and proteases (particularly elastase) by neutrophils after repeated rounds of infection and inflammation lead to the permanent and incurable structural damage of the airways also known as bronchiectasis (Cantin et al., 2015). For a long time this excessive inflammatory response was thought to be the major process that leads to the bronchiectasis. However, studies with miscarried or aborted CF fetuses (Hubeau et al., 2001; Khan et al., 1995; Verhaeghe et al., 2007) demonstrated increased concentration of inflammatory markers in the lungs, which strongly suggests the presence of inflammation even in the aseptic conditions. Similarly, the lungs of CFTR-deficient mice display higher levels of pro-inflammatory keratinocyte chemoattractant (KC) cytokine (homologue of human IL-8), S100A8 and most importantly IL-1 β (Guilbault et al., 2006; Inoue et al., 1994; Tabary et al., 2001; Thomas et al., 2000). Most recent reports revealed that unlike inflammation resulting from the infection which is driven by Toll-like receptor network, *sterile inflammation* seen in aborted CF fetuses, young uninfected children with CF and non-infected CFTR-KO mice is mediated through the activation of interleukin-1 receptor (IL1-R) (Chen et al., 2007; Fritzsching et al., 2015) (**Figure 1.1.2**).

Figure 1.1.2 Activation of IL-1 α pro-inflammatory cascade in CF.

CAMK2A: Calcium/calmodulin-dependent protein kinase type II subunit α ; EGLN2: Egl-9 Family Hypoxia Inducible Factor 2; IL-1 α : Interleukin-1 α ; IL-1RAcP: interleukin-1 receptor accessory protein; IL-1RI: Interleukin 1 receptor, type I; IKK: I κ B kinase; I κ B: Inhibitor of nuclear factor kappa-B kinase subunit; NF κ B: Nuclear Factor κ B; MyD88 : Myeloid differentiation primary response protein 88; TRAK1: Trafficking kinesin-binding protein 1; TRAF6: TNF receptor-associated factor 6; TAK1: Transforming growth factor β -activated kinase 1; TAB1/2 : TAK1 Binding Protein



It seems that the increased viscosity of the airway surface liquid that arises as the consequence of reduced epithelial Cl⁻ transport, leads to the hypoxia unique to the CF airways (Montgomery et al., 2017). In turn, the lack of oxygen leads to the necrosis of epithelial cells, which release IL-1 α (Fritzsching et al., 2015), that activates IL1-R thereby initiating the pro-inflammatory cascade under sterile conditions (**Figure 1.1.2**). Additionally, hypoxia alone can activate NF- κ B pathway independently from IL-1 α cytokine (Culver et al., 2010; Fitzpatrick et al., 2011), which suggests that there are multiple pathways, some of which remain uncharacterized, that may lead to the inflammation even in the absence of pathogens.

Whatever the mechanism, this sterile inflammation is not protective (Montgomery et al., 2017) and in fact it impedes the ability of an organism to combat the infection (Cohen-Cyberknoh et al., 2013). Therefore, the inflammation (sterile and pathogen-induced) is the central topic of my doctoral thesis around which the themes presented in the forthcoming chapters are revolving.

This chapter is an introduction into different approaches undertaken during my doctoral studies with an aim to control inflammation, and these include diverse disciplines ranging from immunology of B-cells to the biochemistry of ceramides and fatty acids. However, major focus will be on *ceramide imbalance* in CF which is for the first time defined in this thesis. Finally, this thesis concludes with the effects of fenretinide on the expression of two major mucin genes in the lungs (MUC5AC and MUC5B) and on the imbalance of polyunsaturated fatty acids, another major biochemical hallmark of CF.

1.2 Immunological Defense of Lungs

With a large surface area, roughly the size of a tennis court (Salvi and Holgate, 1999), that interacts extensively with the environment outside the body; the respiratory system represents the most challenging immunological dilemma for an organism. Unlike skin or gastrointestinal system whose epithelial structures present a solid natural barrier and whose microbiomes efficiently prevent the outgrowth of pathogenic organisms from the environment, the mostly sterile environment of the lungs and their role as the organs of gas exchange makes their normal functioning critical for the survival and intolerant of collateral damage.

The nose filters many bacteria, viruses and fungi, preventing their incursion into the lower parts of the respiratory tract. Passive mechanisms such as formation of mucus blanket, mucociliary

removal of the inhaled particles and defense molecules secreted by epithelial cells provide a robust defense against all but the most aggressive pathogens. The particles and microorganisms that evaded these mechanical defenses are usually eliminated by alveolar macrophages which serve as the front line of cellular defense against respiratory pathogens (Lloyd and Marsland, 2017). Only after these primeval mechanisms fail to prevent the advances of the most aggressive pathogens, the adaptive immune responses as the final and usually most efficient line of defense must be marshaled in order to maintain the integrity of airway function and ensure the survival of the host.

Adaptive immune responses are mediated by lymphocytes which execute two broad classes of responses against pathogens: antibody responses and cell-mediated responses carried out by B- and T-cells respectively. In antibody responses, B-cells are activated to secrete proteins called antibodies that bind directly to the pathogens thereby marking them for destruction by phagocytic cells, mainly macrophages. In cell-mediated responses, T-cells react directly against an antigen that is presented to them on the surface of infected cells, by secreting the molecules that kill the infected cell and by producing signal molecules that activate macrophages (Abbas et al., 2018).

Clearance of pathogens by one of these mechanisms ensures the return of respiratory system to homeostasis and its normal functioning. However, in the lungs of CF patients, the clearance of pathogens is hindered by the viscous layer of mucus that entraps the pathogens, thereby precluding the very first line of respiratory defense. This initial defect, together with sterile inflammation due to the necrotic death of epithelial cells in this hypoxic environment, initiates a vicious circle of infection and inflammation which after many repeated cycles leaves permanent scars in the lung tissue (Fritzsche et al., 2015).

Antibiotic treatments that are used to prevent the outgrowth of pathogenic bacteria provide only a temporary relief, and during the lifetime of a CF patient the continuous use of antibiotics may lead to the development of resistance of pathogens with which they are continuously being infected.

The major damage during pathogen-induced inflammation is inflicted by neutrophils, the cells of innate immune system that are recruited to clear the pathogens, but which in doing so release

enormous amounts of reactive oxygen species and proteolytic enzyme (Cantin et al., 2015). These substances are toxic not only to the pathogens but also to the host tissue, and following prolonged exposure lung tissue becomes irreversibly fibrotic and dysfunctional.

While the role of neutrophils in this process has been firmly established for a long time (Muhlebach et al., 1999; Tabary et al., 2006; Ulrich et al., 2010) the role of B and T-cells, the two major arms of the adaptive immune system, continues to be explored.

Over the last two decades, a growing body of evidence has emerged to support a physiologically important role for the low levels of CFTR protein expressed in B and T-cells. Central to the phenotype of CF with regards to T-cells appear to be a predilection to mount a type 2 helper T-cell (Th2) response (Hartl et al., 2006), which is pro-allergic and appropriate for fighting parasites, but not bacterial pathogens such as *P. aeruginosa*. Moss and colleagues showed that helper T cells (Th) from patients with CF produce lower levels of IFN- γ , a Th cytokine crucial for mounting anti-bacterial response (Moss et al., 2000). On the other hand, the expression of IL-10 was shown to be upregulated in CF patients (Casaulta et al., 2003; Moss et al., 2000) from Ratner) and recently in uninfected CFTR-KO mice as well (Garić et al., 2018). Additionally, it was demonstrated that CFTR-KO mice that are infected with *P. aeruginosa* can recover from the acute infection, but unlike their wild-type littermates still develop chronic infection despite having higher antibody titers against *P. aeruginosa* (Coleman et al., 2003; Moser et al., 2002).

One emerging explanation for the phenomenon of Th2 skewing seen in CF is that mutant CFTR protein causes increased flux of Ca²⁺ ions across T-cell membrane which shifts T-cells towards Th2 phenotype. It has been known that the absence of the functional CFTR protein in the plasma membrane is associated with hyperactivity of TRPC6 Ca²⁺ channel (Antigny et al., 2011). Therefore, according to this hypothesis, the influx of Ca²⁺ ions leads to the increased translocation of NFAT transcription factor from the cytoplasm into the nucleus, which drives the expression of IL-4, IL-13 and IL-6 cytokines, which further lead to the expression of IgE antibodies and allergic inflammation (Hodge et al., 1996; Ranger et al., 1998; Yoshida et al., 1998). Indeed, the findings that CFTR-KO mice have disproportionate Th2 response upon *A. fumigatus* infection compared to wild-type mice have been supporting this hypothesis whereas CFTR-KO deficiency was characterized with diminished Th1 response (Allard et al., 2006).

Different isoforms of NFAT promote different cytokine expression profiles and determine the type of Th differentiation. In particular, unrestrained NFATc1 activity promotes Th2 differentiation and production of IL-4, IL-5 and IL-6, all of whom lead to the production of high levels of IgE in B cells (Abbas et al., 2018). Therefore, an aberrant Th2 profile present in patients with CF may lead to another abnormality: dysfunction and potentially pathological activation of B-cells.

1.2.1 The role of BAFF in B-cell development

Millions of B lymphocytes that are generated in the adult bone marrow (BM) every day are continuously exported to the periphery where they provide protection to the organism mostly by secreting antibodies. B-cell development begins in the specialized environment of the bone marrow with the asymmetric division of an hematopoietic stem cell (HSC) and continues through a series of progressively more differentiated progenitor stages to the production of common lymphoid progenitors (CLPs), which can give rise to B cells, T cells, or some of the innate lymphoid cells like natural killer (NK) cells (Abbas et al., 2018). CLPs destined to become T cells migrate to the thymus, where they complete their maturation, while those that remain in the BM will enter the B-cell development pathway.

First, HSCs differentiate into multipotent progenitor cells (MPPs), which can produce both lymphoid and myeloid cells but are no longer self-renewing stem cells. MPPs express on their surface a receptor tyrosine kinase called FLT3 that is activated by the membrane-bound FLT3 ligand displayed by stromal cells of the BM and several transcription factors that determine the fate of this lineage. Detailed discussion of these transcription factors and their actions is beyond the scope of this review, but suffice it to say that the levels of PU.1 (Purine box factor 1) transcription factor determine lymphoid versus myeloid differentiation: low levels of PU.1 promote lymphoid whereas high levels of PU.1 promote myeloid differentiation (Anderson et al., 2002; Nerlov and Graf, 1998).

The E2A, EBF1, and Pax-5 transcription factors induce the expression of genes encoding the recombinases Rag-1 and Rag-2 and components of B-cell receptor (BCR). As a CLP destined to become B-cell matures, the chromatin containing the immunoglobulin heavy-chain locus

becomes increasingly accessible, Rag-1 and Rag-2 proteins initiate their recombination and the developing cell is irrevocably committed to the B-cell lineage (Nutt and Kee, 2007).

Rearrangement between D(diversity) and J(joining) segments of the H(heavy)-chain locus takes place at the early pro-B cell stage driven by the actions of Rag-1 and Rag-2 proteins. V-gene segment rearrangement follows in the early pre-B cell stage (Bassing et al., 2002; Hozumi and Tonegawa, 1976).

In pre-B cells, functional H-chains (VDJ-C μ) pair with V-preB and λ -like to form the pre-BCR, which is expressed inside the cell but not on the surface. Signals induced by pre-BCR downregulate the expression of RAG genes, preventing the rearrangement of the second H-chain allele and also induce proliferation. These events ensure that only one of the two heavy-chain alleles can be expressed in a single B-cells, resulting in a phenomenon called *allelic exclusion* (Bassing et al., 2002). The allelic exclusion ensures that each B-cell expresses only one type of antigen-binding site, because an antibody binding site is determined by the combination of a particular H and L chain. B-cells that displays BCRs of a single, defined specificity, can be efficiently activated by corresponding antigen, whereas single B-cell that expresses several combinations of the two different H and L chains (thus expressing a variety of antigen-binding specificities), would not be able to mediate a specific immune response (Bassing et al., 2002).

Next, RAG genes are re-expressed to initiate V-J rearrangement of L-chains. Rearranged L-chains pair with H chains and form IgM. Antigen binding by surface IgM expressed on immature B cells initiates signaling cascade which changes the expression pattern of many genes and ultimately leads to the egress of immature B-cells into the circulation. Immature B cells (called transitional 1 B-cells at this point) travel to the spleen by following higher gradient of sphingosine 1-phosphate (S1P) which they sense through S1P receptor expressed on their surface (Matloubian et al., 2004).

Once they enter the spleen, immature B cells (called at this point transitional or T1 cells) will encounter for the first time a cytokine called **B-cell activating factor** belonging to the TNF family (BAFF), which is produced in the spleen mostly by follicular dendritic cells (FDCs). However, outside the spleen BAFF is produced by neutrophils (Scapini et al., 2008), activated T-cells (Huard et al., 2001), lung epithelial cell (Kato et al., 2006), cytotrophoblasts of placenta

(Langat et al., 2008), fibroblast-like synoviocytes in the synovium of patients with rheumatoid arthritis (Alsaleh et al., 2007), osteoclasts in patients with multiple myeloma (Abe et al., 2006; Geffroy-Luseau et al., 2008), and even salivary gland epithelial cells in patients with Sjögren's syndrome (Ittah et al., 2008). The production of BAFF by non-haematopoietic cells may provide local niches to modulate the survival and function of B cells and plasma cells that are patrolling through these tissues.

BAFF and its paralogous cousin APRIL (A Proliferation-Inducing Ligand) are the two ligands that together with the three corresponding receptors form a "BAFF system" crucial for the homeostasis of B-cells in an adult organism. BAFF is an evolutionary conserved gene and the presence of its homologue in some of the most primitive Vertebrates like lampreys substantiates its essential role in the hematopoiesis of B-cells in all Vertebrates (Das et al., 2016). On the other hand, APRIL is present in amphibians, reptiles and mammals but is absent in birds (Das et al., 2016), which is consistent with its non-essential role in the hematopoiesis of B-cells (Varfolomeev et al., 2004).

By the time they reach spleen, immature B-cells will start expressing BAFF-R on their surface. The receptors of the BAFF system are: BAFF receptor (BAFF-R), transmembrane activator and calcium-modulating cyclophilin ligand interactor (TACI) and B-cell maturation antigen (BCMA). BAFF binds very strongly to BAFF-R and with a much lower affinity to BCMA and TACI, whereas APRIL binds both BCMA and TACI (Day et al., 2005). Of all these interactions, the most relevant one for the homeostasis of B-cells is the one between BAFF and its receptor BAFF-R, since mice with a deletion in both BAFF-R and BAFF gene show a profound reduction in B-cell numbers and a developmental block at the transitional T2 stage. In contrast, the deficiency of APRIL does not lead to significant abnormalities in the B-cell development (Varfolomeev et al., 2004) and therefore will not be discussed further here, but it is important to mention that in April-deficient mice class switching to IgA is compromised (Castigli et al., 2004).

A role for BAFF and BAFF-R in the survival of B cells during B cell maturation was shown in BAFF- and BAFF-R-deficient animals, in which maturation of marginal zone and B2 type of B-cells is impaired beyond the T1 stage (Mackay et al., 2003) (**Table 1.2.1**). However, B1 type of

B cells, memory B cells and a small population of mature splenic B cells do not require BAFF or APRIL for survival (Benson et al., 2008; Gorelik et al., 2003; Scholz et al., 2008).

Mouse Model	Phenotype	Reference
<i>Baff</i> ^{-/-} mice	<ul style="list-style-type: none"> • Impaired B cell maturation beyond the T₁ stage • Decreased immunoglobulin levels • Decreased T cell-dependent and T cell-independent immune responses • Modest increase of allograft survival, improved with a non-effective low dose of cyclosporine 	Mackay et al. <i>Annu. Rev. Immunol.</i> (2003).
<i>Baff</i> -transgenic mice	<ul style="list-style-type: none"> • Development of B cell hyperplasia from the T₂ B cell stage • Development of T cell-independent but MYD88-dependent autoimmunity involving the production of autoantibodies, glomerulonephritis, inflammation and destruction of the salivary glands • Decreased saliva production; B₁ B cells present in the kidney and marginal zone-like B cells present in the salivary glands • Expansion of the effector and regulatory T cell compartments 	Mackay et al. <i>Semin. Immunol.</i> (2006). Groomet al. <i>J. Exp. Med.</i> (2007). Mackay et al. <i>Curr. Dir. Autoimmun.</i> (2005).
<i>Baffr</i> ^{-/-} mice	<ul style="list-style-type: none"> • Same as <i>Baff</i>^{-/-} mice • Decreased lifespan of germinal centres • Impaired class switch recombination 	Shulga-Morskaya et al. <i>J. Immunol.</i> (2004).

Table 1.2.1 Phenotypes of BAFF and BAFF-R knockout mice and BAFF transgenic mice.

Courtesy of Ms. Juhi Shah

In addition to the studies with genetically engineered mouse models, Rauch et al demonstrated central role for BAFF-BAFF-R signaling in the survival and maintenance of both follicular and marginal zone B cell pools of B-cells *in vivo* by injecting mice with anti-BAFF antibody (Rauch et al., 2009).

BAFF is synthesized as a membrane-bound protein that can be released as a soluble cytokine by proteolytic cleavage. Membrane-bound form of BAFF is cleaved by furin convertase (Schneider et al., 1999) to generate soluble form of BAFF. Like most ligands of TNF family, processed and soluble BAFF molecules usually form homotrimers. However, BAFF is the only member of TNF family that can form multimers as large as a capsid-like assembly of 20 trimers (60-mer). Trimeric form of BAFF activates BAFF-R, while BAFF 60-mers but not BAFF trimers signal through TACI (Bossen et al., 2008).

Binding of the trimeric form of BAFF to BAFF-R leads to the recruitment of TNF receptor-associated factor 3 (TRAF3) to the trimeric BAFF-R. This leads to the degradation of TRAF3 and release of the inhibition imposed by unbound TRAF3 on the alternative nuclear factor-κB2

pathway. On the other hand, recruitment of TRAF2 or TRAF6 to the trimeric TACI receptor results in a positive signal (classical NF- κ B1 pathway) only when at least two trimeric TRAFs are recruited in response to higher order oligomers of ligand, such as BAFF 60-mers (Mackay and Schneider, 2009).

The mechanistic details of the early BAFF-R signaling have long remained elusive because BAFF-R binds only TRAF3 which does not activate neither classical nor alternative NF- κ B pathway. TRAF3 directly interacts with NF- κ B Inducing Kinase (NIK) kinase and this interaction recruits TRAF2 to NIK. TRAF2 further recruits cellular Inhibitor of Apoptosis Protein 1 (cIAP), which acts as an E3 ubiquitin ligase for NIK, thereby tagging it for degradation. Upon binding of BAFF trimer to BAFF-R, TRAF3 is recruited to BAFF-R and is degraded in TRAF2-dependent manner. This liberates NIK kinase from degradation, and now NIK is free to activate alternative NF- κ B2 pathway. NIK activates I κ B Kinase α (IKK α) which phosphorylates p100, leading to its partial proteolysis to generate p52 (Xiao et al., 2001). This creates transcriptionally competent NF- κ B complex RelB/p52 that translocates to the nucleus and induces activation of NF- κ B target genes (Mackay and Schneider, 2009).

On the other hand, TRAF2 and TRAF6 engaged by TACI receptor induce K63-linked polyubiquitination of receptor-interacting protein 1 (RIP1) and this noncanonical polyubiquitin chain recruits both the TGF- β -activated kinase 1 (TAK1) complex (consisting of TAK1, TAB2, and TAB3) and the IKK complex (consisting of IKK α , β , and γ), by binding directly to the ubiquitin-binding domains present on TAB2 and IKK γ , respectively. Once hooked by polyubiquitinated RIP1, TAK1 directly activates IKK β through proximity-mediated phosphorylation (Chen, 2005; Ea et al., 2006; Wu et al., 2006). IKK β eventually phosphorylates an inhibitory subunit of NF- κ B called I κ B α . I κ B α is then polyubiquitinated through Lys48-linked polyubiquitin chains by the β -TrCP E3 ubiquitin ligase, leading to its degradation by the proteasome and to nuclear translocation of free NF- κ B dimmers (RelA/p50), ultimately ending in activation of NF- κ B target genes.

Stimulation of BAFF-R strongly activates the alternative NF- κ B2 pathway and weakly activates the classical NF- κ B1 pathway in primary B cells whereas TACI receptor strongly activates classical NF- κ B1 pathway. Nevertheless, both pathways are required for B-cell survival.

Additionally, BAFF-R activates PI3K-mTOR-AKT axis (Patke et al., 2006; Woodland et al., 2008), which further contributes to the growth and the survival of B-cells.

All together, the activation by multiple signaling pathways by BAFF cytokine contributes to the survival and metabolic fitness of B-cells. On the other hand, excessive production of BAFF is detrimental to the host, as demonstrated with transgenic mice overexpressing BAFF. These mice suffer from increased production of autoantibodies, proteinuria, salivary gland destruction, immunoglobulin deposits in the kidney and splenomegaly, all of which are symptoms reminiscent of autoimmune diseases like systemic lupus erythematosus and Sjögren's syndrome (Groom et al., 2002; Gross et al., 2000; Mackay et al., 1999). The development of these phenotypes in BAFF transgenic mice is largely due to the excessive expansion of B-cells beyond T2 stage, namely marginal zone B cells and T2 cells. Interestingly, BAFF-transgenic mice have more effector T cells, but they also have more Treg cells (Walters et al., 2009). However, autoimmune phenotypes develop to the same extent in T-cell-sufficient and T-cell-deficient BAFF transgenic mice (Groom et al., 2007), which indicates that T cells are not responsible for autoimmune phenotypes observed in BAFF-transgenic mice.

1.2.2 The role of BAFF in lung immune defense

For a long time it was thought that the primary immune responses could only be generated in secondary lymphoid organs (Moyron-Quiroz et al., 2004), but studies in lymphotoxin α -deficient mice, which lack lymph nodes and have completely disorganized spleen demonstrated that antigen-specific B and T cells can be primed in non-lymphoid tissues as well (Lee et al., 2000; Lund et al., 2002). In fact, many studies revealed the presence of ectopic (also called tertiary) lymphoid-like structures in tissues affected by chronic inflammation, including respiratory system (reviewed in (Aloisi and Pujol-Borrell, 2006)). Unlike well organized secondary lymphoid organs, these ectopic lymphoid structures are relatively disorganized and transient structures that develop in response to infection, chronic inflammation or both (Aloisi and Pujol-Borrell, 2006; Carragher et al., 2008). However, they do contain all the necessary cellular and biochemical components to induce activation and promote the survival of B-cells. Even though these structures evolved as the local mechanisms to control infection, their prolonged activity may amplify the detrimental effects of chronic inflammation to the surrounding tissues (Aloisi and Pujol-Borrell, 2006).

Although BAFF plays a critical roles in B-cell development and survival during normal immune responses, its continuous presence in ectopic lymphoid structures may prevent the proper resolution of inflammation and therefore exacerbate tissue damage. Indeed, elevated levels of BAFF were reported to correlate with disease severity in the CD4⁺ T cells of patients infected with *Mycobacterium tuberculosis* (Liu et al., 2012). Furthermore, the levels of BAFF were increased in the bronchoalveolar lavage fluid (BALF) of infants with severe respiratory syncytial virus (RSV) infection, as well as in the upper airway secretions from children with human metapneumovirus, influenza virus (H1N1), bocavirus, rhinovirus and *Mycoplasma pneumoniae* infections (McNamara et al., 2013). Perhaps of the most immediate relevance for the patients with CF was the finding that BAFF is increased at the protein level in the BALF of children with CF irrespective of their infection status with *P. aeruginosa* and that its levels are increased in mice upon infection with *P. aeruginosa* (Neill et al., 2014). Furthermore, BAFF mRNA was found to be among the top 50 up-regulated genes in the bronchial epithelium of patients with CF who were not infected with *P. aeruginosa* when compared with non-CF bronchial epithelium (Ogilvie et al., 2011).

These studies opened a possibility that BAFF is an element of sterile inflammation, known to be one of the contributing factors that ultimately lead to the permanent lung dysfunction known as bronchiectasis in the lungs of CF patients. If this was the case, BAFF could be targeted in patients with CF with an available therapeutic antibody (Belibumab) in order to control sterile inflammation and therefore prevent or at least postpone bronchiectasis. However, neither of these studies (Neill et al., 2014; Ogilvie et al., 2011) established whether BAFF is increased in the lungs of CF mice compared to wild-type littermates therefore leaving an open possibility that the increased level of BAFF observed in these studies are due to the subclinical bacterial and/or viral infections known to be very common in patients with CF (Belessis et al., 2012; Zemanick and Wainwright, 2016).

Therefore, in order to explore this possibility, we measured the level of BAFF cytokine in the lung homogenates of CFTR-KO mice and their wild-type littermates without collecting BAL fluid at the baseline and upon infection with *P. aeruginosa* (Garić et al., 2018). We discovered that BAFF levels are not increased in uninfected CFTR-KO mice compared to their wild-type counterparts. However, the levels of BAFF sharply rise upon infection with *P. aeruginosa* in the

lungs of both CFTR-KO and wild-type mice (Garić et al., 2018). Interestingly, the levels of an anti-inflammatory cytokine IL-10 were increased in CFTR-KO mice compared with their wild-type littermates, which is probably a negative-feedback loop response to the sterile inflammation present in CFTR-KO mice. Furthermore, we wanted to examine whether this increase in BAFF levels is important for the ability of animals to combat infection or it could be a part of cytokine storm and non-essential for the immune defense of the lungs. In order to test this hypothesis, we used Sandy-2 antibody known to deplete BAFF very efficiently *in vivo* (Kowalczyk-Quintas et al., 2016), and we demonstrated that reducing the level of BAFF in both wild-type and CF-KO mice increases their susceptibility to infection determined by significantly higher bacterial burden in Sandy-2 treated animals. Furthermore, depleting BAFF in CF-KO but not wild-type mice further compromised lung function measured by metacholine-induced lung resistance. Interestingly, we also discovered that the depletion of BAFF with Sandy-2 antibody decreases the population of Treg cells in the lungs but not in the spleen. These results are consistent with the previous finding that BAFF transgenic mice overexpressing BAFF protein have increased the number of Treg cells (Walters et al., 2009).

Taken together, these results point out to an essential role of BAFF cytokine in the immune defense of lungs and raise important concerns regarding the prospects of lung infection in patients treated with Belimumab[®] or any other antibody that decreases the levels of BAFF. On the other hand, this study corroborates the previous findings which suggest that the incorporation of BAFF as an adjuvant into vaccines could boost pathogen-specific antibody titers. Indeed, it was shown that co-administration of BAFF with the T-cell independent vaccine Pneumovax23 resulted in significantly higher IgM and IgA titers, while both IgM and IgG were boosted against T-cell independent antigens (Do et al., 2000). Additionally, co-administration of BAFF with heat-killed *Pseudomonas aeruginosa* significantly improves pathogen-specific immune response (Tertilt et al., 2009).

In conclusion, BAFF is an important cytokine for the production of mature B-cells in all Vertebrates. The presence of BAFF in the lungs is essential for the host defense against any invading pathogen. The application of BAFF cytokine for the production of more efficient vaccines is an area with a great translational potential yet to be explored.

This subchapter was adapted from a recently published review article Garić D, De Sanctis JB, Shah J, Dumut DC, Radzioch D. *Biochemistry of very-long-chain and long-chain ceramides in cystic fibrosis and other diseases: The importance of side chain*. Prog Lipid Res. 2019 Mar 12. pii: S0163-7827(19)30011-6. doi: 10.1016/j.plipres.2019.03.001.

1.3 Ceramides

1.3.1 Metabolism of sphingolipids

In the late 19th century, JWL Tudichum was the first to recognize the enigmatic nature of a brain lipid that he isolated and named it “sphingosine” after the Sphinx, a creature from Greek mythology that devoured all the passengers who could not answer the riddle it was posing to them (Thudichum, 1884). Indeed, sphingosine, an amino-alcohol of 18 carbons, and its relatives known as sphingolipids continue to present an enigma to all of us studying them to this day. Biochemical steps in the synthesis of sphingolipids, including its salvage pathways, are illustrated in the **Figure 1.3.1**, whereas **Figure 1.3.2** depicts subcellular localization of the enzymes involved in their metabolism.

The sphingosine backbone, in all sphingolipids, is initially produced in the form of 3-ketosphinganine from palmitic acid and serine which are coupled by the enzymes called serine palmitoyltransferases (Sptlc1 and Sptlc2) in the smooth endoplasmic reticulum. As depicted in the **Figure 1.3.1**, in the next step, 3-ketosphinganine is reduced by 3-ketosphinganine reductase (Kdsr) to sphinganine. Sphinganine is then acylated by one of the six ceramide synthases (Cers1-6) in vertebrates, each of which uses fatty acid of the specific length as the substrate, giving rise to dihydroceramides with side chains of different lengths. Even though ceramide synthases directly produce dihydroceramides and not ceramides in the *de novo* pathway, their name as such became common and in this review we will retain this nomenclature.

The length of the acyl chain of the fatty acids used by ceramide synthases in this reaction usually ranges from 14 to 26 carbons and the specificity towards the acyl-chains is determined by a short 11-residue sequence located in an intraluminal loop of each enzyme (Tidhar et al., 2018). Therefore, the length of the side chain of all sphingolipids is determined at this step by a relative tissue-specific composition of ceramide synthases (see below) and the relative affinity of the dimers formed by the ceramide synthases (Mullen et al., 2012). Depending on the length of their

acyl side chain, all ceramides can be grouped as long-chain (C14:0-C20:0), very –long-chain ceramides (C22:0-C26:0) and ultra-long-chain ceramides (more than 26 carbons) (Grosch et al., 2012; Jennemann et al., 2012). Therefore, ceramide is not a single species but should be considered a family of closely related but distinct molecules with emerging distinct functions (Hannun and Obeid, 2011).

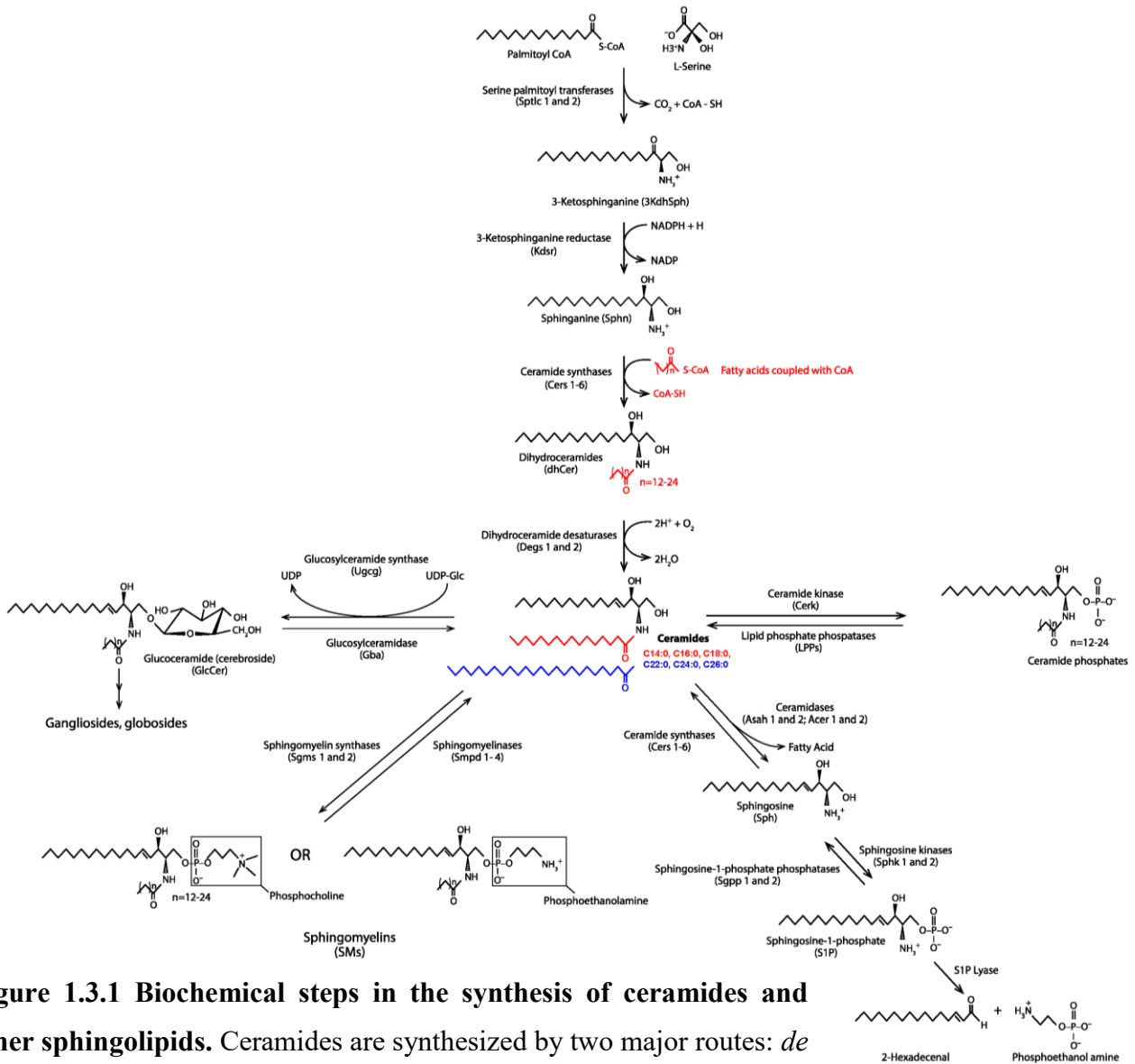


Figure 1.3.1 Biochemical steps in the synthesis of ceramides and other sphingolipids. Ceramides are synthesized by two major routes: *de novo*, from palmitoyl-CoA and L-serine, and in different salvage pathways that are used to recycle complex sphingolipids like cerebroside, sphingomyelins or phosphorylated ceramides. The length of the main chain is constant and is determined during *de novo* synthesis of the ceramide backbone. However, the length of the side chain varies and is determined by the expression of particular types of ceramide synthases in the cell.

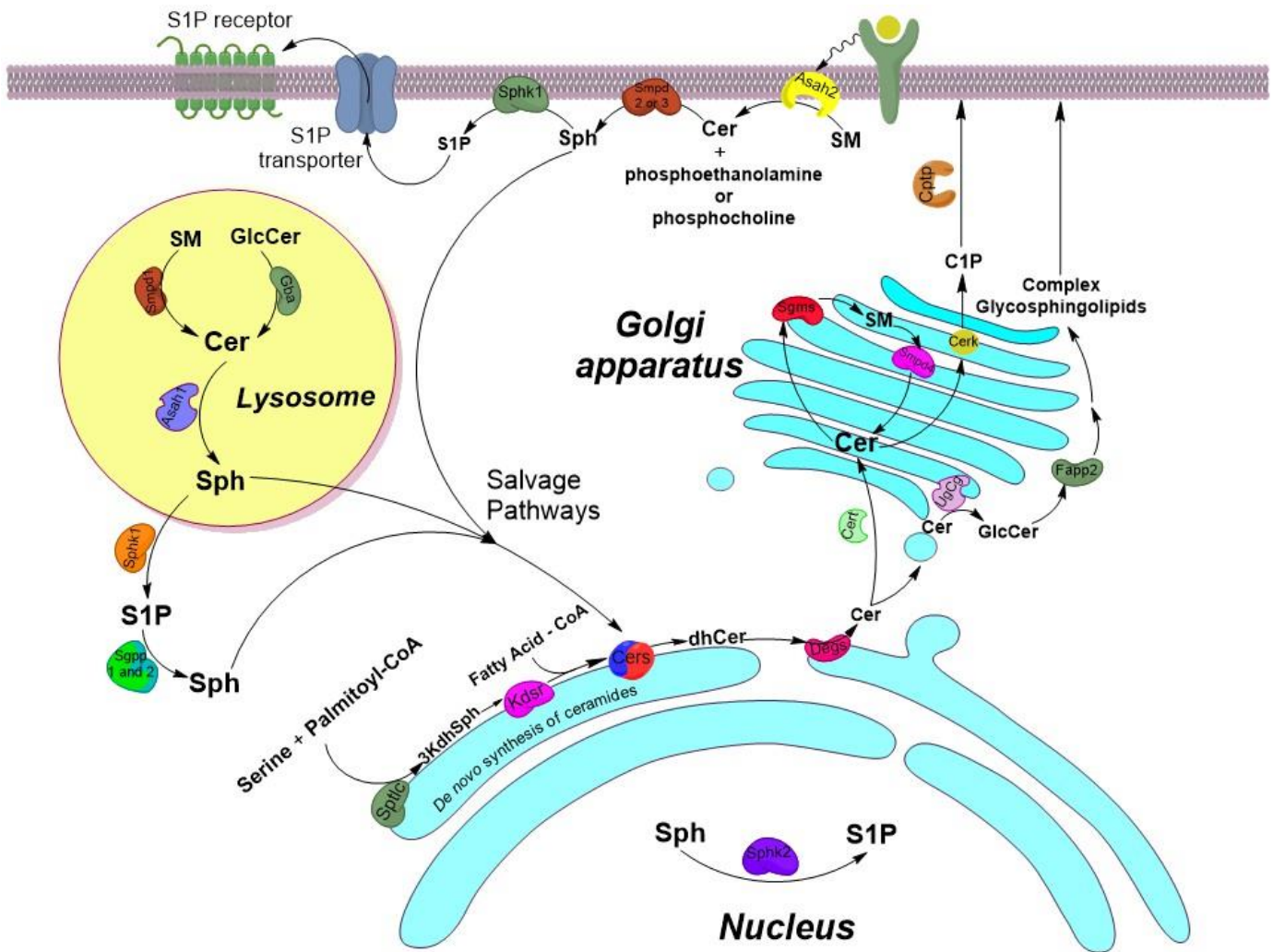


Figure 1.3.2 Subcellular localization of the enzymes involved in the metabolism of sphingolipids. *De novo* synthesis of ceramides is always initiated in the membrane of a smooth endoplasmic reticulum. Ceramides are transported to Golgi apparatus where the synthesis of sphingomyelins and cerebroside (glycosphingolipids) takes place. These complex sphingolipids are subsequently transported to the cell membrane where they exert their functions. Degradation of complex sphingolipids takes place mostly in the lysosomes but also in the plasma membrane. Molecules arising from these catabolic reactions (sphinganine and fatty acids) may be reused through one of salvage pathways for the synthesis of ceramides. (3KdhSph-3-ketosphinganine; Cer-ceramides; dhCer-dihydroceramides; GlcCer-Glucoceramides/Cerebrosides; C1P-ceramide 1-phosphate; SM-Sphingomyelin; S1P-Sphingosine 1-phosphate; Sph-Sphingosine)

Importantly, ceramide synthases can use either sphinganine and sphingosine as a substrate, and thus they are involved both in the *de novo* synthesis and salvage pathways. Dihydroceramides produced by ceramide synthases are further dehydrogenated to ceramides by one of the two desaturases located in ER (Degs1 and Degs2).

Ceramides are named after the Latin word for wax (*cerum*) because they have a waxy consistency and an amide bond which is not present in other lipids. They are the key intermediates in the metabolism of all sphingolipids, since the ceramide skeleton is present in all of them, and they can be mutually converted from one another by being reduced to corresponding ceramides and additional moieties.

Ceramides are transported from the smooth endoplasmic reticulum to the Golgi apparatus by the ceramide transfer protein (Cert) for the purpose of sphingomyelin synthesis or by vesicular transport for glucosylceramide synthesis (Maceyka and Spiegel, 2014). Sphingomyelins are synthesized in the Golgi by the action of sphingomyelin synthases (Sgms1 and Sgms2) which transfer phosphatidylcholine onto the primary hydroxyl group of ceramides. The reverse reactions are carried out by one of the four sphingomyelinases. Acidic sphingomyelinase (Smpd1/aSMase) is located mainly in the lysosomes. The neutral sphingomyelinases are localized either in the plasma membrane, Golgi or perinuclear ER. Specifically, Smpd2/nSMaseI is located mainly in the plasma membrane, Smpd3/nSMaseII is located in the plasma membrane and Golgi, and Smpd4/nSMaseIII is located in the perinuclear endoplasmic reticulum (**Figure 1.3.2**).

Metabolism of the vast array of complex glycosphingolipids (cerebrosides, globosides and gangliosides) starts with the transfer of glucose to ceramides catalyzed by glucosylceramide synthase (Ugcg, located in Golgi) and reversed by glucosylceramidase (Gba and Gba2 located in lysosomes and Golgi, respectively). Four-phosphate adaptor protein (Fapp2) transports simple glucosylceramides to the trans-Golgi for the biosynthesis of complex glycosphingolipids.

Ceramides can also be phosphorylated in the Golgi at the OH group originating from serine by ceramide kinase (Cerk) to form ceramide-1-phosphate (C1P), a rare species which is transported to the cell membrane by C1P transport protein (Ctp). Phosphorylation by Cerk can be reversed by some of the Lipid Phosphate Phosphatases (LPPs) (Tang et al., 2015).

Finally, ceramides may be degraded by one of the ceramidases (Asah1, Asah2, Acer1, Acer2) to sphingosine which may serve as the substrate for ceramide synthases in the reverse reaction. Alternatively, it can be phosphorylated into a potent signaling molecule sphingosine-1-phosphate (reviewed extensively elsewhere) (Maceyka and Spiegel, 2014) through the action of sphingosine kinases (Sphk1 and Sphk2). Sphk1 is located mainly in the plasma membrane and it gets activated by extracellular stimuli, whereas Sphk2 is located in the nucleus and produces S1P which inhibits histone deacetylases (Hait et al., 2009). S1P may be degraded through action of S1P lyase to 2-hexadecenal and phosphoethanolamine and this marks an irreversible exit of this metabolite from sphingolipid metabolism.

Therefore, all sphingolipids, whether they are sphingomyelins, cerebroside, gangliosides or globosides contain a **ceramide backbone** as their intramembranous component which consists of a sphingosine linked through an amide bond to an acyl chains of various lengths (**Figure 1.3.1**).

1.3.2 Metabolic actions of ceramides

Ceramides have long been known to be ubiquitous building blocks of eukaryotic cell membranes and signaling molecules produced mostly upon various exogenous stimuli like inflammation or stress. Therefore, the roles of ceramides in the cell can be viewed as **structural** components of the cellular membranes and as **metabolic/bioactive**, as the signaling molecules produced upon various stimuli.

Despite their involvement in numerous biological processes, remarkably little mechanistic insight has been gained so far into the function of specific ceramides as signaling molecules. The reason for this is that naturally occurring long-chain and very-long chain ceramides are not water-soluble and it is very difficult to insert them exogenously into a phospholipid bilayer. In the early studies, synthetic short-chain ceramides (particularly C2:0, C6:0 and C8:0), which are water soluble (form micelles) were widely used as experimental tools. However, it became clear that the use of these exogenous short-chain ceramides as a tool to study the role of endogenous ceramides is not justified because they have completely different partitioning and behavior in biomembranes, and unlike natural ceramides they can easily translocate to the cytosol (van

Blitterswijk et al., 2003). Hence, there are only a few firmly established examples of the interaction between endogenous ceramides and their target proteins (**Figure 1.3.3**).

One of the first discovered proteins interacting with ceramide in a manner that depends on the length of the side chain was the ceramide transporter (Cert) (**Figure 1.3.2**). Cert is a cytosolic protein shown to transfer long-chain (C14, C16:0, C18:0 and C20:0) but not very-long chain ceramides, from the smooth ER to Golgi (Kumagai et al., 2005). Therefore, it remains unknown how VLCCs get transported from the place of their synthesis (ER) to the plasma membrane.

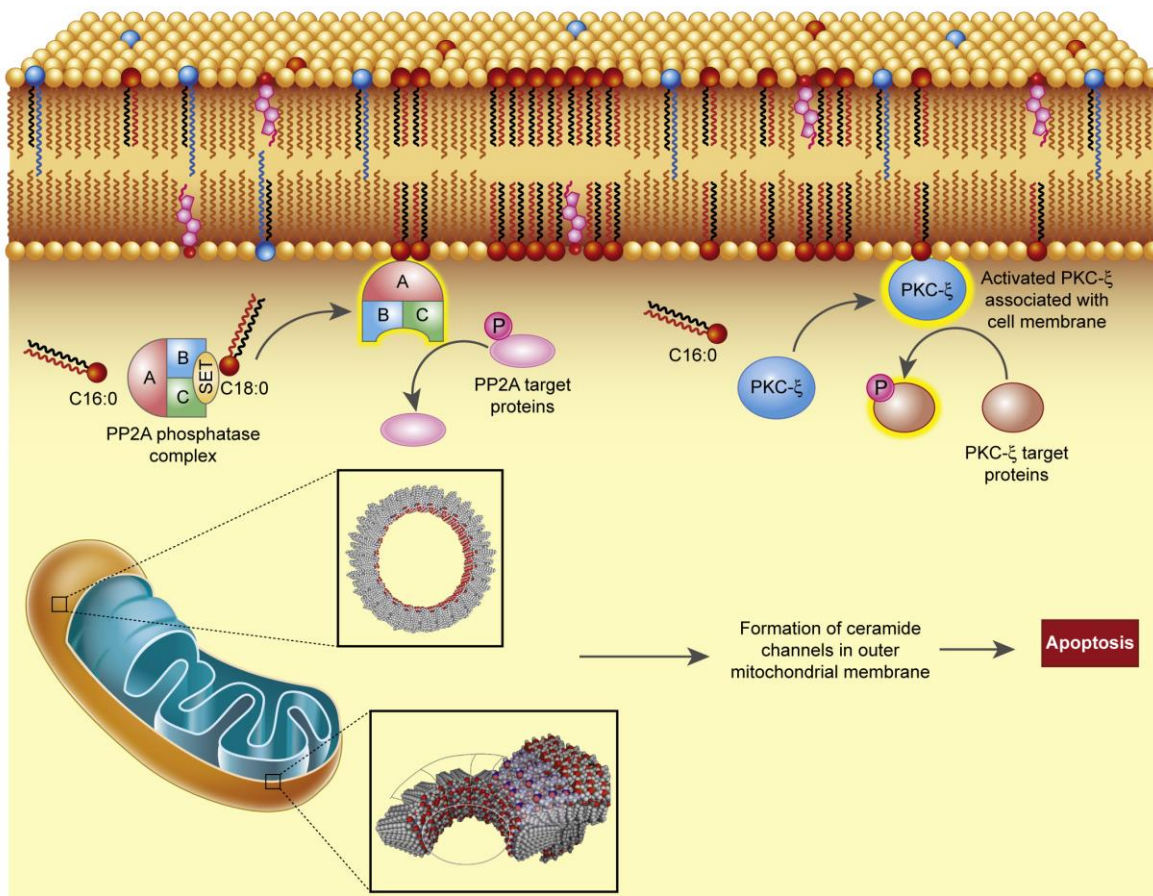


Figure 1.3.3 Metabolic actions of endogenous ceramides There are very few studies describing the interaction between endogenous ceramides and their target proteins. Long-chain ceramides (C16:0 and C18:0) indirectly activate protein phosphatase 2A (PP2A) by binding to its inhibitor I2PP2A (Inhibitor-2 of PP2A) or SET (S(var)3-9, Enhancer-of-zeste and Trithorax), thereby relieving its inhibitory action on PP2A. PP2A enzymes are composed of A, B and C subunits which have different isoforms and can assemble in an array of combinatorial associations each controlling different cell functions.
continued...

...continued. Binding of C16:0 ceramide to PKC- ζ leads to its activation and association with the inner leaflet of cell membrane. Long-chain ceramides (e.g C16:0) form large transmembrane channels in the outer mitochondrial membrane that may lead to permeabilization, release of cytochrome c and initiation of apoptosis. Very-long-chain ceramides may counteract formation of pores by long-chain ceramides. Phosphoglycerides (yellow patterns), Long-chain ceramides (red/black patterns), Very-long-chain ceramides (blue/black patterns), cholesterol (red/pink patterns). See further **Figure 1.3.7**

Next, it was shown that ceramides indirectly activate PP2A phosphatase by binding to its inhibitor which is called either I2PP2A (Inhibitor-2 of PP2A) or SET (S(var)3-9, Enhancer-of-zeste and TriThorax) and thereby relieving its inhibitory action on PP2A (Mukhopadhyay et al., 2009; Saddoughi et al., 2013) (**Figure 1.3.3**). This interaction seems to be dependent on the length of the side chain as it was subsequently shown that C18:0 binds to I2PP2A/SET protein with a higher affinity than C16:0 but only a minute binding of C24:0 was demonstrated (Saddoughi et al., 2013). The protein phosphatase 2A (PP2A) is one of the major Ser/Thr phosphatases that counteract the action of Ser/Thr kinases and they are implicated in a plethora of cellular functions including regulation of many signaling pathways, cell cycle progression, apoptosis, DNA replication, gene transcription, and protein translation. PP2A enzymes are oligomeric enzymes composed of a conserved catalytic (C) subunits (two isoforms), scaffolding(A) subunit (two isoforms), and one large array of B subunits (over 15 in mammalian genomes). A huge diversity of biochemically distinct PP2A complexes can be assembled in cells due to combinatorial association of these three types of subunits (Shi, 2009). Therefore, indirect activation of PP2A complexes by ceramides can have profound consequences on fundamental cellular processes. C16:0 ceramide binds directly to PP2A phosphatase, however it remains uncertain to which subunit it binds, and subsequently acts as an allosteric activator (Grosch et al., 2012). Binding of C18:0 ceramide to I2PP2A/SET inhibitor reduces its interaction with PP2A and therefore indirectly activates PP2A (Grosch et al., 2012).

Initially, synthetic ceramide C6:0 was shown to activate PKC- ζ (Bourbon et al., 2000) but subsequently long-chain ceramide C16:0 was found to bind PKC- ζ directly as well (Wang et al., 2009). Protein phosphatase 1 (PP1) seems to be activated by intramembraneous ceramides but the importance of chain length was not examined in this study (Canals et al., 2012).

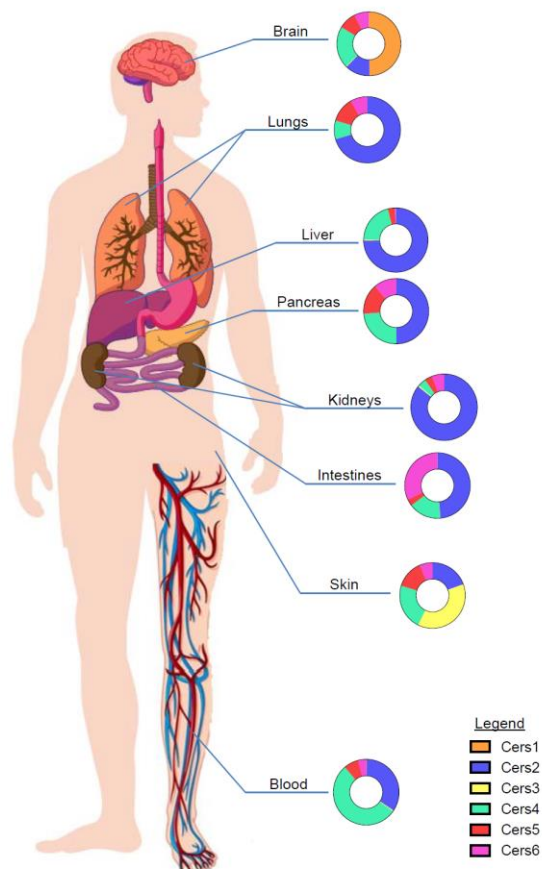
All of these biochemical studies examined the effect of artificial short ceramides or long-chain ceramides on cellular targets, however as of 2018, direct intracellular targets of very-long-chain ceramide (C22:0-C26:0) remain unknown. Clearly, interaction of cellular proteins with specific endogenous ceramides may lead to their localized activation near cell membrane (**Figure 1.3.3**).

The ability of synthetic short-chain ceramides (C2:0, C6:0 and C8:0) to induce apoptosis was known for a long time (Escargueil-Blanc et al., 1998; Martin et al., 1995) and an association between increased level of C16:0 ceramides and apoptosis was found in Jurkat cells following exposure to ionizing radiation (Thomas et al., 1999) as well. Since then many other investigators observed increased level of C16:0 under different pro-apoptotic conditions (Eto et al., 2003; Kroesen et al., 2001; Osawa et al., 2005; Schiffmann et al., 2010). The exact protein targets involved in apoptosis that may be affected by specific ceramides remain uncertain. However, C16:0 ceramide is able to form large transmembrane channels in the outer mitochondrial membrane (Siskind et al., 2002) that may eventually lead to the permeabilization of the outer mitochondrial membrane, release cytochrome c, and initiation of apoptosis (Chang et al., 2015) (**Figure 1.3.3**). Interestingly, it seems that VLCCs interfere with the formation of this channel (Stiban and Perera, 2015), therefore, potentially inhibiting apoptosis. In addition to the differences regarding their structural role in the regulation of cellular membrane fluidity discussed below, these results provided mechanistic insight in the earlier observation that the long-chain ceramides have opposite effects from the very-long-chain ceramides on the proliferation of cells *in vitro* (Hartmann et al., 2012; Sassa et al., 2012).

Due to inherent difficulties in working with endogenous ceramides in cell culture, the biochemical characterization of their cellular functions, especially with regards to the length of their side chain, had to await development of genetic knockout models for ceramide synthases. Even though interpretation of the results generated using KO mice for specific ceramide synthases is challenging because of tissue-specific expression of these enzymes shows significant overlap (**Figure 1.3.4**) and because these enzymes form dimers which are responsible for production of specific ceramide species (Laviad et al., 2012), physiological roles of certain ceramide species has been uncovered based on the analysis of the phenotypes of KO mice for specific ceramide synthases.

Two strains of mice, flincher (fln) and toppler (to) spontaneously arose at the Jackson Laboratories. Both mutations caused a complete loss of Cers1 activity that was accompanied by dramatic changes in the levels of sphingolipids (Zhao et al., 2011). In the brain of fln mice, total ceramide levels decreased, mainly because of a decrease in C18:0 and C18:1 ceramides. The levels of C14:0 and C16:0 increased whereas C20:0, C22:0 and C24:0 were unaltered. Flincher and toppler mice developed cerebellar ataxia with concomitant degeneration of cerebellar Purkinje cells. Accordingly, mice with targeted disruption of Cers1 gene, had profound defects in cerebellum which was associated with a decrease in major brain gangliosides (GM1, GD1a, GD1b, and GT1b) (Ginkel et al., 2012). These results highlight the importance of C18:0 ceramide in the normal function of the cerebellum.

Figure 1.3.4 Tissue-specific distribution of ceramide synthases Ceramides synthases (Cers) are the central enzymes in the metabolism of ceramides. Their relative abundance in each organ or tissue determines the amount of specific ceramide class that is produced. Pie chart for each organ represents the distribution of Cers-es, which are color-coded as in the Legend. The data is based on the (references (Laviad et al., 2012; Petrache et al., 2013) and GXA database)



Cers3 knockout mice die shortly after birth from transepithelial water loss, and the synthesis of ultra-long-chain ceramides is completely abrogated in these mice (Jennemann et al., 2012). A missense mutation that inactivates Cers3 has been identified in human congenital ichthyosis that results in the loss of ultra-long-chain ceramides and generalized scaling of the skin in affected

patients (Eckl et al., 2013), and Cers3 appears essential for spermatogenesis as well (Rabionet et al., 2015).

Cers4 knockout mice show progressive loss of hair (alopecia) starting at 7 weeks of age and a strong decrease of Cers4-produced ceramides (C18:0 and C20:0) in the skin, whereas C16:0 was not affected and C24:0 was only slightly upregulated (Ebel et al., 2014).

Cers5 is one of the two predominant forms of ceramide synthases in the lungs, the other one being ubiquitously expressed Cers2. Cers5 dimerizes with Cers2 and these heterodimers produce very-long-chain ceramides, whereas Cers5 homodimers produce long-chain ceramides (Laviad et al., 2012). Cers5 KO mice are viable, fertile and do not show any obvious morphological alterations. However, Cers5 deficiency leads to a specific reduction of C16:0 ceramide levels in the lungs, spleen, muscle, liver, as well as in the white adipose tissue, and is associated with reduced inflammation of adipose tissue after challenge with high fat diet (Gosejacob et al., 2016).

Deletion of Cers6 in mice leads to the reduction of C16:0 levels in the kidneys and small intestine. These mice display clasping abnormality of their hind limbs and a habituation deficit (Ebel et al., 2013). Similarly to Cers5 knockout mice, Cers6 knockout mice are protected from obesity when fed high-fat-diet and have reduced inflammation of adipose tissue after being challenge with a high fat diet (Turpin et al., 2014).

Finally, Cers2 is the most ubiquitously and most abundantly expressed form among all ceramide synthases (**Figure 1.3.4**). Therefore, it is not surprising that Cers2 KO mice display the most profound range of phenotypes compared to KO models of all other Cers-es. Cers2 KO mice were generated independently in the laboratories of Klaus Willecke and Anthony Futerman and both Cers2KO mouse models display almost identical phenotypes. As expected, these mice exhibit strongly reduced levels of VLCCs, particularly C24:0, in the liver (Imgrund et al., 2009; Pewzner-Jung et al., 2010b), brain (Imgrund et al., 2009), kidneys (Ebel et al., 2014) and lungs (Petrache et al., 2013) while at the same time they exhibit strong increase in the levels of LCCs, particularly C16:0 in the liver (Imgrund et al., 2009; Pewzner-Jung et al., 2010a), kidneys (Imgrund et al., 2009; Pewzner-Jung et al., 2010a) and lungs (Petrache et al., 2013). Consequently, the total amount of ceramides is not different between Cers2 KO and WT animals

(Petrache et al., 2013; Pewzner-Jung et al., 2010b). This imbalance of LCC and VLCC species can be explained by the fact that Cers2:Cers2 homodimers have only weak catalytic activity, Cers2:Cers5 and Cers2:Cers6 heterodimers synthesize VLCCs whereas Cers5:Cers5 and Cers6:Cers6 homodimers synthesize LCCs (Laviad et al., 2012).

Starting from the early adulthood, Cers2 KO mice show progressive loss of myelin and starting around 9 months of age, both the medullary tree and the internal granular layer of the cerebellum show signs of degeneration (Imgrund et al., 2009). In older mice progressive hepatomegaly is initially seen (around 4th month) followed by the development of the aggressive hepatocellular carcinoma (7-10th month) (Imgrund et al., 2009; Pewzner-Jung et al., 2010a). Interestingly, even though the kidneys show as high levels of Cers2 mRNA expression as the liver, and display similar changes in the levels of ceramides as seen in the kidneys of Cers2 KO animals, there were no pathological abnormalities seen in the kidneys of Cers2 KO mice (Pewzner-Jung et al., 2010a). These results emphasize the different role of VLCCs in the homeostasis of brain and liver compared to kidneys.

Finally, a Cers2 KO mouse exhibits strong pro-inflammatory changes in their lungs. As in the liver of Cers2 KO mice (Pewzner-Jung et al., 2010a), the levels of C24:0 and C24:1 are greatly reduced, accompanied by a 10-fold increase in the levels of C16:0, but the total level of ceramides remains unaltered when compared with wild-type animals (Petrache et al., 2013). Lungs from adult Cers2 KO mice (3 months or older) display patchy areas of perivascular inflammation, increased inflammatory cell content, and strongly increased airflow resistance (Petrache et al., 2013). The changes seen in Cers2 KO mice in the relative ratio between VLCCs (C24:0, C24:1, C26:0) and LCCs (C14:0, C16:0) are strongly reminiscent of the pro-inflammatory phenotype previously seen in CFTR knockout mice (CFTR-KO) (Kent et al., 1997) and will be discussed in more details below. Interestingly, the inflammatory response triggered in the lungs of Cers2 KO mice is not protective, and in fact Cers2 KO mice are much more susceptible to bacterial infection than their littermate wild-type controls (Pewzner-Jung et al., 2014), similarly as we observed in the CFTR-KO mice compared to their littermate wild-type controls (Guilbault et al., 2005; Guilbault et al., 2009). Finally, it is important to emphasize that Cers-es are evolutionary extremely well conserved proteins, present in all eukaryotic cells. While the sequence homology between animal and fungal enzymes is clear, *Arabidopsis* has three

proteins (LOH 1, 2 and 3) with Cers activity whose homology to animal enzymes is not obvious from sequence comparisons (Voelzmann and Bauer, 2010). All fungal and animal Cers-es have a conserved Lag1p motif (longevity assurance gene 1) named after yeast mutants, which is essential for the synthesis of ceramides. Lag1p motif is located within a TLC domain named after the three protein families in which it was originally found (Tram, Lag and CLN8)(Winter and Ponting, 2002). All vertebrate and insect Cers orthologues, with a notable exception of Cers1, contain a homeodomain derived from homeobox proteins, sequence-specific transcription factors important in development. However, the first 15 amino acids of this domain are missing in ceramide synthases of vertebrates, as is the key residue (N51) involved in DNA binding(Levy and Futerman, 2010). Therefore, it is highly unlikely that vertebrate Cers-es function like genuine transcription factors, but the homeodomain of Cers5 and Cers6 is essential for their Cers activity(Mesika et al., 2007). Surprisingly however, the only Cers in *Drosophila* known as Schlank can bind DNA through its homeodomain and directly regulate transcription of the genes involved in fat metabolism (Sociale et al., 2018). In this case, Schlank acts as a sensor of fatty acids level and transcriptional repressor of lip3 (lipase 3) gene (Sociale et al., 2018).

1.3.3 Ceramides as structural elements of biological membranes

The mechanistic basis and the biochemical pathways behind the phenotypes seen in the ceramide synthases knockout mice have not been fully explored yet. Part of the answer to these questions seems to lie in the structural role of ceramides as the fundamental building blocks of all eukaryotic cell membranes.

Ceramides form the intramembraneous backbone of all sphingolipids, including sphingomyelins. Sphingomyelins consist of phosphocholine or phosphoethanolamine bound to a ceramide backbone through an OH group of a given ceramide species that resides in the cell membranes with its two aliphatic chains (**Figure 1.3.1**).

The original “Fluid Mosaic” model of cell membrane initially proposed by Singer and Nicholson in 1972 predicted totally free lateral diffusion of both lipids and proteins (Singer and Nicholson, 1972). However, by late seventies, it became clear that “lipid clusters” may be a common feature of biological membranes. Cholesterol and sphingolipids were found to belong to one type of a lipid cluster already decades ago (Demel et al., 1977; Estep et al., 1979). Even though the

concept of “lipid domains” in biological membranes was formalized already in 1982 (Karnovsky et al., 1982), it was not until 1997 that the interest in these “microdomains” exploded when Kai Simons introduced the concept of “lipid rafts”(Simons and Ikonen, 1997). Lipid rafts are defined as cholesterol- and sphingolipids-rich liquid ordered state platforms (microdomains) that float in a liquid disordered matrix (the rest of cell membrane). The acyl chains of lipid rafts are more saturated than the acyl chains of the surrounding membrane matrix, and so they pack more tightly, producing a liquid ordered state. It is believed that the cholesterol acts like a “glue” that holds together the lipid rafts because it has very high affinity for sphingolipids. Indeed, the level of cholesterol in the lipid rafts is about twice as high than in non-raft portions of the membrane. The concentration of sphingomyelin in the lipid rafts is about 50% higher than in non-raft portions of the membrane. As a result of tight packing, the portions of the membrane that contain lipid rafts are thicker than the surrounding, more loosely packed sections of the membrane, and so the lipid rafts protrude above the membrane surface.

An original hallmark of lipid rafts is their ability to be isolated from the remaining membrane portions by extraction in cold (4°C) nonionic detergents (like Triton-X or Brij-98) (Schuck et al., 2003). Under these conditions, lipid rafts are insoluble whereas the remaining portions of the cell membrane are dissolved. Due to this property they are also referred to as “Detergent Resistant Membranes (DRMs). Lipid rafts are believed to cover small areas (10-200 nm) but they are highly dynamic and their size may be affected by various biochemical processes that affect the composition of cellular sphingolipids and cholesterol. Therefore, any domain of the plasma membrane isolated in this way and has these biochemical constituents, can be defined as a *bona fide* lipid raft.

Currently, two basic types of lipid rafts can be distinguished: **planar lipid rafts** (also known as non-caveolar or glycolipid rafts) and **caveolae** (Staubach and Hanisch, 2011) (**Figure 1.3.5**). Planar rafts are continuous with the surface of the cell membrane and protrude above while caveolae are flask-shaped invaginations. Each of these rafts is distinguished by the presence of the characteristic proteins: flotillins in the planar lipid rafts and caveolins in caveolae (**Figure 1.3.5**). It is believed that the function of these proteins is to recruit signaling molecules from the cytosol and organize the initial events of the signal transduction pathways that emanate from the plasma membrane.

While the existence of lipid rafts is not disputed anymore, the role of lipid rafts in the regulation of expression and stability of membrane and transmembrane proteins remains a mystery. Lipid rafts are clearly involved in the organization of multiple signal transduction pathways that start at the level of cell membrane. These pathways include, but are not limited to, activation of PI3K and Akt kinases which is important for growth and survival, clustering of Fas/CD95 proapoptotic receptors, and the activation of erythropoietin and TCR receptors. The role of lipid rafts in signal transduction has been extensively reviewed elsewhere (Mollinedo and Gajate, 2015; Simons and Toomre, 2000; Varshney et al., 2016) and will not be further discussed here.

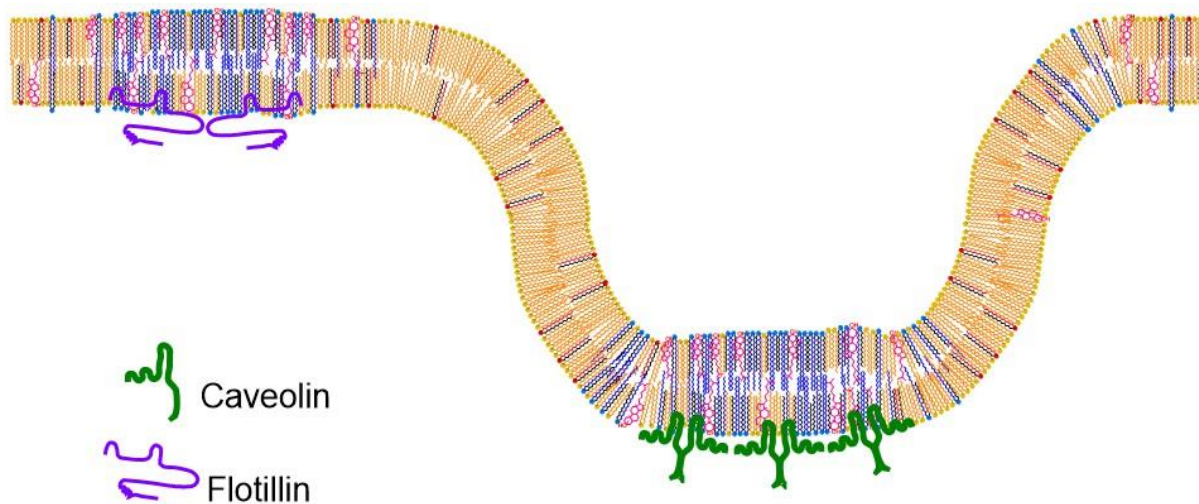


Figure 1.3.5 Planar lipid rafts and caveolae. Planar lipid rafts are continuous with the surface of the cell membrane, under normal conditions they protrude from the cell membrane and are characterized by the presence of proteins called flotillins. Caveolae are flask-shaped invaginations distinguished by the presence of proteins called caveolins. The function of both flotillins and caveolins is to attract and retain signaling molecules into lipid rafts. Phosphoglycerides (yellow patterns), Long-chain ceramides (red/black patterns), Very-long-chain ceramides (blue/black patterns), cholesterol (red/pink patterns)

Lipid rafts are built of sphingolipids and cholesterol, however, the composition and ratios of specific ceramides that serve as building blocks of sphingolipids within lipid rafts have never been firmly established. It is likely that the abundance of ceramide species which is tissue-specific also determines their abundance in lipid rafts in the cells in the specific organs. For

example, C24:0 ceramides represents about 72% of total ceramides whereas C16:0 only 18% in the cells of healthy mouse lungs.

The group of Kateřina Vávrová established important biophysical differences between C16:0 and C24:0 ceramides that could confer fairly different behaviour to these ceramide species within the lipid rafts. Using infrared spectroscopy and artificial lipid bilayers, they showed markedly different phase behaviour of C16:0 ceramides compared to C24:0 ceramides, which was found to be due to the less ordered side chain of C16:0 (Skolova et al., 2014). Subsequently these authors demonstrated that the membranes containing C16:0 were significantly more permeable to water and some organic molecules than the membranes containing C24:0 ceramides. Also, the membrane monolayers containing C16:0 ceramides were shown to be less condensed than monolayers formed by C24:0 ceramides (Pullmannova et al., 2017). Therefore, these biophysical differences between C16:0 and C24:0 ceramides explain the differences seen in the membranes of *Cers2* KO mice compared to their wild-type counterparts: Microsomal vesicles prepared from *Cers2*-KO mice have distorted membranes of much higher fluidity than vesicles prepared from wild-type animals (Silva et al., 2012). These vesicles also display morphological changes that include areas of different curvature in the same vesicle and tubule-like structures emerging from a single vesicle, as opposed to the vesicles derived from wild-type animals which were of perfectly spherical shape (Silva et al., 2012) (**Figure 1.3.6**).

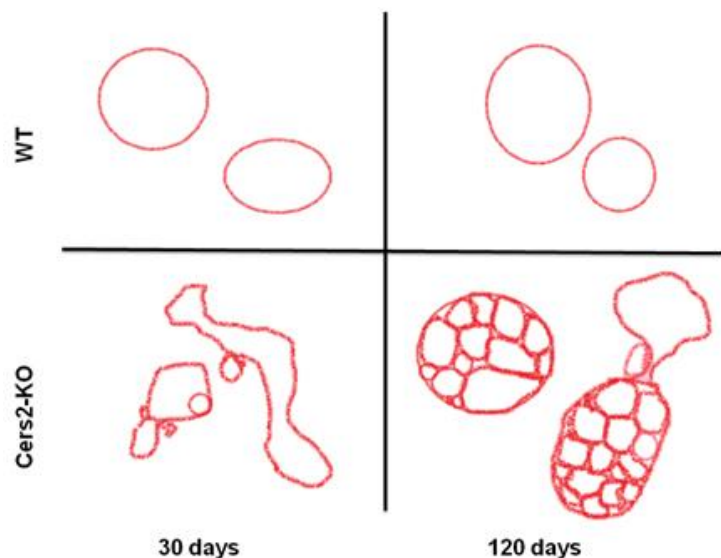
Figure 1.3.6 Effect of CerS2 ablation

on the membrane morphology of microsomal vesicles

Depiction of the giant microsomal vesicles labeled with Rho dye (1,2-Dioleoyl-sn-Glycero-3-Phosphoethanolamine-N-

(Lissamine Rhodamine B Sulfonyl) and imaged by confocal microscopy (based on the work of (Laviad et al., 2012; Silva et al., 2012)).

Microsomal vesicles were prepared from the livers of wild-type (upper panels) and *CerS2* null (lower panels) mice of different ages.



Since total glycerophospholipid and cholesterol levels were unaltered in *Cers2* KO mice compared with their wild-type littermates (Pewzner-Jung et al., 2010b), these biophysical differences in the membranes derived from *Cers2* KO mice must be due to the changes in their sphingolipids composition, i.e. increase in ceramide C16:0.

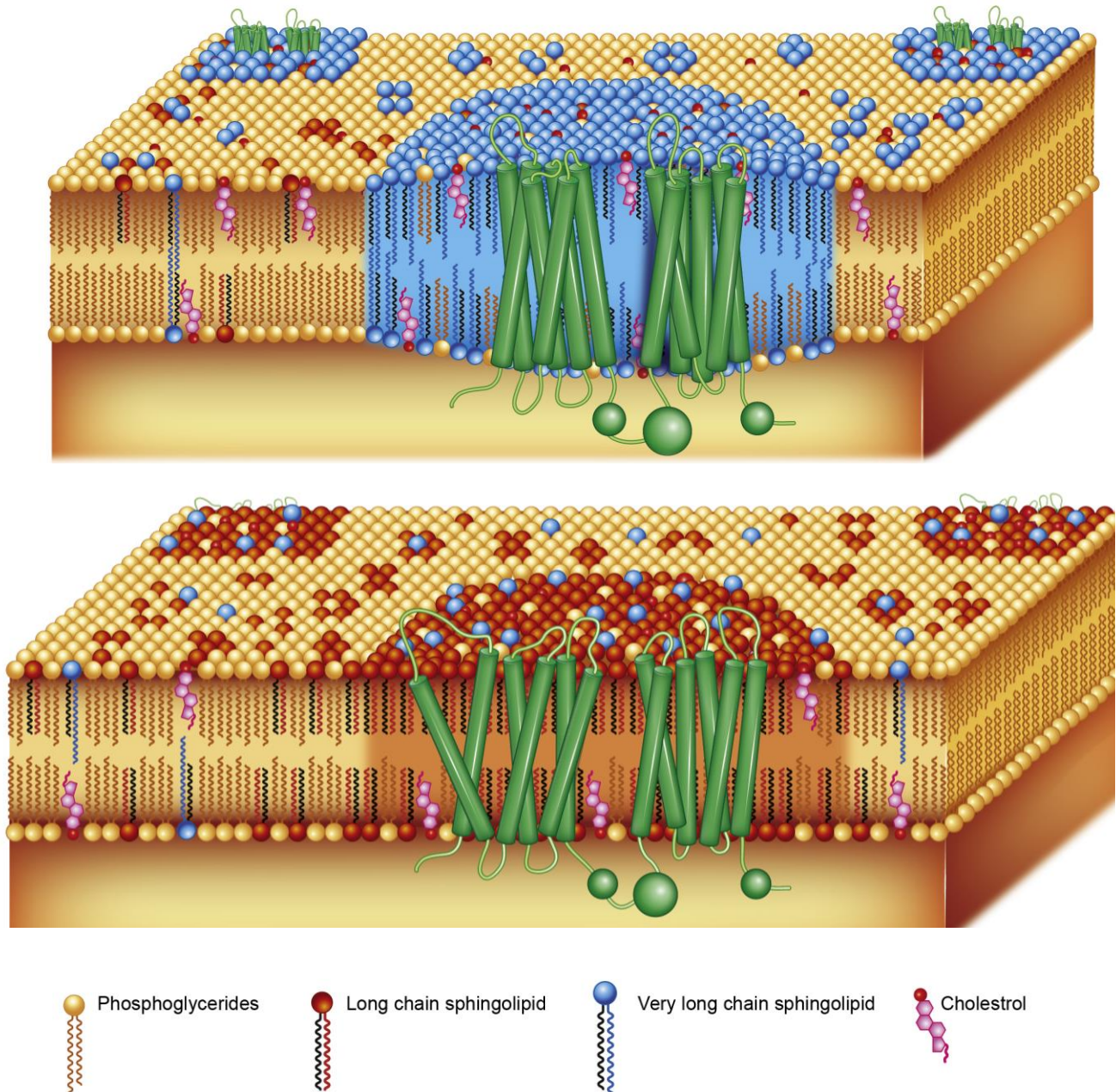


Figure 1.3.7. Structures of lipid rafts under normal and pathological conditions Under normal conditions (A), when VLCCs are more abundant than LCCs, tight packing of VLCCs whose acyl chain interdigitate from both leaflets of the cell membrane forms a gel-like environment in the lipid rafts that may stabilize the folding of large transmembrane proteins (green), like CFTR. *continued...*

continued... On the other hand, in the membranes of cells from Cers2-KO mice or cells from patients with CF (**B**), where LCCs are more abundant than VLCCs, lipid rafts are more fluid, because their side chain do not interdigitate from the two leaflets of the cell membrane, and under these conditions the folding of large transmembrane proteins (green), like CFTR, may be compromised. Phosphoglycerides (yellow patterns), Long-chain ceramides (red/black patterns), Very-long-chain ceramides (blue/black patterns), cholesterol (red/pink patterns).

Based on these findings, it is very likely that under normal conditions, when VLCCs are more abundant than LCCs in cellular membranes, tight packing of C24:0 ceramides whose acyl and sphingosine chains interdigitate from both sides of the cell membrane, forms a gel-like environment of much lesser fluidity than in the membranes enriched in C16:0 ceramides (Niemela et al., 2006). Overall, a tightly packed lipid environment created by VLCCs, including C24:0 is likely to stabilize large, intrinsically disordered transmembrane proteins, such as CFTR (**Figure 1.3.7 A**).

On the other hand, sphingomyelins formed from C16:0 ceramide may act disruptively in the formation of lipid rafts as opposed to their more ordered and less permeable structures formed primarily from C24:0, and the folding of large transmembrane proteins, like CFTR situated in the lipid rafts enriched in LCCs, can be compromised (**Figure 1.3.7 B**).

Indeed, the differences between intramembraneous environments created by C16:0 and C24:0 ceramides are fully supported by the recent molecular dynamics simulations (Moore et al., 2018).

Finally, some authors proposed making a distinction between sphingomyelin-enriched and ceramide-enriched lipid rafts (Ziobro et al., 2013). However, these two types of sphingolipids are mutually convertible from each other in the cell membrane by the actions of sphingomyelinases and sphingomyelin synthases, and since both types of rafts fall under the original definition of a *bona fide* lipid raft, we will not make such distinction here. Further studies are required to characterize the specific contribution of the subclasses of ceramides in lipid rafts formation. A detailed analysis of various subtypes of sphingomyelin-enriched lipid rafts would be particularly interesting in assessing the role of lipid rafts in the regulation of expression of membrane protein's localization and stability.

1.3.4 Ceramides in CF

The first connection between ceramides and pulmonary infection with *P. aeruginosa*, the most common pathogen in the lungs in CF patients, was made by the group of Richard Blumberg. In their study, Nieuwenhuis and colleagues treated immunodeficient CD1d $-/-$ mice with (2S, 3S, 4R)-1-O-(α -D-Galactosyl)-N-hexacosanoyl-2-amino-1,3,4-octadecanetriol (shortly named KRN7000), a compound similar to the naturally occurring α -galactosylceramide which is a ligand that activates NK cells and macrophages when presented by CD1d lymphocytes (Nieuwenhuis et al., 2002). KRN7000 lacks a double bond in the sphingosine and therefore contains 16 carbons long chain and 26 carbons long the acyl portion of the ceramide backbone, therefore effectively mimicking very-long chain dihydroceramide dC26:0. This study demonstrated that pre-treatment of mice with KRN7000 greatly enhanced the clearance of *P. aeruginosa* in acute pneumonia model. However, the biochemical mechanism underlying this effect had not been investigated.

Next line of evidence for the involvement of ceramides in the host defense against *P. aeruginosa* came from the studies of lipid raft formation upon infection in the laboratory of Erich Gulbins. In their studies, Grassmé and colleagues followed the formation of lipid rafts in cultured cells by analyzing distribution of ganglioside GM1 by fluorescently labelled cholera toxin (Grassme et al., 2003). They observed rapid (10-15 min) reorganization of cholera toxin-positive patches in the cell membrane upon infection of lung epithelial cells with *P. aeruginosa*. Interestingly, they also observed clustering of CFTR molecules within these GM1-enriched domains. Furthermore, they showed that the release of pro-inflammatory cytokines in the lungs of mice was negatively regulated by the formation of these membrane structures. Therefore, a failure to generate these structures in infected cells results in an unabated inflammatory response, massive release of interleukin-1 (IL-1), and septic shock in mice. By following localization of acidic sphingomyelinase (Smpd1/aSMase) and fluorescently labelled 15B4 antibody (Sigma) against ceramides, they postulated that these membrane structures are enriched in ceramides. However, 15B4 anti-ceramide antibody used in this study recognizes not only both long-chain and very-long chain ceramides but also cholesterol esters among many lipid species as shown in the **Figure 1.3.8**. Therefore, the relative content of each of the specific classes of ceramides or other

lipids components present in these rafts could not be conclusively established due to lack of the specificity of the antibody used.

The association between an increase in the pro-inflammatory C16:0 ceramide levels and constitutive inflammation in the lungs of CF mice which strongly increases with age was established in the laboratory of Erich Gulbins. In that study, Teichgräber and colleagues (Teichgraber et al., 2008) used S58-9 antibody, which similarly to 15B4 anti-ceramide antibody recognizes both long- and very-long chain ceramides (**Figure 1.3.8**), but they quantified only the level of C16:0 ceramides by mass spectroscopy in the lungs of *Cftr*^{tm1Unc}-Tg(FABPCFTR) mice and in the lungs of CF patients undergoing transplantation. Therefore, even though no conclusions could be drawn about VLCCs, this study provided for the first time a link between age-dependent accumulation of C16:0 ceramide in the respiratory tract of uninfected CF mice and constitutive pulmonary inflammation in the mice hyper-susceptible to *P. aeruginosa* infection. Teichgräber and colleagues further showed that the accumulation of C16:0 ceramide in the lungs results in the increase of respiratory cell death and formation of DNA deposits on the respiratory epithelium which are crucial for high adherence of *P. aeruginosa* to the respiratory epithelium of CF mice. These findings are fully consistent with the early reports by Thomas and colleagues suggesting that C16:0 induces apoptosis of epithelial cells, which results in deposition of DNA and cellular debris on the respiratory epithelium, eventually leading to hyperinflammatory phenotype of CF lungs (Thomas et al., 1999). Interestingly, Teichgräber and colleagues also showed that the treatment of CF mice with amitriptyline or genetic deficiency of SMPD1 enzyme which produces ceramides from sphingomyelins corrects this defect. There are four Smpd enzymes (acidic sphingomyelinases) in both the mouse and human genomes (**Figure 1.3.1**). The specificity of these sphingomyelinases with regards to the length of the fatty acid side chain in the sphingomyelins is unknown. It is therefore unknown how the treatment of cells with amitriptyline affects the levels of any of the specific ceramide species. In a phase IIb clinical trial, treatment of CF patients with amitriptyline (25 mg daily for 28 days) resulted in a small increase in the percentage of predicted FEV1: in the per-protocol groups (patients who completed the allocated treatment), patients treated with amitriptyline (n=16) had absolute-to-baseline increase of $+2.2 \pm 5.2\%$ and relative-to-baseline increase of $+3.6 \pm 7.9\%$ while placebo-treated patients experienced a slight decrease of $-2.7 \pm 5.0\%$ in the absolute-to-baseline and -

4.9±10.1% in the relative-to-baseline FEV1 (see Table 2. in the ref. (Nahrlich et al., 2013)). Comparison (Student's t-test) between amitriptyline- and placebo- treated group was statistically significant for both absolute-to baseline and relative-to-baseline FEV1 (p=0.013).

Importantly, testing only the levels of C16:0 ceramide which represents 18% of total ceramides present in the lungs (Petrache et al., 2013), without analyzing any of the other ceramide species present in the lungs leaves many questions unanswered.

Indeed, the work of Teichgräber and colleagues (Teichgraber et al., 2008) was preceded by another important milestone, when Guilbault and colleagues (Guilbault et al., 2008) performed a comprehensive analysis of long-chain and very-long-chain ceramides extracted by Folch method (Folch et al., 1957) from human plasma of healthy volunteers and patients with CF using high-performance liquid chromatography (HPLC) coupled with mass spectrometry (MS). The results of this study demonstrated for the first time that the plasma of CF patients had a much lower concentration of C24:0 ceramides than healthy controls. Furthermore, both healthy controls and CF patients had many fold lower levels of C16:0 than C24:0 and no significant differences in the level of C16:0 were found in CF patients compared to healthy controls.

In the next study done by Garić and colleagues (Garic et al., 2017), the specific ceramide species were also quantified by HPLC-MS where molecular decomposition performed using Parent Ion scan of common fragments attributed to ceramides, after the entire pool of ceramides was first purified by thin-layer chromatography and then quantified by ELISA using 15B4 antibody. The latter study (Garic et al., 2017) revealed that C24:0 and other VLCCs were strongly decreased in the lungs of CF mice, plasma of CF patients and CFBE41o- epithelial cells, whereas C16:0 ceramide and other LCCs were increased. Importantly, CF mice used in this study were not fed on Peptamen, therefore avoiding potentially confusing effects of cholesterol and vitamin A from the food. The CFTR-KO mice used in this study did not have the CFTR protein restored in their intestines. This is important to keep in mind when comparing the data generated using different mouse model of CF lung disease since the intestinal expression of CFTR introduced under FABP promoter in the gut-corrected mice, was previously shown to be leaky in the lungs as well (see Figure 1B in (Zhou et al., 1994)). Obviously, none of CF patients enrolled in this study were eating Peptamen either, therefore eliminating food as a potential source of bias. Finally, the study published by Garić and colleagues (Garic et al., 2017) demonstrated that similar imbalance in

relative ratio of VLCCs and LCCs was also found in the lung epithelial cells derived from a CF patients (CFBE41o-) demonstrating for the first time this phenomenon can be observed and studied *in vitro*.

These two studies (Garic et al., 2017; Guilbault et al., 2008), together with the studies published by Grassmé (Grassme et al., 2003), Teichgräber and colleagues (Teichgraber et al., 2008) represent the cornerstone for our modern understanding of ceramides in cystic fibrosis. Taken together, these studies defined the **imbalance of ceramides in cystic fibrosis**, characterized by the abnormally low levels of C24:0 ceramide and other VLCCs and increased levels of C16:0 ceramide and other LCCs. This situation seen in CFTR-KO mice is strikingly reminiscent of the ceramide imbalance seen in *Cers2*-KO mice where the levels of C24:0 are strongly decreased and the levels of C16:0 are increased (Petrache et al., 2013). The phenotypes of lung hyperinflammation and hypersusceptibility of *Cers2*-KO mice to pulmonary infection with *P. aeruginosa* are even more tantalizing. While the reason for the imbalance of ceramides in *Cers2*-KO model is clear, since *Cers2* is essential for the synthesis of VLCCs, in CFTR-KO mice the underlying cause of this phenomenon still remains a mystery and the mechanistic connection between these two models (*Cers2*-KO and CFTR-KO) is still unclear since *Cers2* enzyme is not downregulated in CF mice (DG, unpublished observation). Therefore, the conclusion from these studies taken together is that the decreased levels of C24:0 ceramides and increased levels of C16:0, as seen in *Cers2*-KO and CFTR-KO mice, strongly correlate with the compromised ability of these mice, to fight off pulmonary infections. Whatever the cause is, the consequences of ceramide imbalance in CFTR-KO mice for the stability of CFTR protein in the membrane are starting to emerge and will be discussed in more details below.

Interestingly, low doses (1.25 μ M) of fenretinide (N-(4-hydroxy-phenyl) retinamide), which is a synthetic retinoid molecule, reverses this imbalance, by upregulating the levels of C24:0 and other VLCCs while concurrently downregulating the levels of C16:0 and other LCCs in CF mice, CFBE41o- cells and partially in CF patients (Garic et al., 2017). This effect is mediated through the downregulation of *Cers5* enzyme (Garic et al., 2017) which produces LCCs as a homodimer and VLCCs as a heterodimer with *Cers2*. Importantly, the reversal of ceramide imbalance coincided with a dramatic improvement of the ability of CF-KO mice to combat *P. aeruginosa* infection. In particular, CFTR-KO mice treated with fenretinide showed a 10-fold

decrease in the bacterial load in the lungs compared with placebo-treated animals (Guilbault et al., 2008).

These results offer a hope that the CF patients treated with fenretinide will have not only their ceramide imbalance corrected, but that they will also fight off pulmonary infections with higher efficiency. The efforts to translate these findings in the clinic are currently underway in the Phase II (APPLAUD) trial (NCT03265288), an International Phase II, double-blind, randomized, placebo-controlled study to evaluate the safety and efficacy of LAU-7b in CF patients administered once-daily for 6 months.

1.3.5 Ceramides and CFTR

CFTR is a large, intrinsically disordered protein (Baker et al., 2007) that is primarily localized at the apical domain of epithelial cells (Li and Naren, 2010). Each CFTR molecule contains two membrane –spanning domains (MSD1 and MSD2), two nucleotide binding domains that participate in ATP binding and hydrolysis (NBD1 and NBD2), and a regulatory domain (R) whose phosphorylation by protein kinase A (PKA) regulates opening of the channel (Lukacs and Verkman, 2012). The folding of the wild-type CFTR protein is slow and relatively inefficient due to the large size of this protein and the requirement of multiple interactions between the domains for a functional conformation of the protein to be achieved (Abu-Arish et al., 2015; Lukacs and Verkman, 2012).

There are two populations of CFTR protein in the apical cell membrane: one freely floating in the lipid bilayer and the other one is confined to the lipid rafts (Abu-Arish et al., 2015; Wang et al., 2008). In the human bronchial epithelial cells (HBE) cultured in vitro, proportion of CFTR protein that is confined to the lipid rafts represents about 25% (Abu-Arish et al., 2015) whereas in Calu-3 cells this population reaches up to 50% (Wang et al., 2008).

Many different pro-inflammatory stimuli, like activation of TNF receptor, viral, or bacterial infection (Abu-Arish et al., 2015; Dudez et al., 2008; Kowalski and Pier, 2004) that trigger activation of sphingomyelinases and hydrolysis of sphingomyelin into ceramides and phosphocholine or phosphoethanolamine, lead to recruitment of freely floating CFTR molecules and fusion of those that are already confined in the lipid rafts into larger (1-2 μm) ceramide-enriched platforms. The consequences of this reorganization with regards to CFTR function and

the content of the various species of VLCCs and LCCs present in these platforms are not yet characterized.

However, taking into consideration our previous discussion of the fundamental biophysical differences between long-chain and very-long chain ceramides, we hypothesize that the tight packing in the lipid environment of VLCC-enriched platforms created by C24:0 and other VLCCs due to their acyl chains that interdigitate from both leaflets of the plasma membrane (Moore et al., 2018; Skotland et al., 2017), might stabilize the folding of CFTR and perhaps also other large transmembrane proteins localized in this type of rafts (**Figure 1.3.7A**). On the other hand, the environment of LCC-enriched platforms may adversely impact on the folding of large transmembrane proteins, like CFTR, due to the high fluidity of LCC-enriched membranes (**Figure 1.3.7 B**).

The ΔF_{508} mutation entirely abrogates the proper folding of CFTR protein, leading to its degradation in the endoplasmic reticulum. Therefore, even though CFTR proteins are synthesized, they never reach the apical cell membrane, because they are destroyed by the surveillance mechanisms in the endoplasmic reticulum that recognizes and degrades misfolded and damaged proteins via ubiquitin-proteasome pathway (Lukacs and Verkman, 2012).

The discovery that lowering the temperature of cells in culture (down to 26° C) can rescue CFTR protein from degradation (Denning et al., 1992), indicated for the first time that even the unstable mutant ΔF_{508} CFTR protein can become functional if the folding of the protein is affected by an extrinsic manipulation (in this case, lowering the temperature of the cells expressing the protein). Even though, this discovery cannot be clinically translated, it opened a possibility that someday a pharmacological chaperon, in the form of a small organic molecule could be developed that binds directly to the mutant protein and modify its folding in such a way that it resembles wild-type protein, thereby effectively correcting the phenotypes of cystic fibrosis in patients.

High throughput drug discovery strategies employed by pharmaceutical companies utilize separate functional assays to screen for the compounds which promote the exit of a mutant ΔF_{508} protein from endoplasmic reticulum and its accumulation in the apical plasma membranes (so called “correctors”) and compounds that increase the probability for the opening of CFTR channel (so called “potentiators”). The distinction between the drug which are called correctors

and potentiators is artificial, as normalization of channel gating and protein processing in the endoplasmic reticulum both depend on ΔF_{508} refolding. Many compounds identified thus far have limited *in vivo* efficiency in the CF patients who have the $\Delta F_{508}/\Delta F_{508}$ alleles.

The efforts undertaken by Vertex Pharmaceuticals company yielded two compounds that reached CF patients in the clinic. The first compound was VX770 (Ivacaftor, Kalydeco®), a potentiator, that was shown to increase the probability that the CFTR channel affected by rare non-synonymous mutation resulting in the substitution Gly551Asp of CFTR protein (G551D CFTR genotype accounts for only 3% of CF cases) (Van Goor et al., 2009). Indeed, the patients affected by G551D mutation substantially benefit from the treatment with this drug (Accurso et al., 2010; Ramsey et al., 2011). Unfortunately, patients affected by the most common ΔF_{508} mutation do not benefit significantly from this drug (Flume et al., 2012).

The second compound was VX809 corrector described in 2011 (Lumacaftor, never commercialized as a single therapeutic agent), which binds mutant ΔF_{508} protein and corrects its folding defect, thereby rescuing it from degradation in the endoplasmic reticulum (Van Goor et al., 2011). Despite spectacular results obtained *in vitro* (Van Goor et al., 2011), the success of VX809 has been disappointing in clinical studies and no sufficient levels of mature ΔF_{508} CFTR protein was observed in the cell membrane after the treatment (Clancy et al., 2012).

Since an increase in the function of mutant ΔF_{508} CFTR protein was observed after acute administration of VX770 in primary human airway epithelial cells from CF patients (Van Goor et al., 2011) and the human organoids derived from CF ($\Delta F_{508}/\Delta F_{508}$) intestinal tissues (Dekkers et al., 2013), clinical trials were designed to test the efficacy of VX809 + VX770 combination known as Orkambi (Vertex Pharmaceuticals). The results of the studies which utilized this combination of the drugs demonstrated very modest benefit (De Boeck et al., 2013; Galietta, 2013). In $\Delta F_{508}/\Delta F_{508}$ patients only small improvements in the lung function (up to 4% increase in FEV1) and up to 39% lower rate in pulmonary exacerbation were observed (Wainwright et al., 2015). One of the reasons for these disappointing results might be that VX770 causes a dose-dependent reversal of VX809-mediated CFTR correction, and in fact decreases the expression of ΔF_{508} protein corrected by VX809 at the cell surface, therefore effectively counteracting the effects of VX809 (Cholon et al., 2014; Veit et al., 2014). Unfortunately, chronic VX770 treatment also reduces expression and function of the wild-type CFTR (Cholon et al., 2014),

therefore, precluding its utility in other diseases where CFTR function is diminished, such as chronic obstructive lung disease (COPD). Recently, a combination known as Symdeko® consisting of a novel corrector called VX661(Tezacaftor) with VX770 demonstrated excellent safety profile and was shown to reduce sweat chloride and improve lung function in subjects homozygous for ΔF_{508} or compound heterozygous $\Delta F_{508}/G551D$ (Donaldson et al., 2018). Furthermore, the addition of VX445 (CFTR corrector) to Symdeko® resulted in significantly improved ΔF_{508} CFTR protein processing, trafficking, and Cl^- transport *in vitro* compared with any two of these agents in dual combination and 11.0-point increase in the percentage of predicted FEV₁ ($p < 0.001$) in $\Delta F_{508}/\Delta F_{508}$ patients (Keating et al., 2018). Finally, in patients who have only one responsive ΔF_{508} allele (ΔF_{508} -Minimal Function genotypes), the addition of VX659 (CFTR corrector) to Symdeko® resulted in an increase of up to 13.3 points in the percentage of predicted FEV₁ ($p < 0.001$) and further 9.7-point increase in the percentage of predicted FEV₁ in $\Delta F_{508}/\Delta F_{508}$ patients who were already receiving Symdeko® (Davies et al., 2018b).

Importantly, a novel approach to rescue ΔF_{508} protein using a combination of three chemically distinct pharmacological chaperones instead of one compound has been recently reported (Veit et al., 2018a). Application of each of these compounds individually had only a modest effect on the rescue of ΔF_{508} protein, but the combination (named by the authors 3C) of all three compounds simultaneously was able to restore the function of ΔF_{508} protein to approximately ~50% of the wt level, a value deemed sufficient to alleviate clinical manifestation of $\Delta F_{508}/\Delta F_{508}$ patients, as heterozygous carriers do not display any disease symptoms (Griesenbach et al., 1999).

The reason for the failure of VX809 treatment could also be the fact that the effectiveness of this compound is diminished under inflammatory conditions. Perhaps the overall effect can be improved if the lipid imbalance associated with a constitutive hyper-inflammation phenotype intrinsic to CF would be corrected prior or during the treatment with VX809 or other drug. The hyper-inflammatory phenotype and progressive airway hyperplasia might be directly linked with the aberrant composition of membrane lipids as demonstrated using *Cers2*-KO mice which have no genetic mutations in the CFTR gene. Interestingly, *Cers2*-KO mice display extreme susceptibility to lung infection (Petrache et al., 2013) which resembles the progressive lung

disease we observed in our CFTR-KO mouse model in the mice which are at least 4 months old (Kent et al., 1997).

Furthermore, the forced expression of wild-type CFTR in the cell line derived from the $\Delta F_{508}/\Delta F_{508}$ patient (CFBE41o-) by plasmid transfection reverses imbalance among ceramide species (Garic et al., 2017), suggesting that these two phenomena (lack of the functional CFTR protein and ceramide imbalance) may be biochemically connected. However, the expression of the corrected ΔF_{508} protein after VX809 treatment alone is still not sufficient to correct the distortion of cellular membranes caused by high level of LCCs and low levels of VLCCs. Therefore, we can envision that in the future any pharmacological agent that would be able to correct the imbalance of ceramides, independently from the correction of CFTR folding, could contribute to the increased stability of the corrected ΔF_{508} CFTR protein after treatment with appropriate correctors.

1.3.6 Technical challenges in ceramide quantification

Much of the confusion in the current literature about the role of ceramides in health and disease arises from the flaws in the methods used for their quantification. Traditionally, ceramides have been quantified in biological samples using antibodies and mass spectroscopy. The results obtained from these studies sometimes led to fundamentally different conclusions (Guilbault et al., 2008; Teichgraber et al., 2008).

In our previous work, we utilized 15B4 anti-ceramide monoclonal antibody from Sigma to quantify the total ceramide levels in the lipid pool after their purification from other lipids by thin layer chromatography. The total ceramide levels were normalized using total phospholipid levels among the tested samples prior to the subsequent mass spec analysis allowing for adequate characterization of the relative changes in the distribution of various species of ceramides during the course of infection or chronic inflammation.

We found that 15B4 antibody not only cannot distinguish different species of ceramides (very-long-chain vs. long-chain vs. dihydroceramides) and it also recognizes other species of lipids as we now show on **Figure 1.3.8 A**. We also tested the antibody employed by others (anti-ceramide polyclonal antibody; Glycobiotech, clone S58-9) (Becker et al., 2010; Teichgraber et al., 2008; Ulrich et al., 2010) and found that it shows the same lack of specificity, and recognizes non-

discriminately not only ceramides but also cholesterol, cholesterol esters, triglycerides, phosphatidylcholine and sphingomyelins (**Figure 1.3.8 A**). Importantly, neither the monoclonal antibody 15B4 nor the polyclonal antibody S58-9 can distinguish different lipids from each other if such lipids contain ceramide skeletons with the various acyl chains lengths in their structure (**Figure 1.3.8 B**).

Using mass spectrometry with standards containing an extensive panel of both very long and long chain ceramides, we quantified the specific ceramide species content in the lysate of cell lines, murine lungs, and the plasma of patients with CF (Garic et al., 2017). This work showed that C24:0 and other species of ceramide containing very-long-chain were downregulated both

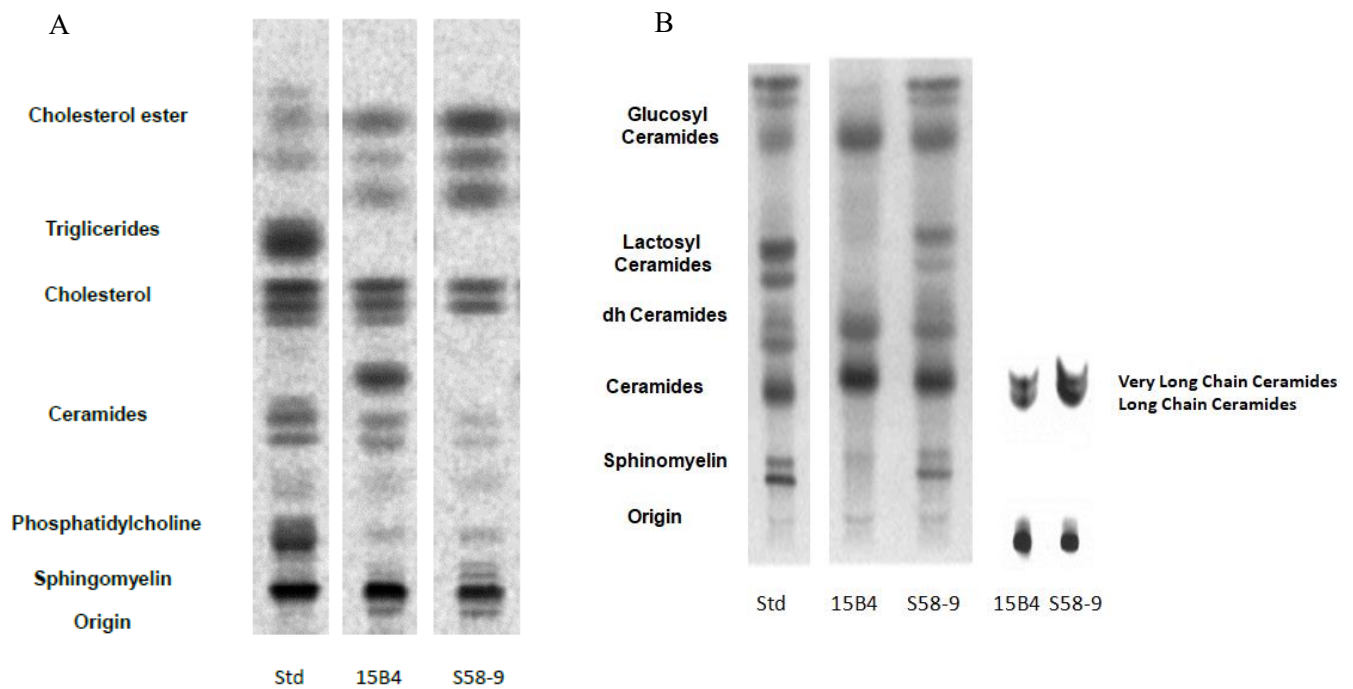


Figure 1.3.8 Commercially available antibodies for ceramide detection recognize lipids other than ceramides and do not distinguish between long-chain and very-long-chain ceramides A. Comparison of polyclonal S58-9 and monoclonal 15B4 antibodies with respect to their affinity to different lipid species. Standard (Brain Lipid Extract; Avanti) were visualized by iodine vapours. Lipids were detected by Mono - 15B4 antibody (Sigma) and Poly – S58-9 (Glycobiotech) antibodies on the nytran paper after thin-layer chromatography. *continued...*

...continued **B.** *Comparison of polyclonal S58-9 and monoclonal 15B4 antibodies with respect to their abilities to recognize different species of lipids that contain ceramide skeleton as a part of their structure.* Standard (ceramides C14:0, C16:0, C18:0, C18:1, C20:0, C24:0 and C24:1 all from Avanti Polar Lipids) were visualized by iodine vapours (see **Supplement A1.0** in the APPENDIX). Lipids were detected by Mono - 15B4 antibody (Sigma) and Poly-S58-9 (Glycobiotech) antibodies on the nytran paper after thin-layer chromatography. Courtesy of Dr. Juan B. De Sanctis.

in the younger and older cystic fibrosis patients and older CFTR-KO mice consistently with our previous findings, and in addition we also found that not only C16:0, as previously published (Teichgraber et al., 2008), but also other species of long-chain ceramides, such as C14:0, are upregulated in the lungs of CF cell line, older mice, as well and the blood of CF patients (Garic et al., 2017).

Finally, we would like to point out that the severe ceramide imbalance was also reported in the lungs in two independent reports characterizing knockout mice for Cers2 enzyme specifically (Petrache et al., 2013) and other organs as well (Imgrund et al., 2009). Indeed, Petrache and colleagues have demonstrated a strong decrease in the C24:0 levels in the Cers2-KO mice compared to wt mice. The level of C24:0 represented 72% of total ceramides in wt mice whereas in Cers2-KO there was only 7% of C24:0 ceramides. This depletion of the C24:0 ceramide observed in the Cers2-KO mice was associated with an increase in the level of C16:0 ceramide in the lung of Cers2-KO mice (Petrache et al., 2013). Similarly, Willecke's group (Imgrund et al., 2009) showed the same effect in the liver, kidneys and brain of Cers 2-KO mice (Imgrund et al., 2009). However, there was no significant difference in the total amount of ceramide in the liver (Pewzner-Jung et al., 2010b) nor in the lungs (Petrache et al., 2013) of adult Cers2-KO mice (120 days) compared to their wild-type counterparts. Also, the total amount of ceramide was actually lower in the liver, and no difference in total levels of ceramides was seen in the brain and kidneys of adult Cers2-KO mice (10 weeks) mice developed in Willecke's lab (Imgrund et al., 2009). These results open a new question of what was actually recognized by S58-9 antibody in the lungs of Cers2-KO mice stained with this antibody (Pewzner-Jung et al., 2014) since the total amounts of ceramides were not be significantly different in the lungs of Cers2-KO compared to the lungs from wt mice and the antibodies used are not able to recognize selectively C16:0 ceramides.

Therefore, currently available commercial antibodies (15B4 from Sigma and S58-9 from Glycobiotech) are both suitable for the assessment of the total pool of ceramides if the ceramides are purified from the rest of lipids present in the samples, but are not reliable tools for the quantification of specific ceramides levels in biological samples.

For all these reasons, visualizing subcellular localization of naturally occurring ceramides has been very difficult in practice. Additional challenge comes from the fact that unlike other lipids that can be specifically recognized by certain protein domains (eg. phosphatidylinositol lipids or PIPs are recognized by pleckstrin-homology domain), there are no binding protein domains that can be used as highly specific probes for ceramides (Canals et al., 2018). Some of the previously discussed intracellular ceramide targets were used to visualize ceramides in the cell and these efforts were summarized in a recent review (Canals et al., 2018)

Therefore, mass spectrometry, using an extensive panel of ceramides of different side-chain length, remains the only reliable method for unambiguous quantification of ceramides. Due to the lack of specificity of the existing antibodies, as of now, there is no generally accepted method for the subcellular localization of ceramides. Combining results obtained by these different methodologies may lead to fundamentally different and confounding conclusions.

1.4 Polyunsaturated fatty acids (PUFAs) and their metabolism in CF

Unsaturated fatty acids are carboxylic acids that contain one or more double bonds and more than 4 carbons in the acyl chain. Monounsaturated fatty acids (MUFAs) contain one double bond whereas polyunsaturated fatty acids (PUFAs) carry two or more double bonds. The most common naturally occurring PUFAs are ω -3 and ω -6 PUFAs. The designation ω refers to the position of the most distal double bond counted from the last carbon of the acyl chain (e.g. ω -3 PUFAs have its first double bond 3 carbons away from the most distal methyl group. Alternatively, n letter instead of ω can be used with the same meaning and fatty acids can be designated as n-3 and n-6. For example, docosahexanoic acid (DHA) is an ω -3 fatty acid that has 22 carbons and 6 alternating double bonds counted from the most distal carbon atom and thus can be labeled as 22:6n-3. Similarly, arachidonic acid (AA) is an ω -6 PUFA that has 20 carbons and 4 alternating double bonds counted from the 20th carbon and thus can be labeled as 20:4n-6.

Mammals do not have the ability to introduce double bonds in fatty acids beyond carbon 9 and 10 (counted from the carbonyl carbon), and therefore they must obtain some PUFAs from the food (Di Pasquale, 2009). The two essential fatty acids for humans are linoleic acid (18:2n-6) and α -linolenic acid (18:3n-3) which are metabolized through the pathways shown in the (Figure 1.4.1) Therefore, linoleic acid is the precursor for AA and α -linolenic acid is the precursor for docosahexanoic acid (DHA). Importantly, both AA and DHA can be introduced in the metabolism directly from the food. Indeed, AA and its precursors are found in plant-derived oils (corn, peanut, sunflower), red meat and eggs (Saini and Keum, 2018), while DHA is found in fish oil and algae (Horrocks and Yeo, 1999).

Both AA and DHA are transported in the bloodstream either in the esterified form (incorporated into triglycerides or cholesteryl esters) or as “free fatty acids” bound to lipoproteins, but once inside cell, they become incorporated into phospholipids which are principal lipid constituents of cellular membranes. Upon activation of various signaling pathway initiated either by endogenous (hormones, cytokines) or exogenous factors (bacterial lipopolysaccharide), AA and DHA are released from phospholipids through the action of the enzymes called phospholipases. There are three major categories of phospholipases: cytosolic phospholipases (cPLA₂), secreted phospholipases (sPLA₂) which are Ca²⁺-dependent and Ca²⁺-independent phospholipases

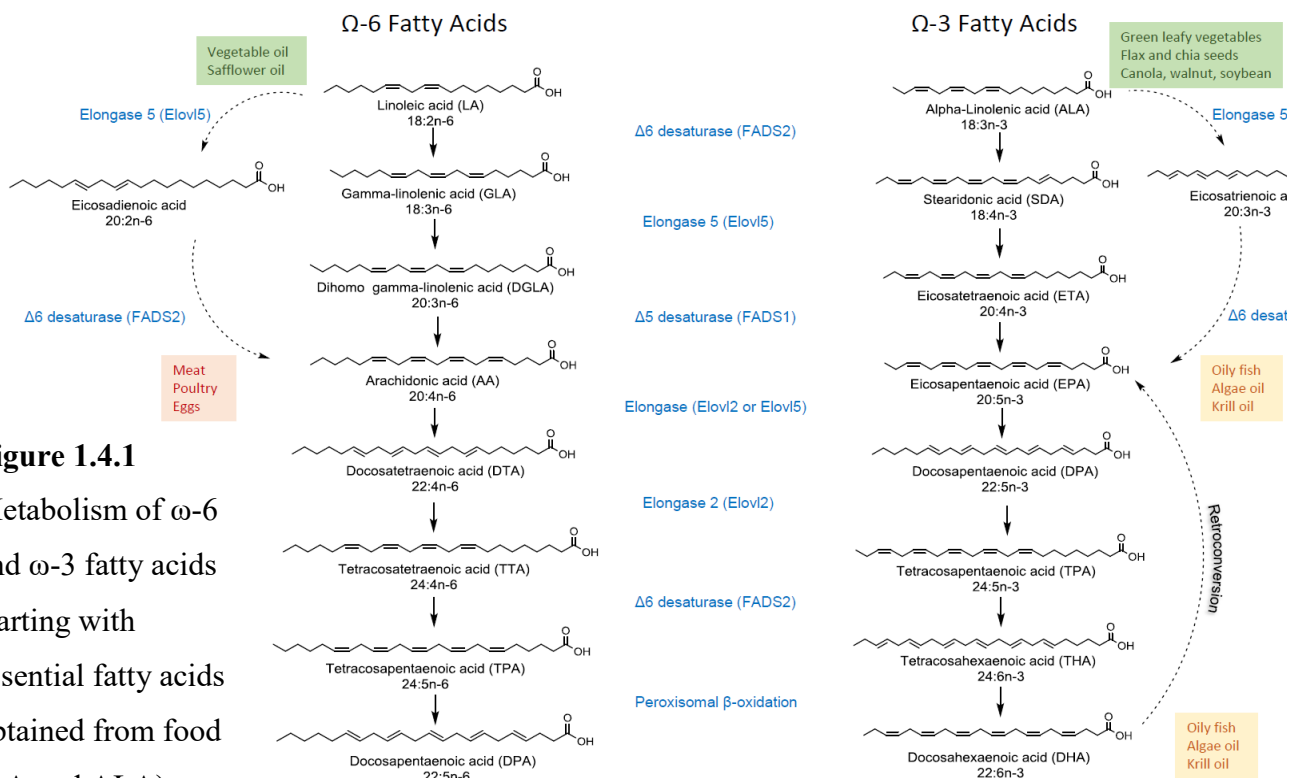


Figure 1.4.1
Metabolism of ω -6 and ω -3 fatty acids starting with essential fatty acids obtained from food (LA and ALA).

Courtesy of Catalina Daciana Dumut.

Each of these categories of enzymes is coded by multiple paralogous genes. For example, in the human genome there are six genes for cytosolic phospholipases (PLA2G4A, PLA2G4B, PLA2G4C, PLA2G4D, PLA2G4E and PLA2G4F coding for cPLA₂-α, cPLA₂-β, cPLA₂-γ, cPLA₂-δ, cPLA₂-ε and cPLA₂-ζ proteins respectively), eleven genes for secreted phospholipases (PLA2G2A, PLA2G2D, PLA2G2F, PLA2G3, PLA2G5, PLA2G10, PLA2G1B, PLA2G2C, PLA2G2E, PLA2G12A and PLA2G12B coding for group IIA sPLA₂, group IID sPLA₂, group IIF sPLA₂, group III sPLA₂, group V sPLA₂, group X sPLA₂, sPLA₂-IB, sPLA₂-IIC, sPLA₂-IIE, sPLA₂-XIIA and sPLA₂-XIIB proteins respectively) and six genes for iPLA₂ (PNPLA9, PNPLA8, PNPLA6, PNPLA3, PNPLA2 and PNPLA4 coding for iPLA₂β, iPLA₂γ, iPLA₂δ, iPLA₂ε, iPLA₂ζ and iPLA₂η proteins respectively) (Dennis et al., 2011; Murakami et al., 2016).

AA is released from the phospholipids mostly through the actions of cPLA₂ and sPLA₂ enzymes (Dennis et al., 2011; Murakami et al., 2016) while DHA can be released through the action of iPLA₂ enzymes (Cheon et al., 2012; Strokin et al., 2003) and sPLA₂ (Murakami et al., 2011; Murase et al., 2016). Interestingly, once released from the membrane DHA can inhibit cPLA₂ and thus limit the release of AA (Shikano et al., 1994).

Once released from the membrane, AA and DHA are metabolized through the series of enzymatic steps into molecules with potent pro- and anti-inflammatory properties.

AA is the substrate for cyclooxygenases: constitutively expressed COX-1 and inflammation-inducible COX-2 are both well-known target of aspirin and other non-steroidal anti-inflammatory drugs (NSAIDs) (Rouzer and Marnett, 2009). These two enzymes initially convert AA into an unstable intermediate called prostaglandin H₂ which is further converted to different biologically active prostanoids depending on the presence of different tissue-specific isomerases. These are prostaglandins (PGE₂, PGD₂, PGF₂α), prostacyclin (PGI₂) and thromboxanes (TXA₂, TXB₂) (McGiff, 1981). AA is also the substrate for lipoxygenases (5-LOX, 12-LOX and 15-LOX) which convert it into leukotrienes, lipoxins and hepoxilins (Samuelsson et al., 1987). 5-LOX produces leukotriene A₄ (LTA₄) which is further converted into cysteinyl-leukotrienes (LTC₄, LTD₄ and LTE₄, leukotriene B₄ (LTB₄) and lipoxins (LXA₄ and LXB₄). 12-LOX converts AA into 12-hydroxyeicosatetraenoic acid (12-HETE) and 15-LOX converts AA into LXA₄ and LXB₄ (Dobrian et al., 2011).

All secondary metabolites produced from AA, with the notable exception of lipoxins, are potent pro-inflammatory molecules. The activation of numerous G-protein coupled receptors (GPCRs) through which these derivatives of AA act leads to the well known hallmarks of inflammation such as chemotaxis of neutrophils and degranulation of platelets at the site of their production, synthesis of pyrogenic cytokines which raise body's temperature etc (Serhan and Ward, 1999).

On the other hand, all known metabolites of DHA have anti-inflammatory properties (Duvall and Levy, 2016). Once released from the membrane by the action of phospholipases, DHA serves as the substrate for 15-LOX and 12-LOX enzymes. 15-LOX converts DHA into the intermediate 17S-hydroperoxy-DHA which is further converted by neutrophil-derived 5-LOX to the D-series of resolvins (RvD1-RvD4) (Hong et al., 2003; Serhan et al., 2002). DHA can also be converted by 15-LOX into 16, 7-epoxy-protectin intermediate and then to protectin D1 (Hong et al., 2003; Serhan et al., 2002). Finally, 12-LOX in macrophages converts DHA into *Macrophage Mediators in Resolving Inflammation* or maresins (Dalli et al., 2013; Serhan et al., 2009). Resolvins, protectins and maresins are potent anti-inflammatory molecules that also act through specific GPCRs and activate multiple signaling pathways that lead to the resolution of inflammation (Duvall and Levy, 2016). These include reduction of neutrophils chemotaxis, stimulation of phagocytosis of apoptotic neutrophils, clearance of allergens and many others (Duvall and Levy, 2016).

1.4.1 PUFAs in CF

The first association of abnormal metabolism of PUFAs with CF was made back in 1962 when Kuo et al (Kuo et al., 1962) described abnormally low levels of linoleic acid (18:2n-6) in the plasma and tissues of children with CF. The next two important milestones were the discoveries that the levels of DHA are decreased in different tissues of CF patients examined *post mortem* (Underwood et al., 1972) whereas the level of AA is increased in leukocytes (Carlstedt-Duke et al., 1986; Gilljam et al., 1986; Strandvik et al., 2001). These historical findings were later confirmed in both CF patients (Freedman et al., 2004) and CFTR-KO (Freedman et al., 1999; Guilbault et al., 2009). Taking into consideration the previously discussed pro- and anti-inflammatory roles of AA and DHA respectively, these findings collectively defined what is nowadays known as a **proinflammatory imbalance of fatty acids** in CF, shortly expressed as a high AA/DHA or low DHA/AA ratio.

However, with the cloning of CFTR gene in 1989 which sparked the hope that the genetic defect itself could be corrected by gene therapy, the initial description of proinflammatory imbalance of fatty acids fell into obscurity. New interest in this field was rekindled in the early 2000s with the finding that the dietary supplementation with DHA of *cftr* $-/-$ mice ameliorated many of the CF-related pathologic phenotypes, including reduction of villus hypertrophy, reversal of pancreatic duct dilation, and most importantly restrain LPS-stimulated pulmonary inflammation (Freedman et al., 1999; Freedman et al., 2002). Despite encouraging results obtained in mice (Beharry et al., 2007; Freedman et al., 1999; Freedman et al., 2002; Portal et al., 2018), the supplementation of DHA alone and other n-3 PUFAs alone did not confer significant clinical benefit to patients with CF (Coste et al., 2007; Lloyd-Still et al., 2006; Van Biervliet et al., 2008a). Nevertheless, it was shown that the pharmacological correction of pro-inflammatory AA/DHA ratio by fenretinide that leads to the simultaneous decrease in AA and increase in DHA (which may not be achieved with DHA treatment alone) resulted in the significantly improved ability of *cftr* $-/-$ mice to resolve pulmonary infection with *P. aeruginosa* (Guilbault et al., 2009).

For a long time it was thought that the proinflammatory imbalance of fatty acids observed in patients with CF is the consequence of pancreatic insufficiency and the resultant lipid malabsorption (Farrell et al., 1985; Hubbard et al., 1977; Rogiers et al., 1983). However, several independent lines of evidence undoubtedly disproved the malabsorption hypothesis. First, fatty acid imbalance persists in CF patients in whom pancreatic insufficiency has been successfully corrected with enzyme replacement and nutritional support (Aldamiz-Echevarria et al., 2009; Roulet et al., 1997). Second, the proinflammatory imbalance of fatty acids is seen in *cftr* $-/-$ mice (Freedman et al., 1999; Guilbault et al., 2009), mostly in the tissues that express high level of CFTR protein such as lungs, pancreas and intestine, but not in tissues such as brain, kidney or heart (Freedman et al., 1999; Mimoun et al., 2009). Finally, the presence of the proinflammatory imbalance of fatty acids even in cultured cells derived from the lungs of CF patients indicates that this phenomenon is not secondary to pancreatic insufficiency or pathogen-induced lung inflammation but is indeed causally linked to lack of functional CFTR protein and is therefore intrinsic defect of CF (Andersson et al., 2008) (Garić et al *Biochimica et Biophysica Acta (BBA) - Molecular and Cell Biology of Lipids*, 2019 submitted).

Several non-conflicting hypotheses were proposed in order to explain the proinflammatory imbalance of fatty acids in CF, but none of them provides mechanistic connection between the absence of functional CFTR protein and high AA/DHA ratio. Historically the first described abnormality of fatty acids in CF, ie. the LA deficiency, as well as the increased level of AA could simply be explained by the rapid turnover of LA into AA (Al-Turkmani et al., 2008). Indeed, increased conversion of radioactively labelled LA into AA was demonstrated in CF cells compared with wild-type controls (Njoroge et al., 2011). These changes were accompanied with the increased expression of $\Delta 5$ - and $\Delta 6$ -desaturases (coded by FADS1 and FADS2 genes respectively) and could be recapitulated by the treatment of cells with a small molecule inhibitor of CFTR (CFTR_{inh}-172). However, these results do not explain the low levels of DHA observed in CF, which is the least understood defect of all. Interestingly, DHA is known to suppress the expression of $\Delta 5$ - and $\Delta 6$ -desaturases in cultured cells (Njoroge et al., 2012) and mice (Freedman et al., 1999; Mimoun et al., 2009), but the causal connection between CFTR deficiency and low DHA levels remains unclear. It is clear that the metabolism of EPA to DHA is decreased in cultured CF cells (Njoroge et al., 2011), but the level of 22:5n-3 which is the immediate downstream product of EPA was not decreased in this study. On the other hand, retroconversion of DHA to EPA which occurs through the modified β -oxidation in peroxisomes (Gronn et al., 1991; Hiltunen et al., 1986) was also described in CF (Njoroge et al., 2012). Additionally, an abnormal metabolism of phosphatidylcholine (PC) was invoked to explain lower levels of DHA in CF: PC formed *de novo* through the methylation of phosphatidylethanolamine (PE) is known to have higher DHA content than PC formed using choline derived from the diet (DeLong et al., 1999; Pynn et al., 2011). CF cells appear to have a defect in the metabolism of methyl group such that the *de novo* synthesis of PC is favoured, thereby depleting DHA levels (Innis and Davidson, 2008; Watkins et al., 2003). Whatever the mechanism of DHA deficiency in CF is, it is clear that this abnormality can result in the lower level of anti-inflammatory lipid mediators derived from it, as it was indeed reported for Resolvin E1 in CF patients (Yang et al., 2012).

Finally, numerous studies have convincingly demonstrated that the increased release of AA in CF cells from the cell membrane is mediated by cytosolic phospholipases (cPLA₂) (Berguerand et al., 1997; Carlstedt-Duke et al., 1986; Dif et al., 2010; Levistre et al., 1993; Miele et al., 1997). In this scenario, the increased conversion of LA to AA could be merely a compensatory response

to this change, which inadvertently contributes to even higher levels of AA. The relationship between these two pathways, if any, remains to be explored.

Nevertheless, it has never been established which one out of six cytosolic phospholipases contributes the most to the increased levels of AA. We examined the mRNA levels of all six cytosolic phospholipases in CFBE 41o- cells derived from a $\Delta F508/\Delta F508$ patient and we could not observe any difference in mRNA between parental cells and those transfected with wt-CFTR protein (Garic et al *Biochimica et Biophysica Acta (BBA) - Molecular and Cell Biology of Lipids*, 2019 submitted). However, this leaves an open possibility that the protein levels and/or activities of cPLA₂ enzymes are affected by posttranslational modifications. Indeed, the treatment of CFBE41o- parental cells with fenretinide, an orphan drug which was previously reported to decrease the level of AA and increase the level of DHA (Guilbault et al., 2009) was found to decrease the total cPLA₂ activity assayed by colorimetric assay (Garic et al *Biochimica et Biophysica Acta (BBA) - Molecular and Cell Biology of Lipids*, submitted). The mechanism of this change remains to be further explored.

1.4.2 Fenretinide

Understanding the mechanisms of proinflammatory fatty acid imbalance in CF is of direct relevance to dietary therapy (Borowitz et al., 2002; Smith et al., 2012). Unfortunately, the typical modern Western diet contains high ratio of ω -6 to ω -3 PUFAs (Blasbalg et al., 2011; Simopoulos, 1998), and therefore may exacerbate the already present intrinsic defect of high AA and low DHA production in CF patients. This, in turn, may result in an increased production of pro-inflammatory lipid mediators for which AA serves as a precursor and decreased production of anti-inflammatory lipid mediators for which DHA serves as the starting metabolite. Unfortunately, the supplementation of DHA alone and other n-3 PUFAs alone did not confer significant clinical benefit to patients with CF (Coste et al., 2007; Lloyd-Still et al., 2006; Van Biervliet et al., 2008a).

Fenretinide (4-hydroxy(phenyl)retinamide; 4-HPR) is a synthetic analogue of retinoic acid which has a phenyl moiety instead of carboxylic group linked through an amide bond (**Figure 1.4.2**).

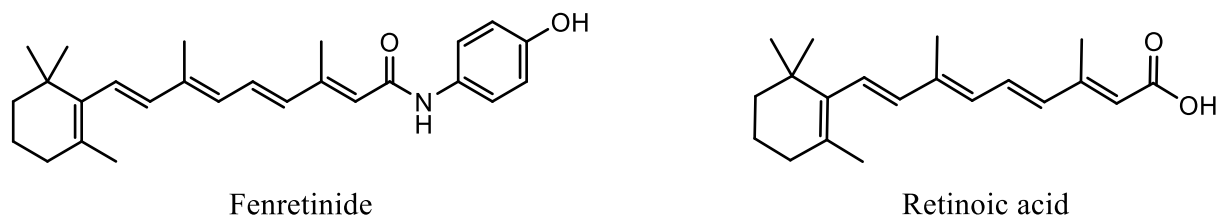


Figure 1.4.2 Structures of fenretinide and retinoic acid.

We have previously reported that low doses of fenretinide correct proinflammatory lipid imbalance in CFTR-KO mice by decreasing the levels of AA while simultaneously upregulating the level of DHA (Guilbault et al., 2009). Fenretinide was used at lower doses as a chemopreventive agent in patients with breast cancers (Veronesi et al., 1999) and at relatively high doses for treatment of patients with neuroblastoma (Children's Oncology et al., 2006). In both cases fenretinide was shown to be a relatively safe agent and the most common adverse effects reported were minor visual disturbances such as diminished dark adaptation. This adverse effect is most likely due to the ability of fenretinide to decrease endogenous retinol concentrations by competing for the same transport protein RBP4 (Berni and Formelli, 1992). Fenretinide binds strongly to RBP4, but this complex does not bind to transthyretin (Berni et al., 1993). However, the fenretinide-RBP4 complex is eliminated through renal filtration, thereby depleting the level of RBP4 necessary to transport retinol, which eventually results in lower retinol levels in fenretinide-treated patients (Berni et al., 1993).

Similarly to retinoic acid, which is a physiologically active metabolite of retinol, fenretinide binds to retinoid receptors (RARs), which belong to the family of nuclear receptors. Upon binding of their ligand (which may be either all-trans-retinoic acid or 9-cis retinoic acid), several isoforms of RARs, known as RAR- α , - β and - γ , bind to the DNA sequence known as retinoic acid receptor elements (RAREs) and regulate transcription of hundreds of genes (Al Tanoury et al., 2013). On the other hand, retinoid X receptors (RXR- α , - β and - γ) bind only 9-cis retinoic acid (Leblanc and Stunnenberg, 1995). Fenretinide was found to bind strongly to RAR γ , weakly to RAR β (Bu and Wan, 2007; Fanjul et al., 1996) and not at all to RXR α (Fanjul et al., 1996). On the other hand, fenretinide activates transcription by a nuclear receptor called PPAR γ (Harris et al., 2005; Lin et al., 2016) although there is no evidence for the direct interaction with PPAR γ . The consequences of these actions are certainly cell-type dependent and result in the downregulation or upregulation of the transcription of the genes normally controlled by these

nuclear receptors. Additionally, fenretinide was found to prevent the activation of NF- κ B pathway by inhibiting the phosphorylation of I κ B α kinase (Shishodia et al., 2005) and to inhibit phosphorylation of Erk kinase (Lachance et al., 2013) thereby inhibiting the signals that emanate from multiple Tyr-phosphorylated growth factor receptors.

Due to its pleiotropic effects outlined above, it is very difficult to pinpoint the exact mechanism whereby fenretinide affects the activity of cytosolic phospholipases. Additionally, fenretinide was found to increase the level of anti-inflammatory very-long-chain ceramides while decreasing the levels of pro-inflammatory long-chain ceramides and this effect could be attributed to the downregulation of Cers5 enzyme (Garic et al., 2017).

Even though the exact mechanism of fenretinide action on different lipid species is still unknown, it is certain that fenretinide holds promise as the safe agent for the pharmacological correction of aberrant lipid metabolism in patients with CF. Long-term safety of fenretinide was well established in the population of breast cancer patients (Camerini et al., 2001; Veronesi et al., 2006). However, the safety profile of fenretinide in CF patients was evaluated for the first time in a Phase Ib clinical trial with a novel orally bioavailable formulation of fenretinide (LAU-7B). The reassuring safety profile and excellent pharmacokinetics of the LAU-7B formulation obtained in Phase Ib, led to the Phase II (APPLAUD) trial (NCT03265288). This is a currently ongoing international Phase II, double-blind, randomized, placebo-controlled study to evaluate the safety and efficacy of LAU-7b in CF patients administered escalating doses (100 mg, 200 mg, 300 mg) once-daily for 6 months.

Finally, since the signaling through retinoid receptors and NF- κ B pathway are known to be important for constitutive and pathogen-induced expression of mucin genes (Binker et al., 2015; Blanco et al., 2009; Morin et al., 2015), we examined how fenretinide treatment affects the expression of MUC5AC and MUC5B genes in a goblet cell line derived from rat lungs. Interestingly, our recent results demonstrate that the low dose of fenretinide (1.25 μ M) selectively prevents MUC5AC overexpression, without significantly affecting MUC5B expression (Garić et al. *Biochimica et Biophysica Acta (BBA) - Molecular and Cell Biology of Lipids*, 2019 submitted). These results are especially important considering significant biological differences between MUC5AC and MUC5B (Evans et al., 2015; Roy et al., 2014). Indeed, it was recently demonstrated that MUC5B is required for mucociliary clearance and immunological

defense of the lungs whereas MUC5AC is dispensable and is in fact responsible for pathological plugging and airway obstruction (Evans et al., 2015). Nevertheless, the mechanistic connection between proinflammatory lipid imbalance and the regulation of mucin gene expression remains unexplored. Most likely, such a connection would be indirect, through the metabolites of fatty acids such as eicosanoids (Marom et al., 1981) or 12(R)-HETE (Garcia-Verdugo et al., 2012).

In conclusion, the pro-inflammatory imbalance of PUFAs reflected in a high AA/DHA ratio is an important component of sterile inflammation which is detrimental for the lung defense of CF patients. This underexplored biochemical aspect of CF may lead to the development of novel therapeutic interventions in the future. To this end, fenretinide holds promise as a safe pharmacological agent for the correction of abnormal lipid metabolism and as a novel mucoregulatory agent.

Based on the preceding discussion the Hypotheses and Objectives of my doctoral thesis were:

1. CF patients have higher level of BAFF in their plasma. Hyperinflammation in CF is not protective, since CF patients are more susceptible to lung infections despite higher antibody titers. We hypothesize that BAFF is a component of sterile inflammation in CFTR-KO mice and that the neutralization of BAFF may improve lung function in CF-KO mice. Therefore, the objectives were to examine the level of BAFF in both wild-type and CFTR-KO mice and to examine the susceptibility of both groups of mice to lung infection with *Pseudomonas aeruginosa* upon depletion of BAFF with a neutralizing antibody.
2. There is a link between CFTR expression and the aberrant profile of phospholipid subclass called ceramides in CF and this imbalance in ceramides can be corrected by treatment with fenretinide. We hypothesized that fenretinide restores the balance of LCC and VLCC species *via* modulation of the enzymes specific for the chain length of these ceramide species. Therefore, our objective was to elucidate the identity of these enzymes and the effect of fenretinide on their expression.
3. It was shown that the downregulation of CFTR gene with antisense RNA leads to pro-inflammatory imbalance of fatty-acids. Therefore, we hypothesized that the upregulation of

CFTR gene in $\Delta F508/\Delta F508$ cell line would lead to the correction of this imbalance and that this effect could be mimicked by fenretinide treatment. Since, fenretinide is an antagonist of retinoic acid and an agonist of PPAR- γ transcription factor, we hypothesized that it may transcriptionally regulate the expression of MUC5AC and MUC5B genes. Therefore, the objectives were to assess the levels of AA and DHA in $\Delta F508/\Delta F508$ lung epithelial cell line upon overexpression of CFTR and to assess the levels of MUC5AC and MUC5B genes in a goblet cell line and murine lungs upon infection with *Pseudomonas aeruginosa* and fenretinide pre-treatment.

Chapter 2

Depletion of BAFF cytokine exacerbates infection in *Pseudomonas aeruginosa* infected mice

This chapter examines the role of BAFF cytokine in the immunological defense of lungs. It was adapted from the published manuscript: Garić D, Tao S, Ahmed E, Youssef M, Kanagaratham C, Shah J, Mazer B, Radzioch D. *Depletion of BAFF cytokine exacerbates infection in Pseudomonas aeruginosa* infected mice. **J Cyst Fibros. 2018 Dec 7. pii: S1569-1993(18)30864-6. doi: 10.1016/j.jcf.2018.11.015. [Epub ahead of print] (*original article*)**

2.1 Abstract

Background: Cystic fibrosis (CF) is a genetic disease characterized by chronic inflammation of the lungs that is ineffective at clearing pathogens. B-cell activating factor (BAFF), a cytokine involved in the development of B-cells, is known to be elevated in CF patients with subclinical infections. We postulate that the elevated BAFF levels in CF patients might be triggered by *Pseudomonas aeruginosa* infection and it might play a protective role in the regulation of lung responses to infection.

Methods: To address this hypothesis, we used a well characterized model of CFTR.KO mice infected with a clinical strain of *P. aeruginosa* (PA508). We quantified cell types with flow cytometry, concentration of cytokines by ELISA tests, bacterial load by colony counting and lung physiology by metacholine-induced lung resistance.

Results: Our data demonstrates that BAFF is not elevated in uninfected CF mice, and infection with *Pseudomonas* leads to significant induction of this regulatory cytokine. We also demonstrate that the maintenance of BAFF levels and its induction during the infection is important for clearance of *Pseudomonas* infection as its depletion during the course of infection leads to decrease in the resolution of infection both in WT and CFTR-KO mice. Interestingly, the depletion of BAFF not only results in a depletion of B cells numbers but also to a significant decrease in the number of regulatory T cells in the non-infected lungs.

Conclusions: Overall, our data demonstrate for the first time that BAFF is an important regulatory molecule helping to maintain the immunological response to infection and clearance of lung infection.

2.2 Introduction

Patients with cystic fibrosis (CF) demonstrate impaired ability to clear both bacterial and fungal pathogens and subsequently suffer from chronic pulmonary inflammation. This persistent, high-intensity inflammation is dominated by neutrophils that release proteases, particularly elastase, that cleave structural proteins of the lungs (Cantin et al., 2015; Elizur et al., 2008). These proteolytic activities contribute to bronchiectasis, a permanent structural damage of the lungs that can lead to respiratory failure and even death. Therefore, better understanding of which

regulatory molecules are essential for clearing lung pathogens in CF subject is of great importance.

To this end, several pharmacological approaches to control excessive inflammation have been investigated including corticosteroids, high-dose ibuprofen and azithromycin (Cantin et al., 2015). Unfortunately, the improvements seen after the treatment with systemic corticosteroids was modest and transient. The benefits were lost after the treatment was stopped and toxicity was high (Lai et al., 2000). Treatment with high-dose ibuprofen has not been widely adopted due to the challenges associated with obtaining pharmacokinetics for appropriate dosing and concerns over adverse effects (Konstan, 2008). Azithromycin is an antibiotic that may have anti-inflammatory properties independent of its bactericidal action, and has been recommended for the treatment of CF patients over the age of six, irrespective of their infection status with *P. aeruginosa* (Saiman et al., 2010; Saiman et al., 2012). The effect of these therapies on the regulatory molecules important for the maintenance of proper immune response and clearing infection have not yet been assessed adequately.

B cell activating factor (BAFF) is a cytokine required for the generation and maintenance of B cells, the major factories of antibody production (Schneider et al., 1999; Thompson et al., 2001). Even though the production of pathogen-specific antibodies by B-cells is normally an important mechanism of airway defense, it was shown that early production of IgA and IgG antibodies to *P. aeruginosa* alginate did not prevent development of chronic infection and furthermore the higher levels of *P. aeruginosa*-specific IgA antibodies correlate with poor lung function (Pedersen et al., 1990). Recently it was found that the expression of BAFF was increased at both mRNA (Ogilvie et al., 2011) and protein levels (Neill et al., 2014) in the lungs of CF patients compared to healthy controls, irrespective of their infection status with *P. aeruginosa*. These findings prompted us to hypothesize that the increased levels of BAFF could represent a feedback response and an inherent feature of chronically infected lungs observed in vast majority of CF patients. We hypothesize that BAFF could be important mediator in the regulation of lung inflammation and specific targeting of BAFF could establish if its ablation would impair ability to fight the infection worsening of the lungs physiology or decrease excessive inflammation preventing bronchiectasis, potentially without compromising the host's immune response against the pathogen.

We had previously reported that IL-10-KO mice and WT mice treated with neutralizing antibodies against IL-10 are more susceptible to *P. aeruginosa* infection in the lungs than their wild-type counterparts (Guilbault et al., 2002). Using S489X (B6.129P2-Cftr^{tm1Unc}) mice, Soltys et al. (Soltys et al., 2002) reported that the IL-10 level is lower in the BALF of these CF mice. IL-10 is an anti-inflammatory cytokine produced by B and T cells, dendritic cells and macrophages in response to inflammatory stimuli (Saraiva and O'Garra, 2010), and therefore its production might be affected when the BAFF levels would be depleted. In order to investigate the potential source of IL-10 in the lungs of CF mice, we focused on two major populations of immunosuppressive lymphocytes, namely B-regulatory (Breg) and T-regulatory (Treg) cells. Breg and Treg cells are subsets of lymphocytes whose function is to maintain immunological tolerance through production of immunosuppressive cytokines such as IL-10 and TGF- β . CD4⁺CD25⁺ Treg cells are defined by the expression of transcription factor Foxp3. In contrast to the CD4⁺CD25⁺Foxp3⁺ Treg cells, there are currently no known transcription factors specific to the development of Breg cells. In addition to being CD19 positive, Bregs are defined by their production of inhibitory ligands such as PD-1 and immunosuppressive cytokines.

In this study we examined the effect of blocking BAFF ligand with a neutralizing antibody Sandy-2. Our results show the effect of BAFF depletion on the level of IL-10 and some of its major producers, namely Breg and Treg cells and clearly demonstrate that the depletion of BAFF has deleterious effects on the bacterial burden and lung physiology in wild-type C57BL/6 and CFTR-KO mice during infection with *P. aeruginosa*.

2.3 Methods

2.3.1 Mice

Inbred C57BL/6-Cftr^{-/-} (CF-KO) mice with an increased susceptibility to pulmonary *P. aeruginosa* infection compared to their littermate controls and without intestinal correction of CFTR were previously described (Gosselin et al., 1998). All experiments were conducted in accordance with the Canadian Council on Animal Care guidelines and approved by the Facility Animal Care Committee of the MUHC-RI.

2.3.2 Neutralization of BAFF cytokine

For the neutralization of BAFF cytokine, mice were injected intraperitoneally with either PBS as a placebo control or with 2mg/kg of Sandy-2 antibody (Adipogen, #AG-20B-0063PF), as this dose was previously described to fully deplete B-cells(Kowalczyk-Quintas et al., 2016).

2.3.3 Preparation of bacterial inoculums and lung infection

Bacteria (*P. aeruginosa* strain DNC235) were entrapped in agar beads (150-200 μm in size) and mice were infected ($1 \cdot 10^6$ cfu/animal) non-invasively through the trachea as previously described (Guilbault et al., 2005). Mice were sacrificed 3 days after infection by CO₂ overdose and lungs were collected for further analyses.

2.3.4 CFU quantification

Lungs from infected mice were harvested and homogenized for 45 seconds at speed 6 (PT10135; Brinkmann Instruments Co., Mississauga, ON, Canada) in 3 ml of sterile PBS. Serial 10-fold dilutions of lung homogenates were plated on Petri dishes containing trypticase soy agar (TSA). The number of cfu per lung was counted after overnight incubation at 37°C. An aliquot of the lung homogenate was preserved with protease inhibitors (Roche) for ELISA tests.

2.3.5 ELISA tests

Concentration of total protein in each sample was determined with a BCA kit (Thermo Fischer Scientific) and an equal amount of protein (100 μg per well) was used in ELISA test. Quantification of the BAFF level was done using the Quantikine[®] ELISA BAFF immunoassay (MBLYS0, RnD Systems) and IL-10 was done using ELISA immunoassay (DY417-05, R&D Systems) according to the manufacturer's instructions.

2.3.6 Pulmonary resistance

Pulmonary resistance in mice was measured as previously described (Kanagaratham et al., 2014). The maximum resistance for each mouse, in response to PBS or increasing doses of methacholine exposure was determined using Buxco plethysmograph system (Buxco Research System, Wilmington, NC, USA).

2.3.7 Flow Cytometry

Spleens were harvested and macerated in 1X PBS. Lungs were injected with 1mL of digestion buffer (1X Hanks' Balanced Salt Solution (14025092, Life Technologies), 3U/mL collagenase D (11088866001, Roche), and 10 mg/mL DNase I (90083, ThermoFisher Scientific) through the trachea. The lungs were digested for 30 minutes at 37°C with GentleMACSOcto Dissociator (130096427, MiltenyiBiotec Inc). The resulting cell suspensions were filtered through a 40µM nylon mesh. Following RBC lysis, splenocytes and lung epithelial cells were re-suspended in medium (RPMI 1640 containing 10% FBS, 1% Sodium Pyruvate, 1% Pen/Strep, 1% HEPES, and 50µM β-mercaptoethanol) and cultured for 4 hours in the presence of a cell activation cocktail containing PMA, ionomycin, and Brefeldin A (Cat. 423303, BioLegend) at 37°C. For the staining of B cell from the spleen, stimulated cells were first stained for 30 min at 4°C with CD19-PerCP (115532, BioLegend), and fixable viability dye (FVD) Zombie-Aqua (423102, BioLegend). For the staining of B cells in lungs, stimulated cells were stained for 25 min at 4°C with CD45-APC (103112, BioLegend), CD19-PerCP, CD138-BV421, and FVD Zombie-Aqua. Following incubation in Fixation/Permeabilization buffer (00-5523-00, eBioScience) for 20 min at RT, splenocytes and lung cells were stained with IL-10-PE (505008, BioLegend) in Perm/Wash buffer for 30 min at 4°C, washed in Perm/Wash buffer, and then re-suspended in FACS buffer. For staining of T cells from spleen, stimulated cells were first stained for 30 min at 4°C with CD4-FITC (100510, BioLegend), CD25-PE (101904, BioLegend), and FVD-eFluor780 (65086514, eBioScience). For staining of T cells from lungs, cells were stained with CD45.2-eFluor450 (48-0454-82, eBioscience), CD4-FITC, CD25-PE, and FVD-eFluor780. Following incubation in fixation/permeabilization buffer for 30 min at RT, splenocytes and lung cells were stained with FoxP3-APC (17577382, eBioScience) in Perm/Wash buffer for 1 hour at RT, washed in Perm/Wash buffer, then re-suspended in FACS buffer. All cells were kept on ice until acquisition. Samples were run using a FACS Canto II (BD) on the same day. The flow cytometry data were analyzed using FlowJo version 10.1 software.

2.3.8 Statistical Analysis

All statistical analyses were performed using GraphPad (GraphPad, San Diego, CA, USA). Statistical analysis was performed using ANOVA test with Holm-Sidak's correction whenever multiple comparisons (more than two groups) for a single variable were compared and *t*-tests

with Welch's correction when only two conditions for a single variable were compared at a time. Data is represented as means \pm SD (* $p \leq 0.05$, ** $p \leq 0.01$, *** $p \leq 0.001$).

2.4 Results

2.4.1 Increased level of IL-10 and not BAFF is an inherent feature of cystic fibrosis.

Experimental design and the timeline of the treatment of mice with Sandy-2 and subsequent infection is outlined in **Figure 2.1**.

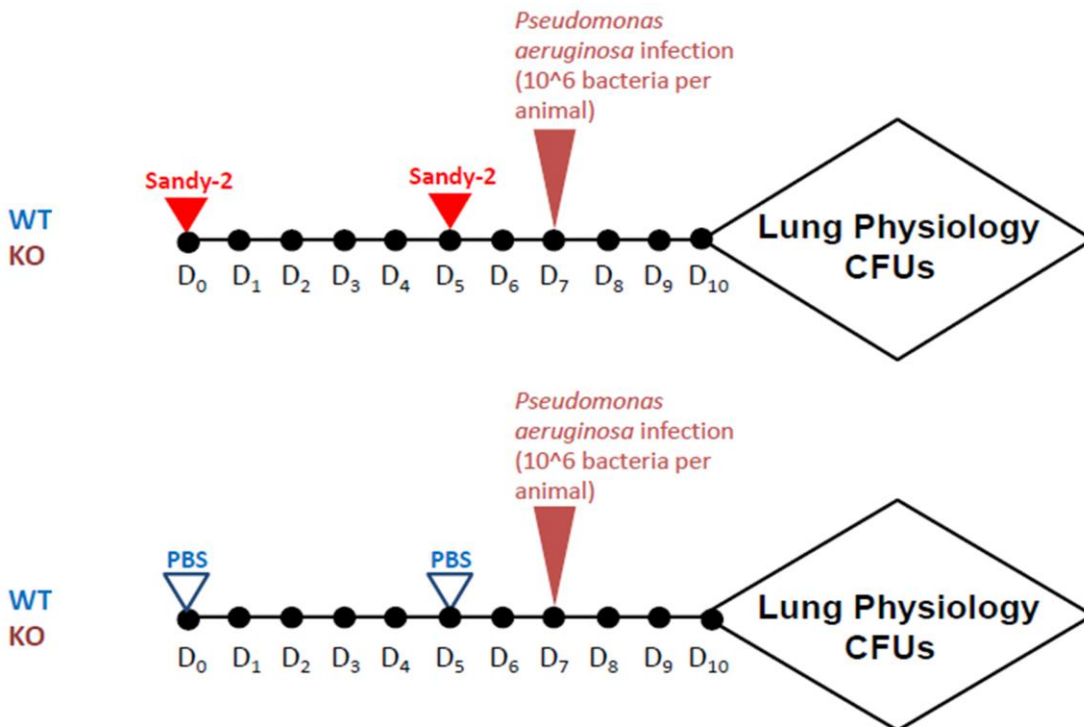


Figure 2.1 Experimental design/timeline of placebo (PBS) and Sandy-2 treatment followed by *P. aeruginosa* (PA508) infection.

We did not observe any adverse effects upon Sandy-2 treatment based on visual examination and measurement of weight even after repeated administration of the antibody (**Figure S2.1**). In order to examine whether an elevated level of BAFF is associated with the CFTR^{-/-} genotype, we analyzed the levels of BAFF by ELISA test in lung homogenates of CFTR homozygous knockout mice (CF-KO) and their wild-type littermates housed under standard conditions. With regards to BAFF, we did not observe any significant differences between the lungs of wild-type and CF-KO mice (**Figure 2.2A**). Next, we examined the levels of BAFF during pulmonary infection with *P. aeruginosa* in CF-KO mice. To this end, we measured the level of BAFF in CF-

KO mice and their wild-type littermates. Indeed, we found that infection with *P. aeruginosa* strongly increased the level of BAFF in the lungs of both wild-type and CF-KO mice and that this increase could be efficiently prevented with Sandy-2 treatment (**Figure 2.2 A**).

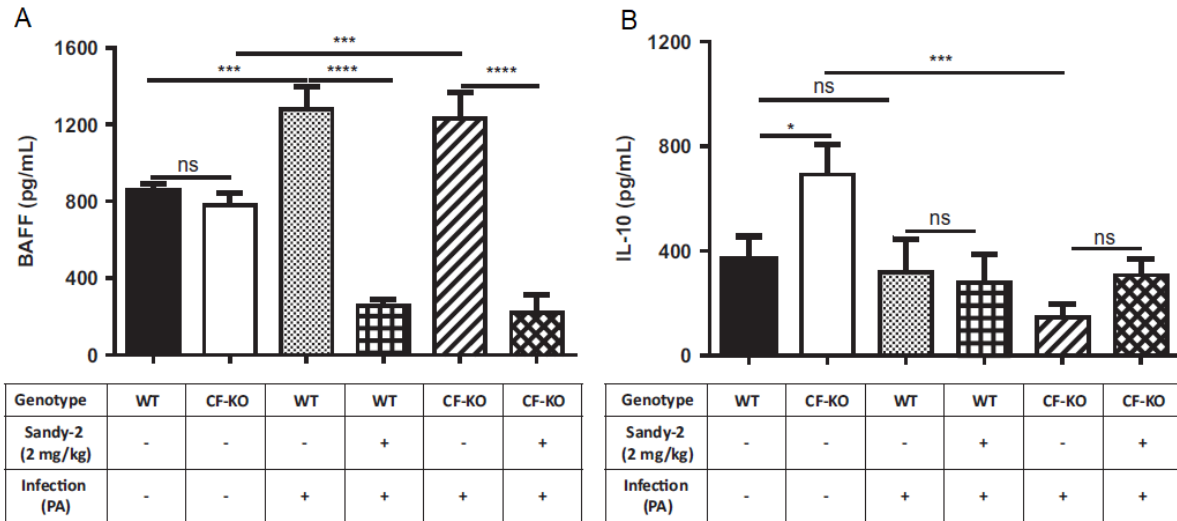


Figure 2.2 A. BAFF levels in uninfected WT and CFTR-KO mice, after *P. aeruginosa* (PA508) infection, and after Sandy-2 treatment. **B.** IL-10 levels in uninfected WT and CFTR-KO mice, after *P. aeruginosa* (PA508) infection, and after Sandy-2 treatment.

Each group consisted of n=3-5 WT or CFTR-KO mice which were either untreated and uninfected controls or treated with placebo (PBS) or Sandy-2 (2 mg/kg) and infected with PA508 strain of *P. aeruginosa* (10^6 CFU/animal). Data is represented as means \pm SD (* $p \leq 0.05$, ** $p \leq 0.01$, *** $p \leq 0.001$, **** $p \leq 0.0001$).

In order to test how the reduction of BAFF levels affects the ability of mice to control *P. aeruginosa* infection, we treated mice with Sandy-2 antibody two times prior to bacterial infection (**Figure 2.1**). There are several antibodies available to neutralize BAFF and we selected Sandy-2 as it was shown to be the most efficient antibody for the neutralization of BAFF (Kowalczyk-Quintas et al., 2016). Indeed, we observed that following the treatment with Sandy-2 mice BAFF levels were lower than in non-treated mice and even after infection BAFF levels were not increased in Sandy-2 treated mice and they remained lower than the levels observed in uninfected animals (**Figure 2.2 A**). Furthermore, we wanted to examine the level of IL-10 in the lung homogenates of infected and non-infected CF-KO mice and their corresponding wild-type controls. Interestingly, the levels of IL-10 were significantly higher in the lungs of non-infected

CF-KO mice compared with their wild-type and controls (**Figure 2.2 B**). Treatment of mice infected with *P. aeruginosa* with Sandy-2 did not lead to an increase in the level of IL-10 in wild-type animals and only resulted in slight increase of IL-10 in CF-KO mice.

2.4.2 BAFF depletion does not have significant impact on Breg cells

At baseline, we did not observe any significant difference in the presence of B cells between wild-type and CF-KO mice in the lungs (**Figure 2.3 A**) nor in the spleen (**Figure 2.3 B**). We also did not observe any significant difference in the number of CD19+IL10+ B cells between wild-type and CF-KO mice in the lungs nor spleen (**Figure 2.3 C**). As expected anti-BAFF treatment efficiently depleted the total numbers of B-cells both in the lungs and spleen of both infected and non-infected mice (**Figures 2.3 A and B**, respectively). As shown in **Figure 2.3 A**, 72 hours after infection, the relative percentage of B cells, dramatically decreased in the lungs of both wild-type and KO mice. Interestingly, in the spleens of Sandy-2 treated non-infected mice, the percentage of CD19+IL10+ cells was not significantly altered and it was even higher in the spleens of infected CF-KO mice compared with placebo-treated controls, as illustrated in **Figure 2.3 D**.

Overall our findings demonstrate the effect of BAFF depletion has much greater impact on the the IL10+ Breg population in the lungs but not in the spleen which does not seem to be dependent on pathways regulated by BAFF even during course of infection.

2.4.3 Treg cells are not significantly altered in CF-KO mice but they are strongly depleted by anti-BAFF treatment

BAFF-KO mice were shown to be fully depleted of B cells but did not show any significant difference in T cell counts (Schiemann et al., 2001). However, the impact on BAFF gene deletion on CD45+CD4+CD25+FoxP3+ Treg cells was not evaluated in that study. Therefore, we wanted to evaluate how depletion of BAFF impacts this subpopulation of T cells in CF mouse model which displays CF lung disease (Guilbault et al., 2005; Kent et al., 1997).

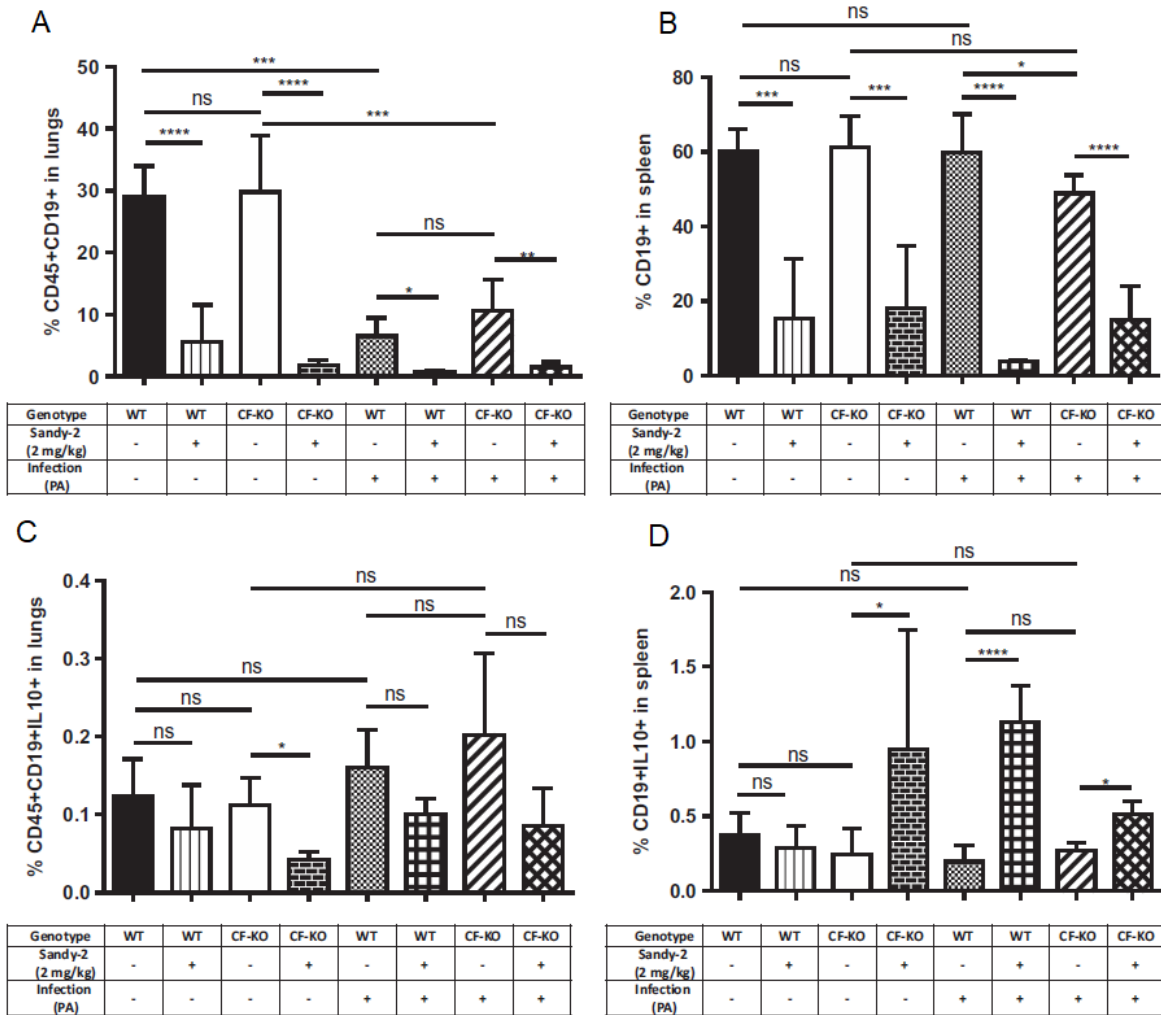


Figure 2.3 Anti-BAFF treatment efficiently depleted B-cells in both the lungs and spleen of infected and non-infected WT and CFTR-KO mice. A. % of CD45+CD19+ B cells in the lungs of uninfected WT and CFTR-KO mice, after Sandy-2 treatment, after *P. aeruginosa* (PA508) infection, and after Sandy-2 treatment of infected WT and CFTR-KO mice. **B.** % of CD19+ B cells in the spleen of uninfected WT and CFTR-KO mice, after Sandy-2 treatment, after *P. aeruginosa* (PA508) infection, and after Sandy-2 treatment of infected WT and CFTR-KO mice. **C.** % of CD45+CD19+IL10+ B cells in the lungs of uninfected WT and CFTR-KO mice, after Sandy-2 treatment, after *P. aeruginosa* (PA508) infection, and after Sandy-2 treatment of infected WT and CFTR-KO mice. **D.** % of CD19+IL10+ B cells in the spleen of uninfected WT and CFTR-KO mice, after Sandy-2 treatment, after *P. aeruginosa* (PA508) infection, and after Sandy-2 treatment of infected WT and CFTR-KO mice. Each group consisted of n=3-5 WT or CFTR-KO mice which were either untreated and uninfected controls or treated with placebo (PBS) or Sandy-2 (2 mg/kg) and infected with PA508 strain of *P. aeruginosa* (10^6 CFU/animal). Data is represented as means \pm SD (* $p \leq 0.05$, ** $p \leq 0.01$, *** $p \leq 0.001$, **** $p \leq 0.0001$).

We discovered that BAFF depletion selectively decreased the percentage of Treg cells in the lungs of both wild-type and CF-KO mice, but did not have any effect on the percentage of Tregs in the spleen (**Figures 2.4 A and 2.4 B**). These results are consistent with a previous finding that BAFF transgenic mice have increased the number of Treg cells (Walters et al., 2009). Also, a previous report (Hector et al., 2015) suggested that Treg cells may be decreased in the gut-corrected $Cftr^{tm1Unc} - Tg^{(FABPCFTR)}$ mouse model of cystic fibrosis. Our mouse model has been extensively characterized in several prior publications (Guilbault et al., 2005; Kent et al., 1997) which similarly to CF patient do not express CFTR in the gut tissue. We did not observe Treg cells to be decreased at baseline in the lungs our CFTR mouse model. Neither infection alone nor infection combined with Sandy-2 treatment had a significant effect on Treg population in the spleen of wild-type mice (**Figure 2.4 B**).

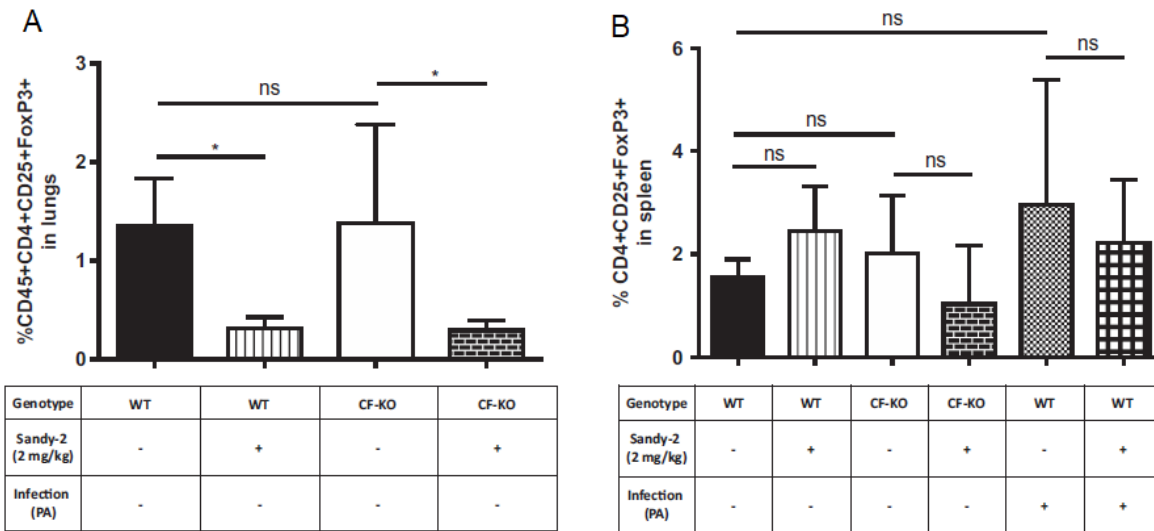


Figure 2.4 BAFF depletion selectively decreased the % of Treg cells in the lungs of both WT and CFTR-KO mice, but did not have any effect in the spleen. **A.** % of CD45+CD4+CD25+FoxP3+Treg cells in the lungs of uninfected WT and CFTR-KO mice, after Sandy-2 treatment, and after Sandy-2 treatment of infected WT mice. **B.** % of CD4+CD25+FoxP3+ Treg cells in the spleen of uninfected WT and CFTR-KO mice, after Sandy-2 treatment, after *P. aeruginosa* (PA508) infection and after Sandy-2 treatment of infected WT mice. Each group consisted of n=3-5 WT or CFTR-KO mice which were either untreated and uninfected controls or treated with placebo (PBS) or Sandy-2 (2 mg/kg) and infected with PA508 strain of *P. aeruginosa* (10^6 CFU/animal). Data is represented as means \pm SD (* $p \leq 0.05$, ** $p \leq 0.01$, *** $p \leq 0.001$, **** $p \leq 0.0001$).

2.4.4 Reducing the level of BAFF in both wild-type and CF-KO mice increases their susceptibility to infection

CFU counts in lung homogenates of CF-KO mice treated with PBS were significantly higher than in wild-type mice treated with PBS, consistent with our previously reported results (Guilbault et al., 2005). As shown in **Figure 2.5 A**, bacterial burden was significantly higher in CF-KO mice treated with Sandy-2 than in CF-KO mice treated with PBS, indicating that reduction of BAFF levels or depletion of B-cells in CF-KO mice impairs their ability to control infection. We also observed significant differences in CF counts between wild-type mice treated with PBS and Sandy-2. These results are consistent with the previously published findings that a temporal increase in systemic BAFF levels together with administration of heat-killed *P. aeruginosa* augments a pathogen-specific immune response and protects mice against a lethal pulmonary challenge with *P. aeruginosa* (Tertilt et al., 2009).

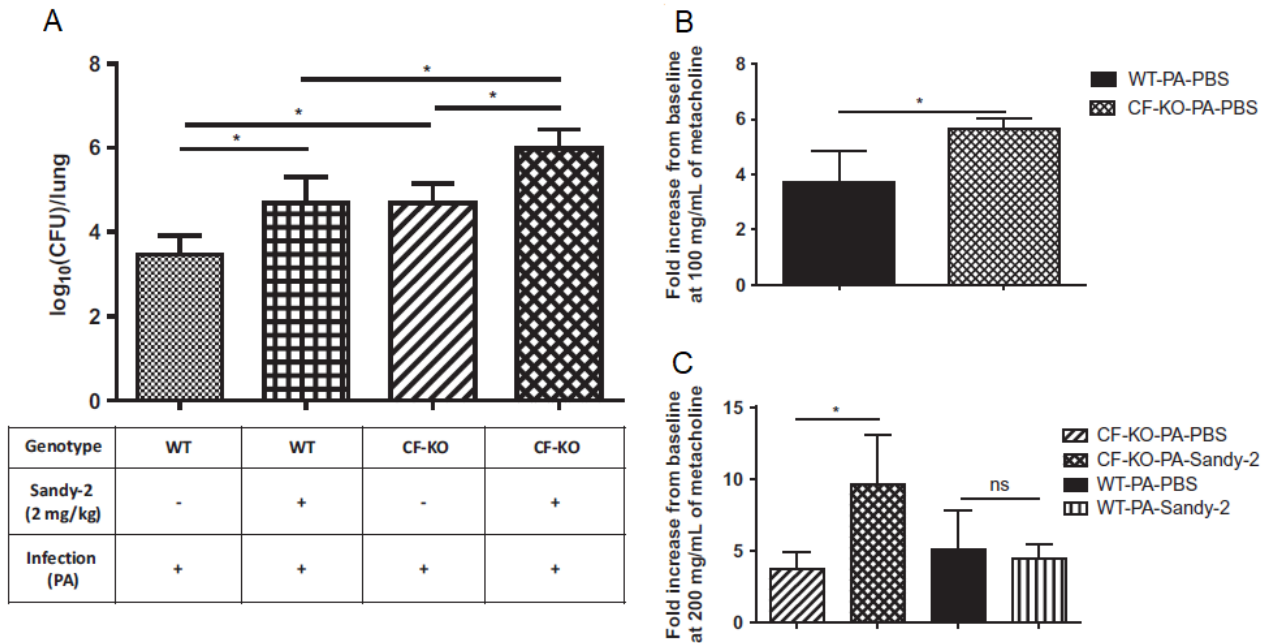


Figure 2.5 BAFF depletion exacerbates pulmonary infection and in CF-KO mice contributes to the increase of lung resistance **A.** Bacterial counts in the lungs of mice treated with Sandy-2 and placebo (PBS), 3 days after infection with PA508 strain of *P. aeruginosa*. **B.** Fold increase from baseline at 100 mg/ml methacholine in placebo-treated (PBS) CFTR-KO mice and their wild-type littermates after infection with *P. aeruginosa* (PA508). *continued...*

...continued C. Fold increase from baseline at 200 mg/ml methacholine in placebo treated (PBS) and anti-BAFF (Sandy-2) treated CFTR-KO mice after infection with *P. aeruginosa* (PA508). Each group consisted of n=3-5 WT or CFTR-KO mice which were either untreated and uninfected controls or treated with placebo (PBS) or Sandy-2 (2 mg/kg) and infected with PA508 strain of *P. aeruginosa* (10^6 CFU/animal). Data is represented as means \pm SD (* $p \leq 0.05$, ** $p \leq 0.01$, *** $p \leq 0.001$, **** $p \leq 0.0001$).

2.4.5 Reducing the level of BAFF in CF-KO but not in wild-type mice increases their lung airway resistance

One way to quantify the physiology of lungs is to test the lung responsiveness to methacholine, a non-selective muscarinic receptor agonist which is commonly used for diagnosing bronchial hyperreactivity. C57Bl/6 strain of mice are relatively resistant to methacholine compared to other strains, therefore the higher doses of methacholine needs to be used during the analysis of lung resistance. Therefore, the range of the methacholine doses suitable for assessment of lung physiology in this strain of mice was first established. In the subsequent experiments we have used 50 mg/ml to 200 mg/ml range of methacholine doses while assessing lung physiology in these mice. The dose of 100 mg was skipped in some experiments in order to avoid fatigue of the lungs. Our results demonstrated a statistically significant difference in the lung resistance between CF-KO and wild-type at the dose of 100 mg/ml of methacholine (**Figure S2.2 A** and **Figure 2.5B**). Therefore in the second set of experiments using mice infected with a clinical strain of *P.aeruginosa* (PA508) and treated with Sandy-2 antibody, we increased the doses of methacholine and the final dose reached 200 mg/ml of methacholine. As seen in **Figures S2.2B** and **Figure 2.5C**, airway resistance of infected CF-KO mice treated with Sandy-2 was significantly higher than the airway resistance of infected CF-KO mice treated with PBS as a control. BAFF depletion in wild-type mice treated with Sandy-2 (**Figure 2.5C**) has not affected the lung physiology to the same extent as we had observed in the CFTR-KO mice. Overall, our results clearly demonstrate physiological relevance of BAFF as a regulatory molecule in maintenance of lung physiology of CFTR-KO during the lung infection.

2.5 Discussion

In this study we analyzed physiological importance of BAFF in CF mouse model of pulmonary infection. To achieve this objective we have tested the effect of BAFF depletion in CF-KO mice and their wild-type littermates on their ability to control *P. aeruginosa* infection. We also analyzed the change in number of Breg and Treg cells.

Previous reports found significantly increased expression of BAFF in BAL fluid (Neill et al., 2014) and bronchial brushings (Ogilvie et al., 2011) from the lungs of CF patients. Since we did not observe such a difference at baseline in uninfected CF-KO mice and their wild-type counterparts, we believe that these differences were due to the chronic infection in the lungs known to be perpetually present in this population of patients (Zemanick and Hoffman, 2016). In the previously published study using BAL fluids collected from S489X (B6.129P2-Cftr^{tm1Unc}) mice and controls (Soltys et al., 2002), it was shown that the level of IL-10 were lower in CF mice than controls. In our study we used whole lung homogenate without collecting BAL fluid prior to collection, which we believe represents better the entire lung environment. Our findings demonstrated significantly increased levels of IL-10 in CF-KO mice at the baseline. We believe that our results indicate the existence of a low-grade simmering inflammation present in the CF-KO mice that triggers production of IL-10. We have previously described in detail the importance of IL-10 in the control of lung infection with *Pseudomonas* in female and male C57BL/6 mice (Guilbault et al., 2002). The IL-10 levels are typically increased during the first 24 hours of acute lung infection and eventually decrease as the infection gets resolved. In CF mice after 72h infection has still not been resolved. At this time point post infection, the levels of IL-10 were already down regulated in the infected CF-KO compared to uninfected CF-KO suggesting that resolution phase of inflammatory response in CF-KO is aberrantly regulated.

CD19⁺IL10⁺ cells were mostly unaffected by Sandy-2 treatment suggesting that anti-BAFF treatment selectively depletes B cells that are not producing IL-10 and partially spares the population of anti-inflammatory B-cells, particularly during inflammation. These results may be especially important with regards to the development of novel therapies targeting BAFF in systemic lupus erythematosus (SLE). Indeed, targeting BAFF by Belimumab[®] has shown promising results in the phase III trial of patients with SLE (Furie et al., 2011; Manzi et al., 2012; Navarra et al., 2011). However, there have been conflicting reports with regards to the role of IL-

10 in lupus, with some describing disease-promoting (Ishida et al., 1994; Ravirajan et al., 2004) whereas others describing its protective (Blenman et al., 2006; Yin et al., 2002) role in murine lupus models. Nevertheless, several studies have found that the level of IL-10 is significantly higher in patients with SLE and that the higher IL-10 levels correlate with higher severity of the disease, indicating that the elevated levels of circulating IL-10 in SLE patients cannot control constitutive inflammation present in these patients (Houssiau et al., 1995; Liu et al., 2011; Park et al., 1998). To the best of our knowledge, this is the first report describing selective depletion of B-cells that are not Breg cells using anti-BAFF treatment.

In a previous study, using $Cftr^{tm1\text{Unc}} - Tg^{(FABPCFTR)}$ mice in which CFTR expression is restored in the intestines, Hector et al. (Hector et al., 2015) found that Treg cells are significantly decreased in these KO mice compared with their WT controls. However, we did not observe such a difference using our CF-KO mice. Again, we believe that these differences are due to the simmering inflammation perpetually present in the lungs of CF-KO mice (Gosselin et al., 1998), which is partially corrected in the lungs of $Cftr^{tm1\text{Unc}} - Tg^{(FABPCFTR)}$ mice.

Furthermore, BAFF knockout mice are known to be fully devoid of B cells, whereas they show no changes in total T cell counts (Schiemann et al., 2001). However, our study provides new evidence that the depletion of BAFF strongly decreased the number of Treg cells in the lungs in non-infected mice. Given the controversial status of Treg cells in SLE, with some investigators reporting their beneficial role in the murine model of SLE (Scalapino et al., 2006), while others reporting increased number of Tregs in human SLE that correlated with the severity of the disease (Alexander et al., 2013; Golding et al., 2013), it will be of interest to further investigate the consequences of BAFF depletion by therapeutic antibodies in SLE.

Here we show that neutralizing BAFF is detrimental for the defense against *P. aeruginosa* infection. Indeed, the bacterial load measured as CFU per lung was significantly higher in both WT and CF-KO animals that were treated with Sandy-2 compared to placebo-treated controls. Still, the bacterial load was higher in CF-KO Sandy-2 treated animals than in WT mice treated with Sandy-2, probably because CF-KO mice are more susceptible to infection than their WT counterparts.

Finally, our results demonstrated that lung function during infection, assessed by measuring lung resistance, was more compromised during infection in Sandy-2 treated CF-KO mice compared to placebo-treated CF-KO mice. Although WT mice treated with anti-BAFF treatment became more susceptible to lung infection similarly as CF-KO mice, the effect of BAFF depletion at the level of lung physiology in WT was not significant. Lung resistance of CF-KO mice was very clearly affected by the depletion of this regulatory protein than lung resistance of WT mice.

In conclusion, in this study we demonstrate that elevated levels of IL-10 but not BAFF are an inherent feature of the lungs of CF-KO mice due to the persistent inflammation continuously present in these animals even in the absence of infection. Interestingly, depletion of BAFF does not affect IL-10 population of B cells as much as other subtypes of B cells but strongly depletes Treg cells in the non-infected lungs. Finally, depletion of BAFF impairs the ability of CF-KO mice to fight off *P. aeruginosa* lung infection and compromises lung function as demonstrated by higher bacterial load and higher methacholine-induced lung resistance.

2.6 Acknowledgements

We want to acknowledge financial support from by Anthera Inc. and Cystic Fibrosis Canada. We would like to thank Mr. Daniel Houle for technical assistance.

2.7 Author Contributions

D.G. and D.R. designed all experiments. D.R. and B.M. supervised the study. D.G. participated in all experiments and wrote the entire manuscript. S.T. and E.A. performed flow cytometry analyses. C.K. performed lung resistance measurements. J.S. performed all statistical analyses, prepared all the figures and helped with experiments. M.Y. participated in lung resistance studies.

2.8 Conflict of Interest

None declared by any of the authors in this study.

2.9 Supplementary Figures

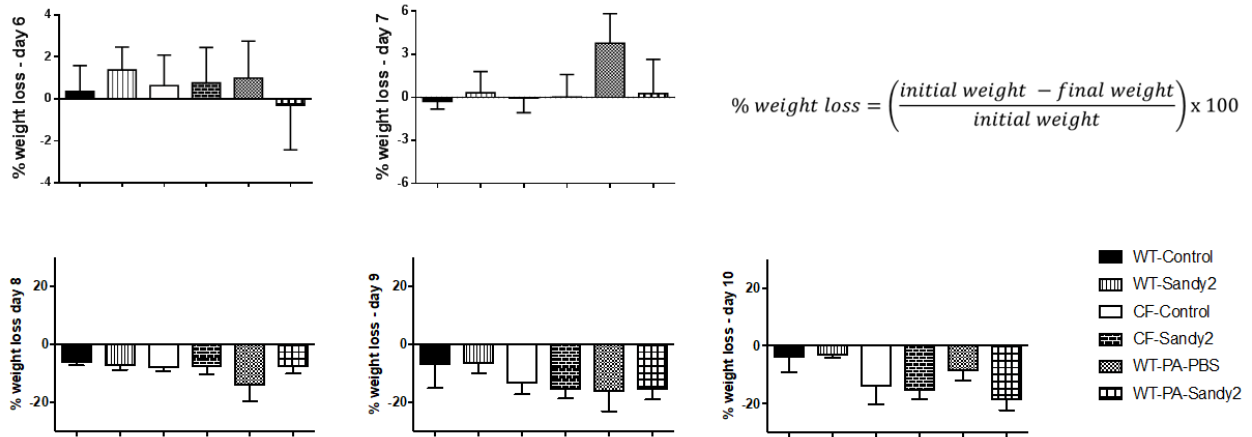


FIGURE S2.1 Changes in % weight loss of mice after Sandy-2 treatment (on days 6 and 7) and *P. aeruginosa* (PA508) infection (on days 8, 9 and 10). Weight loss % was calculated using the formula given above.

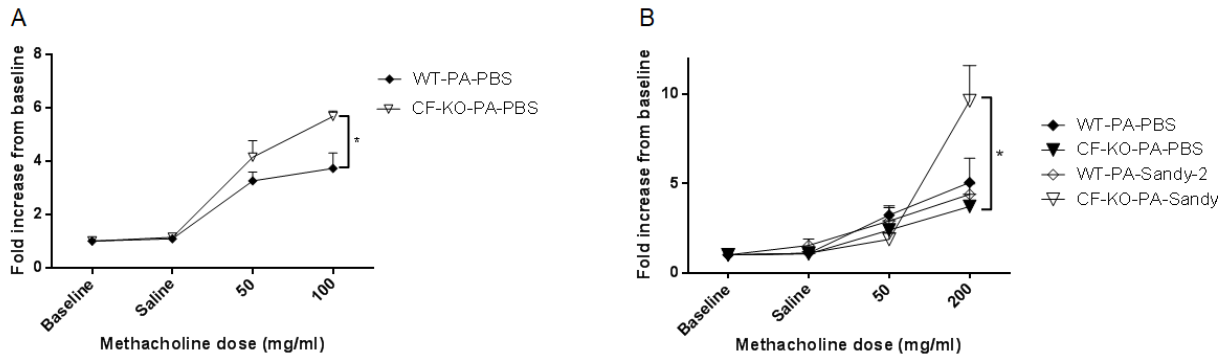


FIGURE S2.2 Reduction of BAFF level in CFTR-KO mice contributes to the increase of lung resistance during pulmonary infection with *P. aeruginosa* (PA508). **A.** Effect of placebo (PBS) on lung physiology (lung resistance at 100 mg/ml of methacholine) in CFTR-KO mice and their wild-type littermates after infection with *P. aeruginosa* (PA508). **B.** Effect of placebo (PBS) and anti-BAFF (Sandy-2) treatment on lung physiology (lung resistance at 200 mg/ml of methacholine) in CFTR-KO mice and their wild-type littermates after infection with *P. aeruginosa* (PA508). Each group consisted of n=3-5 WT or CFTR-KO mice which were either untreated and uninfected controls or treated with placebo (PBS) or Sandy-2 (2 mg/kg) and infected with PA508 strain of *P. aeruginosa* (10^6 CFU/animal). Data is represented as means \pm SD (* $p \leq 0.05$, ** $p \leq 0.01$, *** $p \leq 0.001$, **** $p \leq 0.0001$).

Chapter 3

Fenretinide differentially modulates the levels of long- and very-long-chain ceramides by downregulating Cers5 enzyme: evidences from bench to bedside

This chapter examines the levels of pro-inflammatory long-chain ceramides and anti-inflammatory very-long-chain ceramides in cystic fibrosis, the causality between the expression of CFTR and their levels as well as the effect of fenretinide on them. It was adapted from the published manuscript: Garić D, De Sanctis JB, Wojewodka G, Houle D, Cupri S, Abu-Arish A, Hanrahan JW, Hajduch M, Matouk E, Radzioch D. *Fenretinide differentially modulates the levels of long- and very long-chain ceramides by downregulating Cers5 enzyme: evidence from bench to bedside. J Mol Med (Berl)*. 2017 Oct; 95(10):1053-1064. (original article)

3.1 Abstract

Cystic fibrosis is the most common genetic disease whose symptoms may be alleviated but not fully eliminated. Ceramides have long been implicated in the inflammatory etiology of cystic fibrosis, with contradicting reports with regards to their role. Recently, significant biological and biophysical differences have been observed between long- and very-long-chain ceramides. This work reveals that long-chain ceramides are upregulated whereas very-long-chain ceramides are downregulated in cell lines, mouse animal model and patients with cystic fibrosis, compared with their controls. Treatment with fenretinide decreases the levels of long-chain ceramides and increases the levels of very-long-chain ceramides. Our results show that restoration of cystic fibrosis conductance regulator (CFTR) expression is associated with normalization of aberrant levels of specific ceramides. This demonstrates for the first time a correlation between CFTR protein expression and regulation of specific ceramide levels. Furthermore, using cystic fibrosis lung epithelial cell lines, we demonstrate that this effect can be attributed to the transcriptional downregulation of ceramide synthase 5 (*Cers5*) enzyme. We also discovered a partial synergism between fenretinide and zinc (Zn^{2+}), whose deficiency has been reported in patients with cystic fibrosis. Overall, in addition to having direct translational application, we believe that our findings contribute to the understanding of ceramide metabolism in cystic fibrosis, as well as other inflammatory diseases where imbalances of ceramides have also been observed.

3.2 Introduction

Despite the new personalized approaches, cystic fibrosis (CF) still remains the most common lethal genetic disease in Caucasians affecting on average 1 in 3000 newborns (Cutting, 2013). However, an amazing effect on life expectancy of patients with CF is anticipated from the correction of the effects of specific mutations in CFTR gene by a small-molecule therapy targeting the defective CFTR protein (Corvol et al., 2016). The disease is caused by various mutations in the CFTR gene (Cutting, 2015; Lucarelli et al., 2015) that abrogate its function as a chloride channel in the pulmonary epithelium, the most common being F508del that disrupts the folding and causes premature degradation of the CFTR protein. The absence of functional CFTR protein leads to the accumulation of viscous mucus in the lungs and to the colonization of opportunistic pathogens, the most common of which is *Pseudomonas aeruginosa* (*P. aeruginosa*). This initiates a vicious cycle of recurrent infections and inflammation that may be

sporadically interrupted by antibiotic treatment but that inevitably results in the permanent tissue damage which is the principal cause of morbidity in patients with CF (Cutting, 2013). Several studies have highlighted a connection between lipid rafts of lung epithelial cells (Grassme et al., 2003; Kowalski and Pier, 2004) and their ability to initiate signaling cascades that activate immune response against *P. aeruginosa*. Lipid rafts are micro-domains in the plasma membrane, highly enriched in cholesterol and sphingolipids that serve as the origin of receptor-mediated signaling events. Stimulation of receptors, such as CD95 or CD40, activates acid sphingomyelinase in the lipid rafts which produces ceramides by degrading sphingomyelins (Cremesti et al., 2001; Grassme et al., 2001). Ceramides induce the fusion of small sphingolipid-enriched rafts into larger membrane platforms that cluster receptor molecules and initiate receptor signaling (Bollinger et al., 2005). Ceramides are sphingolipids made of a sphingosine and an acyl chain of different lengths. It is this acyl moiety that confers specific and sometimes fundamentally different biophysical and biochemical properties to ceramides of different classes (Skolova et al., 2014). Recently it became clear that ceramides containing long acyl chain (LCCs), have opposing biological effects on cellular viability as compared to ceramides containing very long acyl chain (VLCCs) (Grosch et al., 2012; Hartmann et al., 2012). How ceramide species of different acyl-chain length exert opposing biological effects remains unclear. Specificity of the acyl chain length is achieved by the addition of acyl-CoA of different lengths (C14-C26) to sphinganine by ceramide synthases (Cers-es) located in the endoplasmic reticulum (Levy and Futerman, 2010). Of the six mammalian Cers-es, Cers2 represents the most ubiquitously expressed form and the one with the highest expression in lung epithelial cells (Petrache et al., 2013). Cers2 forms heterodimers with Cers5 that produce VLCCs, whereas Cer5:Cers5 homodimers produce LCCs and Cers2:Cers2 homodimers display very low or no catalytic activity (Laviad et al., 2012). Previously, it was shown that the failure to generate ceramide-enriched signaling platforms in lung epithelial cells leads to an uncontrolled inflammatory response, massive release of interleukin-1- β (IL-1 β) and septic shock-induced death of mice upon *P. aeruginosa* infection (Grassme et al., 2003). Treatment of infected mice with galactosylceramide was shown to enhance clearance of *P. aeruginosa* from infected lungs (Nieuwenhuis et al., 2002). We showed, for the first time, that both patients with CF and CF-knockout (CF-KO) mice have lower total amount of certain species of ceramides, as compared to their controls (Guilbault et al., 2009), the most abundant of which is C24:0. Treatment of CF-KO

mice with fenretinide (N-4-hydroxyphenyl-retinamide), normalized the level of ceramide species in the lungs and decreased bacterial burden after *P. aeruginosa* lung infection (Guilbault et al., 2008). Fenretinide is a semisynthetic retinoid that acts as an agonist of PPAR γ receptor (Harris et al., 2005; Lin et al., 2016), a well-known transcription factor that requires Zn²⁺ ions for its action (Meerarani et al., 2003). On the other hand, Teichgräber *et al* (Teichgraber et al., 2008) showed that accumulation of LCCs, specifically C16:0, causes age-dependent constitutive pulmonary inflammation, death of pulmonary epithelial cells and increases susceptibility of CF-KO mice to *P. aeruginosa* infection. However, in that report, C24:0, the most abundant of all species of ceramides, was not examined. As a secondary endpoint in a Phase Ib clinical trial of fenretinide, we measured the effect of the drug on specific ceramide species. Due to seemingly discordant reports regarding the role of ceramides in CF, we set out to more specifically examine the levels of specific ceramide species (LCCs vs. VLCCs), presumed to have opposing biological effects. Here we report the major differences in CF between the two best explored and most abundant representatives of LCCs (C16:0) and VLCCs (C24:0) as well as other ceramide species (**Figures S3.2-S3.8**) demonstrating the effect of fenretinide on both classes of ceramides; decreasing the LCCs and increasing diminished levels of VLCCs.

3.3 Methods and Materials

3.3.1. Cell culture

Pulmonary epithelial cell line CFBE41o- (CFTR-F508del/F508del) (Kunzelmann et al., 1993), further referred to as CFBE41o-(P) and CFBE41o- transduced with wild-type CFTR and further referred to as CFBE41o- (wt-CFTR) (Bebok et al., 2005), were grown as described in **Supplementary Materials and Methods** section. For each experiment, the 80% confluent monolayer was treated for 72h with 1.25 μ M fenretinide (AMRI Global, Albany, New York USA, formerly Grafton and Cedarburg Pharmaceuticals) and/or 12.5 μ M zinc sulfate (Sigma). Physiological concentrations of Zn²⁺ in human plasma are 10.1-17.9 μ M (Rink and Gabriel, 2001).

3.3.2 Measurement of mRNA expression by quantitative RT-PCR

RNA was extracted with Aurum Total RNA kit (Biorad) and quantitative real time PCR was done as described in **Supplementary Materials and Methods** section. Primers for ceramide

synthases were specifically designed to distinguish each member of the family from another one. Specificity of each primer set was confirmed by manual comparisons of primer sequences against cDNA sequences using ClustalOmega (EMBL) (**Table S3.1.**) and the specificity of RT-PCR products was confirmed by sequencing.

3.3.3 Western Blot

Protein extraction, measurement of protein concentration and SDS-PAGE, are described in **Supplementary Materials and Methods** section and the fast transfer of proteins to nitrocellulose membrane was done as previously described (Garic et al., 2013). The anti-Cers2 antibody against a 20-mer peptide of the C-terminal region (SRLLANGHPILNNNHPKND) was produced by Willecke laboratory, and extensively characterized, as previously described (Kremser et al., 2013). The anti-Cers5 antibody (ThermoScientific #PA-20647) used in this study was produced using as an immunogen a peptide of the 14 amino acids from the N-terminus of the protein that specifically distinguishes Cers5 from all other members of this family.

3.3.4 Mice

Inbred C57BL/6-Cftr^{+/-} were maintained in the animal facility of the McGill University Health Center Research Institute (MUHC-RI, Montreal, Canada) as described in **Supplementary Materials and Methods**. CF-KO mice used in the experiments were obtained by breeding C57BL/6-Cftr^{+/-} heterozygous mice. CF-KO mice and wild-type littermate controls were treated via intraperitoneal route with 10 mg/kg of fenretinide dissolved in 1% ethanol daily for 4 weeks and then sacrificed. Plasma and lungs were collected and analyzed from CF-KO mice and their wild-type littermate controls.

3.3.5 Patients and Clinical Trial

The Phase Ib clinical trial was conducted at MUHC, Montreal Chest Institute with the primary aim of evaluating the safety of fenretinide in CF patients (clinicaltrials.gov, NCT02141958). A total of 15 patients (**Table 3.1**) were treated with escalating multiple daily doses of a novel oral solid dosage form of fenretinide or matching placebo, randomized 3:1, respectively (Laurent Pharmaceuticals Inc., Montréal, Canada) during cycles of 21 consecutive days, spaced by minimum 7-days drug-free periods: 100 mg per day in Cycle 1 (C1), 200 mg per day in Cycle

two (C2) and 300 mg per day in Cycle three (C3) (**Figure S3.1**). One patient withdrew in C3 due to upcoming elective surgery. A design and a small number of CF patients enrolled in this Phase Ib double blind placebo-controlled design of safety trial have not allowed to randomize adequately the placebo group vs. drug treated group regarding their respective annual frequencies of exacerbations. Postulated therapeutic drug concentration range (1-2 μ M) was reached in the plasma of all drug treated patients in C3 (**Table 3.1**) as of Day 1. Blood samples were also collected from fifteen healthy volunteers to determine at the same time the reference ranges in healthy controls described in detail in **Table S3.2**. (Ethics review# A-16296.b, Proposal # SC090443 and Award # W81XWH-10-1-0858). All genotypes of patients are presented according to the traditional and new Human Genome Variation Society (HGVS) nomenclature (Berwouts et al., 2011).

3.3.6 Measurement of ceramide levels by mass spectroscopy

Ceramide levels were assessed in blood and lung tissue collected from CF mice and in blood from clinical trial participants. Plasma and lung samples were preserved in 1 ml of 1 mM of butyl-hydroxyanisole (BHA) in a chloroform/methanol solution (2:1 vol/vol) (Folch et al., 1957; Van Handel and Zilversmit, 1957). Ceramides were analyzed using high-performance liquid chromatography coupled with mass spectrometry (LC/MS/MS) after their initial separation on thin layer chromatography and silica extraction as previously described (Guilbault et al., 2008).

3.3.7 Statistical Analysis

All statistical analyses were performed using GraphPad (GraphPad, San Diego, CA, USA). For the cell lines, statistical significance of differences was evaluated using unpaired *t*-test with Welch's correction. For mice, statistical significance of differences was evaluated using a one-way ANOVA test. For the comparisons of patients with healthy controls (HC), unpaired *t*-test with Welch's correction was used, while Wilcoxon's matched-pairs test was used to evaluate the statistical significance of differences within patients before and after fenretinide or placebo treatment. We always refer to the significance represented by * sign (or multiple * signs) above the particular line. In all cases only two conditions are compared at the time, even when there are multiple conditions on the graph.

Patient Number	Sex	Age (years)	BMI (kg/m ²)	Genotypes		Fen (μM)	C24:0 (pmol/nmol of phosphate) at the baseline	C24:0 (pmol/nmol of phosphate) in C3 after fenretinide administration	C16:0 (pmol/nmol of phosphate) at the baseline	C16:0 (pmol/nmol of phosphate) in C3 after fenretinide administration	
				Traditional Nomenclature	HGVS Nomenclature						
High Responders (C24:0 ↑, C16:0 ↓)											
CF3	M	29	18.9	ΔF508/ΔF508	c.[1521_1523delCTT(+)]1521_1523delCTT	2.278	3.9	4.2	1.2	0.92±0.21 (C3 vs baseline; p=0.03)	
CF5	M	22	23.5	ΔF508/ΔF508	c.[1521_1523delCTT(+)]1521_1523delCTT	4.594	4.5	5.2	0.9		
CF7	M	18	19.0	F508/621+1G-T	c.[1521_1523delCTT(+)]489+1G>T	3.326	3.9	5.9	1.1		
CF10	M	25	19.4	ΔF508/ΔF508	c.[1521_1523delCTT(+)]1521_1523delCTT	1.978	4.3	5.2	1.3		
CF14	M	33	19.0	ΔF508/ΔF508	c.[1521_1523delCTT(+)]1521_1523delCTT	N/A*	3.2	4.9	1.5		
Partial Responders											
CF1	M	36	24.4	ΔF508/ΔF508	c.[1521_1523delCTT(+)]1521_1523delCTT	1.008	3.5	3.5	1.7	1.0±0.43 (C3 vs baseline; p=0.41)	
CF6	M	18	21.0	ΔF508/G85E	c.[1521_1523delCTT(+)]254G>A	1.702	4.2	5.7	0.8		
CF9	M	36	24.9	ΔF508/3849+10kbC-T	c.[1521_1523delCTT(+)]3718-2477C>T	3.981	4.0	4.9	0.6		
CF12	M	57	16.5	ΔF508/R352G	c.[1521_1523delCTT(+)]1054C>G	2.966	3.3	5.3	0.8		
CF15	F	52	19.7	ΔF508/ΔF508	c.[1521_1523delCTT(+)]1521_1523delCTT	N/A*	5.3	4.5	1.1		
Placebos											
CF4	F	21	24.2	ΔF508/ΔF508	c.[1521_1523delCTT(+)]1521_1523delCTT	0	3.8	3.3	0.9	0.8±0.2 (C3 vs baseline; p=0.50)	
CF8	M	29	26.6	ΔF508/S549N	c.[1521_1523delCTT(+)]1646G>A	0	4.8	6.0	0.8		
CF11	F	31	23.6	ΔF508/unknown	c.[1521_1523delCTT(+)]?	0	4.5	5.0	0.7		
CF13	M	29	21.2	ΔF508/711+1G>T	c.[1521_1523delCTT(+)]579+1G>T	0	3.8	5.6	0.9		
HC (n=15)	M/F*	41.6 ± 12.9	24.7±3.1	WT/WT	c.[-]=[-]	0		5.72±0.4	N/A	0.44±0.20	N/A

Table 3.1 Demographic data of patients and healthy controls and response of patients to fenretinide in the third cycle of phase Ib clinical trial. BMI - Body Mass Index; HGVS - Human Genome Variation Society; Fen - Fenretinide; N/A - Not Applicable *Footnote:* * Male sex : 46 %; # According to the approved ethical protocol for clinical trial phase Ib pharmacokinetic analysis was approved for 12 patients, including placebos.

For patients who are followed in time Wilcoxon's matched-pairs test was used to evaluate the statistical significance of differences within patients before and after fenretinide or placebo treatment. In case when ANOVA was used (only for mice), Bonferroni correction was applied. In all cases, the threshold of statistical significance was set at $p \leq 0.05$.

3.4 Results

3.4.1 Mice

3.4.1A Very-Long-Chain Ceramide species are downregulated and Long-Chain Ceramide species are upregulated in CF-KO mice compared with WT controls

We have previously shown that VLCCs, in particular C24:0, are constitutively downregulated in CF-KO mice and CF patients compared with their WT-counterparts and Healthy Controls, respectively (Guilbault et al., 2009). Here, we aimed to closely examine the level of each ceramide species from the available panel of ceramides by mass spectroscopy. Our analysis revealed that shorter ceramide species with side-chain length from 14 to 18 carbons (C14:0, C16:0, C18:0), although much less abundant compared to VLCCs, are significantly up-regulated in the plasma and lungs of CF-KO mice compared with their wild-type controls. On the other hand, VLCCs (C22:0, C24:0, C26:0) were significantly downregulated in both plasma and lungs of CF-KO mice compared with WT controls (**Figure 3.1 A-D; Figures S3.2. and S3.3**). Recent studies done by Petrache *et al* (Petrache et al., 2013) suggest that the increase of LCCs concomitant to *Cers2* knockout leads to constitutive inflammatory phenotype in the lungs. However, biological significance of these changes as well as the molecular mechanisms behind them remain to be fully elucidated.

3.4.1B Fenretinide normalizes the levels of ceramides in CF-mice by downregulating long-chain ceramide species and upregulating very-long chain ceramide species

In order to assess the effect of fenretinide on distinct ceramide species, we treated mice daily with 10 mg/kg of fenretinide for 28 days. We assessed the levels of ceramides in plasma (**Figure 3.1 A and C**) and lungs (**Figure 3.1 B and D**) of treated mice. Our analysis showed that fenretinide consistently downregulated the levels of C16:0 and other LCCs in both wild-type and CF-KO mice; however, the magnitude of this effect was much larger in CF-KO mice. Additionally, fenretinide treatment corrected aberrantly low levels of C24:0 and most of the other VLCCs in CF-KO mice (**Figure 3.1 A-D, Figure S3.2, and Figure S3.3**).

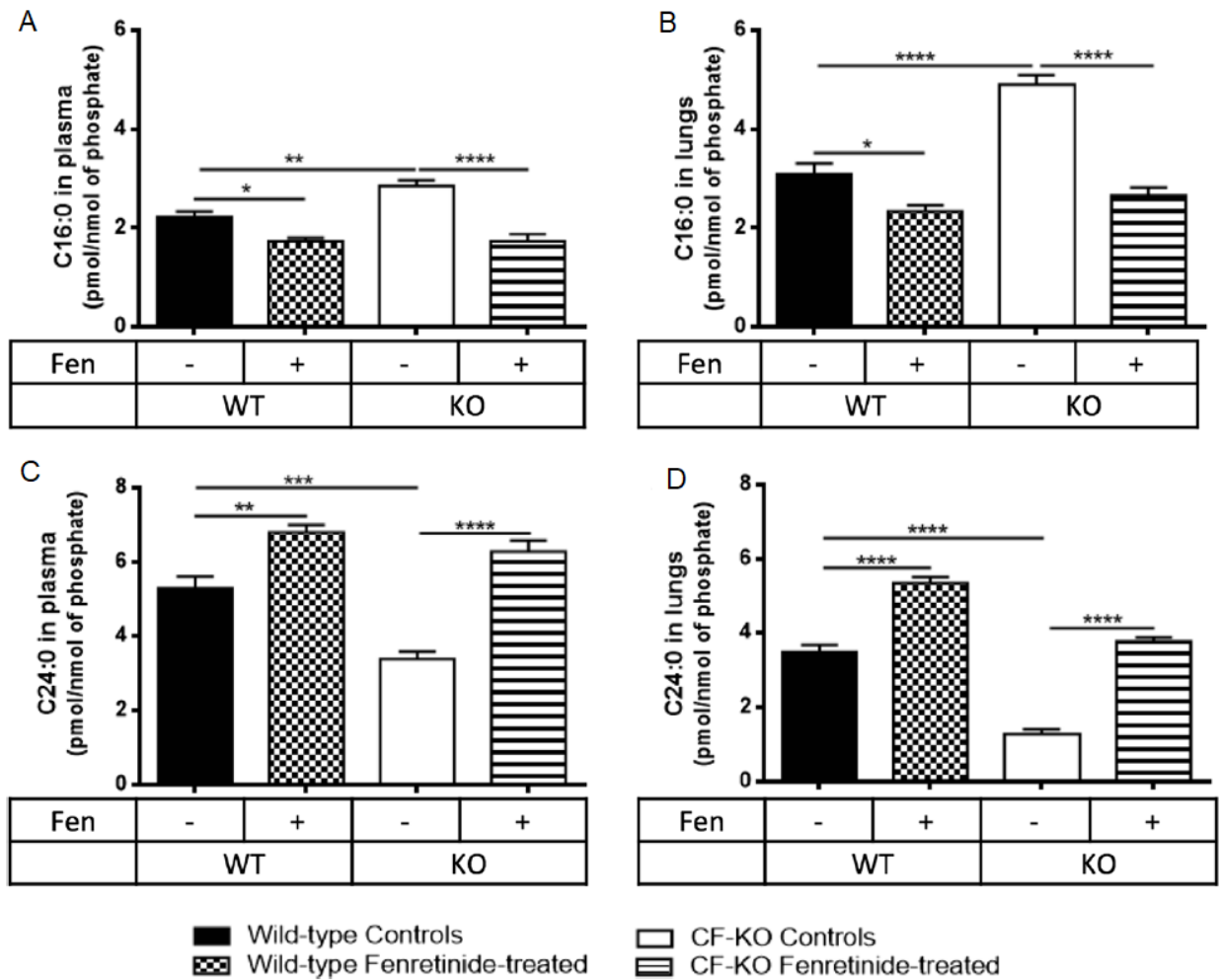


Figure 3.1 Levels of C16:0 and C24:0 ceramides in plasma and lungs of CF-KO mice and wild-type littermates treated with fenretinide and vehicle-treated (ethanol) controls. C16:0 is upregulated in the plasma (A) and lungs (B), whereas C24:0 is downregulated in the plasma (C) and lungs (D) of CF mice (n=7 for both ethanol and fenretinide treated group) compared with their WT littermates (n=8 for both fenretinide and ethanol treated group). In all cases these imbalances were reversed with fenretinide (Fen) treatment. For mice, statistical analysis was done using one-way ANOVA test. Bars show means \pm SD (* $p \leq 0.05$, ** $p \leq 0.01$, *** $p \leq 0.001$, **** $p \leq 0.0001$)

3.4.2 CF Patients

LCCs are upregulated and VLCCs are downregulated in patients with CF compared with healthy controls and this imbalance is corrected by fenretinide treatment

In order to assess whether the effects of fenretinide can be translated from mice to humans, we compared the levels of ceramides in the plasma of HC, patients with CF at baseline before the start of the Phase Ib clinical trial and at the end of the third cycle of fenretinide treatment (C3) where a therapeutically effective plasma concentration was achieved. Indeed, levels of C16:0 were significantly higher in the plasma of patients with CF prior to the study treatment, compared with HC (**Figure 3.2 A and 2B**). On the other hand, the levels of C24:0 and most other VLCCs were significantly lower in the plasma of patients with cystic fibrosis compared with HC (**Figure 3.2 C and 2D, Figure S3.4**). During our analysis, we found that the fifteen patients enrolled (10-11 patients treated with active drug, depending on the drug treatment cycle) segregated in two groups with regards to the changes in ceramide levels: high responders in which both C24:0 and C16:0 were corrected, and partial responders in which only C24:0 was corrected. Therefore, we grouped the patients receiving fenretinide into high responders (HR) (n=5), partial responders (PR) (n=5) alongside patients on placebo (P) (n=4), as outlined in **Table 3.1**. In HR CF patients, the ceramide imbalance was corrected by 300 mg per day fenretinide treatment. The high levels of C16:0 and other LCCs were downregulated by fenretinide, whereas the low levels of C24:0 and other VLCCs were increased (**Figure 3.2 A and 2C, Figure S3.4**). In the PR group of patients, in which usually only one of the two ceramide species of interest was corrected, mixed responses were also observed for several other ceramide species (**Figure S3.6, Table 3.1**). All but one patient (RDZ #15) had increased C24:0 in response to fenretinide treatment, however this patient has been the only patient with the C24:0 levels within the normal range at baseline. The increased levels of C16:0 at baseline in this patient seem to be brought down within the range observed in HC. In the group of partial responders, C16:0 decreased in two patients (RDZ #1 and #15), and increased in three patients (RDZ #6, #9 and #12). Importantly, we did not see any significant changes in the placebo group neither in C24:0 (p=0.18; C3 vs. baseline) nor C16:0 (p=0.50; C3 vs. baseline) (**Figure 3.2 B and D, Figure S3.5**). Due to the small sizes of both drug-treated and placebo-treated groups and variabilities between patients enrolled in Phase Ib trial with regards to their lung function and frequency of exacerbation parameters at the baseline and genotypes, true comparisons would only be possible in the Phase II trial.

3.4.3 Lung epithelial cell lines

In order to understand the mechanism behind the changes in LCCs and VLCCs induced by treatment with fenretinide, in the pulmonary epithelium of mice and patients, we used a well characterized lung epithelial cell line homozygous for F508del CFTR mutation developed from

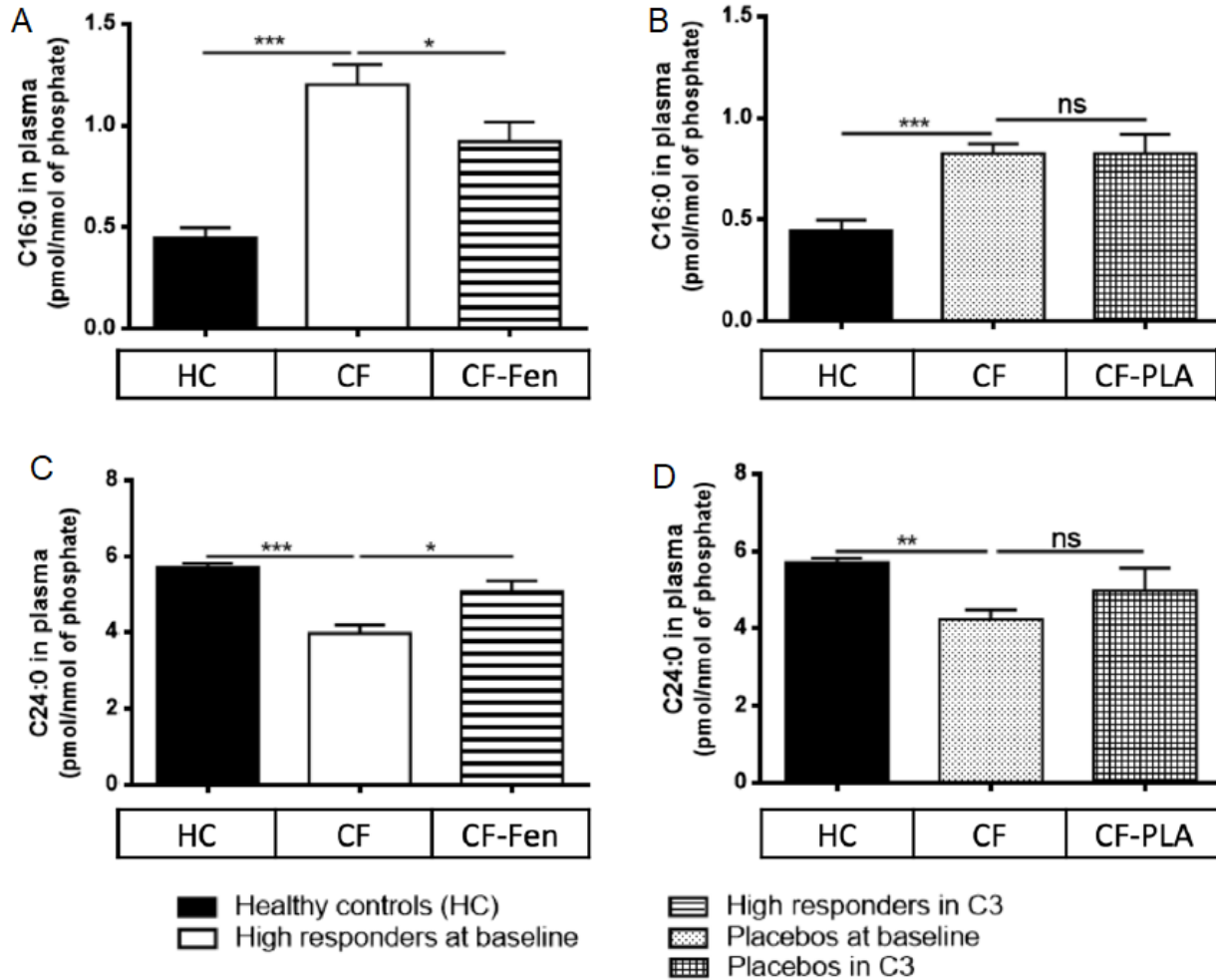


Figure 3.2 C16:0 is higher in the plasma of both patients to be treated (A) (n=5) and placebos (PLA; n=4) (B) at the baseline compared to healthy controls (HC, n=15). Fenretinide (Fen) treatment decreases the level of C16:0 in 5 patients (A), but not in placebos (B). C24:0 is lower in the plasma of both patients to be treated (C) and placebos (D) at the baseline compared to healthy controls. Fenretinide treatment increases the level of C24:0 in 5 patients (C) but not placebos. For patients, unpaired t-test with Welch's correction was used to compare patients at the baseline with healthy controls while Wilcoxon's matched-pairs test was used to evaluate the differences seen in patients before and after the treatment with fenretinide. Bars show means \pm SD (* $p \leq 0.05$, ** $p \leq 0.01$, *** $p \leq 0.001$, **** $p \leq 0.0001$).

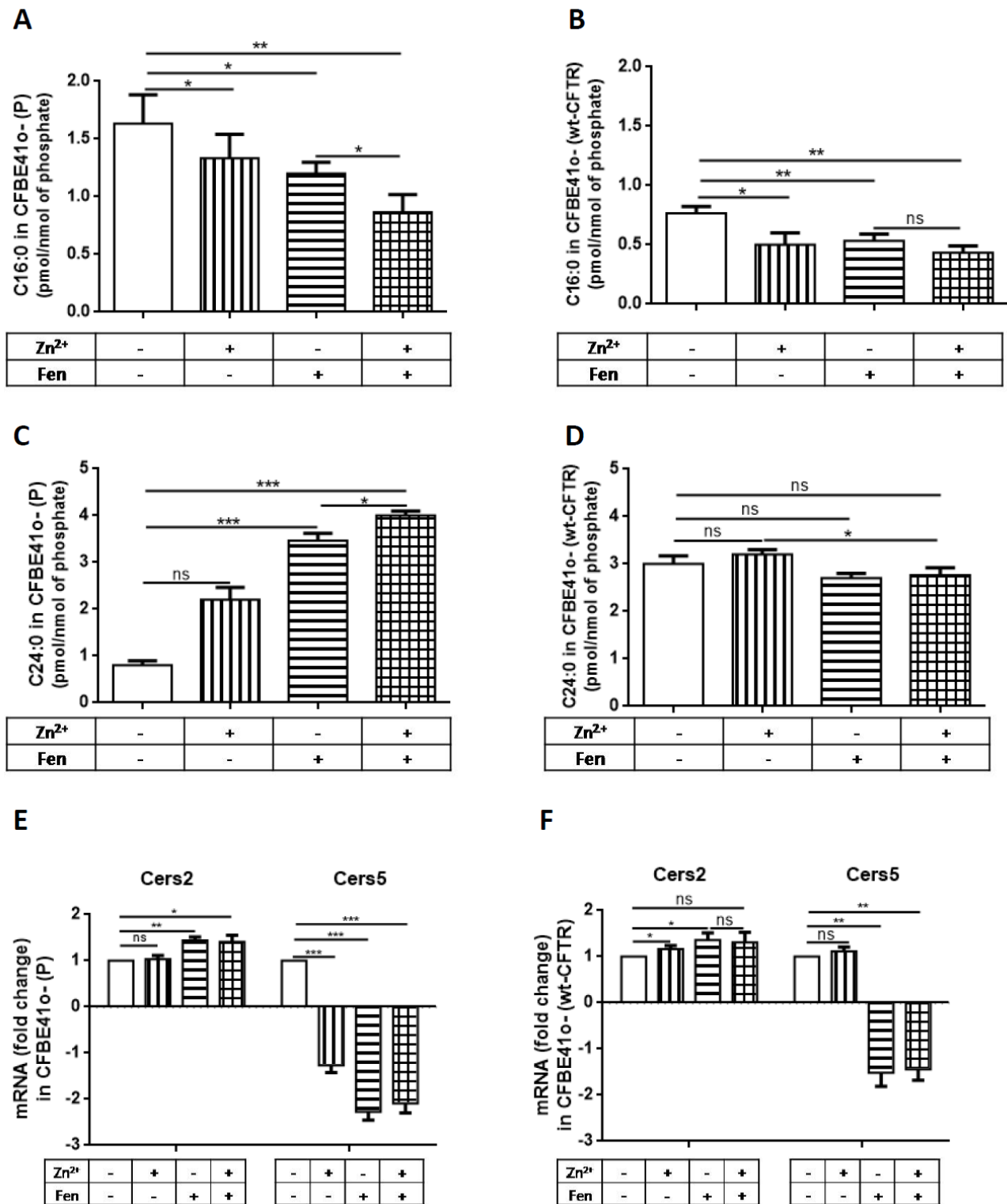


Figure 3.3 The level of C16:0 in CFBE41o- (P) cells is partially decreased by the treatment with either Zn²⁺ or fenretinide alone but is strongly decreased in the combined treatment with fenretinide and Zn²⁺ (A). Level of C16:0 is significantly lower in CFBE41o- (wt-CFTR) cells than in its parental line and is even further brought down by fenretinide and Zn²⁺ treatment (B). *continued...*

continued... Level of C24:0 is not affected by the treatment with Zn^{2+} alone but is strongly upregulated by the treatment with either fenretinide (Fen) alone or combined treatment with Zn^{2+} and fenretinide (C). Level of C24:0 is significantly higher in CFBE41o- (wt-CFTR) cells than in its parental line and is not affected by fenretinide and/or Zn^{2+} treatment (D). In CFBE41o- (P) (F508del/F508del), treatment with fenretinide slightly (fold change = 1.43) but significantly (** $p \leq 0.01$) upregulates the expression of mRNA for Cers2 enzyme whereas treatment with Zn^{2+} alone does not have any significant effect and combined treatment with fenretinide has only marginal effect (fold change = 1.40, * $p \leq 0.05$) on the expression of Cers2 mRNA (E). On the other hand, both fenretinide alone and fenretinide combined with Zn^{2+} had a strong and statistically significant effect on the expression of Cers5 enzyme (E), whereas Zn^{2+} alone had a marginal (fold change = -1.26;*** $p \leq 0.001$) effect on the expression of Cers5. In CFBE41o- (wt-CFTR) cells, mRNA for Cers2 was slightly affected by fenretinide and Zn^{2+} treatment, whereas combined treatment had no effect (F). On the other hand, mRNA for Cers5 was strongly downregulated by fenretinide (fold change = -1.52) and combined treatment (fold change = -1.44) whereas Zn^{2+} alone did not have any significant effect (F). Data are represented as means \pm SD (* $p \leq 0.05$, ** $p \leq 0.01$, *** $p \leq 0.001$, **** $p \leq 0.0001$). All experiments were done in triplicates (n=3).

CF bronchial epithelial cells by Gruenert and colleagues, further referred to as parental CFBE41o-(P) cell line (F508del/F508del). We also used a derivative cell line produced by transduction with lentiviral vector directing the expression of wild-type CFTR as previously described (Bebok et al., 2005) and further referred to as CFBE41o-(wt-CFTR). CFBE41o-(P) cells inherently express high levels of C16:0 ceramide and following treatment with fenretinide, the levels decreased. Interestingly, treatment with Zn^{2+} ions alone was also able to decrease the levels of C16:0 ceramides (Figure 3.3 A), and these effects were enhanced in the combination with fenretinide. On the other hand, CFBE41o- (wt-CFTR) cell line expresses much lower level of C16:0 in comparison with its parental cell line CFBE41o-(P), and these levels are brought down even further with fenretinide and Zn^{2+} treatment (Figure 3.3 B).

Also, CFBE41o-(P) cell line expresses low levels of C24:0. Following the treatment with fenretinide, the levels of C24:0 ceramide increased, reaching the range close to those observed in human and mouse controls (Figure 3.3 C). When the cells were treated with both fenretinide and with Zn^{2+} ions, a further increase of the C24:0 levels was observed.

On the other hand, correction of CFTR protein deficiency in CFBE41o- (wt-CFTR) cell line by transfection of lentiviral vector encoding functional CFTR protein, resulted in much higher levels of C24:0 compared to CFBE41o-(P), and these were not further modified by Zn²⁺ and fenretinide treatment (**Figure 3.3 D**).

The fact that CFBE41o- (wt-CFTR) cell line expresses much lower levels of C16:0 and much higher levels of C24:0 than its CF counterpart with mutated CFTR seems to suggest a causal link between CFTR expression, and ceramide metabolism deserves further exploration

Since Cers-es are the only enzymes of the ceramide pathway specific for acyl or side chain length, we hypothesized that fenretinide may affect the levels of LCCs and VLCCs by transcriptionally regulating some of these enzymes. The most abundant ceramides in the lungs are C16:0 and C24:0, respectively synthesized by Cers5:Cer5 homodimers and Cers5:Cers2 heterodimers (Laviad et al., 2012).

Indeed, in both CFBE41o- (P) and CFBE41o-(wt-CFTR) cells fenretinide downregulated Cers5 enzyme at the level of mRNA (**Figure 3.3E and 3.3F, respectively**) and these changes were reflected at the level of Cers5 protein as well (**Figure 3.4**). On the other hand, in both cell lines, fenretinide slightly upregulated the levels of Cers2 enzyme at mRNA level (**Fig 3.3E and 3.3F**) however no changes were seen at Cers2 protein level (**Figure 3.4**). Overall, by downregulating the levels of Cers5, without significantly affecting the level of Cers2 enzyme, the formation of Cers5:Cers5 homodimers is disadvantaged in respect to Cers2:Cers5 heterodimers after fenretinide and/or Zn²⁺ treatment. Therefore, the production of C16:0 is decreased and the production of C24:0 is increased (**Figure 3.5 C**).

3.5 Discussion

The importance of lipid rafts in the activation of signaling pathways leading to regulated host response against acute *P. aeruginosa* infection has long been recognized (Grassme et al., 2003). However, there have been conflicting reports with regards to the role of specific ceramide species within lipid rafts. All ceramides consist of a sphingosine backbone of 18 carbons and an acyl chain of variable length (**Figure 3.5 A**), and depending on the length of this acyl chain, they can be grouped in LCCs (C₁₄-C₂₀) and VLCCs (C₂₂-C₂₆).

Teichgräber *et al* (Teichgraber et al., 2008) previously reported that age-dependent accumulation of LCCs (specifically C16:0 species; see [22] Supplementary Information) causes inflammation, cell death and increases susceptibility of CF-KO mice to *P. aeruginosa* infection. However, there were no results reported on C24:0 or any other VLCCs levels in their study. Our group showed that CF-KO mice have lower content of VLCCs, specifically C24:0 species, and that this deficiency could be corrected by treatment with fenretinide (Guilbault et al., 2008). Importantly, fenretinide treatment of CF-KO mice significantly decreased bacterial burden upon *P. aeruginosa* infection (Guilbault et al., 2008).

Hartmann and colleagues investigated the role of ceramides and reported that effects of LCCs are opposite of the effects of VLCCs on the growth of human breast and colon cancer cells, with LCCs having pro-apoptotic effect while VLCCs exhibiting anti-apoptotic effect (Hartmann et al., 2012). In line with these reports, Brodlie *et al* reported that C16:0, C18:0 and C20:0 ceramides, but not C22:0, were upregulated in CF patients with advanced stage lung disease; the study did not include analysis of C24:0 levels (Brodlie et al., 2010).

Interestingly, Pewzner-Jung *et al* recently reported (Pewzner-Jung et al., 2014) that the "sphingoid very-long chain bases" were able to kill a broad spectrum of bacteria at nanomolar to low micromolar concentrations including *P. aeruginosa* and even *Burholderia cepacia*. Further, they demonstrated that very long chain sphingoid bases are abundantly expressed on the luminal surface of the nasal epithelium and lungs of HCs but were almost undetectable in CF patients. Importantly, restoration of surface sphingoid very-long chain bases by inhalation reversed susceptibility of CF mice and cured existing *P. aeruginosa* infection.

The exact molecular mechanism behind the opposing effects of the ceramides containing fatty acids of different side-chain lengths is still unclear. Biophysical investigations done by Školova *et al* suggest that C16:0, particularly its acyl chain, is less organized than the very long chain of C24:0 and therefore may be disruptive for the formation of lipid rafts and other sphingomyelin-containing structures in the cell, especially when overproduced (Školova et al., 2014).

Here we aimed to explore how fenretinide treatment impacts the level of specific ceramide species and to gain insight into the molecular mechanisms responsible for these effects. We have systematically examined the level of LCCs and VLCCs in the CF patients, CF mice and a CF cell

line treated with fenretinide and their controls. Indeed, our results demonstrate that VLCCs including C22:0, C24:0, C24:1, C26:0 and C26:1 were consistently downregulated in CF mice and CF patients and LCCs including C14:0 and C16:0 were upregulated both in CF mice and CF patients compared to controls. We did not observe consistency in modulation of the level of C18:0 and C20:0 ceramides among CF patients, CF mice CF cell line treated with fenretinide (Figures S3.2, S3.3, S3.4, S3.7 and S3.8). The synthesis of C18:0 and C20:0 is controlled by Cers1 and Cers4, two enzymes which do not seem to be modulated by fenretinide treatment (see Table A1.0 in the APPENDIX). We further went on to examine the mechanism responsible for the observed changes in LCCs and VLCCs caused by fenretinide treatment. The steady state levels of ceramides in the cell are critically dependent on the amount of ceramides produced by either *de novo* (from palmitate and serine) or salvage pathway (from sphingosine) and the amount of ceramides consumed by their incorporation into either sphingomyelins or complex glycosphingolipids (Figure 3.5 B).

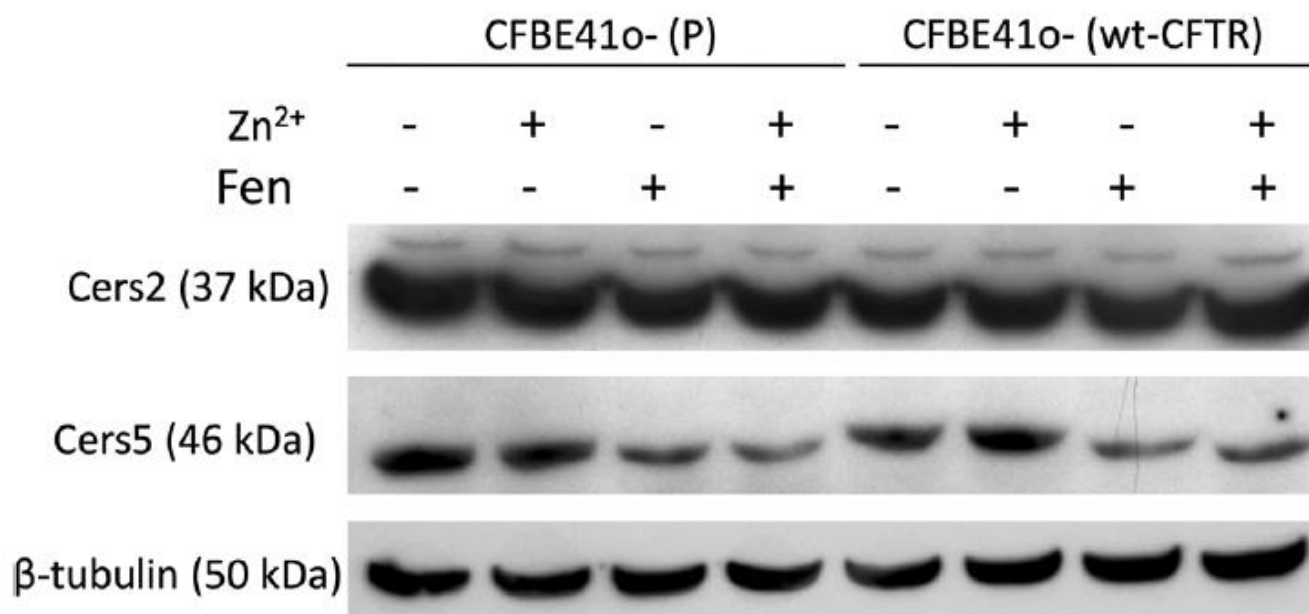


Figure 3.4 Measurement of protein levels by Western blot in CFBE41o-(P) (F508del/F508del) and CFBE41o-(wt-CFTR) cells shows that Cers2 is not affected in either of these cell lines by fenretinide and/or Zn²⁺ treatment. On the other hand, the levels of Cers5 are decreased in both CFBE41o-(P) (F508del/F508del) and CFBE41o-(wt-CFTR) cells following treatment with fenretinide and combined treatment with fenretinide and Zn²⁺, but are unaffected by treatment with Zn²⁺ alone.

As can be seen in **Figure 3.5 B**, Cers-es are the critical enzymes involved in both pathways of ceramide production. There are six mammalian Cers-es (Cers1-6) and they catalyze addition of the side chain to the dihydrosphingosine in the *de novo* pathway or sphingosine in the salvage pathway. Therefore, they are the only enzymes in both pathways that are specific with regards to the length of the side chain. In lungs, of the six mammalian Cers-es, the predominantly expressed forms are Cers2, Cer4 and Cers5 (Petrache et al., 2013). In order to produce LCCs, Cers5 enzymes homodimerize, while the production of VLCCs requires heterodimerization between Cers5 and Cers2 enzymes (Laviad et al., 2012). Therefore, production of VLCCs depends on the balance between enzymes produced by different isoforms of Cers-es. Based on the observed changes in the levels of specific ceramides, we examined how treatment with fenretinide affects the level of Cers-es. As a model we used the well characterized human bronchial epithelial cell line CFBE41o-(P) and its derivative overexpressing wild-type CFTR, CFBE41o-(wt-CFTR).

We showed that fenretinide treatment leads to significant downregulation of Cers5 at mRNA and protein levels whereas Cers2 mRNA levels and protein levels were not significantly affected (**Figures 3.3 and 3.4**). Therefore, by downregulating Cers5 levels, fenretinide changes the ratio of Cers5/Cers2 enzymes in favour of the formation of Cers5:Cers2 heterodimers over Cers5:Cers5 homodimers. Consequently, LCC species are decreased and VLCC species are increased upon fenretinide treatment. There are multiple explanations on how fenretinide treatment might downregulate the mRNA level of Cers5. For example, it might upregulate the expression of the repressor for Cers5 gene or upregulate miRNA that binds to Cers5 mRNA.

Fenretinide has been known to exert some of its multiple cellular effects by acting as a ligand for PPAR γ receptor (Kocdor et al., 2009). On the other hand, PPAR γ receptor has long been recognized as a potential therapeutic target in CF and its function has been known to be severely reduced in CF (Dekkers et al., 2012; Ollero et al., 2004; Perez et al., 2008). This deficiency is most likely caused by the lack of endogenous PPAR γ ligands like 15-keto-PGE2, linoleic acid and DHA (Dekkers et al., 2012). Indeed, pharmacological activation of PPAR γ by rosiglitazone has been shown to confer some therapeutic benefits in CF mice (Harmon et al., 2010). Unfortunately, rosiglitazone has been withdrawn from the market due to the side effects leading to the elevated risk of heart attacks in diabetic patients (Nissen and Wolski, 2007).

Additionally, zinc deficiency has been described in children affected by CF (Yadav et al., 2014) and supplementation of zinc decreased respiratory infections in children with CF (Abdulhamid et al., 2008; Van Biervliet et al., 2008b). Interestingly, zinc ions are required for the transcriptional actions of PPAR γ receptor (Meerarani et al., 2003; Reiterer et al., 2004). Dekkers and colleagues proposed that PPAR γ should be considered as a therapeutic target in CF (Dekkers et al., 2012). Therefore, we decided to test the effect of fenretinide alone, zinc (Zn²⁺) treatment alone and a combined treatment of zinc (Zn²⁺) and fenretinide on CF lung epithelial cells. Indeed, this combination resulted in an additive effect in the downregulation of LCCs and upregulation of VLCCs, warranting further investigation of the potential therapeutic value of using a combined treatment with zinc (Zn²⁺) and fenretinide.

In conclusion, this study demonstrates that fenretinide normalizes the imbalance among several specific ceramide species in CF patients and CF mice. Interestingly, our data show for the first time a strong correlation between CFTR expression and levels of C16:0 and C24:0 ceramides. Specifically, we report that fenretinide upregulates the levels of VLCCs which were reported to have anti-inflammatory and anti-apoptotic role in 80% of patients and downregulates the levels of LCCs which were reported to have pro-inflammatory effect and pro-apoptotic role in epithelial cells in 70% of patients (Grosch et al., 2012; Hartmann et al., 2012). It is possible that the differences in expression of gene modifiers in partial responders might influence the regulation of *Cers5* gene in response to fenretinide or that the 21 days of treatment was not sufficient to change the levels of these phospholipids. We cannot exclude the possibility that the patient's nutritional habits, individual to each patient, and the differences in the degree of zinc (Zn²⁺) levels among patients also had a significant impact on the variability of the corrective effect on specific species of ceramides among patients. We were unable to assess the potential influence of these factors because the clinical trial was not designed for this purpose. Our findings suggest that the therapeutic effect might be enhanced if fenretinide treatment is accompanied by zinc supplementation in the diet. Furthermore, our findings might also be of relevance in designing potential therapies for diseases other than CF, where an imbalance between LCCs and VLCCs has also been documented like atopic dermatitis and eczema (Imokawa et al., 1991; Janssens et al., 2012; Park et al., 2012).

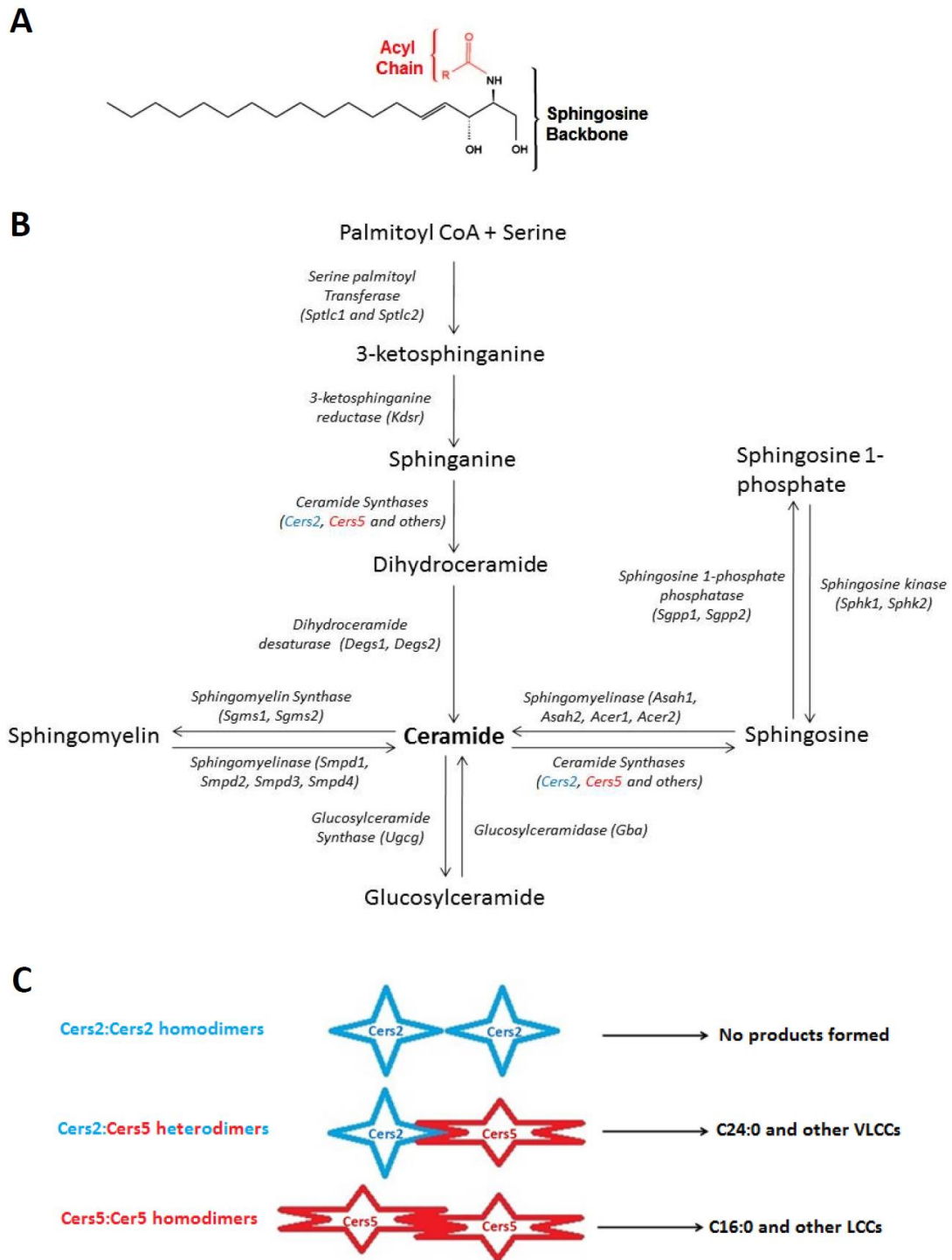


Figure 3.5 Overview of ceramide structure, biosynthesis, and dimerization based mechanism of action. Ceramides consist of sphingosine backbone of 18 carbons originating from palmitic acid and an acyl chain of different lengths (A). Ceramide synthases are the key enzymes in the metabolism of sphingolipids, involved in both de novo and salvage pathway of ceramide production (B) (adapted and modified from (Laviad et al., 2012; Levy and Futerman, 2010)). *continued...*

...continued. Cers2:Cers2 homodimers display very low or no catalytic activity, Cers2:Cer5 heterodimers produce very long-chain ceramides, the most prominent of which is C16:0 whereas Cers5:Cers5 homodimers produce long-chain ceramides, the most prominent of which is C24:0 (c). Cers2 levels are constitutively expressed in most tissues at relatively high levels (Laviad et al., 2012; Levy and Futerman, 2010). After downregulation of Cers5 by fenretinide, the formation of Cers5:Cers5 homodimers is disadvantaged in respect to Cers2:Cers5 heterodimers and the formation of very long-chain ceramides is therefore favored.

3.6 Acknowledgements

We would like to thank Dr. Klaus Willecke and Dr. Andreas Bickert from Molecular Genetics, Life and Medical Sciences (LIMES)-Institute, University of Bonn for providing a highly specific antibody against Cers2 protein. We would like to thank late Dr. Dieter Gruenert from University of California, San Francisco for providing CFBE41o- parental cell line. We would like extend our acknowledgements to Radu Pislariu, Patrick Colin, Jean-Marie Houle and Irenej Kianicka (Laurent Pharmaceuticals Inc.) for the critical review of this manuscript. The study reports data from an Investigator-sponsored clinical trial by the McGill University Health Center (MUHC).

3.7 Author Disclosure

The study reports data from an Investigator-sponsored clinical trial by the McGill University Health Center (MUHC).GW received funding from the Frederick Banting and Charles Best Canada Graduate Scholarships Doctoral Award from the Canadian Institutes of Health Research and QC-IRDI and FRQ (MITACS) funding. JBdS received funding from FONACIT (G2005000389). DR and EM received funding from Ministère du DéveloppementÉconomique, de l'Innovationet de l'Exportation (MDEIE/MESRST), MSBiValorisation and Cystic Fibrosis Canada. A.A.A. received fellowship support from the Natural Sciences and EngineeringResearch Council of Canada (NSERC), Cystic Fibrosis Canada (CFC), and Groupe de Recherche Axé sur la Structure des Protéins (GRASP). J.W.H. was funded by the Canadian Institutes of Health Research(CIHR) and the Cystic Fibrosis Foundation. The funders had no role in study design, data collection and analysis, decision to publish, or preparation of the manuscript. DR, JDS and GW hold USA, Canadian and European patents applications (Method for correcting a lipid

imbalance in a subject; PCT/ CA/2006/002041). DR has been one of the founders of Laurent Pharmaceuticals Inc.

3.8 Supplementary Materials and Methods

3.8.1 Cell culture

Pulmonary epithelial cell lines, parental CFBE41o- (CFTR-F508del/F508del) CFBE41o- constitutively overexpressing CFTR, were grown in Eagle's Minimal Essential Medium (Invitrogen) supplemented with 10% Fetal Bovine Serum (Wisent), 2 mM L-glutamine(Wisent), 50 U/ml penicillin (Wisent) and 50 µg/ml streptomycin (Wisent), in a 5% CO₂-95% air incubator at 37°C. For each experiment, cells were 80% confluent at the beginning of the treatment and they were treated for 72h with 1.25 µM fenretinide (Grafton, formerly Cedarburg Pharmaceuticals, Grafton, WI, USA) and/or 12.5 µM zinc sulphate (Sigma), as indicated. Physiological concentrations of zinc in plasma are 10.1-17.9 µM [25]. For each subsequent step, monolayer of cells was washed two times with PBS and lysed in an appropriate buffer.

3.8.2 Measurement of mRNA expression by quantitative RT-PCR

For RNA extraction, cells were lysed in Lysis Buffer supplied in the Aurum Total RNA kit (Biorad), and RNA was extracted according to manufacturer's instructions. cDNA was produced using iScript RT Supermix RT-qPCR (Biorad) and quantitative real time PCR was done with SSoFastEvaGreen Supermix (Biorad) with an annealing temperature of 54°C. The annealing temperature of the qPCR reaction was set to 54°C, due to the somewhat lower melting point of our primers. The final concentration of primers was 400 nM and 15 ng of cDNA was used in a 20 µl reaction volume. Primers for ceramide synthases (Cers) were specifically designed to distinguish each unique Cers. From the initially tested three different housekeeping genes (GAPDH, β-actin and β-tubulin), β-tubulin was selected as a housekeeping gene because it did not fluctuate between the samples. Specificity of each primer set was confirmed by manual comparisons of primer sequences against cDNA sequences using Clustal Omega (EMBL) (**Table S3.1**). In order to calculate the fold change, formula $2^{(-\Delta\Delta C_t)}$ was used where $\Delta\Delta C_t = (Ct(\text{target gene, test}) - Ct(\text{reference gene, test})) - (Ct(\text{target gene, control}) - Ct(\text{reference gene, control}))$. Whenever fold change was less than 1, negative inverse value was plotted ($-1/(2^{(-\Delta\Delta C_t)})$).

3.8.3 Western Blot

For protein extraction, cells were lysed in homemade RIPA buffer (50 mM Tris, 150 mM NaCl, 50 mM NaF, 0.2 mM Na₃VO₄, 0.1% SDS, 2 mM EDTA, 1% NP-40, 0.5% Na-deoxycholate, pH=7.4) with freshly dissolved tablet of protease inhibitors (Roche). Concentration of protein was determined using BCA Protein Assay Kit (Thermo Scientific) and proteins were denatured in 2x urea buffer (40 mM Tris, 1 mM EDTA, 9M urea, 5% (w/v) SDS, 0.01% (w/v) bromophenol blue, 5% (v/v) 2-mercaptoethanol, pH=8.0), 35 µg of total protein was loaded on a gel and proteins were resolved by SDS-PAGE. Proteins were transferred onto nitrocellulose membrane using semi-dry transfer and the fast semi-dry transfer buffer (1X, final) containing 48mM Tris, 15 mM HEPPS with freshly added sodium bisulfite (1 mM final), EDTA (1.0 mM final) and N, N-dimethylformamide (1.3 mM final) as previously described [26]. Membranes were incubated with primary antibodies: against Cers2 (developed by Willecke laboratory, University of Bonn), against Cers5 (ThermoScientific # PA5-20647) and against β-tubulin (3F3-G2; sc-53140). Subsequently, membranes were incubated with secondary antibodies: goat anti-mouse (IgG-HRP (sc-2005) and Pierce Gt anti-RB IgG (H+L) Super Clonal secondary antibody (Thermo Scientific #A27036). Finally, membranes were developed using chemiluminescent kit (Biorad, #170-5060).

3.8.4 Mice

Inbred C57BL/6-Cftr^{+/-} were maintained in the animal facility of the McGill University Health Center Research Institute (MUHC-RI, Montreal, Canada). All pups were genotyped within two weeks of age. Mice were kept in cages with corn bedding (Anderson, Bestmonro, LA) and were fed NIH31-modified irradiated mouse diet (Harlan Teklan, Indianapolis, IN). CF-KO mice and their wild-type littermate controls were treated with 10 mg/kg of fenretinide dissolved in 1% ethanol solution of ethanol intraperitoneally for 4 weeks and sacrificed. All experiments were conducted in accordance with the Canadian Council on Animal Care guidelines and approved by the Facility Animal Care Committee of the MUHC-RI.

Table S3.1 Sequences of primers for quantitative real-time PCR

Gene	Sense	Sequence (5' to 3')
Human β -tubulin	F	TACTACAATGAAGCCACAG
	R	CAGACTGACCAAATACAAAG
Human Cers2	F	CCTCAATAACAACCATCGTA
	R	TAGTTCCTTGGCTTTATGC
Human Cers5	F	GCTGTTCACGGTCTTATAC
	R	ATAGAGTCACTGAAGAGGTT

Table S3.2 Levels of ceramides in healthy controls

Sample #	Sex	Age	Weight (kg)	Height (cm)	BMI (kg/m ²)	Genotype	Ceramide species (pmol/nmol of phosphate)																Sphingosine species	Sphingosine 1P species	Ceramide 1P
							C14:0	C16:0	C18:0	C18:1	C20:0	C20:1	C20:4	C22:0	C22:1	C24:0	C24:1	C26:0	C26:1	DH					
211B	F	59	70	160	27.3	WT/WT	0.9	0.8	0.8	0.6	0.6	1	2.4	1.2	1.4	6	0.3	0.5	1.1	4.6	4.5	4.7	1.4		
218B	M	56	77	172	26	WT/WT	0.4	0.3	0.5	0.6	0.4	1.5	1.8	1.3	1.2	5.7	0.3	0.1	2.5	4.2	4.4	4.7	2.1		
219B	M	46	55	162	21	WT/WT	0.3	0.3	0.6	0.5	0.3	1.7	1.7	1.2	1.2	5.3	0.4	0.2	2.6	4.2	4.5	5.1	2		
221B	F	30	64	162	24.4	WT/WT	0.6	0.5	0.7	0.5	0.7	1.1	2	1.4	1.5	6.2	0.1	0.3	1.2	5	4.7	5	1.9		
222	F	27	61	172	20.6	WT/WT	0.7	0.6	0.6	0.4	0.6	0.8	2.3	1.1	1.1	4.9	0.4	0.4	1	4.3	4.2	3.9	1.6		
223	M	32	67	176	21.6	WT/WT	0.8	0.6	0.8	0.4	0.8	1.2	2	1.2	1.7	5.9	0.3	0.2	1.4	5.1	5	4.6	2.2		
224	M	61	74	179	23.1	WT/WT	0.8	0.3	0.6	0.6	0.6	1.3	2.1	1.3	1.6	5.8	0.2	0.4	1.3	5.2	4.8	5.3	2.2		
225	F	37	60	168	21.3	WT/WT	0.6	0.4	0.5	0.4	0.5	1.4	2.4	1.1	1.3	5.5	0.2	0.2	2.7	4.6	4.5	5.4	1.9		
226	F	33	55	165	20.2	WT/WT	0.7	0.9	0.9	0.4	0.5	1.1	1.9	1.3	1.3	6.5	0.4	0.6	1.3	5	5.2	4.1	1.5		
227	M	51	90	178	28.4	WT/WT	0.5	0.4	0.8	0.3	0.4	0.9	2.1	1.5	1.6	5.5	0.2	0.4	1.4	5.5	5.3	4.8	2		
228	M	32	90	180	27.8	WT/WT	0.6	0.3	0.7	0.2	0.4	0.7	2.6	1.3	1.3	5.3	0.3	0.5	1.2	4.8	5.5	4.3	2.1		
229	F	21	83	180	25.6	WT/WT	0.5	0.4	0.6	0.5	0.5	1	2.1	1.2	1.5	5.5	0.5	0.4	1.4	5.2	6.2	5	2.3		
230	F	59	71	162	27.1	WT/WT	0.7	0.3	0.5	0.3	0.6	0.9	2.3	1	1.4	6.2	0.4	0.5	1.5	5.4	5.8	4.8	1.8		
231	F	43	79	171	27	WT/WT	0.4	0.4	0.4	0.4	0.6	0.8	2.5	1.2	1	5.8	0.6	0.7	1.2	5.3	5.7	3.8	2.2		
232	M	38	95	180	29.3	WT/WT	0.3	0.2	0.8	0.3	0.5	0.9	1.8	1.1	0.9	5.7	0.4	0.6	1.3	5.1	6.1	4	2.6		
	averag	41.7	72.7	171.1	24.7		0.59	0.45	0.65	0.43	0.53	1.09	2.13	1.23	1.33	5.72	0.33	0.40	1.54	4.90	5.09	4.63	1.99		
	SD=	13.0	12.8	7.5	3.2		0.18	0.20	0.15	0.12	0.13	0.29	0.27	0.13	0.23	0.41	0.13	0.17	0.56	0.43	0.65	0.51	0.32		
F (%)=	53.3																								
M (%)=	46.7																								

Figure S3.1 CONSORT diagram



CONSORT 2010 Flow Diagram

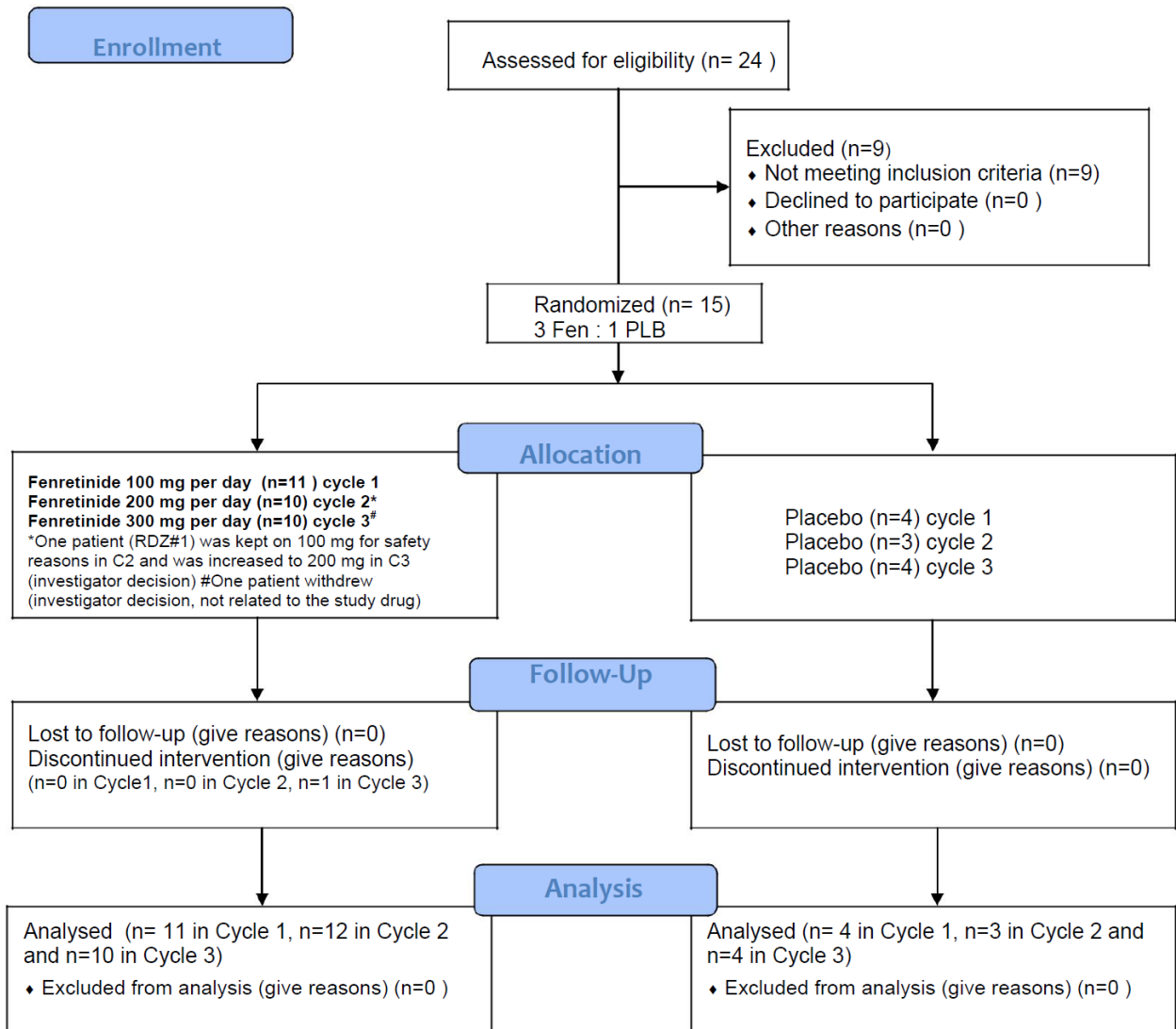


Figure S3.2 Levels of ceramides other than C16:0 and C24:0 in the plasma of CF and WT mice before and after fenretinide treatment

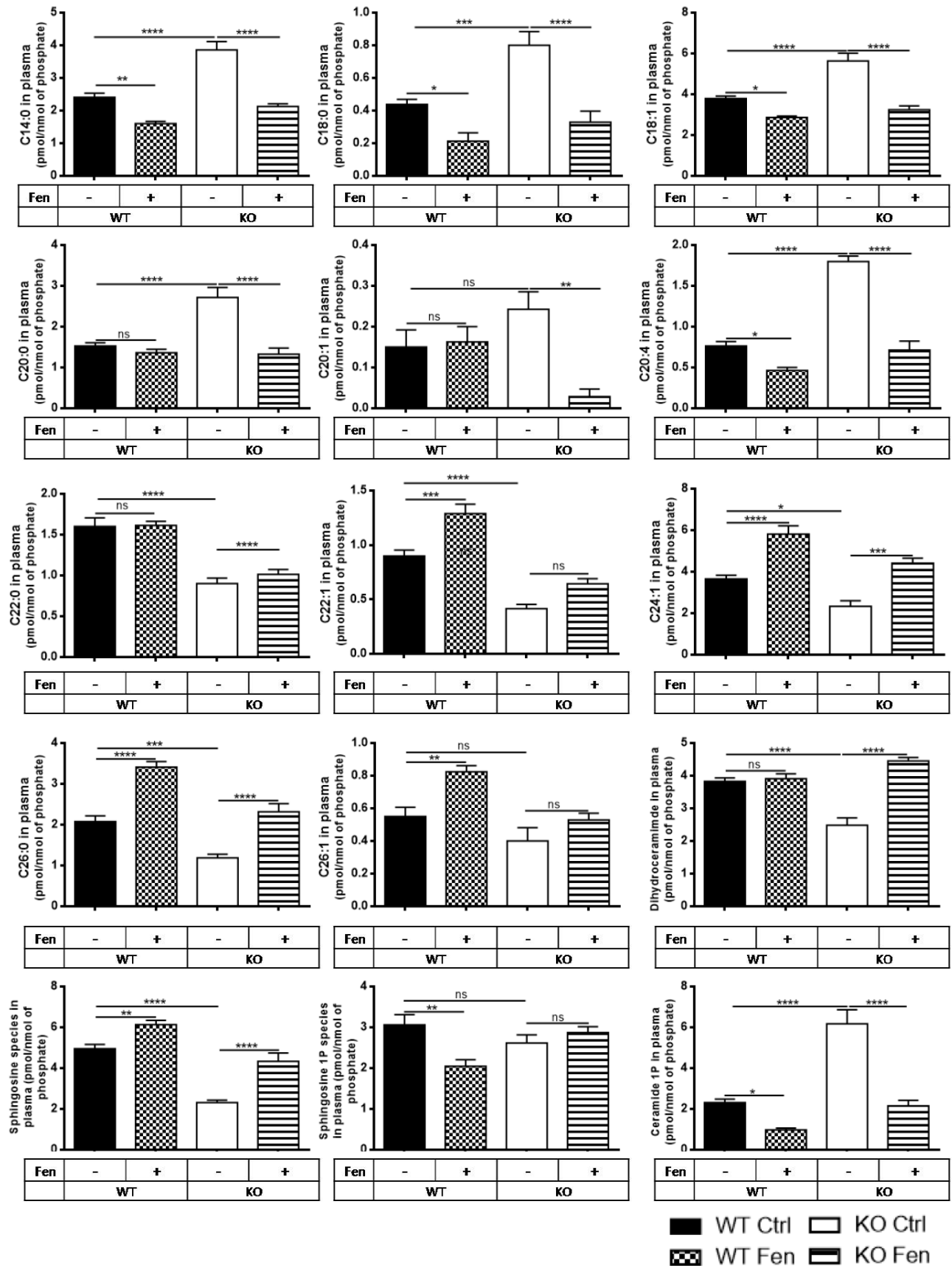


Figure S3.3 Levels of ceramides other than C16:0 and C24:0 in the lungs of CF and WT mice before and after fenretinide treatment

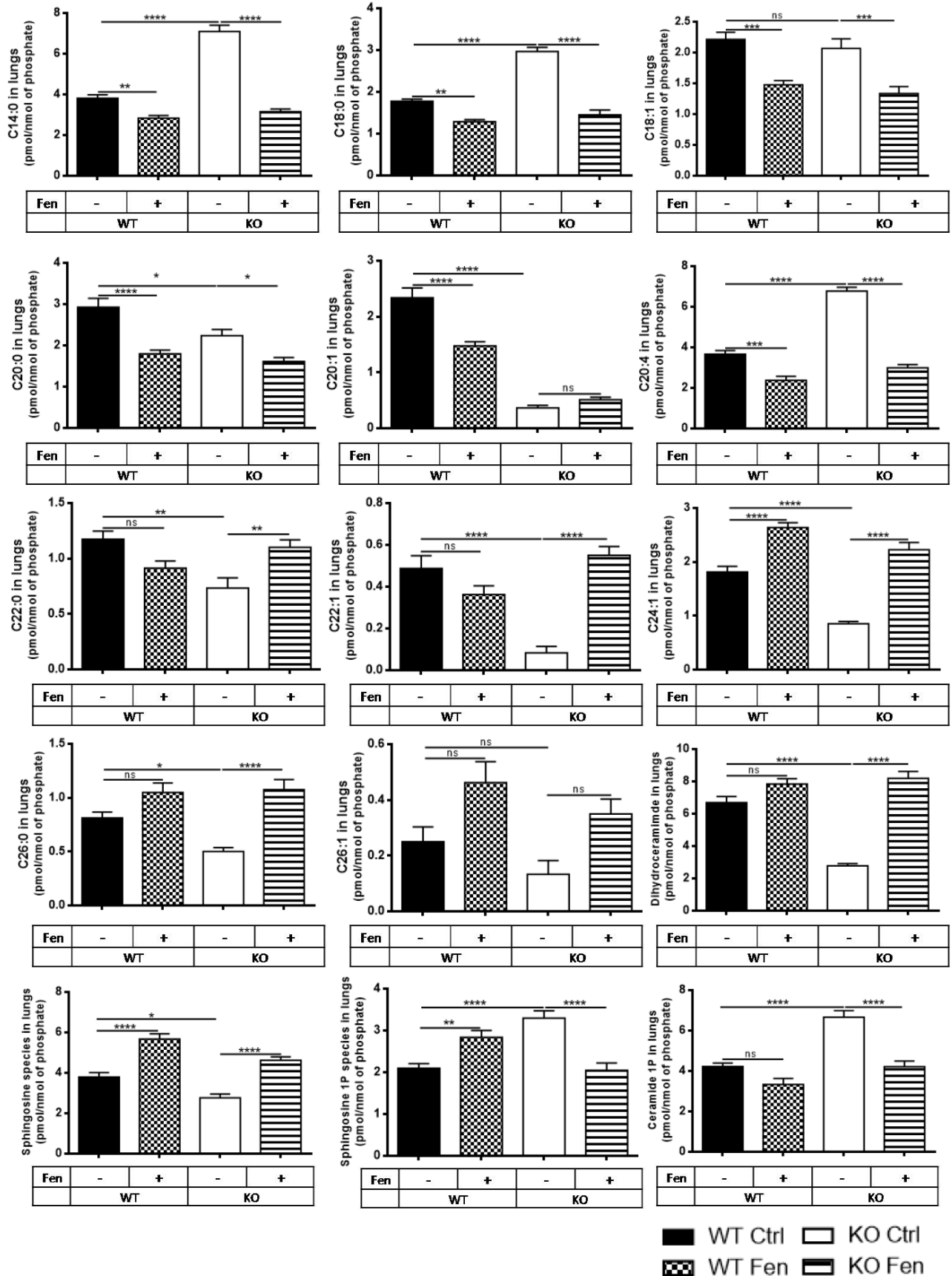


Figure S3.4 Levels of ceramides other than C16:0 and C24:0 in the plasma of responding patients (3, 5, 7, 10, 14) during cycle 3 of phase Ib clinical trial

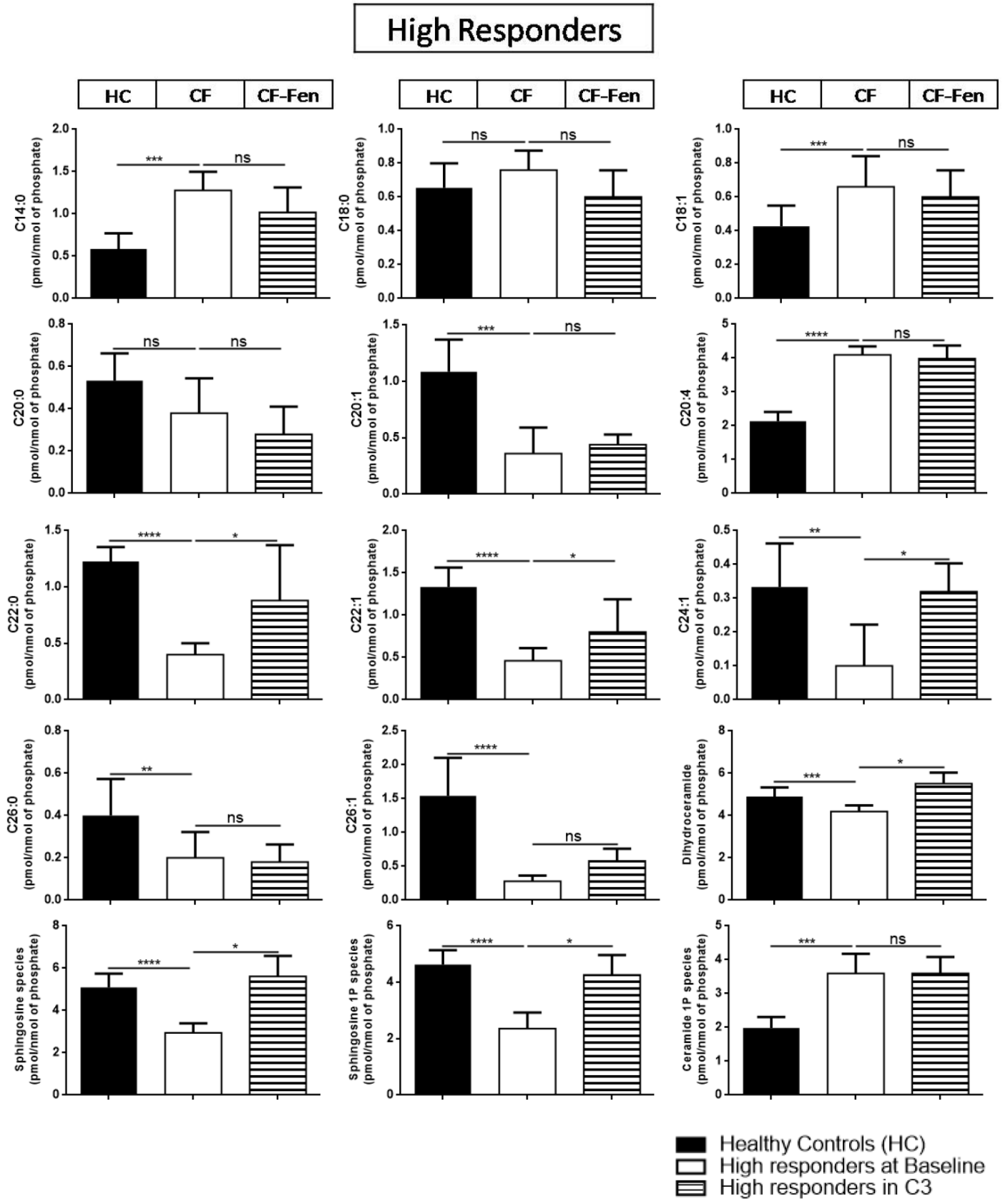


Figure S3.5 Levels of ceramides other than C16:0 and C24:0 in the plasma of placebos (4, 8, 11, 13) during cycle 3 of phase Ib clinical trial

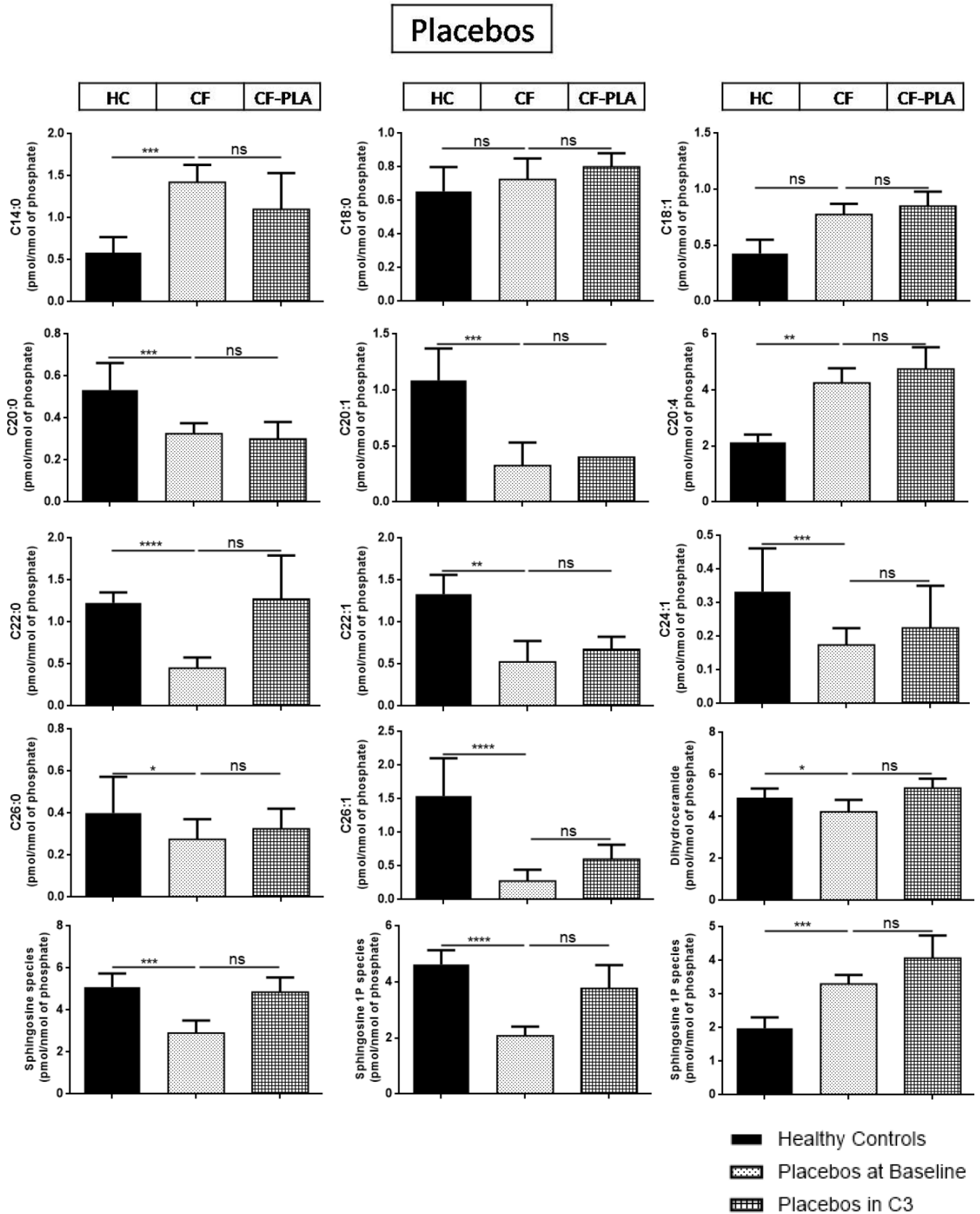


Figure S3.6 Levels of ceramides other than C16:0 and C24:0 in the plasma of partially responding patients (1, 6, 9, 12, 15) during cycle 3 of phase Ib clinical trial

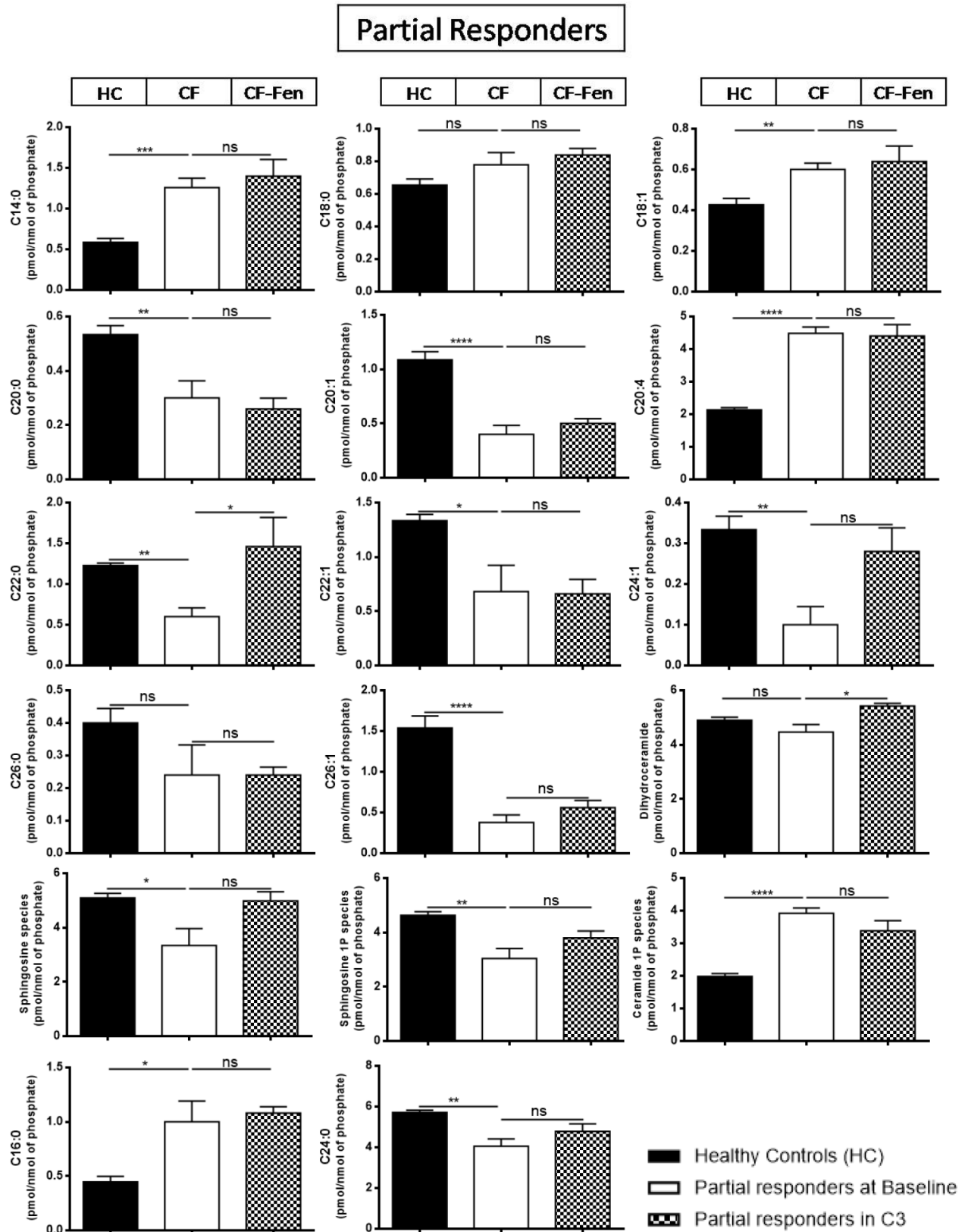


Figure S3.7 Levels of ceramides other than C16:0 and C24:0 in the parental CF cell line CFBE41o- (CFTR-F508del/F508del) before and after the treatment with fenretinide, Zn²⁺ and the two combined. Each experiment was done in triplicates.

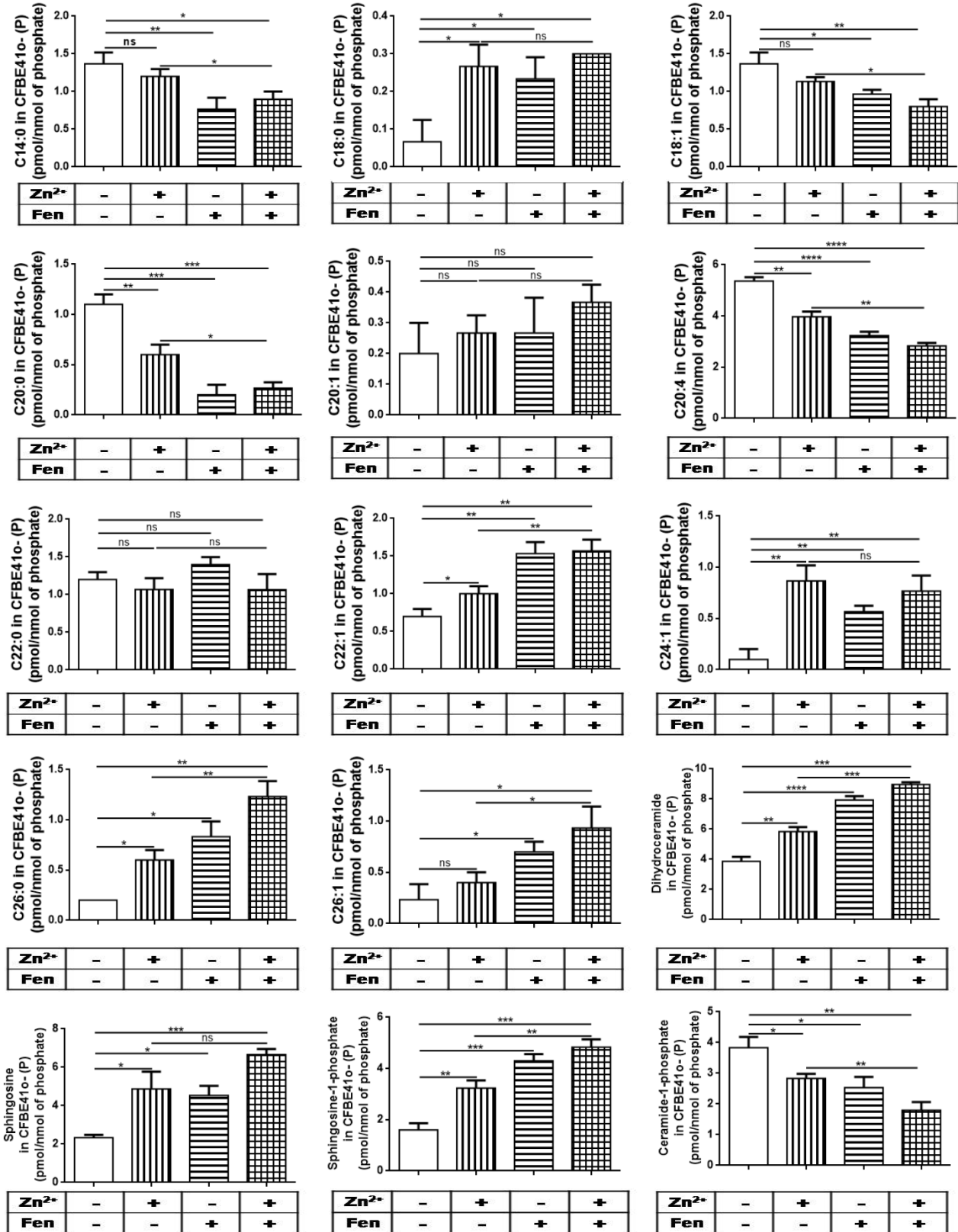
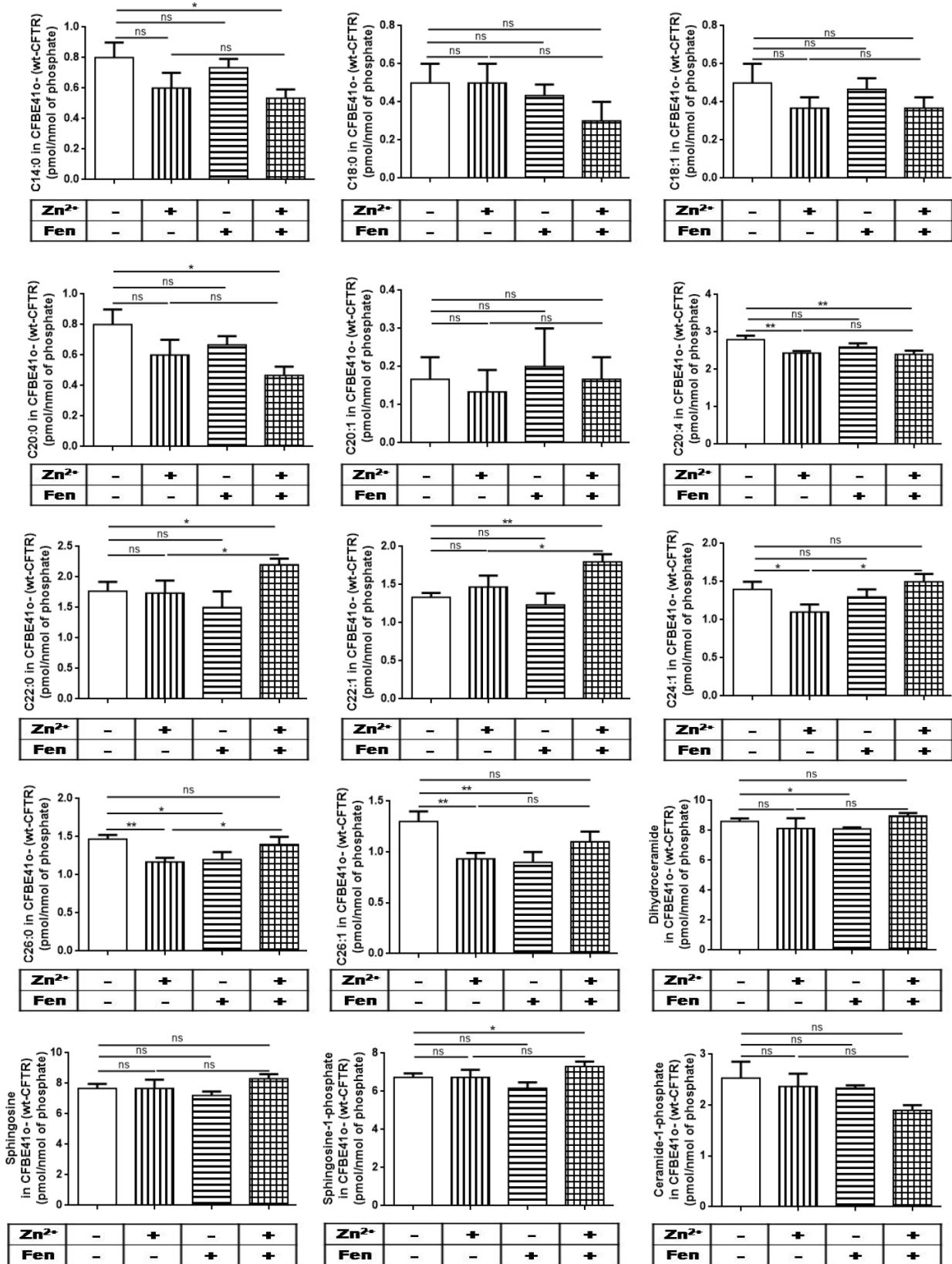


Figure S3.8 Levels of ceramides other than C16:0 and C24:0 in the CFBE41o- cell line over expressing wild-type CFTR before and after the treatment with fenretinide, Zn²⁺ and the two combined.



Chapter 4

Fenretinide mimics CFTR-induced correction of DHA/AA imbalance and blocks LPS-induced MUC5AC overexpression without affecting MUC5B

This chapter examines pro-inflammatory profile of fatty acids in CF cell lines, an important component of the sterile inflammation in CF. Additionally, here we demonstrate for the first time a specific effect of fenretinide on Muc5AC gene expression. This chapter was adapted from a submitted manuscript: “Fenretinide mimics CFTR-induced correction of DHA/AA imbalance and blocks LPS-induced MUC5AC overexpression without affecting MUC5B” by Dušan Garić; Juan B. De Sanctis; Juhi Shah; Daciana Catalina Dumut; Mina Youssef and Danuta Radzioch, Biochimica et Biophysica Acta (BBA) - Molecular and Cell Biology of Lipids 2019.

4.1 Abstract

Cystic fibrosis (CF) is the most common genetic disease in Caucasians. CF manifests through the accumulation of mucus in the lungs, which serves as the fertile soil for the growth of microorganisms, leading to recurrent infections and ultimately lung failure. Mucus in CF patients consists of DNA from dead neutrophils and mucins produced by goblet cells. MUC5AC mucin is responsible for the pathological plugging of the airways whereas MUC5B has a protective role against bacterial infection. Therefore, decreasing the level of MUC5AC without affecting MUC5B would be a desirable mucoregulatory treatment.

We demonstrated that pre-treating mice with fenretinide in a chronic model of *P. aeruginosa* lung infection efficiently prevents the accumulation of mucus. Fenretinide prevented lipopolysaccharide-induced increase of MUC5AC gene expression, without affecting the level of MUC5B in the lung goblet cell line. Furthermore, fenretinide treatment efficiently reversed pro-inflammatory imbalance of fatty acids by increasing the levels of docosahexanoic and decreasing the level of arachidonic acid in lung epithelial cell line and primary leukocytes derived from CF patients.

4.2 Introduction

Cystic fibrosis is the most common autosomal-recessive genetic disorder in Caucasians with the frequencies varying from 1 in 3000 newborns in an average Caucasian population up to 1 in 313 in Hutterites living in Alberta (Canada) (Cutting, 2013). The underlying genetic defects are various mutations in CFTR gene that abrogate its function as a chloride channel in epithelial cells of respiratory and gastrointestinal tracts. The most common mutation is a deletion of phenylalanine at the position 508 ($\Delta F508$) which accounts for 75% of diagnosed patients (Lemna et al., 1990).

Primary causes of morbidity and mortality in CF patients are lung infections that result from the accumulation of mucus that creates a fertile soil for bacterial growth (Emerson et al., 2002). The major component of the mucus in CF is polymerized DNA that comes from dead neutrophils (Lethem et al., 1990). Therefore, inhalation of dornase- α , an enzyme that degrades DNA has been shown to reduce pulmonary exacerbations and improve lung function in CF patients. However, dornase- α remains the only mucolytic agent with proven efficacy in CF (Quan et al., 2001; Robinson et al., 2005; Wilmott et al., 1996).

Mucus of patients with CF consists of dense polymeric mucus, DNA from dead neutrophils as well as mucins, the proteins that are normally produced by goblet cells in the lungs. The mRNA expression MUC5AC and MUC5B genes encoding for mucin proteins is up-regulated in patients with cystic fibrosis (Henderson et al., 2014). The expression of MUC5AC and MUC5B proteins gets further enhanced during pulmonary exacerbation (Henke et al., 2007). Although the treatment with N-acetylcysteine, a mucolytic drug was shown to disrupt mucus polymer by substituting free thiol groups for the disulfide bonds connecting mucin proteins, no improvement in lung function in patients with CF was observed (Conrad et al., 2015; Duijvestijn and Brand, 1999).

Furthermore, macrolides were shown to have intrinsic mucoregulatory in addition to their antibiotic action (Shimizu et al., 2003) and corticosteroids in addition to their anti-inflammatory action also downregulate MUC5AC gene expression (Lu et al., 2005). However, long term use of macrolides results in the increased resistance of *Pseudomonas* in CF patients (Mustafa et al.,

2017) and the long-term use of systemic corticosteroids was associated with serious growth impairment in children with CF and very limited benefits (Lai et al., 2000).

The constitutive inflammation present in the lungs of CF patients weakens their ability to fight infections (Cohen-Cymerknoh et al., 2013). The chronic inflammation is associated with pro-inflammatory lipid imbalance characterized by high levels of arachidonic acid (AA) and low levels of docosahexanoic acid (DHA) (Carlstedt-Duke et al., 1986; Farrell et al., 1985; Lloyd-Still et al., 1981; Underwood et al., 1972), resulting in very high AA/DHA ratio, which has long been known as a biochemical hallmark of CF.

It became clear that malnutrition due to pancreatic insufficiency is not the reason for the increased AA/DHA ratio seen in CF patients, since the same phenomenon can also be observed in cell culture rich in all necessary nutrients (Carlstedt-Duke et al., 1986) and it also persists in CF patients in whom pancreatic insufficiency has been successfully treated by enzyme replacement (Freedman et al., 2004; Roulet et al., 1997). While it is clear that the increased release of AA from cell membranes in cells from CF patients is mediated by cytosolic phospholipase A2 (cPLA2) (Berguerand et al., 1997; Carlstedt-Duke et al., 1986; Dif et al., 2010; Lachance et al., 2013; Levistre et al., 1993; Miele et al., 1997), the reasons for the decreased level of DHA are not well understood and seem to be related to the abnormal metabolism of its precursor, eicosapentaenoic acid (EPA) (Njoroge et al., 2012; Njoroge et al., 2011). Importantly, correction of DHA/AA imbalance was associated with better lung function in CF mice (Freedman et al., 1999; Freedman et al., 2002), significantly improved ability to resolve pulmonary infection with *P. aeruginosa* (Guilbault et al., 2009) and lower level of MUC5AC production (Binker et al., 2015; Morin et al., 2015)

Previously, we showed that 28-day treatment protocol with fenretinide, a synthetic retinoid, resulted in normalization of low DHA/AA ratio in CF mice by lowering the level of AA and upregulating the level of DHA and these changes were accompanied by dramatic improvement of CF mice to fight off *Pseudomonas* infection (Guilbault et al., 2008; Guilbault et al., 2009).

We previously demonstrated that fenretinide prevents goblet cell hyperplasia in the lungs of asthmatic A/J mice upon challenge with an allergen (Kanagaratham et al., 2014), but the specific effect of fenretinide on the expression of MUC5AC and MUC5B genes was not examined. The

importance of retinoic acid in the induction of MUC5AC and MUC5B genes in human tracheobronchial cells was previously established (Koo et al., 1999a; Koo et al., 1999b), and since fenretinide is a synthetic derivative of retinoic acid which might be competing with retinoic acid for the binding site to its receptors, we hypothesized that the treatment with fenretinide may modulate the expression of MUC5AC and MUC5B genes.

4.3 Materials and Methods

4.3.1 Cell Culture

Parental pulmonary epithelial cell lines CFBE41o⁻ (Δ F508/ Δ F508) was previously described (Kunzelmann et al., 1993) and is further referred to as CFBE41o⁻(P). CFBE41o⁻ transduced with wild-type CFTR is further referred to as CFBE41o⁻ (wt-CFTR) (Bebok et al., 2005). Both cell lines were grown in Eagle's Minimal Essential Medium (Invitrogen) supplemented with 10% Fetal Bovine Serum (Wisent), 2 mM L-glutamine(Wisent), 50 U/ml penicillin (Wisent) and 50 μ g/ml streptomycin (Wisent), in a 5% CO₂ - 95% air incubator at 37°C. For each experiment, cells were 80% confluent at the beginning of the treatment and they were treated for 48h or 72h with 1.25 μ M fenretinide (Grafton, formerly Cedarburg Pharmaceuticals, Grafton, WI, USA). Physiological concentrations of Zn²⁺ in human plasma are 10.1-17.9 μ M (Rink and Gabriel, 2001), therefore 12.5 μ M zinc sulphate (Sigma) was added to the culture medium as indicated. For each subsequent step, monolayer of cells was washed two times with PBS and lysed in an appropriate buffer.

SPOC-1 (SPontaneously derived in Complete serum-free medium) is a pulmonary goblet cell line derived from rat lungs which was previously described (Doherty et al., 1995) and characterized as a mucin-producing cell line (Randell et al., 1996). These cells were originally grown in a serum-free medium consisting of DMEM/F12 as the basis with the following components added up to the final concentrations: 2.5 mM L-glutamine, 15 mM HEPES, 0.3 μ M hydrocortisone, 1% Bovine Pituitary Extract, 0.1 μ g/ml cholera toxin, 5 μ g/ml transferrin, 50 μ M phosphoethanolamine, 80 μ M ethanolamine, 25 ng/ml EGF, 0.5 mg/ml Bovine Serum Albumin, 50 nM retinoic acid, 50 units/ml penicillin and 50 μ g/ml streptomycin. However, for the purpose of our experiments, we modified the content of the medium in which we have cultured SPOC-1 cells in a following way: as the basis we used DMEM containing high glucose (4500 mg/l), L-

glutamine (584 mg/ml) and sodium pyruvate (110 mg/l) (Wisent, 319-005-CL) with the following components added up to the final concentrations: 10% Fetal Bovine Serum, 50 units/ml penicillin and 50 µg/ml streptomycin, 25 mM HEPES (from 1500 mM stock prepared as described below), 1.4 µM hydrocortisone (based on (Zaidman et al., 2016)), 2.7 µM epinephrine (based on (Randell et al., 2011) and 50 nM retinoic acid (based on (Randell et al., 2011)). The stocks of hydrocortisone, epinephrine and retinoic acid were prepared as described in (Randell et al., 2011). The stock of 1500 mM HEPES was prepared by dissolving 17.85 grams of HEPES free acid cell culture grade (Akron AK3268-0500) in 34 ml of DMEM (Wisent, 319-005-CL) and vortexing forcefully until complete dissolution of the powder. The pH of HEPES stock solution was adjusted (pH=7.4) with ~2.5 ml of 10 M NaOH and the final volume was adjusted with DMEM up to 50 ml. SPOC-1 cells were treated with 1 µg/ml of LPS (Sigma, L9143) and 1.25 µM fenretinide as outlined in the **Table 4.1**.

	PRE-TREATMENT				TREATMENT							
	Day 1		Day 2		Day 3		Day 4		Day 5		Day 6	
Condition	LPS	FEN	LPS	FEN	LPS	FEN	LPS	FEN	LPS	FEN	LPS	FEN
1	-	-	-	-	-	-	-	-	-	-	-	-
2	+	-	+	-	+	-	+	-	+	-	+	-
3	-	+	-	+	+	-	+	-	+	-	+	-
4	-	+	-	+	-	+	-	+	-	+	-	+
5	-	+	-	+	+	+	+	+	+	+	+	+
6	+	+	+	+	+	+	+	+	+	+	+	+

Table 4.1 Conditions and treatment schedule for SPOC-1 cells

4.3.2 Molecular Biology

For RNA extraction, cells were lysed in Lysis Buffer supplied in the Aurum Total RNA kit (Biorad), and RNA was extracted according to manufacturer's instructions. cDNA was produced using iScript RT Supermix RT-qPCR (Biorad) from 2µg of total RNA in a 40µl RT reaction. Once RT reaction was completed, cDNA was diluted with 150 µl of water and 10 µl of 500 µM xylencyanol in order to visualize cDNA samples for the sake of pipetting accuracy. We have established that the final concentration of 7.5 µM xylencyanol in a qPCR reaction does not inhibit polymerization reaction, neither intereferes with EvaGreen emission, yet greatly facilitates pipetting of cDNA samples into 384-well plate by labeling the wells into which cDNA

was added. A stock of 500 μ M xylencyanol was prepared by dissolving xylencyanol powder (Biorad FF #1610423) in water and passing the solution through 0.2 μ m filter.

Quantitative real time PCR was done with SSoFast EvaGreen Supermix (Biorad) with an annealing temperature of 55°C. The final concentration of primers was 400 nM and 30 ng (3 μ l) of cDNA was used in a 10 μ l qPCR reaction volume. Primers for rat Muc5AC (XM_008760037) and Muc5B (XM_006230608) genes were specifically designed to distinguish Muc5AC and Muc5B genes from each other. From the initially tested three different housekeeping genes (GAPDH, β -actin and β -tubulin), β -actin was selected as a housekeeping gene because it did not fluctuate between the samples. Specificity of each primer set was confirmed by manual comparisons of primer sequences against cDNA sequences using Clustal Omega (EMBL). In order to calculate the fold change, formula $2^{(-\Delta\Delta Ct)}$ was used where:

$$\Delta\Delta Ct = (Ct_{(\text{target gene, test})} - Ct_{(\text{reference gene, test})}) - (Ct_{(\text{target gene, control})} - Ct_{(\text{reference gene, control})}).$$

The sequences of the primers are given in **Table S4.1**.

For protein extraction, cells were lysed in a homemade RIPA buffer (50 mM Tris, 150 mM NaCl, 50 mM NaF, 0.2 mM Na₃VO₄, 0.1% SDS, 2 mM EDTA, 1% NP-40, 0.5% Na-deoxycholate, pH=7.4) with freshly dissolved tablet of protease inhibitors (Roche). Concentration of total protein was determined using BCA Protein Assay Kit (Thermo Scientific).

ELISA tests were used to determine the levels of Muc5AC (Aviva Systems Biology, OKCD02293) and Muc5B (Aviva Systems Biology; OKCD00811) proteins in SPOC-1 cells. Since the level of Muc5AC expression in SPOC-1 cells is much lower (Ct~33 per 30 ng of cDNA) than the level of Muc5B expression (Ct~23 per 30 ng of cDNA), the input of total protein that was loaded in each well was adjusted accordingly: 200 μ g of total protein was loaded for the measurements of Muc5AC and 10 μ g was loaded for the measurements of Muc5B protein. All results were eventually normalized and shown per 1 μ g of total protein input.

For Western Blot, anti-cPLA₂ α a monoclonal antibody from Santa Cruz was used (4-4B-3C).

The activity of cPLA₂ was determined using colorimetric assay, according to manufacturer's instructions (Abcam, ab133090).

4.3.3 Analysis of lipid oxidation, fatty acid levels and protein oxidation.

Monolayer of epithelial cells grown in a T-75 flask was washed twice with PBS and scraped using rubber policeman into 1 ml of 1 mM butylated hydroxyanisole (BHA) in a chloroform/methanol solution (2:1 vol/vol). Peripheral blood mononuclear cells were separated from the blood with Ficoll reagent, washed with PBS and scraped with a policeman into 1 ml of 1 mM butylated hydroxyanisole (BHA) in a chloroform/methanol solution (2:1 vol/vol) as well.

Phospholipids were identified by thin layer chromatography extraction. Diazomethane was used to esterify the released fatty acids and the esters were identified by GC/MS (Hewlett Packard 5880A, WCOT capillary column (Supelco-10, 35 m × 0.5 mm, 1 µm thick)) using commercial standards (Sigma-Aldrich, Oakville, ON, Canada).

Lipid peroxidation was measured fluorometrically using 2-thiobarbituric acid-reactive substances (TBARS) as surrogate for malondialdehyde, the end product of lipid peroxidation (Niehaus and Samuelsson, 1968; Ohkawa et al., 1979). Briefly, the samples were mixed with 8.1% sodium dodecyl sulfate, 20% acetic acid and 0.8% 2-thiobarbituric acid. After vortexing, samples were incubated for 1 h at 95°C after which butanol-pyridine at 15:1 (v/v) ratio was added. The mixture was shaken for 10 min and then centrifuged. The butanol-pyridine layer was measured fluorometrically at 552 nm after excitation at 515 nm (Shimadzu, Japan). The results are expressed in nmole TBARS/mg of protein which reflects the levels of malondialdehyde in the samples as well as any other thiobarbituric acid reactive substances (Lykkesfeldt, 2007).

Oxidative damage of proteins was assessed using 3-nitrotyrosine as a surrogate marker. 3-nitrotyrosine was determined by ELISA as previously described (Montes de Oca et al., 2008) using well characterized antibodies (Ye et al., 1996). Antibodies (mouse IgG monoclonal, polyclonal against nitrotyrosine and polyclonal goat anti-rabbit IgG-peroxidase) were from Upstate Biotechnology (Lake Placid, NY). The quantification of 3-nitrotyrosine was performed using a standard curve with known concentrations of 3-nitrotyrosine from chemically modified bovine serum albumin. The sensitivity of the assay was 50 pg/ml.

4.3.4 Mice

Inbred C57BL/6-Cftr^{-/-}(CFTR-KO) mice with an increased susceptibility to pulmonary *P. aeruginosa* infection compared to their littermate controls and without intestinal correction of CFTR were previously described (Gosselin et al., 1998). All pups were genotyped within 3-4 weeks of age by PCR. Mice were kept in cages with corn bedding (Anderson, Bestmonro, LA) and were fed NIH31-modified irradiated mouse diet (Harlan Teklan, Indianapolis, IN). CFTR-KO mice and their wild-type littermates were treated with LAU-7b formulation of fenretinide by gavage (10 mg/kg) 7 days before infection and during the 3 days after infection with bacteria entrapped in agarose beads. In a control group, mice were treated with methylcellulose as a placebo. Bacteria (*P. aeruginosa* strain PA508) were entrapped in agar beads (150-200 µm in size) and mice were infected ($1 \cdot 10^6$ cfu/animal) non-invasively through the trachea as previously described (Guilbault et al., 2005).

4.3.5 Histology

Mice were sacrificed 3 days after infection by CO₂ overdose and lungs were preserved for histological analysis in PBS-buffered formalin. Lung sections were stained with Alcian Blue-Periodic Acid-Schiff (AB/PAS) and counterstained with hematoxylin and eosin (H&E) in order to visualize mucus production and infiltration of inflammatory cells around the beads. An automated staining with fluorescently labelled lectins was performed using Discovery Ultra Instrument. Briefly, slides were deparaffinised and rehydrated and antigen retrieval was done using standard CC1 buffer for 24min. Discovery Inhibitor was added to block endogenous peroxidase 4min Slides were incubated with conjugated lectins: Jacalin coupled to fluorescein (FL-1151 from Biolyx) at 1:200 dilution and WGA coupled with rhodamin (RL-1022 from Biolyx) at 1:400 dilution for 24min at 37°C. Counterstaining was done with DAPI. A negative control was included which consisted of the tissue sample without lectins. All experiments were conducted in accordance with the Canadian Council on Animal Care guidelines and approved by the Facility Animal Care Committee of the Research Institute of the McGill University Health Centre.

4.3.6 Ex vivo treatment of peripheral mononuclear blood cells (PMBCs)

Blood of CF patients (three lavender tubes, each with ~3 ml of blood) was centrifuged (2000G, 10 min, 5°C) and plasma was removed. The pellet was reconstituted with D-PBS to the original volume and the content was further diluted up to 30 ml with D-PBS. 10 ml of blood cells diluted in D-PBS was added very slowly to the 4 ml of Ficoll reagent in a 15 ml tube. Cells were centrifuged at 1500 rpm for 30 min at 20 °C with acceleration set at 9 and deceleration set at 1. After separation of lymphocytes in the middle layer, cells were washed two more times with D-PBS (1500 rpm for 7 min at 20 °C) and frozen in 90% FBS, 10% DMSO for further use. For the experiment, cells were grown in RPMI medium supplemented with 10% FBS and treated with two doses of fenretinide (1.0 and 2.5 µM) for 12h. After the treatment cells were pelleted and lysed into 1 ml of 1 mM butylated hydroxyanisole (BHA) in a chloroform/methanol solution (2:1 vol/vol).

4.3.7 Statistical Analysis

All statistical analyses were performed using GraphPad (GraphPad, San Diego, CA, USA). For the cell lines and patient-derived PMBCs, statistical analysis was performed using ANOVA test with Holm-Sidak's correction whenever multiple comparisons (more than two groups) for a single variable were compared and t-tests with Welch's correction when only two conditions for a single variable were compared at a time. Data is represented as means ± SD (*p≤0.05, ** p≤0.01, *** p≤0.001).

4.4 Results

4.4.1 Fenretinide prevents over-expression of MUC5AC gene in a lung goblet cell line after inflammatory stimulation

Since the expression of specific mucin genes Muc5AC and Muc5B in SPOC1 cells was not previously examined, we designed highly specific qPCR primers that distinguish Muc5AC and Muc5B genes from each other and from all other genes for mucins. Indeed, we discovered that the predominant form of mucin gene expressed in these cells is MUC5B ($C_T \sim 22$ per 30 ng of cDNA) whereas Muc5AC gene was expressed at the very low level ($C_T \sim 33$ per 30 ng of cDNA).

Next, SPOC1 cells were treated according to the protocol described in **Table 4.1**, which included 2 days pre-treatment in order to induce the expression of Muc5AC by LPS and expose the cells to fenretinide, followed by 4 days of treatment to test whether fenretinide can prevent LPS-induced Muc5AC expression or decrease the expression of Muc5AC which has already been induced by LPS. The expression of mRNA for Muc5AC gene is induced strongly (~20 fold) by day 5 (**Figure 4.1**). The level of Muc5AC protein follows the same kinetics upon LPS treatment (**Figure 4.2**), being strongly increased by day 5 and then falls down to the same levels as control by the end of day 6, most likely due to the secretion of Muc5AC protein outside the cell. The expression of mRNA for Muc5B starts increasing by day 5 (~2 fold) and peaks at day 6 post-LPS treatment (~6 fold) (**Figure 4.1**). The increase in the level of Muc5B protein is evident only after 6 days of LPS treatment (**Figure 4.2**).

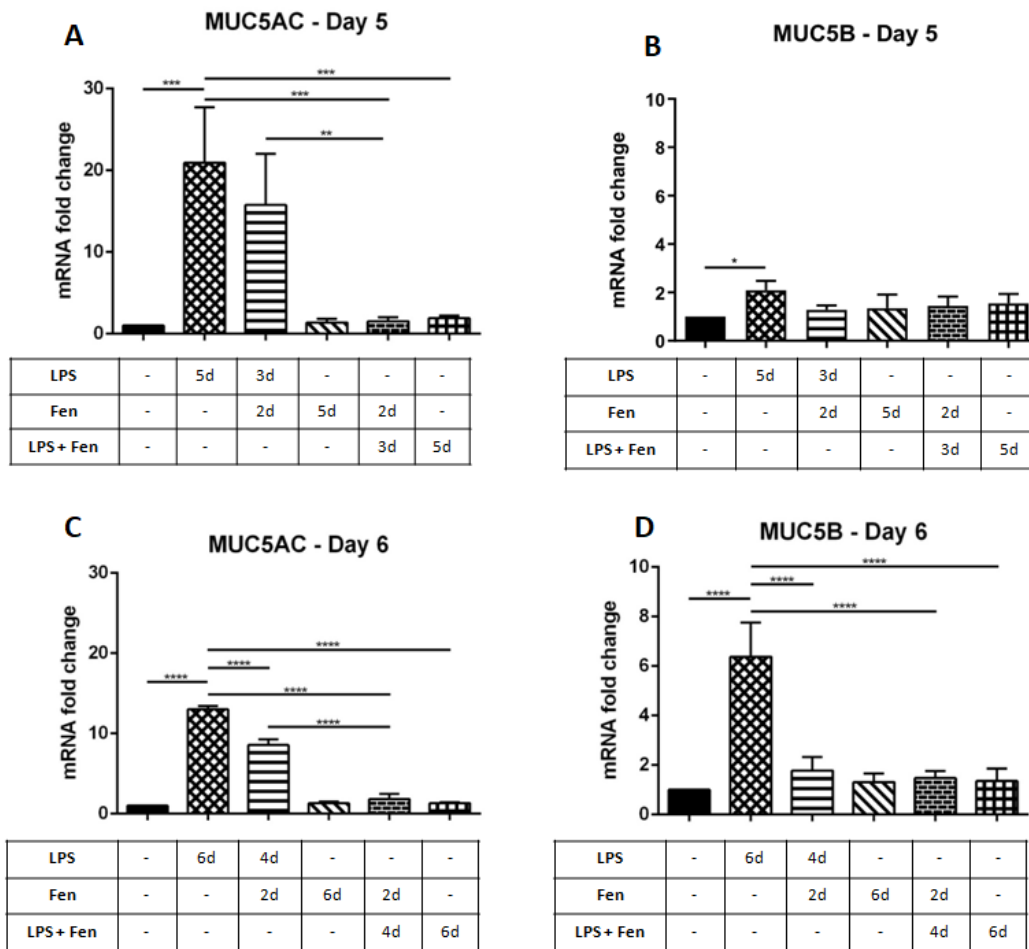


Figure 4.1 In a pulmonary goblet cell line (SPOC-1), LPS treatment strongly induces transcription of MUC5AC mRNA by day 5 and mRNA for MUC5B by day 6 (~6 fold). *continued...*

Figure 4.1 (continued...) Pre-treatment of cells with fenretinide as well as combined treatment with fenretinide and LPS strongly attenuates LPS-induced transcription of mucin genes. All experiments were done in triplicates (n=3). Data is represented as means \pm SD (* $p \leq 0.05$, ** $p \leq 0.01$, *** $p \leq 0.001$, **** $p \leq 0.0001$).

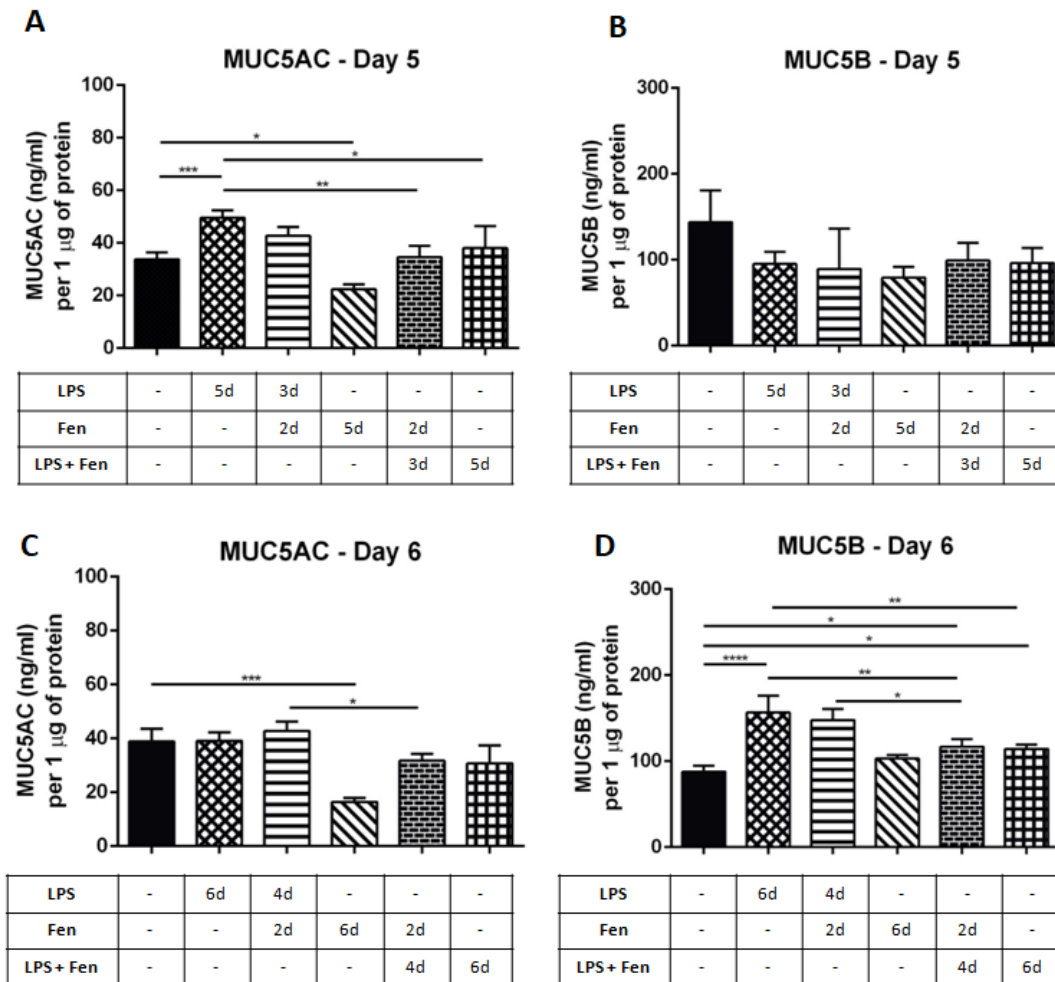


Figure 4.2 Protein levels of the MUC5AC gene follow the kinetics of mRNA induction by LPS in SPOC-1 cells, whereas the protein level of MUC5B gene is strongly induced only after day 6 of LPS treatment. Fenretinide pre-treatment as well as combined fenretinide+LPS treatment prevents LPS-induced increase in MUC5AC protein. The level of MUC5B protein is not significantly affected by fenretinide nor fenretinide+LPS treatment compared with the mock control, but the increase seen in the treatment with LPS alone is diminished by fenretinide treatment. All experiments were done in triplicates. Data is represented as means \pm SD (* $p \leq 0.05$, ** $p \leq 0.01$, *** $p \leq 0.001$, **** $p \leq 0.0001$).

These results demonstrate relatively late kinetics of Muc5AC gene expression in SPOC-1 cells, reminiscent of the situation seen in mouse lungs *in vivo* (see Figure 3 in (Yanagihara et al., 2001)), therefore validating these cells as a model for studying the function of lung goblet cells *in vitro*. Furthermore, these results are consistent with the previous observations that Muc5AC is an inducible gene, whereas Muc5B is a constitutively expressed gene in the lungs (Chen et al., 2001) and shows a very-late kinetics of LPS-mediated induction.

To test whether fenretinide can decrease LPS-induced expression of mucin genes, SPOC-1 cells were treated for 2 days with LPS alone followed with 3 days of treatment with LPS (**Table 4.1**). This experimental setup is modeled to reflect a situation of patients which would start treatment is already infected with *Pseudomonas*. We also to examined how the pre-treatment of SPOC1 cells with fenretinide followed by combined treatment with LPS and fenretinide influences the expression of mucin genes. This experimental setup is supposed to model a condition where a patient who continuously takes fenretinide encounters a pathogen and becomes infected with *Pseudomonas* and/or other bacteria during the course of the treatment.

Indeed, even though Muc5AC is still highly induced when cells are treated with LPS in the presence of fenretinide, induction of mRNA for Muc5AC at the end of day 5 is lower than in LPS group untreated with the drug (**Figure 4.1 A**) and at the end of day 6 is significantly lower even in comparison with cells that were treated with LPS alone (**Figure 4.1 C**). Under these conditions, the level of Muc5AC protein is lower at the end of 5 (**Figure 4.2 A**) when compared with cells treated with LPS alone and becomes indistinguishable at the end of day 6 (**Figure 4.2 C**), most likely due to the secretion. The level of Muc5B mRNA was not significantly altered at day 5 in fenretinide-treated groups (**Figure 4.1 B**) and was significantly lower compared with LPS-treated control at the end of day 6 (**Figure 4.1 D**). The protein level of MUC5B was not significantly altered at in any of the conditions at day 5 (**Figure 4.2 B**), and it was significantly lower in fenretinide pre-treated conditions at the end of day 6 compared with LPS-treated controls (**Figure 4.2 D**).

These results suggest that fenretinide pre-treatment before infection may efficiently prevent pathogen-stimulated over-expression of Muc5AC gene. Under these conditions, neither mRNA nor protein levels of Muc5B gene were significantly altered (**Figures 4.1 B and D; Figures 4.2 B and D**).

Interestingly, fenretinide treatment alone for 5 or 6 days did not significantly change the mRNA levels of both Muc5AC and Muc5B genes (**Figure 4.1**) and only lowered the protein level of Muc5AC (**Figure 4.2**).

Finally, combined treatment with fenretinide and LPS for 5 and 6 days induced very small level of Muc5AC gene transcription (**Figures 4.1 A and C**) which did not reflect on the level of Muc5AC protein (**Figure 4.2 A and 2C**). Under the same conditions, the level of mRNA for Muc5B was not significantly altered (**Figure 4.1 B and D**).

Importantly, at the end of day 5, the level of Muc5AC protein decreased for -33.69 % and at the end of day 6 for -57.57% by fenretinide treatment alone compared to baseline (cell culture medium). At the end of day 5, the level of Muc5B protein were decreased for -44.92 % but at the end of day 6 it was 17.13% higher in cells treated with fenretinide alone compared to baseline (cell culture medium).

Altogether, these results demonstrate that the long-term treatment of SPOC-1 goblet cells with fenretinide *in vitro* can prevent LPS-induced Muc5AC over-expression without significantly affecting expression of Muc5B mucin.

4.4.2 Fenretinide prevents accumulation of MUC5AC mucin in mice upon infection with P. aeruginosa

To test whether our results obtained *in vitro* with SPOC-1 cells can be validated *in vivo*, we treated by gavage wild-type and CFTR-KO mice with a 10 mg/kg of novel formulation of fenretinide, referred to as LAU-7b. Indeed, in the lungs of placebo-treated CFTR-KO mice and their wild-type littermates we observed a significant accumulation of mucus and infiltration of inflammatory cells around the bacteria-coated agarose beads (**Figures 4.3 A and C**) assessed by PAS/Alcian blue staining. On the other hand, in the lungs of the mice treated with fenretinide, the infiltration of inflammatory cells was significantly diminished (**Figures 4.3 B and D**) and the staining of mucus was much less pronounced around the bacteria-coated beads of the same size than in placebo-treated animals (**Figures S4.1 A and B**).

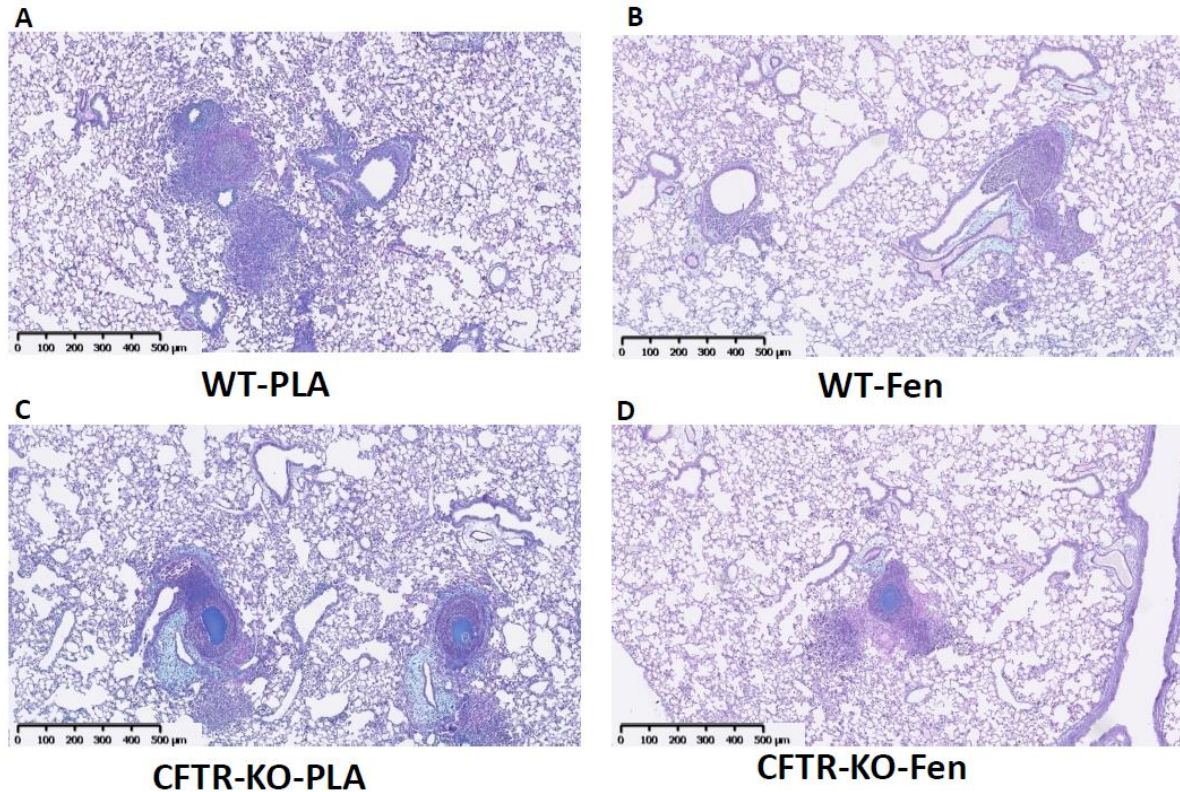


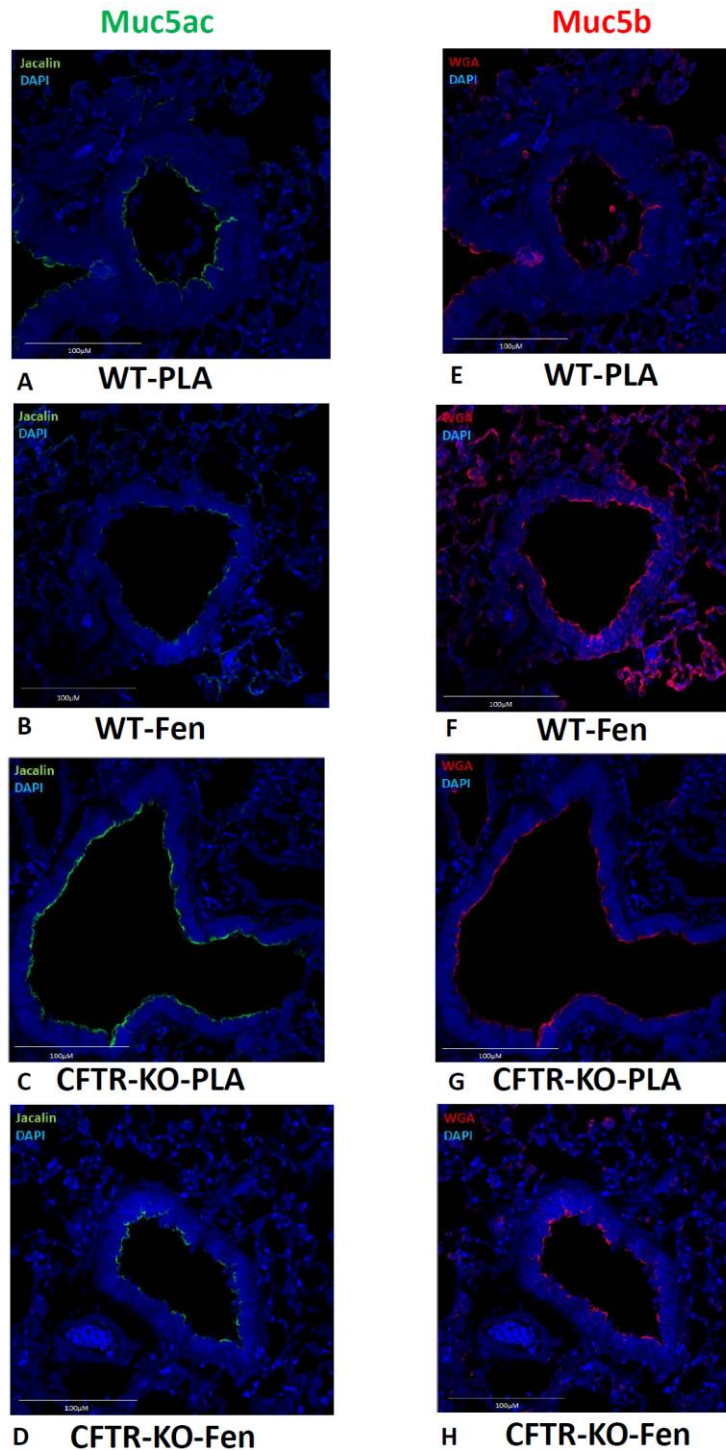
Figure 4.3 Lungs of mice infected with *P.aeruginosa*-coated agarose beads and treated with either placebo (**A** and **C**) or fenretinide (**B** and **D**) were stained PAS/Alcian Blue. Pulmonary infection of mice with *P. aeruginosa*-coated agarose beads results in a massive infiltration of inflammatory cells and production of mucus in WT (**A**) and CFTR-KO (**C**). Fenretinide pre-treatment attenuates these effects in both WT (**B**) and CFTR-KO mice (**D**). 4x magnification, Scale bar = 500 μ m.

Furthermore, we wanted to examine which of the two major mucin proteins expressed in the lungs was affected by fenretinide treatment. Neither PAS nor Alcian Blue can distinguish the Muc5AC from the MUC5B protein. Therefore, we stained the lung sections of *P. aeruginosa*-infected mice with two fluorescently labelled lectins that recognize specific glycosylation patterns present on these two mucin proteins: Fluorescein-coupled jacalin was used to detect Muc5AC and rhodamine-coupled WGA was used to detect Muc5B. Indeed, as can be seen in the **Figure 4.4**, fenretinide treatment efficiently prevented overexpression of Muc5AC mucin upon *P. aeruginosa* infection in both wild-type mice and CFTR-KO, without significantly affecting the expression level of Muc5B mucin. For Muc5AC the effect of fenretinide is noticeable in

both wild-type mice (**Figure 4.4 A vs B**) and CFTR-KO mice (**Figure 4.4 C vs D**), whereas Muc5B staining is somewhat diminished in CFTR-KO mice compared with wild-type mice (**Figure 4.4 F vs H**), probably due to the defective postsecondary maturation of Muc5B in CF airways which has been previously reported (Abdullah et al., 2017).

These results suggest that fenretinide has a potential to be used as a novel muco regulatory and anti-inflammatory agent in the treatment of chronic lung infections.

Figure 4.4 Lungs of mice infected with *P. aeruginosa*-coated agarose beads and treated with either placebo (**A, E, C and G**) or fenretinide (**B, F, D and H**) were stained with fluorescein-coupled jacalin and rhodamine-coupled WGA, the two lectins that recognize Muc5AC and Muc5B mucins respectively. Infection of placebo treated wild-type (**A**) and CFTR-KO (**C**) mice results in a strong induction of Muc5AC, which is blocked in fenretinide-treated mice (**B** and **D**). The expression of Muc5B mucin is not affected by fenretinide treatment in neither wild-type (**E vs F**) nor CFTR-KO mice (**G vs H**). 20x magnification, Scale bar = 100µm.



4.4.3 Fenretinide treatment mimics the re-introduction of wild-type CFTR in $\Delta F508/\Delta F508$ lung epithelial cell line and corrects low DHA/AA ratio in lung epithelial cell line and PMBCs from CF patients

In order to examine the connection between the expression of CFTR protein and the imbalance of fatty acids seen in CF, we used a well characterized lung epithelial cell line homozygous for $\Delta F508$ CFTR mutation developed from CF bronchial epithelial cells by Gruenert and colleagues,

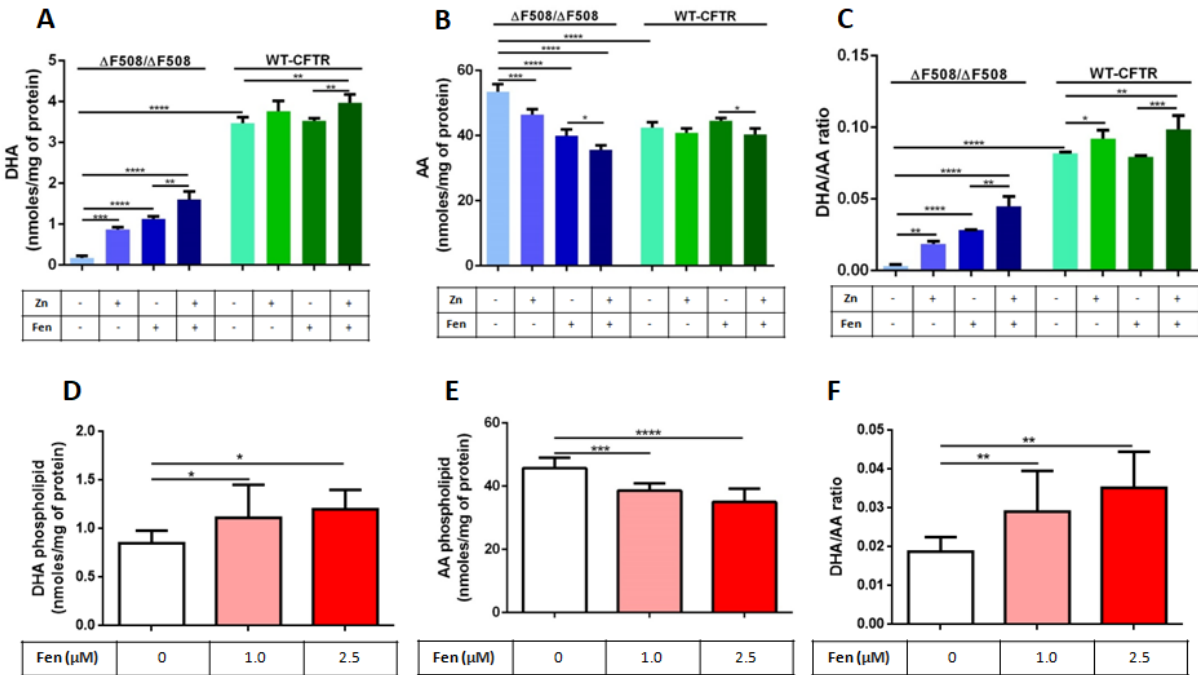


Figure 4.5 Effect of fenretinide (1.25 μM) and Zn^{2+} (12.5 μM) on the levels of AA and DHA in parental CFBE41o- ($\Delta F508/\Delta F508$) and CFBE41o- (CFTR-WT) cells (A-C). Dose-dependent effect of fenretinide on AA and DHA in PMBCs from CF patients (D-F). In CFBE41o- ($\Delta F508/\Delta F508$) cells the level of DHA is increased (A) whereas the level of AA is decreased (B) by the treatment with either Zn^{2+} or fenretinide alone, but the combination of the two has a significantly additive effect, resulting in a strongly increased DHA/AA ratio (C). Reintroduction of wt-CFTR into CFBE41o- ($\Delta F508/\Delta F508$) cells results in a similar effect of AA and DHA. In PMBCs from CF patients, fenretinide causes dose-dependent (1.0 and 2.5 μM) increase in the level of DHA (D) and decrease in the level of AA (E), resulting in a significantly improved DHA/AA ratio (F). Data is represented as means \pm SD (* $p \leq 0.05$, ** $p \leq 0.01$, *** $p \leq 0.001$, **** $p \leq 0.0001$). All experiments were done in triplicates (n=3).

referred to as parental CFBE41o⁻(P) cell line (Δ F508/ Δ F508) (Kunzelmann et al., 1993). We also used a derivative cell line produced by lentiviral transduction of wild-type CFTR as previously described (Bebok et al., 2005) and referred to as CFBE41o⁻(wt-CFTR).

CFBE41o⁻(P) cells inherently express high level of AA and low level of DHA and therefore have very low DHA/AA ratio (**Figures 4.5 A-C**). Interestingly, treatment with Zn²⁺ alone, known to be deficient in CF patients (Abdulhamid et al., 2008; Van Biervliet et al., 2008b; Yadav et al., 2014), increased the level of DHA (**Figure 4.5 A**) and decreased the level of AA in CFBE41o⁻(P) cells (**Figure 4.5 B**). However, treatment with fenretinide strongly increased the level of DHA while also decreasing the level of AA in Δ F508/ Δ F508 CFBE41o⁻(P) cells, and combination of fenretinide and Zn²⁺ further potentiated these effects, resulting in greatly improved DHA/AA ratio (**Figures 4.5 A-B**).

On the other hand, CFBE41o⁻(wt-CFTR) cells expresses much higher level of DHA and much lower level of AA, resulting in greatly elevated DHA/AA in comparison with its parental Δ F508/ Δ F508 alleles expressing cell line CFBE41o⁻(P) (**Figures 4.5 A-C**). The fact that CFBE41o⁻cells expressing wt-CFTR protein cells had much higher DHA and much lower AA levels than parental CFBE41o⁻(P) cells suggests a causal link between the lack CFTR expression and the imbalance of fatty acids observed in CF.

In order to examine the effect of fenretinide on the primary cells from CF patients we treated PMBCs isolated freshly from the blood of CF patients with escalating doses of fenretinide (1.25 μ M and 2.5 μ M) (**Figure 4.5 D-F**). Similarly to lung epithelial cell lines, we observed significant dose-dependent increase in the level of DHA in the membranes of leukocytes (**Figure 4.5 D**) concomitant with the decrease in the level of AA (**Figure 4.5 E**), resulting in a large dose-dependent increase in DHA/AA ratio (**Figure 4.5 F**).

4.4.4 Fenretinide decreases the level of lipid oxidation without affecting protein oxidation in vitro

The level of malondialdehyde, a marker of lipid peroxidation was significantly higher in CFBE41o⁻(P) cells compared with CFBE41o⁻(wt-CFTR) cell line, and it was decreased by the treatment with Zn²⁺ and fenretinide in CFBE41o⁻(P) cells but not in CFBE41o⁻(wt-CFTR) cells

(**Figure 4.6 A**). On the other hand, 3-nitrotyrosine, a marker of oxidative damage of proteins was higher in CFBE41o⁻ (P) compared to CFBE41o⁻ (wt-CFTR) cells and its levels were affected by fenretinide/ Zn²⁺ treatment only in CFBE41o⁻ (P) cells (**Figure 4.6 B**). These results suggest that the absence of CFTR protein is associated with an increase in lipid and protein oxidation in CFBE41o⁻ epithelial cells, and that fenretinide treatment efficiently decreases oxidation of lipids. We also observed significant decrease in lipid peroxidation reflected through dose-dependent decrease in the level of malondialdehyde in PMBCs from CF patients (**Figure 4.6 C**). We did not observe significant change in the level of oxidative stress of proteins, assessed by the level of 3-nitrotyrosine (**Figure 4.6 D**).

4.4.5 Fenretinide inhibits the activity of cytosolic phospholipases (cPLA2)

Several studies have indicated that there is an increased release of AA from cell membranes, mediated by the family of cytosolic phospholipases A2, in cells from CF patients compared with healthy controls (Berguerand et al., 1997; Carlstedt-Duke et al., 1986; Dif et al., 2010; Levistre et al., 1993; Miele et al., 1997). In mammalian genome there are six genes for cytosolic phospholipases (PLA2G4A, PLA2G4B, PLA2G4C, PLA2G4D, PLA2G4E and PLA2G4F) coding for cPLA2- α , cPLA2- β , cPLA2- γ , cPLA2- δ , cPLA2- ϵ and cPLA2- ζ proteins respectively. We examined the mRNA levels of all six members of cPLA2 genes in CFBE41o⁻ cells by qPCR and we observed the expression of only two family members: PLA2G4A (Ct ~22) and PLA2G4C (Ct~28). All other members of this family were not significantly expressed in CFBE41o⁻ (P) and (WT-CFTR) cells as indicated by relatively their relatively high Ct values (Ct > 31). We did not observe any changes in the expression of PLA2G4A at mRNA level between CFBE41o⁻ (P) and CFBE41o⁻ (WT-CFTR) cells (**Figure S4.2**), nor upon fenretinide and/or Zn²⁺ treatment neither the protein level of cPLA2- α by Western blot (**Figure S4.3**). However, we observed that the mRNA level of PLA2G4C was 4-fold higher in the parental CFBE41o⁻ (P) than in CFBE41o⁻ (WT-CFTR) cells, even though the mRNA level of PLA2G4C was not affected by fenretinide treatment. Finally, we hypothesized that fenretinide may change the activity of one of the cytosolic phospholipases by affecting either its post-translational modifications that regulate its activity or post-translationally regulate the level of cPLA2 proteins.

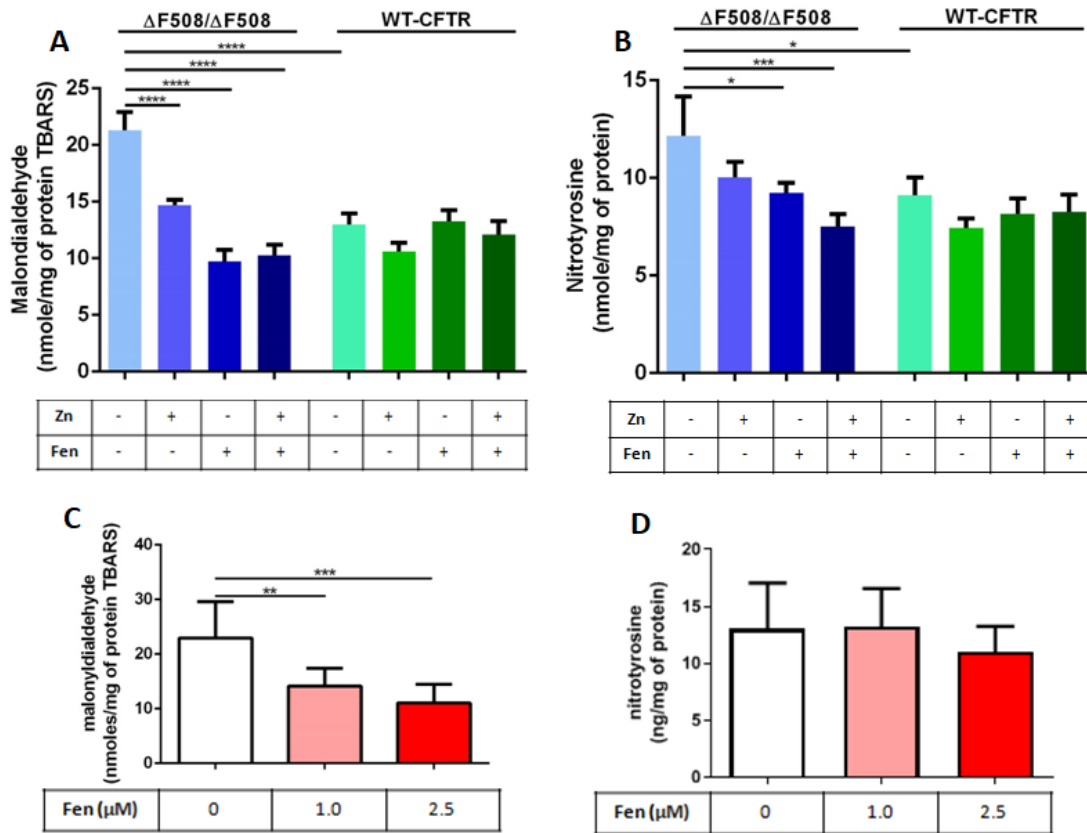


Figure 4.6 Effect of fenretinide (1.25 μM) and Zn^{2+} (12.5 μM) on the levels of malonyldialdehyde and nitrotyrosine in parental CFBE41o- ($\Delta F508/\Delta F508$) and CFBE41o- (CFTR-WT) cells (**A** and **B**). Dose-dependent effect of fenretinide on malonyldialdehyde and nitrotyrosine in PMBCs from CF patients (**C** and **D**). In CFBE41o- ($\Delta F508/\Delta F508$) cells the levels of malonyldialdehyde (**A**) and nitrotyrosine (**B**) are decreased by the treatment with either Zn^{2+} or fenretinide alone but the combination of the two does not have any additive effect. The reintroduction of wt-CFTR into CFBE41o- ($\Delta F508/\Delta F508$) cells results in a strong decrease in the level of malonyldialdehyde (**A**) and nitrotyrosine (**B**). In PMBCs from CF patients, fenretinide causes dose-dependent (1.0 and 2.5 μM) decrease in the level of malonyldialdehyde (**C**) but not in the level of nitrotyrosine (**D**). Data is represented as means \pm SD (* $p \leq 0.05$, ** $p \leq 0.01$, *** $p \leq 0.001$, **** $p \leq 0.0001$). All experiments were done in triplicates ($n=3$).

To test this possibility, we treated CFBE41o- (P) cells for 12, 24, 48 and 72h with a single dose of fenretinide (1.25 μM) known change DHA/AA ratio from lipidomic studies and we measured the activity of cPLA2 enzymes (expressed as nmol/min/ml) by colorimetric assay. Indeed, we

observed a significant decrease in cPLA2 activity starting at 12h post-treatment and very strong decrease of cPLA2 activity after 24, 48 and 72h (**Figure 4.7**). Interestingly Zn²⁺ ions alone had a small but statistically significant effect already after 12h, and much more potent effect again after 72h whereas this effect was not noticeable after 24h and 48h. On the other hand, the effect of fenretinide is evident already at 12h and becomes even stronger at the later time points. Combination of Zn²⁺ ions and fenretinide did not have any additive effect on cPLA2 activity. The mRNA and protein levels of cPLA2- α are not significantly different between CFBE41o- (P) and CFBE41o- (wt-CFTR) cells and they are not affected by fenretinide treatment. Therefore, our data demonstrate that fenretinide affects primarily cPLA2 activity in CFBE41o- (P) cells through the activity of either cPLA2- α or cPLA2- γ enzymes which are the only cytosolic phospholipases expressed in these cells.

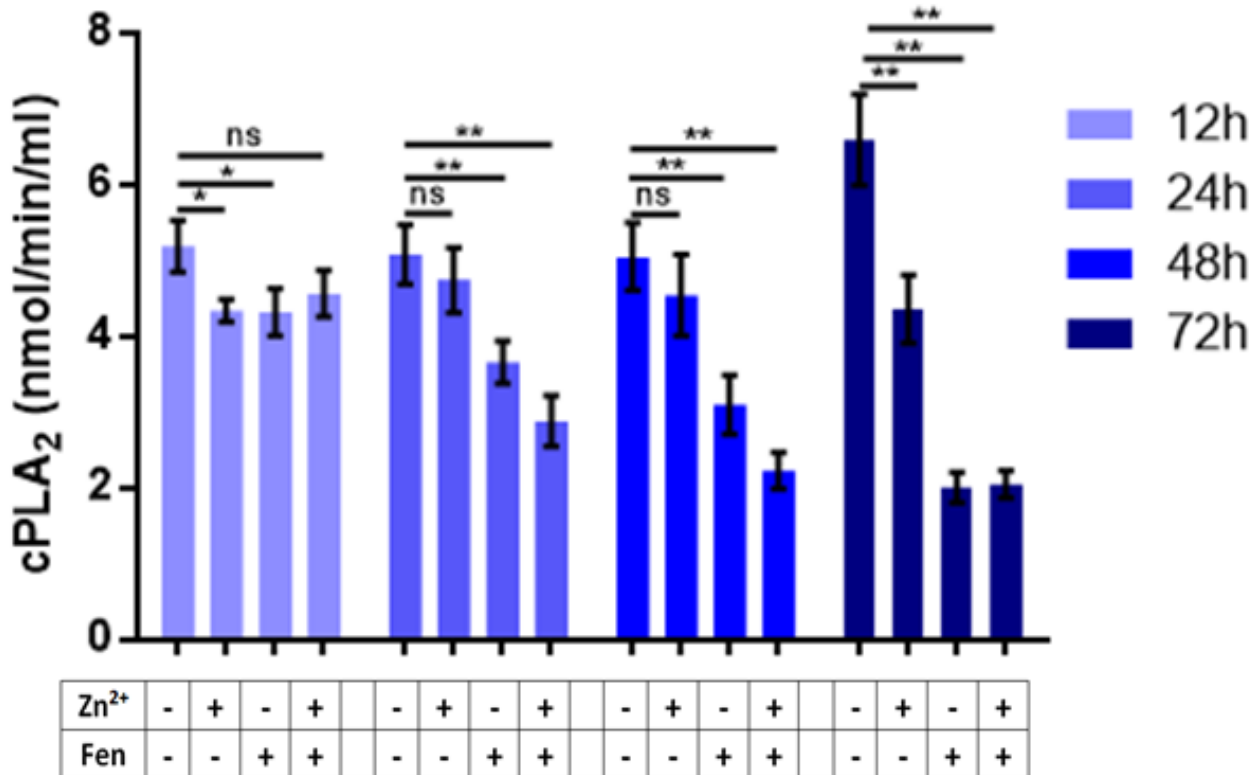


Figure 4.7 Fenretinide (1.25 μ M) and Zn²⁺ (12.5 μ M) inhibit total cPLA2 activity in CFBE41o- (Δ F508/ Δ F508) cells in a time dependent fashion. Data is represented as means \pm SD (* p \leq 0.05, ** p \leq 0.01). All experiments were done in triplicates (n=3).

4.5 Discussion

Accumulation of viscous mucus arising mostly from the DNA of dead neutrophils, but also from the over-expression of mucin genes creates a fertile soil for the growth of microorganisms in the lungs of CF patients. The expression of MUC5AC and MUC5B genes in mucociliary epithelium of the lungs has been known to depend on retinoic acid (RA) (Guzman et al., 1996; Koo et al., 1999a; Koo et al., 1999b) and to be strongly upregulated by NF- κ B signaling (Li et al., 1998a; Li et al., 1998b).

It was also previously reported that of the three retinoic acid receptors (RARs), antagonists of RAR- α strongly inhibited expression of mucin genes caused by RA and RAR- γ antagonists weakly inhibited RAR- α -induced expression of mucin genes whereas RAR- β was not directly involved in RA-induced mucin gene expression (Koo et al., 1999a). Interestingly, a compound Ro41-5253 developed by Hoffman-Roche which acts as an antagonist of RAR- α (Apfel et al., 1992) and an agonist of PPAR- γ (Schupp et al., 2007) prevents the overexpression of MUC5AC in normal human tracheobronchial cells upon various pro-inflammatory stimuli including bacterial lipopolysaccharide (LPS) (Koo et al., 2002). However, even though Ro41-5253 was first described back in 1992 and shown to be relatively safe in mice (Toma et al., 2005), to the best of our knowledge, its safety and efficacy have never been tested in the clinic.

Fenretinide was shown to activate the transcription of PPAR γ -responsive genes (Harris et al., 2005; Lin et al., 2016) and to be a highly selective activator of RAR- γ transcription factor without having any effects on RAR- α (Fanjul et al., 1996). Additionally, fenretinide is known to inhibit NF- κ B pathway (Shishodia et al., 2005).

Therefore, we wanted to test the effect of fenretinide on the expression of Muc5AC and Muc5B genes in the lung goblet cells. To this end, we used SPOC1 cell line which is to the best of our knowledge the only immortalized, non-tumorigenic lung goblet cell line shown to produce mucins after transplantation into syngeneic rats by Alcian Blue/Periodic Acid-Schiff stain (Doherty et al., 1995) and by non-specific mAb RTE11 antibody that recognizes α -linked galactose (Randell et al., 1996). Most commonly used lung cell lines for investigation of mucin production include A549, Calu-3 and many other immortalized cell lines derived from lung tumors. Unlike SPOC1 cells, all of these cell lines are tumorigenic cells with extensive

mutational landscapes and genomic rearrangements that may affect modeling of physiological expression of mucin genes (Blanco et al., 2009). On the other hand, unlike primary lung cells, SPOC1 cells are relatively easy to grow in cell culture, which makes them an attractive model for studying expression of mucin genes *in vitro*.

In this work, we characterized the expression of the two major lung mucins in SPOC-1 cell line and we discovered that Muc5B is constitutively expressed in these cells whereas Muc5AC is expressed only after long term stimulation with LPS. These results also suggest that SPOC1 cells were derived from a clonal population of cells originating from the submucosal glands of a rat and not from the goblet cells of the surface epithelial lining (Groneberg et al., 2002; Ostedgaard et al., 2017).

The induction of MUC5AC gene expression by LPS derived from *P. aeruginosa* was strongly diminished when fenretinide was added even during LPS treatment and was completely abolished if the cells were pre-treated with fenretinide or if fenretinide was applied at the same time as LPS (**Figure 4.1**). The increase in MUC5AC protein level was evident after 5 days of LPS treatment, but decreased at day 6 most likely during protein secretion since the level of mRNA for MUC5AC was still high at this time point (**Figure 4.2**). Pre-treatment with fenretinide diminished the level of MUC5AC protein upon LPS treatment while continuous treatment with fenretinide and/or LPS efficiently prevented LPS-induced production of MUC5AC protein.

On the other hand, the induction of MUC5B gene expression by LPS displayed much slower kinetics with slight increase in mRNA level evident after 5 days of treatment and stronger increase seen only at the end of the sixth day (**Figure 4.1**). Pre-treatment of SPOC-1 cells with fenretinide prevented the increase in MUC5B gene expression and continuous treatment with fenretinide and/or LPS did not result in an increase of MUC5B gene expression (**Figure 4.1**). The level of MUC5B protein was significantly higher only after 6 days of treatment, and pre-treatment with fenretinide did not cause a significant decrease (**Figure 4.2**). On the other hand, the levels of MUC5B protein in the cells pre-treated or continuously treated with fenretinide were significantly lower compared with LPS treated cells.

Fenretinide treatment alone significantly affected only the levels of Muc5AC protein (**Figure 4.2**). Taken together, these results demonstrate that fenretinide can effectively prevent LPS-induced overexpression of Muc5AC without significantly affecting the level of Muc5B protein in lung goblet cells. This is especially important considering the important biological differences between Muc5AC and Muc5B proteins in the lungs: MUC5B is required for mucociliary clearance and effective immunological defense of the lungs as demonstrated with Muc5B *-/-* mice who succumb to opportunistic bacterial infections (Roy et al., 2014). On the contrary, Muc5AC is dispensable for mucociliary clearance and anti-bacterial defense (Roy et al., 2014) and its overproduction causes pathological mucus plugging and airway obstruction (Evans et al., 2015).

Furthermore, we demonstrate here that the results obtained with SPOC-1 cells *in vitro* also translate *in vivo* in wild-type and CFTR-KO mice. Since the administration of free-living bacteria to the murine lung results in rapid bacterial clearance (Bragonzi, 2010), in order to model long-term bacterial infection seen in patients with CF, we used agarose beads coated with living *P. aeruginosa*.

Our results demonstrate that the pre-treatment of mice with fenretinide strongly reduced the infiltration of inflammatory cells and mucus production during infection with *P. aeruginosa*-coated beads (**Figure 4.3**). In particular, when comparing the immune response and mucus production around the bacteria-coated beads of approximately the same size from the lung sections of placebo-treated and fenretinide-treated CFTR-KO mice, we see significantly lower mucus production and diminished infiltration of inflammatory cells in fenretinide-treated CFTR-KO mice (**Figures S4.1 A and B**). Furthermore, the staining of the lung sections with jacalin and WGA, the two lectins that recognize specific glycosylation patterns on Muc5AC and Muc5B respectively, reveals that fenretinide pre-treatment specifically blocked overexpression of Muc5AC in infected mice without affecting the level of Muc5B (**Figure 4.4**).

Taken together, these results suggest that fenretinide has a potential to serve in clinic as a mucoregulatory agent that selectively prevents overproduction of the detrimental MUC5AC mucin upon inflammatory stimulation, without significantly affecting the level of the beneficial MUC5B mucin.

Pro-inflammatory lipid imbalance in patients with CF characterized by high levels of AA (Carlstedt-Duke et al., 1986; Gilljam et al., 1986) and low levels of DHA (Strandvik et al., 2001) (shortly referred to as low DHA/AA ratio) has been known for a long time. Clinical implications of the correction of this biochemical defect have been demonstrated as well, since dietary supplementation of DHA to CFTR-KO mice ameliorated many pathologic features including reduction of ileal villus hypertrophy, reversal of pancreatic duct dilation and suppression of pulmonary hyperinflammation (Freedman et al., 1999; Freedman et al., 2002) and reversal of low DHA/AA ratio by fenretinide treatment improved the ability of CFTR-KO mice to resolve pulmonary infection with *P. aeruginosa* (Guilbault et al., 2009).

The aberrant metabolism of fatty acid resulting in a diminished ratio of DHA/AA in the blood of CF patients could result from acute and chronic infections which CF patients are suffering from. However, comparing fatty acid levels in the $\Delta F508/\Delta F508$ epithelial cells and their counterparts transfected with wt-CFTR grown *in vitro* (ie. under sterile conditions) demonstrate that the mutated CFTR protein expression can be directly linked with the aberrant fatty acid metabolism, therefore providing a proof that the fatty acids aberrant metabolism is not secondary to pancreatic insufficiency or lung inflammation but is indeed causally linked to absence of functional CFTR protein (Andersson et al., 2008).

Our data are also consistent with the studies of Andersson and colleagues (Andersson et al., 2008) in which the authors used 16HBE14o- cells as a model of wild-type lung epithelial cells and IB3-1 cells originating from a compound heterozygous CF patient with $\Delta F508/W1282X$ mutations. In order to decrease the level of CFTR protein, Andersson and colleagues (Andersson et al., 2008) transfected 16HBE14o- cells with a plasmid carrying antisense RNA, and as a wild-type control for IB3-1 cells, they used this cell line transfected with wild-type CFTR (referred to as C38 cells). Indeed, they observed that the decrease of CFTR protein by antisense oligonucleotide in 16HBE14o- cells strongly decreased the level of DHA and increased the level of AA, resulting in a decrease in the DHA/AA ratio. Similar results were obtained when IB3-1 cells were compared with C38 cells.

Since we previously demonstrated that the treatment of CFBE41o-(P) cells with fenretinide and Zn^{2+} corrects their imbalance between long-chain and very-long-chain ceramides (Garic et al., 2017), we wondered how the same treatment would impact on the level of DHA and AA in these

cells. Indeed, we observed that the transfection of the parental CFBE41o- (P) cells with a plasmid carrying wild-type CFTR strongly increased the level of DHA (**Figure 4.5 A**) and decreased the level of AA (**Figure 4.5 B**), resulting in a greatly increased DHA/AA ratio (**Figure 4.5 C**). Interestingly, reintroduction of wild-type CFTR also resulted in a decrease in lipid oxidation. The levels of malondialdehyde, a marker of lipid peroxidation, and 3-nitrotyrosine, a marker of protein oxydation were significantly lowered by transfection of the wt-CFTR (**Figure 4.6 A and B**). The absence of a functional CFTR protein as seen in both 16HBE14o- cells transfected with anti-sense CFTR, parental IB3-1 ($\Delta F508/W1282X$) cells (Andersson et al., 2008) and parental CFBE41o- ($\Delta F508/\Delta F508$) cells results in a low level of DHA and high level of AA (ie. low DHA/AA ratio). Re-introduction of wild-type CFTR corrects this biochemical defect in all cases, therefore unambiguously establishing a causal relationship between the presence of a functional CFTR protein and the metabolism of DHA and AA.

We also demonstrated here that the treatment of CFBE41o- cells with fenretinide mimics the effects of the reintroduction of wild-type CFTR on both DHA and AA levels, effectively correcting low DHA/AA ratio (**Figure 4.5 A-C**). Combined treatment with fenretinide and Zn^{2+} further enhanced this effect. Interestingly even the treatment with Zn^{2+} alone had a small but statistically significant effect improving the aberrant DHA/AA ratio. As a micronutrient, Zn^{2+} is known to be deficient in patients with CF (Yadav et al., 2014), and supplementation with Zn^{2+} was shown to decrease respiratory infections in children with CF (Abdulhamid et al., 2008; Van Biervliet et al., 2008b). These results suggest that the patients treated with fenretinide would benefit from Zn^{2+} supplementation.

Since it is not possible to analyze lipidomic profile of lung epithelial cells of patients with CF without invasive interventions, we wondered whether the improvement in DHA/AA ratio seen in CFBE41o- cell line treated with fenretinide can be seen in also in other cells, which play an important role in regulation of inflammatory responses, such as PMBCs. Indeed, the first description of the abnormal metabolism of AA in CF that results in high levels of this lipid which was not possible to correct by dexamethasone treatment was reported in leukocytes from patients with CF (Carlstedt-Duke et al., 1986). Importantly, leukocytes are known to express CFTR (Johansson et al., 2014) protein, and inhibition of its function results in the production of pro-inflammatory cytokines by macrophages (Gao and Su, 2015) and adhesion deficiency in

monocytes (Sorio et al., 2016). Therefore, we treated PMBCs of eight pediatric patients with two doses of fenretinide *in vitro* and we analyzed the levels of DHA, AA, malondialdehyde and 3-nitrotyrosine. Indeed, as can be seen in **Figure 4.5 D-F**, the treatment of PMBCs with two concentrations of fenretinide caused a dose-dependent increase in DHA and decrease in AA levels, resulting in a strong dose-dependent increase in DHA/AA ratio. Similarly to the results obtained using CFBE41o- cells, the level of malondialdehyde was also decreased, whereas the level of 3-nitrotyrosine was not affected by fenretinide treatment of PMCs (**Figure 4.6 C and D**). Therefore, lipidomic changes seen in CFBE41o-(P) cells upon fenretinide treatment *in vitro* reflect on the leukocytes in patients with CF.

In order to investigate the mechanism whereby fenretinide decreases the level of AA, we treated CFBE41o- (P) cells with fenretinide in a time course dependent manner and we measured the activity of cytosolic phospholipases (cPLA2) by colorimetric assay. A number of studies have indicated that the abnormally high level of AA seen in CF is a consequence of an increased release of AA from cell membranes mediated by cytosolic phospholipases (cPLA2) (Berguerand et al., 1997; Carlstedt-Duke et al., 1986; Dif et al., 2010; Levistre et al., 1993; Miele et al., 1997). Indeed, as shown in **Figure 4.7**, fenretinide-mediated decrease in the activity of cytosolic phospholipases is evident already after 12h and further decrease seen at 24h and 48h, when a stably low level of cPLA2 activity is achieved. Treatment with Zn²⁺ ions significantly decreased cPLA2 activity only after 72h. To further elucidate this effect, we measured by qPCR the levels of all six cytosolic phospholipases present in mammalian genomes (PLA2G4A, PLA2G4B, PLA2G4C, PLA2G4D, PLA2G4E and PLA2G4F) by highly specific primers designed to detect each family member without cross-amplification (**Table S4.1**). Out of these six cytosolic phospholipases only PLA2G4A and PLA2G4C are significantly expressed in CFBE41o- cells whereas all other members are virtually absent as evidenced by high Ct values (Ct>31 per 30 ng of total cDNA). However, fenretinide did not have an effect on mRNA levels of any of the six cytosolic phospholipases (**Figure S4.2**). We also examined whether fenretinide affected the levels cPLA2- α protein in CFBE41o- cells by Western blot after 72h, when the highest inhibition of cPLA2 activity was seen, and we could not observe any changes in the amount of cPLA2- α protein. Since cPLA2- α and cPLA2- γ are the only cytosolic phospholipases present in CFBE41o- cells these results leave an open possibility that fenretinide may affect either the activity these

enzymes by post-translational modifications (e.g. phosphorylation) or affect the level of cPLA2- γ protein.

Additionally, an increase in the level of $\Delta 5$ - and $\Delta 6$ -desaturases has been proposed as an alternative explanation for the high levels of AA in cultured CF cells (Njoroge et al., 2011). We examined the level of both FADS1 and FADS2 genes (coding for $\Delta 5$ - and $\Delta 6$ -desaturases, respectively) in CFBE41o- cells. Indeed, both FADS1 and FADS2 genes are expressed in CFBE41o- cells (Ct~22 per 30 ng of input cDNA), but their mRNA levels were not affected by fenretinide treatment (**Figure S4.4**). Nevertheless, we cannot exclude a possibility that fenretinide affects the protein levels or their activity similarly to cPLA2.

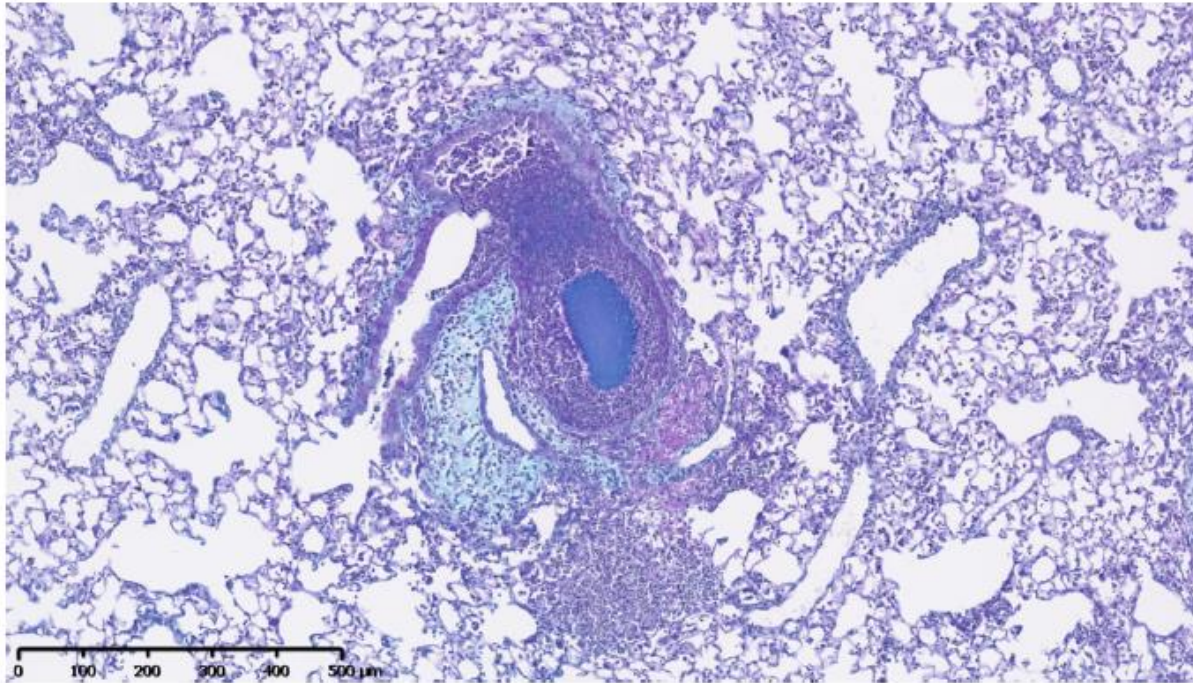
In summary, fenretinide is a novel mucoregulatory agent capable of selectively blocking the expression of MUC5AC gene upon LPS stimulation without significantly affecting the expression of MUC5B gene in pulmonary goblet cells *in vitro*. Pre-treatment of mice with fenretinide efficiently prevents mucus accumulation in a model of chronic lung infection with *P. aeruginosa*. Furthermore, fenretinide treatment of lung epithelial cell line and primary leukocytes isolated from CF patients efficiently mimics the effects wild-type CFTR reintroduction on the levels of AA and DHA, thereby efficiently normalizing aberrant DHA/AA ratio. The ongoing Phase II trial APPLAUD (NCT03265288) will allow adequate evaluation of its therapeutic potential including the frequency and ability of resolve chronic inflammation.

4.6 Supplementary Information

Table S4.1

Gene	Sense	Sequence (5' to 3')
Rat β -actin	F	GTATGGAATCCTGTGGCATC
	R	TGTGTTGGCATAGAGGTCTT
Rat Muc5AC	F	AACCAAGAAGTCCTCCTGA
	R	AAGCAGCAGGTAGGTAGAA
Rat Muc5B	F	GGTTCTGTGTTGTGATTATG
	R	GATGCTGTATGAGTGGTAA
Human PLA2G4A	F	CATTATACGAATCAGGAATTCTGG
	R	TTGACATATAACCAGGTGGAGCC
Human PLA2G4B	F	CAGGCAGCTCAAGAATGTC
	R	GACAACACAGGGTCATCTC
Human PLA2G4C	F	GAGATGAAAGAACAGGGCC
	R	AAGATATTGCCCAAGTGGAT
Human PLA2G4D	F	AGTCAGGTCAAGAATGTTC
	R	GAGATGTCATAGAGAACCTT
Human PLA2G4E	F	AAGGACCATCTCCAACCTG
	R	TCTAGCACGTTCTTCACT
Human PLA2G4F	F	TGCTGTGAAGAACGTCCT
	R	TTCTCAGGTCAAACAGGAG
Human FADS1	F	AGCCCACCAAGAATAAAGA
	R	AGGTACAGCAGGAAGAAG
Human FADS2	F	GCCACCTGTCTGTCTACA
	R	CAGAGGCACCCTTTAAGT

A



B

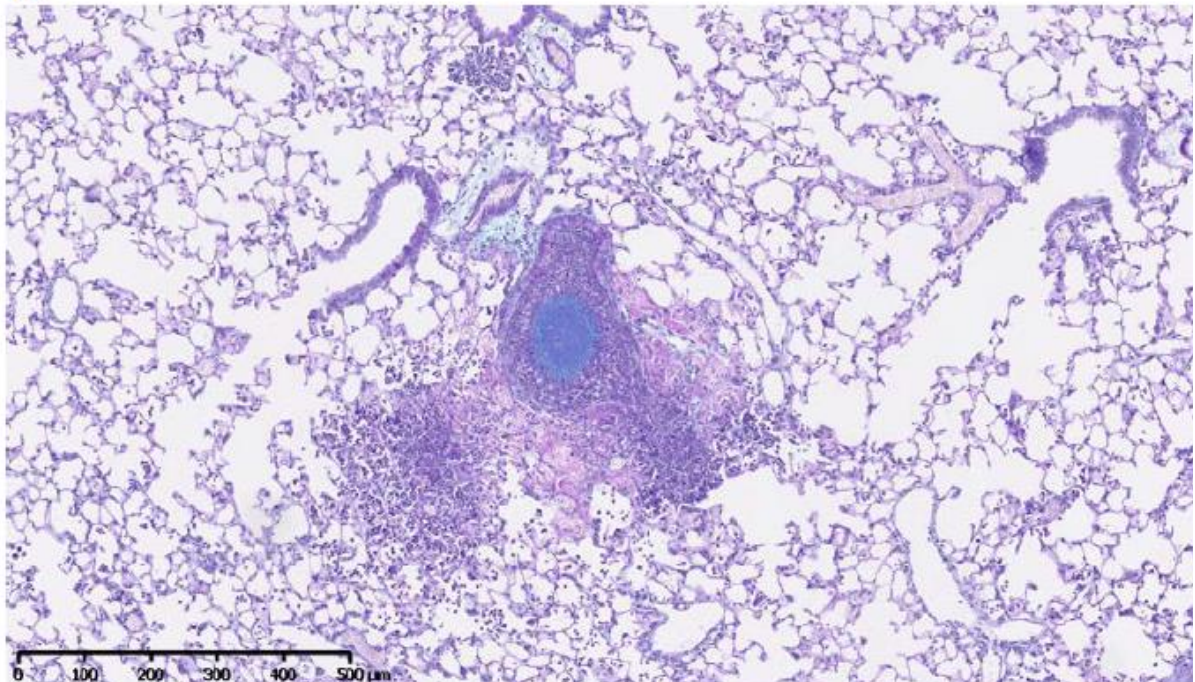


Figure S4.1 Lung sections from the **Figure 4.3** at higher magnification: CFTR-KO mice infected with *P.aeruginosa*-coated beads and treated with either placebo (A) or fenretinide (B). 10x magnification, scale bar = 500 μ m.

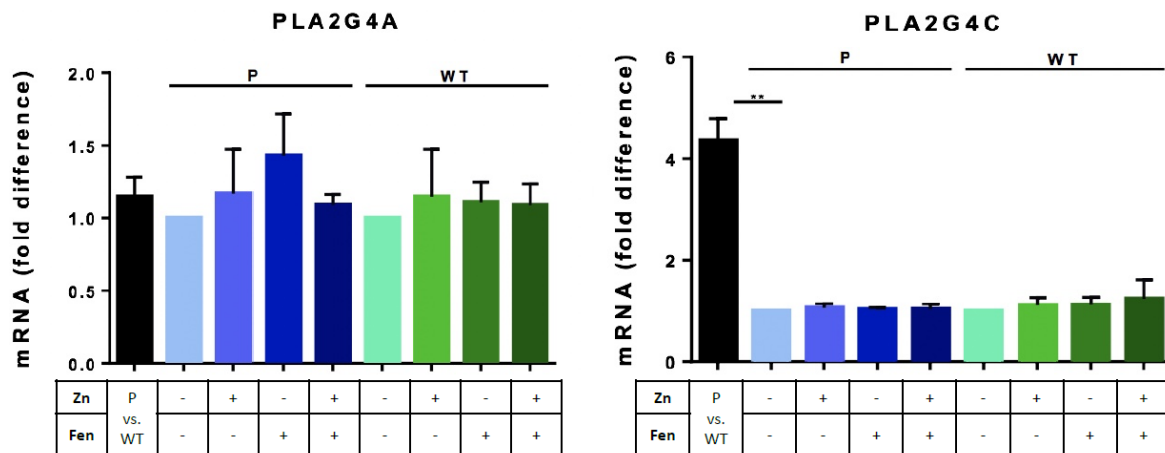


Figure S4.2 The mRNA levels of PLA2G4A and PLA2G4C in CFBE41o- ($\Delta F508/\Delta F508$) and CFBE41o- (wt-CFTR) treated with fenretinide (1.25 μM) and Zn^{2+} (12.5 μM). Data is represented as means \pm SD (** $p < 0.01$). All experiments were done in triplicates ($n=3$).

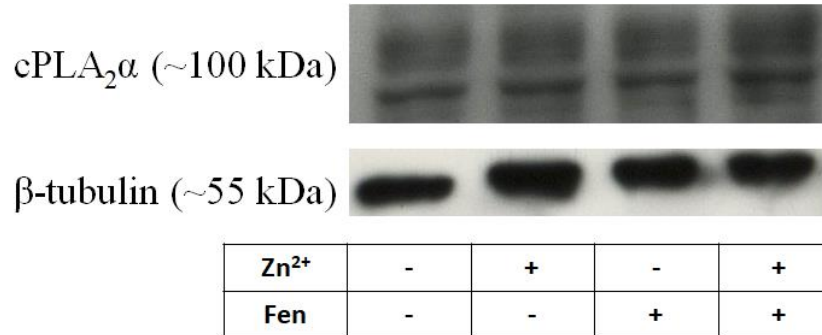


Figure S4.3 The protein level of cPLA₂ α in CFBE41o- ($\Delta F508/\Delta F508$) treated with fenretinide (1.25 μM) and Zn^{2+} (12.5 μM) assessed by Western blot.

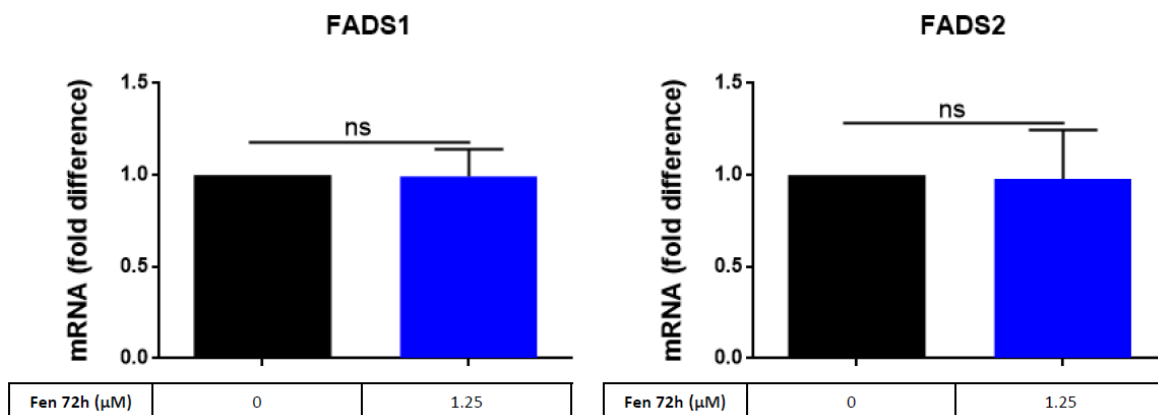


Figure S4.4 The mRNA levels of FADS1 and FADS2 in CFBE41o- ($\Delta F508/\Delta F508$) treated with fenretinide (1.25 μM). Data is represented as means \pm SD (ns= not significant). Both experiments were done in triplicates ($n=3$).

Chapter 5

Discussion, Conclusions and Future Directions

5.1 Discussion

This thesis is a collection of efforts aimed to understand the components and consequences of sterile and pathogen-induced inflammation in CF. These efforts undertaken through very diverse yet complementing approaches that stem from disciplines like immunology, lipidomics and molecular biology led to discoveries presented in **Chapters 2-4**.

Chapter 1 is an introduction into theoretical concepts and practical considerations written in the form of three Review articles that are either already published or are currently under consideration. The first part addresses the previously unappreciated and still largely unexplored role of BAFF cytokine in the immunological defense of lungs and the rationale of using it as an adjuvant in the development of vaccines aimed against pulmonary pathogens. The second part is a comprehensive review of metabolic and structural roles of ceramides in cell biology. Additionally, it is also a discussion on the fundamental physiological differences between long- and very-long chain ceramides revealed through knock-out mouse models for *Cers2* enzyme. Indeed, the work on *Cers2*-KO mice established long-chain-ceramides as the critical components of sterile inflammation in the lungs as very-long-chain-ceramides as anti-inflammatory molecules essential for lung homeostasis. Furthermore, in this Review I outlined for the first time a hypothesis on the impact of the different intramembranous environments created by acyl chains of long- and very-long-chain ceramides on the stability of large and intrinsically disordered proteins such as CFTR.

In **Chapter 2**, I explored the role of BAFF cytokine in the immunological defense of lungs. First, we explored whether BAFF is a component of the constitutive inflammation in CFTR-KO mice which compromises the ability of mice to combat infection or it is component of pathogen-induced protective inflammatory response. Indeed, we discovered that BAFF is not a component of the constitutive (sterile) inflammation in CFTR-KO mice, but is strongly induced upon lung infection with *Pseudomonas*. Depletion of BAFF cytokine by Sandy-2 antibody renders both wild-type and CFTR-KO mice extremely susceptible to the infection with *Pseudomonas* demonstrated by an increased bacterial load and increased metacholine-induced lung resistance upon BAFF deletion. Therefore, these results raise special concerns with regards to the immune defense of the lungs in lupus patients who are treated with Belimumab[®], a monoclonal antibody used to deplete BAFF cytokine in order to control pathologic inflammation. Finally, even though

BAFF-KO mice do not have any noticeable defects in T-cell counts, we discovered that BAFF depletion strongly diminished the levels of Treg cells in the lungs but not in the spleen of non-infected mice. Nevertheless, these results are in accordance with the previously described BAFF transgenic mice where the overexpression of BAFF cytokine surprisingly leads to the increase in the number of Treg cells.

The work of others as well as our own discussed in the **Chapter 1**, served as the basis for our work presented in **Chapter 3**. Here, we systematically examined the levels of LCCs and VLCCs in the CF patients, CF mice and a CF cell line and the effect of fenretinide on these sphingolipids. Our demonstrated that VLCCs were consistently downregulated in CF mice and CF patients and LCCs were upregulated both in CF mice and CF patients compared to the controls. We also noticed that fenretinide reverses this ceramide imbalance by upregulating VLCCs and downregulating LCCs. Furthermore, using CFBE41o- cells as a model, we discovered the mechanism responsible for the observed changes in LCCs and VLCCs caused by fenretinide treatment. In fact, Cers2 requires Cers5 enzyme in order to produce VLCCs (ie. Cers2:Cers2 dimers are catalytically inactive, Cers2:Cers5 heterodimers produce VLCCs and Cers5:Cers5 homodimers produce LCCs). So, by downregulating the mRNA level of Cers5 enzyme which is reflected on the level of Cers5 protein as well, fenretinide changes the ratio of Cers5/Cers2 enzymes in favor of the formation of Cers5:Cers2 heterodimers over Cers5:Cers5 homodimers. Additionally, deficiency of Zn^{2+} which was described in patients with CF prompted us to explore whether the combination with fenretinide would have an additive effect in the downregulation of LCCs and upregulation of VLCCs. Indeed, we discovered that this was the case, although the effect of Zn^{2+} ions alone is much smaller than that of fenretinide. Finally, the fact that the imbalance between LCC and VLCC ceramides species exists even in the cell culture (CFBE41o- cells are derived from a $\Delta F_{508}/\Delta F_{508}$ patient) and that it is corrected upon transfection of cells with a wild-type CFTR gene strongly suggests a causal connection between ceramide imbalance and the absence of a functional CFTR molecule. The mechanistic details of this connection should be an area of active investigation in the future.

Finally, **Chapter 4** describes an attempt to understand mechanistically the connection between the lack of functional CFTR and pro-inflammatory imbalance of fatty acids and established fenretinide as a putative mucoregulatory agent. The pro-inflammatory imbalance of fatty acids,

expressed as increased AA/DHA ratio, is a phenomenon that was described in CF long before discovery of CFTR gene. However, up to this day, the mechanistic connection between the lack of CFTR protein and observed imbalance of fatty acids has not been unequivocally established. For a long time it was thought that malnutrition due to the pancreatic insufficiency or persistent lung inflammation could be the causes of this phenomenon, but the existence of the pro-inflammatory fatty acid imbalance in cell culture eliminated both possibilities. Regardless of the connection with CFTR, increased activity of cPLA2 enzymes was postulate to contribute to the increased levels of AA. Our previous results demonstrated that fenretinide decreases the level of AA in CFTR-KO mice, and the work presented in **Chapter 4**. suggests that it may be exerting this effect by inhibiting the activity of one of cPLA2 enzymes. Interestingly, the re-introduction of wild-type CFTR into CFBE41o- ($\Delta F_{508}/\Delta F_{508}$) cells fully corrects AA/DHA imbalance by decreasing the level of AA and increasing the level of DHA, which further corroborates previous data that the presence of functional CFTR somehow affects the level of these fatty acids.

Finally, we explored the effect of fenretinide on MUC5AC and MUC5B genes because of its known effect on retinoid receptors and NF- κ B pathway. Preliminary results suggest that fenretinide at low doses may block induction of MUC5AC transcription by LPS without significantly affecting MUC5B gene. These results are important because MUC5B gene is known to be essential for the defense of lungs against airborne pathogens, whereas MUC5AC is designated as a culprit for the pathological plugging of the airways.

Fenretinide has already shown very satisfactory safety profile in the long-term treatment of patients with breast cancer in Italy and also in our Phase Ib clinical trial in patients with CF. Currently, LAU-7B formulation of fenretinide is being tested in the Phase II (APPLAUD) trial (NCT03265288), double-blind, randomized, placebo-controlled study to evaluate efficacy in patients with CF. If the results of this clinical trial demonstrate improvement in any of the CF-related symptoms, fenretinide will be an important addition to the very small armamentarium of available drugs for treatment of this incurable disease.

5.2 Conclusions

In the **Chapter 1.** we presented for the first time the evidence for the lack of specificity of currently available commercial antibodies for the detection of ceramides. We believe that these results will lead to the reinterpretation of many previously published results in the biochemistry of ceramides.

The work presented in the **Chapter 2.** revealed for the first time an essential role for BAFF cytokine in the immunological defense of the lungs. These results raise substantive concerns for the health of patients with lupus who are treated with currently approved anti-BAFF therapies (ie. Belimumab®).

The results presented in the **Chapter 3.** established a strong connection between the absence of a functional CFTR protein and the imbalance of an important class of lipids called ceramides. These results also offered for the first time a hope than an intrinsic defect present in the cell membranes of patients with CF could be corrected with a clinically safe drug called fenretinide.

The results presented in the **Chapter 4.** further corroborated a causal link between the expression of functional CFTR protein and a long-known pro-inflammatory imbalance of fatty acids present in patients with CF. Furthermore, this work for the first time examined the potential for fenretinide to specifically block overexpression of Muc5AC gene, the known culprit for pathological plugging of the airways with mucus produced during allergic reaction or infections, without interfering with the expression of Muc5B gene, known to be essential for normal functioning of the lungs.

5.3 Future Directions

The discussion on the fundamental biophysical and biochemical differences between long- and very-long-chain ceramides presented in the **Chapter 1**, together with the results presented in the **Chapter 3**, open a possibility that correction of inherent defects of cell membranes present in CF could also lead to the improved folding of intrinsically disordered, large transmembrane proteins such as CFTR. If this possibility turns out to be correct, the clinically safe drug called fenretinide could be used in combination with approved folding correctors (such as VX809 or VX661) in order to obtain better expression and stability of mutant CFTR proteins on the surface of epithelial cells of patients with CF.

Surprising biological differences between Muc5AC and Muc5B mucins, two major protein components of the mucus in the lungs were recently discovered. The work presented in **Chapter 4**, revealed for the first time that it is possible to selectively block pathogen-induced increases in the levels of a detrimental Muc5AC mucin, in cultured cells and mice, without interfering with the levels of a beneficial Muc5B mucin. Therefore, it will be of interest to investigate whether these results can be translated to the clinic. Currently ongoing Phase II clinical trial (NCT03265288) will offer answers to these questions.

Chapter 6.

References

Abbas, A.K., Lichtman, A.H., and Pillai, S. (2018). Cellular and molecular immunology. (Philadelphia, PA, Elsevier).

Abdulhamid, I., Beck, F.W., Millard, S., Chen, X., and Prasad, A. (2008). Effect of zinc supplementation on respiratory tract infections in children with cystic fibrosis. *Pediatr Pulmonol* 43, 281-287.

Abdullah, L.H., Evans, J.R., Wang, T.T., Ford, A.A., Makhov, A.M., Nguyen, K., Coakley, R.D., Griffith, J.D., Davis, C.W., Ballard, S.T., and Kesimer, M. (2017). Defective postsecretory maturation of MUC5B mucin in cystic fibrosis airways. *JCI Insight* 2, e89752.

Abe, M., Kido, S., Hiasa, M., Nakano, A., Oda, A., Amou, H., and Matsumoto, T. (2006). BAFF and APRIL as osteoclast-derived survival factors for myeloma cells: a rationale for TACI-Fc treatment in patients with multiple myeloma. *Leukemia* 20, 1313-1315.

Abu-Arish, A., Pandzic, E., Goepp, J., Matthes, E., Hanrahan, J.W., and Wiseman, P.W. (2015). Cholesterol modulates CFTR confinement in the plasma membrane of primary epithelial cells. *Biophys J* 109, 85-94.

Accurso, F.J., Rowe, S.M., Clancy, J.P., Boyle, M.P., Dunitz, J.M., Durie, P.R., Sagel, S.D., Hornick, D.B., Konstan, M.W., Donaldson, S.H., *et al.* (2010). Effect of VX-770 in persons with cystic fibrosis and the G551D-CFTR mutation. *N Engl J Med* 363, 1991-2003.

Al-Turkmani, M.R., Andersson, C., Alturkmani, R., Katrangi, W., Cluette-Brown, J.E., Freedman, S.D., and Laposata, M. (2008). A mechanism accounting for the low cellular level of linoleic acid in cystic fibrosis and its reversal by DHA. *J Lipid Res* 49, 1946-1954.

Al Tanoury, Z., Piskunov, A., and Rochette-Egly, C. (2013). Vitamin A and retinoid signaling: genomic and nongenomic effects. *J Lipid Res* 54, 1761-1775.

Aldamiz-Echevarria, L., Prieto, J.A., Andrade, F., Elorz, J., Sojo, A., Lage, S., Sanjurjo, P., Vazquez, C., and Rodriguez-Soriano, J. (2009). Persistence of essential fatty acid deficiency in cystic fibrosis despite nutritional therapy. *Pediatr Res* 66, 585-589.

Alexander, T., Sattler, A., Templin, L., Kohler, S., Gross, C., Meisel, A., Sawitzki, B., Burmester, G.R., Arnold, R., Radbruch, A., *et al.* (2013). Foxp3⁺ Helios⁺ regulatory T cells are expanded in active systemic lupus erythematosus. *Ann Rheum Dis* 72, 1549-1558.

Allard, J.B., Poynter, M.E., Marr, K.A., Cohn, L., Rincon, M., and Whittaker, L.A. (2006). *Aspergillus fumigatus* generates an enhanced Th2-biased immune response in mice with defective cystic fibrosis transmembrane conductance regulator. *J Immunol* 177, 5186-5194.

Aloisi, F., and Pujol-Borrell, R. (2006). Lymphoid neogenesis in chronic inflammatory diseases. *Nat Rev Immunol* 6, 205-217.

Alsaleh, G., Messer, L., Semaan, N., Boulanger, N., Gottenberg, J.E., Sibilia, J., and Wachsmann, D. (2007). BAFF synthesis by rheumatoid synoviocytes is positively controlled by alpha5beta1 integrin stimulation and is negatively regulated by tumor necrosis factor alpha and Toll-like receptor ligands. *Arthritis Rheum* 56, 3202-3214.

Anderson, M.K., Weiss, A.H., Hernandez-Hoyos, G., Dionne, C.J., and Rothenberg, E.V. (2002). Constitutive expression of PU.1 in fetal hematopoietic progenitors blocks T cell development at the pro-T cell stage. *Immunity* 16, 285-296.

Andersson, C., Al-Turkmani, M.R., Savaille, J.E., Alturkmani, R., Katrangi, W., Cluette-Brown, J.E., Zaman, M.M., Laposata, M., and Freedman, S.D. (2008). Cell culture models demonstrate that CFTR dysfunction leads to defective fatty acid composition and metabolism. *J Lipid Res* 49, 1692-1700.

Antigny, F., Norez, C., Dannhoffer, L., Bertrand, J., Raveau, D., Corbi, P., Jayle, C., Becq, F., and Vandebrouck, C. (2011). Transient receptor potential canonical channel 6 links Ca²⁺ mishandling to cystic fibrosis transmembrane conductance regulator channel dysfunction in cystic fibrosis. *Am J Respir Cell Mol Biol* 44, 83-90.

Apfel, C., Bauer, F., Crettaz, M., Forni, L., Kamber, M., Kaufmann, F., LeMotte, P., Pirson, W., and Klaus, M. (1992). A retinoic acid receptor alpha antagonist selectively counteracts retinoic acid effects. *Proc Natl Acad Sci U S A* 89, 7129-7133.

Baker, J.M., Hudson, R.P., Kanelis, V., Choy, W.Y., Thibodeau, P.H., Thomas, P.J., and Forman-Kay, J.D. (2007). CFTR regulatory region interacts with NBD1 predominantly via multiple transient helices. *Nat Struct Mol Biol* 14, 738-745.

Bassing, C.H., Swat, W., and Alt, F.W. (2002). The mechanism and regulation of chromosomal V(D)J recombination. *Cell* 109 Suppl, S45-55.

Bebok, Z., Collawn, J.F., Wakefield, J., Parker, W., Li, Y., Varga, K., Sorscher, E.J., and Clancy, J.P. (2005). Failure of cAMP agonists to activate rescued deltaF508 CFTR in CFBE41o- airway epithelial monolayers. *J Physiol* 569, 601-615.

Becker, K.A., Riethmuller, J., Luth, A., Doring, G., Kleuser, B., and Gulbins, E. (2010). Acid sphingomyelinase inhibitors normalize pulmonary ceramide and inflammation in cystic fibrosis. *Am J Respir Cell Mol Biol* 42, 716-724.

Beharry, S., Ackerley, C., Corey, M., Kent, G., Heng, Y.M., Christensen, H., Luk, C., Yantiss, R.K., Nasser, I.A., Zaman, M., *et al.* (2007). Long-term docosahexaenoic acid therapy in a congenic murine model of cystic fibrosis. *Am J Physiol Gastrointest Liver Physiol* 292, G839-848.

Belessis, Y., Dixon, B., Hawkins, G., Pereira, J., Peat, J., MacDonald, R., Field, P., Numa, A., Morton, J., Lui, K., and Jaffe, A. (2012). Early cystic fibrosis lung disease detected by bronchoalveolar lavage and lung clearance index. *Am J Respir Crit Care Med* 185, 862-873.

Benson, M.J., Dillon, S.R., Castigli, E., Geha, R.S., Xu, S., Lam, K.P., and Noelle, R.J. (2008). Cutting edge: the dependence of plasma cells and independence of memory B cells on BAFF and APRIL. *J Immunol* 180, 3655-3659.

Berguerand, M., Klapisz, E., Thomas, G., Humbert, L., Jouniaux, A.M., Olivier, J.L., Bereziat, G., and Masliah, J. (1997). Differential stimulation of cytosolic phospholipase A2 by bradykinin in human cystic fibrosis cell lines. *Am J Respir Cell Mol Biol* 17, 481-490.

Berni, R., Clerici, M., Malpeli, G., Cleris, L., and Formelli, F. (1993). Retinoids: in vitro interaction with retinol-binding protein and influence on plasma retinol. *FASEB J* 7, 1179-1184.

Berni, R., and Formelli, F. (1992). In vitro interaction of fenretinide with plasma retinol-binding protein and its functional consequences. *FEBS Lett* 308, 43-45.

Berwouts, S., Morris, M.A., Girodon, E., Schwarz, M., Stuhmann, M., and Dequeker, E. (2011). Mutation nomenclature in practice: findings and recommendations from the cystic fibrosis external quality assessment scheme. *Hum Mutat* 32, 1197-1203.

Binker, M.G., Binker-Cosen, M.J., Richards, D., Binker-Cosen, A.A., Freedman, S.D., and Cosen-Binker, L.I. (2015). Omega-3 PUFA docosahexaenoic acid decreases LPS-stimulated MUC5AC production by altering EGFR-related signaling in NCI-H292 cells. *Biochem Biophys Res Commun* 463, 1047-1052.

Blanco, R., Iwakawa, R., Tang, M., Kohno, T., Angulo, B., Pio, R., Montuenga, L.M., Minna, J.D., Yokota, J., and Sanchez-Cespedes, M. (2009). A gene-alteration profile of human lung cancer cell lines. *Hum Mutat* 30, 1199-1206.

Blasbalg, T.L., Hibbeln, J.R., Ramsden, C.E., Majchrzak, S.F., and Rawlings, R.R. (2011). Changes in consumption of omega-3 and omega-6 fatty acids in the United States during the 20th century. *Am J Clin Nutr* 93, 950-962.

Blenman, K.R., Duan, B., Xu, Z., Wan, S., Atkinson, M.A., Flotte, T.R., Croker, B.P., and Morel, L. (2006). IL-10 regulation of lupus in the NZM2410 murine model. *Lab Invest* 86, 1136-1148.

Bollinger, C.R., Teichgraber, V., and Gulbins, E. (2005). Ceramide-enriched membrane domains. *Biochim Biophys Acta* 1746, 284-294.

Borowitz, D., Baker, R.D., and Stallings, V. (2002). Consensus report on nutrition for pediatric patients with cystic fibrosis. *J Pediatr Gastroenterol Nutr* 35, 246-259.

Bosch, L., Bosch, B., De Boeck, K., Nawrot, T., Meyts, I., Vanneste, D., Le Bourlegat, C.A., Croda, J., and da Silva Filho, L. (2017). Cystic fibrosis carriership and tuberculosis: hints toward an evolutionary selective advantage based on data from the Brazilian territory. *BMC Infect Dis* 17, 340.

Bossen, C., Cachero, T.G., Tardivel, A., Ingold, K., Willen, L., Dobles, M., Scott, M.L., Maquelin, A., Belnoue, E., Siegrist, C.A., *et al.* (2008). TACI, unlike BAFF-R, is solely activated by oligomeric BAFF and APRIL to support survival of activated B cells and plasmablasts. *Blood* 111, 1004-1012.

Bourbon, N.A., Yun, J., and Kester, M. (2000). Ceramide directly activates protein kinase C zeta to regulate a stress-activated protein kinase signaling complex. *J Biol Chem* 275, 35617-35623.

Bragonzi, A. (2010). Murine models of acute and chronic lung infection with cystic fibrosis pathogens. *Int J Med Microbiol* 300, 584-593.

Brodie, M., McKean, M.C., Johnson, G.E., Gray, J., Fisher, A.J., Corris, P.A., Lordan, J.L., and Ward, C. (2010). Ceramide is increased in the lower airway epithelium of people with advanced cystic fibrosis lung disease. *Am J Respir Crit Care Med* 182, 369-375.

Bu, P., and Wan, Y.J. (2007). Fenretinide-induced apoptosis of Huh-7 hepatocellular carcinoma is retinoic acid receptor beta dependent. *BMC Cancer* 7, 236.

Camerini, T., Mariani, L., De Palo, G., Marubini, E., Di Mauro, M.G., Decensi, A., Costa, A., and Veronesi, U. (2001). Safety of the synthetic retinoid fenretinide: long-term results from a controlled clinical trial for the prevention of contralateral breast cancer. *J Clin Oncol* 19, 1664-1670.

Canals, D., Roddy, P., and Hannun, Y.A. (2012). Protein phosphatase 1alpha mediates ceramide-induced ERM protein dephosphorylation: a novel mechanism independent of

phosphatidylinositol 4, 5-bisphosphate (PIP₂) and myosin/ERM phosphatase. *J Biol Chem* 287, 10145-10155.

Canals, D., Salamone, S., and Hannun, Y.A. (2018). Visualizing bioactive ceramides. *Chem Phys Lipids* 216, 142-151.

Cantin, A.M., Hartl, D., Konstan, M.W., and Chmiel, J.F. (2015). Inflammation in cystic fibrosis lung disease: Pathogenesis and therapy. *J Cyst Fibros* 14, 419-430.

Carlstedt-Duke, J., Bronnegard, M., and Strandvik, B. (1986). Pathological regulation of arachidonic acid release in cystic fibrosis: the putative basic defect. *Proc Natl Acad Sci U S A* 83, 9202-9206.

Carragher, D.M., Rangel-Moreno, J., and Randall, T.D. (2008). Ectopic lymphoid tissues and local immunity. *Semin Immunol* 20, 26-42.

Casaulta, C., Schoni, M.H., Weichel, M., Cramer, R., Jutel, M., Daigle, I., Akdis, M., Blaser, K., and Akdis, C.A. (2003). IL-10 controls *Aspergillus fumigatus*- and *Pseudomonas aeruginosa*-specific T-cell response in cystic fibrosis. *Pediatr Res* 53, 313-319.

Castigli, E., Scott, S., Dedeoglu, F., Bryce, P., Jabara, H., Bhan, A.K., Mizoguchi, E., and Geha, R.S. (2004). Impaired IgA class switching in APRIL-deficient mice. *Proc Natl Acad Sci U S A* 101, 3903-3908.

Chang, K.T., Anishkin, A., Patwardhan, G.A., Beverly, L.J., Siskind, L.J., and Colombini, M. (2015). Ceramide channels: destabilization by Bel-xL and role in apoptosis. *Biochim Biophys Acta* 1848, 2374-2384.

Chen, C.J., Kono, H., Golenbock, D., Reed, G., Akira, S., and Rock, K.L. (2007). Identification of a key pathway required for the sterile inflammatory response triggered by dying cells. *Nat Med* 13, 851-856.

Chen, Y., Zhao, Y.H., Di, Y.P., and Wu, R. (2001). Characterization of human mucin 5B gene expression in airway epithelium and the genomic clone of the amino-terminal and 5'-flanking region. *Am J Respir Cell Mol Biol* 25, 542-553.

Chen, Z.J. (2005). Ubiquitin signalling in the NF-kappaB pathway. *Nat Cell Biol* 7, 758-765.

Cheng, S.H., Gregory, R.J., Marshall, J., Paul, S., Souza, D.W., White, G.A., O'Riordan, C.R., and Smith, A.E. (1990). Defective intracellular transport and processing of CFTR is the molecular basis of most cystic fibrosis. *Cell* 63, 827-834.

Cheon, Y., Kim, H.W., Igarashi, M., Modi, H.R., Chang, L., Ma, K., Greenstein, D., Wohltmann, M., Turk, J., Rapoport, S.I., and Taha, A.Y. (2012). Disturbed brain phospholipid and docosahexaenoic acid metabolism in calcium-independent phospholipase A(2)-VIA (iPLA(2)beta)-knockout mice. *Biochim Biophys Acta* 1821, 1278-1286.

Children's Oncology, G., Villablanca, J.G., Krailo, M.D., Ames, M.M., Reid, J.M., Reaman, G.H., and Reynolds, C.P. (2006). Phase I trial of oral fenretinide in children with high-risk solid tumors: a report from the Children's Oncology Group (CCG 09709). *J Clin Oncol* 24, 3423-3430.

Cholon, D.M., Quinney, N.L., Fulcher, M.L., Esther, C.R., Jr., Das, J., Dokholyan, N.V., Randell, S.H., Boucher, R.C., and Gentsch, M. (2014). Potentiator ivacaftor abrogates pharmacological correction of DeltaF508 CFTR in cystic fibrosis. *Sci Transl Med* 6, 246ra296.

Clancy, J.P., Rowe, S.M., Accurso, F.J., Aitken, M.L., Amin, R.S., Ashlock, M.A., Ballmann, M., Boyle, M.P., Bronsveld, I., Campbell, P.W., *et al.* (2012). Results of a phase IIa study of VX-809, an investigational CFTR corrector compound, in subjects with cystic fibrosis homozygous for the F508del-CFTR mutation. *Thorax* 67, 12-18.

Cohen-Cymerknoh, M., Kerem, E., Ferkol, T., and Elizur, A. (2013). Airway inflammation in cystic fibrosis: molecular mechanisms and clinical implications. *Thorax* 68, 1157-1162.

Coleman, F.T., Mueschenborn, S., Meluleni, G., Ray, C., Carey, V.J., Vargas, S.O., Cannon, C.L., Ausubel, F.M., and Pier, G.B. (2003). Hypersusceptibility of cystic fibrosis mice to chronic *Pseudomonas aeruginosa* oropharyngeal colonization and lung infection. *Proc Natl Acad Sci U S A* 100, 1949-1954.

Conrad, C., Lymp, J., Thompson, V., Dunn, C., Davies, Z., Chatfield, B., Nichols, D., Clancy, J., Vender, R., Egan, M.E., *et al.* (2015). Long-term treatment with oral N-acetylcysteine: affects lung function but not sputum inflammation in cystic fibrosis subjects. A phase II randomized placebo-controlled trial. *J Cyst Fibros* 14, 219-227.

Corvol, H., Thompson, K.E., Tabary, O., le Rouzic, P., and Guillot, L. (2016). Translating the genetics of cystic fibrosis to personalized medicine. *Transl Res* 168, 40-49.

Coste, T.C., Armand, M., Lebacq, J., Lebecque, P., Wallemacq, P., and Leal, T. (2007). An overview of monitoring and supplementation of omega 3 fatty acids in cystic fibrosis. *Clin Biochem* 40, 511-520.

Cremesti, A., Paris, F., Grassme, H., Holler, N., Tschopp, J., Fuks, Z., Gulbins, E., and Kolesnick, R. (2001). Ceramide enables fas to cap and kill. *J Biol Chem* 276, 23954-23961.

Culver, C., Sundqvist, A., Mudie, S., Melvin, A., Xirodimas, D., and Rocha, S. (2010). Mechanism of hypoxia-induced NF-kappaB. *Mol Cell Biol* *30*, 4901-4921.

Cutting, G.R. (2013). Cystic Fibrosis. In Emery and Rimoin's Principles and Practice of Medical Genetics, R.E.P.a.B.K. David L. Rimoin, ed. (Elsevier).

Cutting, G.R. (2015). Cystic fibrosis genetics: from molecular understanding to clinical application. *Nat Rev Genet* *16*, 45-56.

Dalli, J., Zhu, M., Vlasenko, N.A., Deng, B., Haeggstrom, J.Z., Petasis, N.A., and Serhan, C.N. (2013). The novel 13S,14S-epoxy-maresin is converted by human macrophages to maresin 1 (MaR1), inhibits leukotriene A4 hydrolase (LTA4H), and shifts macrophage phenotype. *FASEB J* *27*, 2573-2583.

Das, S., Sutoh, Y., Hirano, M., Han, Q., Li, J., Cooper, M.D., and Herrin, B.R. (2016). Characterization of Lamprey BAFF-like Gene: Evolutionary Implications. *J Immunol* *197*, 2695-2703.

Davies, J.C., Moskowitz, S.M., Brown, C., Horsley, A., Mall, M.A., McKone, E.F., Plant, B.J., Prais, D., Ramsey, B.W., Taylor-Cousar, J.L., *et al.* (2018a). VX-659-Tezacaftor-Ivacaftor in Patients with Cystic Fibrosis and One or Two Phe508del Alleles. *N Engl J Med*.

Davies, J.C., Moskowitz, S.M., Brown, C., Horsley, A., Mall, M.A., McKone, E.F., Plant, B.J., Prais, D., Ramsey, B.W., Taylor-Cousar, J.L., *et al.* (2018b). VX-659-Tezacaftor-Ivacaftor in Patients with Cystic Fibrosis and One or Two Phe508del Alleles. *N Engl J Med* *379*, 1599-1611.

Day, E.S., Cachero, T.G., Qian, F., Sun, Y., Wen, D., Pelletier, M., Hsu, Y.M., and Whitty, A. (2005). Selectivity of BAFF/BLYS and APRIL for binding to the TNF family receptors BAFFR/BR3 and BCMA. *Biochemistry* *44*, 1919-1931.

De Boeck, K., Kent, L., Davies, J., Derichs, N., Amaral, M., Rowe, S.M., Middleton, P., de Jonge, H., Bronsveld, I., Wilschanski, M., *et al.* (2013). CFTR biomarkers: time for promotion to surrogate end-point. *Eur Respir J* *41*, 203-216.

Dekkers, J.F., van der Ent, C.K., Kalkhoven, E., and Beekman, J.M. (2012). PPARgamma as a therapeutic target in cystic fibrosis. *Trends Mol Med* *18*, 283-291.

Dekkers, J.F., Wiegerinck, C.L., de Jonge, H.R., Bronsveld, I., Janssens, H.M., de Winter-de Groot, K.M., Brandsma, A.M., de Jong, N.W., Bijvelds, M.J., Scholte, B.J., *et al.* (2013). A functional CFTR assay using primary cystic fibrosis intestinal organoids. *Nat Med* *19*, 939-945.

DeLong, C.J., Shen, Y.J., Thomas, M.J., and Cui, Z. (1999). Molecular distinction of phosphatidylcholine synthesis between the CDP-choline pathway and phosphatidylethanolamine methylation pathway. *J Biol Chem* 274, 29683-29688.

Demel, R.A., Jansen, J.W., van Dijck, P.W., and van Deenen, L.L. (1977). The preferential interaction of cholesterol with different classes of phospholipids. *Biochim Biophys Acta* 465, 1-10.

Denning, G.M., Anderson, M.P., Amara, J.F., Marshall, J., Smith, A.E., and Welsh, M.J. (1992). Processing of mutant cystic fibrosis transmembrane conductance regulator is temperature-sensitive. *Nature* 358, 761-764.

Dennis, E.A., Cao, J., Hsu, Y.H., Magrioti, V., and Kokotos, G. (2011). Phospholipase A2 enzymes: physical structure, biological function, disease implication, chemical inhibition, and therapeutic intervention. *Chem Rev* 111, 6130-6185.

Di Pasquale, M.G. (2009). The essentials of essential fatty acids. *J Diet Suppl* 6, 143-161.

Dif, F., Wu, Y.Z., Burgel, P.R., Ollero, M., Leduc, D., Aarbiou, J., Borot, F., Garcia-Verdugo, I., Martin, C., Chignard, M., *et al.* (2010). Critical role of cytosolic phospholipase A2 {alpha} in bronchial mucus hypersecretion in CFTR-deficient mice. *Eur Respir J* 36, 1120-1130.

Do, R.K., Hatada, E., Lee, H., Tourigny, M.R., Hilbert, D., and Chen-Kiang, S. (2000). Attenuation of apoptosis underlies B lymphocyte stimulator enhancement of humoral immune response. *J Exp Med* 192, 953-964.

Dobrian, A.D., Lieb, D.C., Cole, B.K., Taylor-Fishwick, D.A., Chakrabarti, S.K., and Nadler, J.L. (2011). Functional and pathological roles of the 12- and 15-lipoxygenases. *Prog Lipid Res* 50, 115-131.

Doherty, M.M., Liu, J., Randell, S.H., Carter, C.A., Davis, C.W., Nettekheim, P., and Ferriola, P.C. (1995). Phenotype and differentiation potential of a novel rat tracheal epithelial cell line. *Am J Respir Cell Mol Biol* 12, 385-395.

Donaldson, S.H., Pilewski, J.M., Griese, M., Cooke, J., Viswanathan, L., Tullis, E., Davies, J.C., Lekstrom-Himes, J.A., Wang, L.T., and Group, V.X.S. (2018). Tezacaftor/Ivacaftor in Subjects with Cystic Fibrosis and F508del/F508del-CFTR or F508del/G551D-CFTR. *Am J Respir Crit Care Med* 197, 214-224.

Dudez, T., Borot, F., Huang, S., Kwak, B.R., Bacchetta, M., Ollero, M., Stanton, B.A., and Chanson, M. (2008). CFTR in a lipid raft-TNFR1 complex modulates gap junctional intercellular communication and IL-8 secretion. *Biochim Biophys Acta* 1783, 779-788.

Duijvestijn, Y.C., and Brand, P.L. (1999). Systematic review of N-acetylcysteine in cystic fibrosis. *Acta Paediatr* 88, 38-41.

Duvall, M.G., and Levy, B.D. (2016). DHA- and EPA-derived resolvins, protectins, and maresins in airway inflammation. *Eur J Pharmacol* 785, 144-155.

Ea, C.K., Deng, L., Xia, Z.P., Pineda, G., and Chen, Z.J. (2006). Activation of IKK by TNFalpha requires site-specific ubiquitination of RIP1 and polyubiquitin binding by NEMO. *Mol Cell* 22, 245-257.

Ebel, P., Imgrund, S., Vom Dorp, K., Hofmann, K., Maier, H., Drake, H., Degen, J., Dormann, P., Eckhardt, M., Franz, T., and Willecke, K. (2014). Ceramide synthase 4 deficiency in mice causes lipid alterations in sebum and results in alopecia. *Biochem J* 461, 147-158.

Ebel, P., Vom Dorp, K., Petrasch-Parwez, E., Zlomuzica, A., Kinugawa, K., Mariani, J., Minich, D., Ginkel, C., Welcker, J., Degen, J., *et al.* (2013). Inactivation of ceramide synthase 6 in mice results in an altered sphingolipid metabolism and behavioral abnormalities. *J Biol Chem* 288, 21433-21447.

Eckl, K.M., Tidhar, R., Thiele, H., Oji, V., Hausser, I., Brodesser, S., Preil, M.L., Onal-Akan, A., Stock, F., Muller, D., *et al.* (2013). Impaired epidermal ceramide synthesis causes autosomal recessive congenital ichthyosis and reveals the importance of ceramide acyl chain length. *J Invest Dermatol* 133, 2202-2211.

Elizur, A., Cannon, C.L., and Ferkol, T.W. (2008). Airway inflammation in cystic fibrosis. *Chest* 133, 489-495.

Emerson, J., Rosenfeld, M., McNamara, S., Ramsey, B., and Gibson, R.L. (2002). Pseudomonas aeruginosa and other predictors of mortality and morbidity in young children with cystic fibrosis. *Pediatr Pulmonol* 34, 91-100.

Escargueil-Blanc, I., Andrieu-Abadie, N., Caspar-Bauguil, S., Brossmer, R., Levade, T., Negre-Salvayre, A., and Salvayre, R. (1998). Apoptosis and activation of the sphingomyelin-ceramide pathway induced by oxidized low density lipoproteins are not causally related in ECV-304 endothelial cells. *J Biol Chem* 273, 27389-27395.

Estep, T.N., Mountcastle, D.B., Barenholz, Y., Biltonen, R.L., and Thompson, T.E. (1979). Thermal behavior of synthetic sphingomyelin-cholesterol dispersions. *Biochemistry* 18, 2112-2117.

Eto, M., Bennouna, J., Hunter, O.C., Hershberger, P.A., Kanto, T., Johnson, C.S., Lotze, M.T., and Amoscato, A.A. (2003). C16 ceramide accumulates following androgen ablation in LNCaP prostate cancer cells. *Prostate* 57, 66-79.

Evans, C.M., Raclawska, D.S., Ttofali, F., Liptzin, D.R., Fletcher, A.A., Harper, D.N., McGing, M.A., McElwee, M.M., Williams, O.W., Sanchez, E., *et al.* (2015). The polymeric mucin Muc5AC is required for allergic airway hyperreactivity. *Nat Commun* 6, 6281.

Fanconi, G., Uehlinger, E., and Knauer, C. (1936). Das Coelikisyndrom bei angeboren zystischer Pancreafibromatose und Bronchiektasien. *Wien. Med. Wochenschr.*, 753-756.

Fanjul, A.N., Delia, D., Pierotti, M.A., Rideout, D., Yu, J.Q., and Pfahl, M. (1996). 4-Hydroxyphenyl retinamide is a highly selective activator of retinoid receptors. *J Biol Chem* 271, 22441-22446.

Farrell, P.M., Mischler, E.H., Engle, M.J., Brown, D.J., and Lau, S.M. (1985). Fatty acid abnormalities in cystic fibrosis. *Pediatr Res* 19, 104-109.

Fitzpatrick, S.F., Tambuwala, M.M., Bruning, U., Schaible, B., Scholz, C.C., Byrne, A., O'Connor, A., Gallagher, W.M., Lenihan, C.R., Garvey, J.F., *et al.* (2011). An intact canonical NF-kappaB pathway is required for inflammatory gene expression in response to hypoxia. *J Immunol* 186, 1091-1096.

Flume, P.A., Liou, T.G., Borowitz, D.S., Li, H., Yen, K., Ordonez, C.L., Geller, D.E., and Group, V.X.S. (2012). Ivacaftor in subjects with cystic fibrosis who are homozygous for the F508del-CFTR mutation. *Chest* 142, 718-724.

Folch, J., Lees, M., and Sloane Stanley, G.H. (1957). A simple method for the isolation and purification of total lipides from animal tissues. *J Biol Chem* 226, 497-509.

Freedman, S.D., Blanco, P.G., Zaman, M.M., Shea, J.C., Ollero, M., Hopper, I.K., Weed, D.A., Gelrud, A., Regan, M.M., Laposata, M., *et al.* (2004). Association of cystic fibrosis with abnormalities in fatty acid metabolism. *N Engl J Med* 350, 560-569.

Freedman, S.D., Katz, M.H., Parker, E.M., Laposata, M., Urman, M.Y., and Alvarez, J.G. (1999). A membrane lipid imbalance plays a role in the phenotypic expression of cystic fibrosis in *cftr(-/-)* mice. *Proc Natl Acad Sci U S A* 96, 13995-14000.

Freedman, S.D., Weinstein, D., Blanco, P.G., Martinez-Clark, P., Urman, S., Zaman, M., Morrow, J.D., and Alvarez, J.G. (2002). Characterization of LPS-induced lung inflammation in *cftr*^{-/-} mice and the effect of docosahexaenoic acid. *J Appl Physiol* (1985) *92*, 2169-2176.

Fritzsching, B., Zhou-Suckow, Z., Trojanek, J.B., Schubert, S.C., Schatterny, J., Hirtz, S., Agrawal, R., Muley, T., Kahn, N., Sticht, C., *et al.* (2015). Hypoxic epithelial necrosis triggers neutrophilic inflammation via IL-1 receptor signaling in cystic fibrosis lung disease. *Am J Respir Crit Care Med* *191*, 902-913.

Furie, R., Petri, M., Zamani, O., Cervera, R., Wallace, D.J., Tegzova, D., Sanchez-Guerrero, J., Schwarting, A., Merrill, J.T., Chatham, W.W., *et al.* (2011). A phase III, randomized, placebo-controlled study of belimumab, a monoclonal antibody that inhibits B lymphocyte stimulator, in patients with systemic lupus erythematosus. *Arthritis Rheum* *63*, 3918-3930.

Galiotta, L.J. (2013). Managing the underlying cause of cystic fibrosis: a future role for potentiators and correctors. *Paediatr Drugs* *15*, 393-402.

Gao, Z., and Su, X. (2015). CFTR regulates acute inflammatory responses in macrophages. *QJM* *108*, 951-958.

Garcia-Verdugo, I., BenMohamed, F., Tattermusch, S., Leduc, D., Charpigny, G., Chignard, M., Ollero, M., and Touqui, L. (2012). A role for 12R-lipoxygenase in MUC5AC expression by respiratory epithelial cells. *Eur Respir J* *40*, 714-723.

Garic, D., De Sanctis, J.B., Wojewodka, G., Houle, D., Cupri, S., Abu-Arish, A., Hanrahan, J.W., Hajduch, M., Matouk, E., and Radzioch, D. (2017). Fenretinide differentially modulates the levels of long- and very long-chain ceramides by downregulating *Cers5* enzyme: evidence from bench to bedside. *J Mol Med (Berl)* *95*, 1053-1064.

Garic, D., Humbert, L., Fils-Aime, N., Korah, J., Zarfavian, Y., Lebrun, J.J., and Ali, S. (2013). Development of buffers for fast semidry transfer of proteins. *Anal Biochem* *441*, 182-184.

Garić, D.a., Tao, S., Ahmed, E., Youssef, M., Kanagaratham, C., Shah, J., Mazer, B., and Radzioch, D. (2018). Depletion of BAFF cytokine exacerbates infection in *Pseudomonas aeruginosa* infected mice. *Journal of Cystic Fibrosis*.

Geffroy-Luseau, A., Jego, G., Bataille, R., Campion, L., and Pellat-Deceunynck, C. (2008). Osteoclasts support the survival of human plasma cells in vitro. *Int Immunol* *20*, 775-782.

Gilljam, H., Strandvik, B., Ellin, A., and Wiman, L.G. (1986). Increased mole fraction of arachidonic acid in bronchial phospholipids in patients with cystic fibrosis. *Scand J Clin Lab Invest* 46, 511-518.

Ginkel, C., Hartmann, D., vom Dorp, K., Zlomuzica, A., Farwanah, H., Eckhardt, M., Sandhoff, R., Degen, J., Rabionet, M., Dere, E., *et al.* (2012). Ablation of neuronal ceramide synthase 1 in mice decreases ganglioside levels and expression of myelin-associated glycoprotein in oligodendrocytes. *J Biol Chem* 287, 41888-41902.

Golding, A., Hasni, S., Illei, G., and Shevach, E.M. (2013). The percentage of FoxP3+Helios+ Treg cells correlates positively with disease activity in systemic lupus erythematosus. *Arthritis Rheum* 65, 2898-2906.

Gorelik, L., Gilbride, K., Dobles, M., Kalled, S.L., Zandman, D., and Scott, M.L. (2003). Normal B cell homeostasis requires B cell activation factor production by radiation-resistant cells. *J Exp Med* 198, 937-945.

Gosejacob, D., Jager, P.S., Vom Dorp, K., Frejno, M., Carstensen, A.C., Kohnke, M., Degen, J., Dormann, P., and Hoch, M. (2016). Ceramide Synthase 5 Is Essential to Maintain C16:0-Ceramide Pools and Contributes to the Development of Diet-induced Obesity. *J Biol Chem* 291, 6989-7003.

Gosselin, D., Stevenson, M.M., Cowley, E.A., Griesenbach, U., Eidelman, D.H., Boule, M., Tam, M.F., Kent, G., Skamene, E., Tsui, L.C., and Radzioch, D. (1998). Impaired ability of Cfrt knockout mice to control lung infection with *Pseudomonas aeruginosa*. *Am J Respir Crit Care Med* 157, 1253-1262.

Grassme, H., Jekle, A., Riehle, A., Schwarz, H., Berger, J., Sandhoff, K., Kolesnick, R., and Gulbins, E. (2001). CD95 signaling via ceramide-rich membrane rafts. *J Biol Chem* 276, 20589-20596.

Grassme, H., Jendrossek, V., Riehle, A., von Kurthy, G., Berger, J., Schwarz, H., Weller, M., Kolesnick, R., and Gulbins, E. (2003). Host defense against *Pseudomonas aeruginosa* requires ceramide-rich membrane rafts. *Nat Med* 9, 322-330.

Griesenbach, U., Geddes, D.M., and Alton, E.W. (1999). The pathogenic consequences of a single mutated CFTR gene. *Thorax* 54 Suppl 2, S19-23.

Groneberg, D.A., Eynott, P.R., Oates, T., Lim, S., Wu, R., Carlstedt, I., Nicholson, A.G., and Chung, K.F. (2002). Expression of MUC5AC and MUC5B mucins in normal and cystic fibrosis lung. *Respir Med* 96, 81-86.

Gronn, M., Christensen, E., Hagve, T.A., and Christophersen, B.O. (1991). Peroxisomal retroconversion of docosahexaenoic acid (22:6(n-3)) to eicosapentaenoic acid (20:5(n-3)) studied in isolated rat liver cells. *Biochim Biophys Acta* 1081, 85-91.

Groom, J., Kalled, S.L., Cutler, A.H., Olson, C., Woodcock, S.A., Schneider, P., Tschopp, J., Cachero, T.G., Batten, M., Wheway, J., *et al.* (2002). Association of BAFF/BLyS overexpression and altered B cell differentiation with Sjogren's syndrome. *J Clin Invest* 109, 59-68.

Groom, J.R., Fletcher, C.A., Walters, S.N., Grey, S.T., Watt, S.V., Sweet, M.J., Smyth, M.J., Mackay, C.R., and Mackay, F. (2007). BAFF and MyD88 signals promote a lupuslike disease independent of T cells. *J Exp Med* 204, 1959-1971.

Grosch, S., Schiffmann, S., and Geisslinger, G. (2012). Chain length-specific properties of ceramides. *Prog Lipid Res* 51, 50-62.

Gross, J.A., Johnston, J., Mudri, S., Enselman, R., Dillon, S.R., Madden, K., Xu, W., Parrish-Novak, J., Foster, D., Lofton-Day, C., *et al.* (2000). TACI and BCMA are receptors for a TNF homologue implicated in B-cell autoimmune disease. *Nature* 404, 995-999.

Guilbault, C., De Sanctis, J.B., Wojewodka, G., Saeed, Z., Lachance, C., Skinner, T.A., Vilela, R.M., Kubow, S., Lands, L.C., Hajdych, M., *et al.* (2008). Fenretinide corrects newly found ceramide deficiency in cystic fibrosis. *Am J Respir Cell Mol Biol* 38, 47-56.

Guilbault, C., Martin, P., Houle, D., Boghdady, M.L., Guiot, M.C., Marion, D., and Radzioch, D. (2005). Cystic fibrosis lung disease following infection with *Pseudomonas aeruginosa* in *Cftr* knockout mice using novel non-invasive direct pulmonary infection technique. *Lab Anim* 39, 336-352.

Guilbault, C., Novak, J.P., Martin, P., Boghdady, M.L., Saeed, Z., Guiot, M.C., Hudson, T.J., and Radzioch, D. (2006). Distinct pattern of lung gene expression in the *Cftr*-KO mice developing spontaneous lung disease compared with their littermate controls. *Physiol Genomics* 25, 179-193.

Guilbault, C., Stotland, P., Lachance, C., Tam, M., Keller, A., Thompson-Snipes, L., Cowley, E., Hamilton, T.A., Eidelman, D.H., Stevenson, M.M., and Radzioch, D. (2002). Influence of gender

and interleukin-10 deficiency on the inflammatory response during lung infection with *Pseudomonas aeruginosa* in mice. *Immunology* *107*, 297-305.

Guilbault, C., Wojewodka, G., Saeed, Z., Hajdich, M., Matouk, E., De Sanctis, J.B., and Radzioch, D. (2009). Cystic fibrosis fatty acid imbalance is linked to ceramide deficiency and corrected by fenretinide. *Am J Respir Cell Mol Biol* *41*, 100-106.

Guzman, K., Gray, T.E., Yoon, J.H., and Nettlesheim, P. (1996). Quantitation of mucin RNA by PCR reveals induction of both MUC2 and MUC5AC mRNA levels by retinoids. *Am J Physiol* *271*, L1023-1028.

Hait, N.C., Allegood, J., Maceyka, M., Strub, G.M., Harikumar, K.B., Singh, S.K., Luo, C., Marmorstein, R., Kordula, T., Milstien, S., and Spiegel, S. (2009). Regulation of histone acetylation in the nucleus by sphingosine-1-phosphate. *Science* *325*, 1254-1257.

Hannun, Y.A., and Obeid, L.M. (2011). Many ceramides. *J Biol Chem* *286*, 27855-27862.

Harmon, G.S., Dumlao, D.S., Ng, D.T., Barrett, K.E., Dennis, E.A., Dong, H., and Glass, C.K. (2010). Pharmacological correction of a defect in PPAR-gamma signaling ameliorates disease severity in *Cftr*-deficient mice. *Nat Med* *16*, 313-318.

Harris, G., Ghazallah, R.A., Nascene, D., Wuertz, B., and Ondrey, F.G. (2005). PPAR activation and decreased proliferation in oral carcinoma cells with 4-HPR. *Otolaryngol Head Neck Surg* *133*, 695-701.

Hartl, D., Griese, M., Kappler, M., Zissel, G., Reinhardt, D., Rebhan, C., Schendel, D.J., and Krauss-Etschmann, S. (2006). Pulmonary T(H)2 response in *Pseudomonas aeruginosa*-infected patients with cystic fibrosis. *J Allergy Clin Immunol* *117*, 204-211.

Hartmann, D., Lucks, J., Fuchs, S., Schiffmann, S., Schreiber, Y., Ferreiros, N., Merkens, J., Marschalek, R., Geisslinger, G., and Grosch, S. (2012). Long chain ceramides and very long chain ceramides have opposite effects on human breast and colon cancer cell growth. *Int J Biochem Cell Biol* *44*, 620-628.

Hector, A., Schafer, H., Poschel, S., Fischer, A., Fritzsching, B., Ralhan, A., Carevic, M., Oz, H., Zundel, S., Hogardt, M., *et al.* (2015). Regulatory T-cell impairment in cystic fibrosis patients with chronic *pseudomonas* infection. *Am J Respir Crit Care Med* *191*, 914-923.

Henderson, A.G., Ehre, C., Button, B., Abdullah, L.H., Cai, L.H., Leigh, M.W., DeMaria, G.C., Matsui, H., Donaldson, S.H., Davis, C.W., *et al.* (2014). Cystic fibrosis airway secretions exhibit mucin hyperconcentration and increased osmotic pressure. *J Clin Invest* *124*, 3047-3060.

Henke, M.O., John, G., Germann, M., Lindemann, H., and Rubin, B.K. (2007). MUC5AC and MUC5B mucins increase in cystic fibrosis airway secretions during pulmonary exacerbation. *Am J Respir Crit Care Med* 175, 816-821.

Hiltunen, J.K., Karki, T., Hassinen, I.E., and Osmundsen, H. (1986). beta-Oxidation of polyunsaturated fatty acids by rat liver peroxisomes. A role for 2,4-dienoyl-coenzyme A reductase in peroxisomal beta-oxidation. *J Biol Chem* 261, 16484-16493.

Hodge, M.R., Ranger, A.M., Charles de la Brousse, F., Hoey, T., Grusby, M.J., and Glimcher, L.H. (1996). Hyperproliferation and dysregulation of IL-4 expression in NF-ATp-deficient mice. *Immunity* 4, 397-405.

Hong, S., Gronert, K., Devchand, P.R., Moussignac, R.L., and Serhan, C.N. (2003). Novel docosatrienes and 17S-resolvins generated from docosahexaenoic acid in murine brain, human blood, and glial cells. Autacoids in anti-inflammation. *J Biol Chem* 278, 14677-14687.

Horrocks, L.A., and Yeo, Y.K. (1999). Health benefits of docosahexaenoic acid (DHA). *Pharmacol Res* 40, 211-225.

Houssiau, F.A., Lefebvre, C., Vanden Berghe, M., Lambert, M., Devogelaer, J.P., and Renauld, J.C. (1995). Serum interleukin 10 titers in systemic lupus erythematosus reflect disease activity. *Lupus* 4, 393-395.

Hozumi, N., and Tonegawa, S. (1976). Evidence for somatic rearrangement of immunoglobulin genes coding for variable and constant regions. *Proc Natl Acad Sci U S A* 73, 3628-3632.

Huard, B., Schneider, P., Mauri, D., Tschopp, J., and French, L.E. (2001). T cell costimulation by the TNF ligand BAFF. *J Immunol* 167, 6225-6231.

Hubbard, V.S., Dunn, G.D., and di Sant'Agnese, P.A. (1977). Abnormal fatty-acid composition of plasma-lipids in cystic fibrosis. A primary or a secondary defect? *Lancet* 2, 1302-1304.

Hubeau, C., Puchelle, E., and Gaillard, D. (2001). Distinct pattern of immune cell population in the lung of human fetuses with cystic fibrosis. *J Allergy Clin Immunol* 108, 524-529.

Imgrund, S., Hartmann, D., Farwanah, H., Eckhardt, M., Sandhoff, R., Degen, J., Gieselmann, V., Sandhoff, K., and Willecke, K. (2009). Adult ceramide synthase 2 (CERS2)-deficient mice exhibit myelin sheath defects, cerebellar degeneration, and hepatocarcinomas. *J Biol Chem* 284, 33549-33560.

Imokawa, G., Abe, A., Jin, K., Higaki, Y., Kawashima, M., and Hidano, A. (1991). Decreased level of ceramides in stratum corneum of atopic dermatitis: an etiologic factor in atopic dry skin? *J Invest Dermatol* 96, 523-526.

Innis, S.M., and Davidson, A.G. (2008). Cystic fibrosis and nutrition: linking phospholipids and essential fatty acids with thiol metabolism. *Annu Rev Nutr* 28, 55-72.

Inoue, H., Massion, P.P., Ueki, I.F., Grattan, K.M., Hara, M., Dohrman, A.F., Chan, B., Lausier, J.A., Golden, J.A., and Nadel, J.A. (1994). Pseudomonas stimulates interleukin-8 mRNA expression selectively in airway epithelium, in gland ducts, and in recruited neutrophils. *Am J Respir Cell Mol Biol* 11, 651-663.

Ishida, H., Muchamuel, T., Sakaguchi, S., Andrade, S., Menon, S., and Howard, M. (1994). Continuous administration of anti-interleukin 10 antibodies delays onset of autoimmunity in NZB/W F1 mice. *J Exp Med* 179, 305-310.

Ittah, M., Miceli-Richard, C., Gottenberg, J.E., Sellam, J., Eid, P., Lebon, P., Pallier, C., Lepajolec, C., and Mariette, X. (2008). Viruses induce high expression of BAFF by salivary gland epithelial cells through TLR- and type-I IFN-dependent and -independent pathways. *Eur J Immunol* 38, 1058-1064.

Janssens, M., van Smeden, J., Gooris, G.S., Bras, W., Portale, G., Caspers, P.J., Vreeken, R.J., Hankemeier, T., Kezic, S., Wolterbeek, R., *et al.* (2012). Increase in short-chain ceramides correlates with an altered lipid organization and decreased barrier function in atopic eczema patients. *J Lipid Res* 53, 2755-2766.

Jennemann, R., Rabionet, M., Gorgas, K., Epstein, S., Dalpke, A., Rothermel, U., Bayerle, A., van der Hoeven, F., Imgrund, S., Kirsch, J., *et al.* (2012). Loss of ceramide synthase 3 causes lethal skin barrier disruption. *Hum Mol Genet* 21, 586-608.

Johansson, J., Vezzalini, M., Verze, G., Caldreller, S., Bolognin, S., Buffelli, M., Bellisola, G., Tridello, G., Assael, B.M., Melotti, P., and Sorio, C. (2014). Detection of CFTR protein in human leukocytes by flow cytometry. *Cytometry A* 85, 611-620.

Kanagaratham, C., Kalivodova, A., Najdekr, L., Friedecky, D., Adam, T., Hajduch, M., De Sanctis, J.B., and Radzioch, D. (2014). Fenretinide prevents inflammation and airway hyperresponsiveness in a mouse model of allergic asthma. *Am J Respir Cell Mol Biol* 51, 783-792.

Karnovsky, M.J., Kleinfeld, A.M., Hoover, R.L., and Klausner, R.D. (1982). The concept of lipid domains in membranes. *J Cell Biol* 94, 1-6.

Kato, A., Truong-Tran, A.Q., Scott, A.L., Matsumoto, K., and Schleimer, R.P. (2006). Airway epithelial cells produce B cell-activating factor of TNF family by an IFN-beta-dependent mechanism. *J Immunol* 177, 7164-7172.

Keating, D., Marigowda, G., Burr, L., Daines, C., Mall, M.A., McKone, E.F., Ramsey, B.W., Rowe, S.M., Sass, L.A., Tullis, E., *et al.* (2018). VX-445-Tezacaftor-Ivacaftor in Patients with Cystic Fibrosis and One or Two Phe508del Alleles. *N Engl J Med* 379, 1612-1620.

Kent, G., Iles, R., Bear, C.E., Huan, L.J., Griesenbach, U., McKerlie, C., Frndova, H., Ackerley, C., Gosselin, D., Radzioch, D., *et al.* (1997). Lung disease in mice with cystic fibrosis. *J Clin Invest* 100, 3060-3069.

Kerem, B., Rommens, J.M., Buchanan, J.A., Markiewicz, D., Cox, T.K., Chakravarti, A., Buchwald, M., and Tsui, L.C. (1989). Identification of the cystic fibrosis gene: genetic analysis. *Science* 245, 1073-1080.

Khan, T.Z., Wagener, J.S., Bost, T., Martinez, J., Accurso, F.J., and Riches, D.W. (1995). Early pulmonary inflammation in infants with cystic fibrosis. *Am J Respir Crit Care Med* 151, 1075-1082.

Kocdor, H., Kocdor, M.A., Canda, T., Gurel, D., Cehreli, R., Yilmaz, O., Alakavuklar, M., and Guner, G. (2009). Chemopreventive efficacies of rosiglitazone, fenretinide and their combination against rat mammary carcinogenesis. *Clin Transl Oncol* 11, 243-249.

Konstan, M.W. (2008). Ibuprofen therapy for cystic fibrosis lung disease: revisited. *Curr Opin Pulm Med* 14, 567-573.

Koo, J.S., Jetten, A.M., Belloni, P., Yoon, J.H., Kim, Y.D., and Nettlesheim, P. (1999a). Role of retinoid receptors in the regulation of mucin gene expression by retinoic acid in human tracheobronchial epithelial cells. *Biochem J* 338 (Pt 2), 351-357.

Koo, J.S., Kim, Y.D., Jetten, A.M., Belloni, P., and Nettlesheim, P. (2002). Overexpression of mucin genes induced by interleukin-1 beta, tumor necrosis factor-alpha, lipopolysaccharide, and neutrophil elastase is inhibited by a retinoic acid receptor alpha antagonist. *Exp Lung Res* 28, 315-332.

Koo, J.S., Yoon, J.H., Gray, T., Norford, D., Jetten, A.M., and Nettesheim, P. (1999b). Restoration of the mucous phenotype by retinoic acid in retinoid-deficient human bronchial cell cultures: changes in mucin gene expression. *Am J Respir Cell Mol Biol* 20, 43-52.

Kowalczyk-Quintas, C., Schuepbach-Mallepell, S., Vigolo, M., Willen, L., Tardivel, A., Smulski, C.R., Zheng, T.S., Gommerman, J., Hess, H., Gottenberg, J.E., *et al.* (2016). Antibodies That Block or Activate Mouse B Cell Activating Factor of the Tumor Necrosis Factor (TNF) Family (BAFF), Respectively, Induce B Cell Depletion or B Cell Hyperplasia. *J Biol Chem* 291, 19826-19834.

Kowalski, M.P., and Pier, G.B. (2004). Localization of cystic fibrosis transmembrane conductance regulator to lipid rafts of epithelial cells is required for *Pseudomonas aeruginosa*-induced cellular activation. *J Immunol* 172, 418-425.

Kremser, C., Klemm, A.L., van Uelft, M., Imgrund, S., Ginkel, C., Hartmann, D., and Willecke, K. (2013). Cell-type-specific expression pattern of ceramide synthase 2 protein in mouse tissues. *Histochem Cell Biol* 140, 533-547.

Kroesen, B.J., Pettus, B., Luberto, C., Busman, M., Sietsma, H., de Leij, L., and Hannun, Y.A. (2001). Induction of apoptosis through B-cell receptor cross-linking occurs via de novo generated C16-ceramide and involves mitochondria. *J Biol Chem* 276, 13606-13614.

Kumagai, K., Yasuda, S., Okemoto, K., Nishijima, M., Kobayashi, S., and Hanada, K. (2005). CERT mediates intermembrane transfer of various molecular species of ceramides. *J Biol Chem* 280, 6488-6495.

Kunzelmann, K., Schwiebert, E.M., Zeitlin, P.L., Kuo, W.L., Stanton, B.A., and Gruenert, D.C. (1993). An immortalized cystic fibrosis tracheal epithelial cell line homozygous for the delta F508 CFTR mutation. *Am J Respir Cell Mol Biol* 8, 522-529.

Kuo, P.T., Huang, N.N., and Bassett, D.R. (1962). The fatty acid composition of the serum chylomicrons and adipose tissue of children with cystic fibrosis of the pancreas. *J Pediatr* 60, 394-403.

Lachance, C., Wojewodka, G., Skinner, T.A., Guilbault, C., De Sanctis, J.B., and Radzioch, D. (2013). Fenretinide corrects the imbalance between omega-6 to omega-3 polyunsaturated fatty acids and inhibits macrophage inflammatory mediators via the ERK pathway. *PLoS One* 8, e74875.

Lai, H.C., FitzSimmons, S.C., Allen, D.B., Kosorok, M.R., Rosenstein, B.J., Campbell, P.W., and Farrell, P.M. (2000). Risk of persistent growth impairment after alternate-day prednisone treatment in children with cystic fibrosis. *N Engl J Med* 342, 851-859.

Langat, D.L., Wheaton, D.A., Platt, J.S., Sifers, T., and Hunt, J.S. (2008). Signaling pathways for B cell-activating factor (BAFF) and a proliferation-inducing ligand (APRIL) in human placenta. *Am J Pathol* 172, 1303-1311.

Laviad, E.L., Kelly, S., Merrill, A.H., Jr., and Futerman, A.H. (2012). Modulation of ceramide synthase activity via dimerization. *J Biol Chem* 287, 21025-21033.

Leblanc, B.P., and Stunnenberg, H.G. (1995). 9-cis retinoic acid signaling: changing partners causes some excitement. *Genes Dev* 9, 1811-1816.

Lee, B.J., Santee, S., Von Gesjen, S., Ware, C.F., and Sarawar, S.R. (2000). Lymphotoxin-alpha-deficient mice can clear a productive infection with murine gammaherpesvirus 68 but fail to develop splenomegaly or lymphocytosis. *J Virol* 74, 2786-2792.

Lemna, W.K., Feldman, G.L., Kerem, B., Fernbach, S.D., Zevkovich, E.P., O'Brien, W.E., Riordan, J.R., Collins, F.S., Tsui, L.C., and Beaudet, A.L. (1990). Mutation analysis for heterozygote detection and the prenatal diagnosis of cystic fibrosis. *N Engl J Med* 322, 291-296.

Lethem, M.I., James, S.L., Marriott, C., and Burke, J.F. (1990). The origin of DNA associated with mucus glycoproteins in cystic fibrosis sputum. *Eur Respir J* 3, 19-23.

Levistre, R., Lemnaouar, M., Rybkine, T., Bereziat, G., and Masliah, J. (1993). Increase of bradykinin-stimulated arachidonic acid release in a delta F508 cystic fibrosis epithelial cell line. *Biochim Biophys Acta* 1181, 233-239.

Levy, M., and Futerman, A.H. (2010). Mammalian ceramide synthases. *IUBMB Life* 62, 347-356.

Li, C., and Naren, A.P. (2010). CFTR chloride channel in the apical compartments: spatiotemporal coupling to its interacting partners. *Integr Biol (Camb)* 2, 161-177.

Li, D., Gallup, M., Fan, N., Szymkowski, D.E., and Basbaum, C.B. (1998a). Cloning of the amino-terminal and 5'-flanking region of the human MUC5AC mucin gene and transcriptional up-regulation by bacterial exoproducts. *J Biol Chem* 273, 6812-6820.

Li, J.D., Feng, W., Gallup, M., Kim, J.H., Gum, J., Kim, Y., and Basbaum, C. (1998b). Activation of NF-kappaB via a Src-dependent Ras-MAPK-pp90rsk pathway is required for

Pseudomonas aeruginosa-induced mucin overproduction in epithelial cells. *Proc Natl Acad Sci U S A* 95, 5718-5723.

Lin, C.H., Lee, S.Y., Zhang, C.C., Du, Y.F., Hung, H.C., Wu, H.T., and Ou, H.Y. (2016). Fenretinide inhibits macrophage inflammatory mediators and controls hypertension in spontaneously hypertensive rats via the peroxisome proliferator-activated receptor gamma pathway. *Drug Des Devel Ther* 10, 3591-3597.

Liu, K., Zhang, Y., Hu, S., Yu, Y., Yang, Q., Jin, D., Chen, X., Jin, Q., and Liu, H. (2012). Increased levels of BAFF and APRIL related to human active pulmonary tuberculosis. *PLoS One* 7, e38429.

Liu, Y., Zhu, T., Cai, G., Qin, Y., Wang, W., Tang, G., Zhao, D., and Shen, Q. (2011). Elevated circulating CD4⁺ ICOS⁺ Foxp3⁺ T cells contribute to overproduction of IL-10 and are correlated with disease severity in patients with systemic lupus erythematosus. *Lupus* 20, 620-627.

Lloyd-Still, J.D., Johnson, S.B., and Holman, R.T. (1981). Essential fatty acid status in cystic fibrosis and the effects of safflower oil supplementation. *Am J Clin Nutr* 34, 1-7.

Lloyd-Still, J.D., Powers, C.A., Hoffman, D.R., Boyd-Trull, K., Lester, L.A., Benisek, D.C., and Arterburn, L.M. (2006). Bioavailability and safety of a high dose of docosahexaenoic acid triacylglycerol of algal origin in cystic fibrosis patients: a randomized, controlled study. *Nutrition* 22, 36-46.

Lloyd, C.M., and Marsland, B.J. (2017). Lung Homeostasis: Influence of Age, Microbes, and the Immune System. *Immunity* 46, 549-561.

Lu, W., Lillehoj, E.P., and Kim, K.C. (2005). Effects of dexamethasone on Muc5AC mucin production by primary airway goblet cells. *Am J Physiol Lung Cell Mol Physiol* 288, L52-60.

Lucarelli, M., Bruno, S.M., Pierandrei, S., Ferraguti, G., Stamato, A., Narzi, F., Amato, A., Cimino, G., Bertasi, S., Quattrucci, S., and Strom, R. (2015). A Genotypic-Oriented View of CFTR Genetics Highlights Specific Mutational Patterns Underlying Clinical Macrocategories of Cystic Fibrosis. *Mol Med* 21, 257-275.

Lukacs, G.L., Chang, X.B., Bear, C., Kartner, N., Mohamed, A., Riordan, J.R., and Grinstein, S. (1993). The delta F508 mutation decreases the stability of cystic fibrosis transmembrane conductance regulator in the plasma membrane. Determination of functional half-lives on transfected cells. *J Biol Chem* 268, 21592-21598.

Lukacs, G.L., and Verkman, A.S. (2012). CFTR: folding, misfolding and correcting the DeltaF508 conformational defect. *Trends Mol Med* 18, 81-91.

Lund, F.E., Partida-Sanchez, S., Lee, B.O., Kusser, K.L., Hartson, L., Hogan, R.J., Woodland, D.L., and Randall, T.D. (2002). Lymphotoxin-alpha-deficient mice make delayed, but effective, T and B cell responses to influenza. *J Immunol* 169, 5236-5243.

Lykkesfeldt, J. (2007). Malondialdehyde as biomarker of oxidative damage to lipids caused by smoking. *Clin Chim Acta* 380, 50-58.

Maceyka, M., and Spiegel, S. (2014). Sphingolipid metabolites in inflammatory disease. *Nature* 510, 58-67.

Mackay, F., and Schneider, P. (2009). Cracking the BAFF code. *Nat Rev Immunol* 9, 491-502.

Mackay, F., Schneider, P., Rennert, P., and Browning, J. (2003). BAFF AND APRIL: a tutorial on B cell survival. *Annu Rev Immunol* 21, 231-264.

Mackay, F., Woodcock, S.A., Lawton, P., Ambrose, C., Baetscher, M., Schneider, P., Tschopp, J., and Browning, J.L. (1999). Mice transgenic for BAFF develop lymphocytic disorders along with autoimmune manifestations. *J Exp Med* 190, 1697-1710.

Manzi, S., Sanchez-Guerrero, J., Merrill, J.T., Furie, R., Gladman, D., Navarra, S.V., Ginzler, E.M., D'Cruz, D.P., Doria, A., Cooper, S., *et al.* (2012). Effects of belimumab, a B lymphocyte stimulator-specific inhibitor, on disease activity across multiple organ domains in patients with systemic lupus erythematosus: combined results from two phase III trials. *Ann Rheum Dis* 71, 1833-1838.

Marom, Z., Shelhamer, J.H., and Kaliner, M. (1981). Effects of arachidonic acid, monohydroxyeicosatetraenoic acid and prostaglandins on the release of mucous glycoproteins from human airways in vitro. *J Clin Invest* 67, 1695-1702.

Martin, S.J., Newmeyer, D.D., Mathias, S., Farschon, D.M., Wang, H.G., Reed, J.C., Kolesnick, R.N., and Green, D.R. (1995). Cell-free reconstitution of Fas-, UV radiation- and ceramide-induced apoptosis. *EMBO J* 14, 5191-5200.

Matloubian, M., Lo, C.G., Cinamon, G., Lesneski, M.J., Xu, Y., Brinkmann, V., Allende, M.L., Proia, R.L., and Cyster, J.G. (2004). Lymphocyte egress from thymus and peripheral lymphoid organs is dependent on S1P receptor 1. *Nature* 427, 355-360.

McGiff, J.C. (1981). Prostaglandins, prostacyclin, and thromboxanes. *Annu Rev Pharmacol Toxicol* 21, 479-509.

McNamara, P.S., Fonceca, A.M., Howarth, D., Correia, J.B., Slupsky, J.R., Trinick, R.E., Al Turaiki, W., Smyth, R.L., and Flanagan, B.F. (2013). Respiratory syncytial virus infection of airway epithelial cells, in vivo and in vitro, supports pulmonary antibody responses by inducing expression of the B cell differentiation factor BAFF. *Thorax* 68, 76-81.

Meerarani, P., Reiterer, G., Toborek, M., and Hennig, B. (2003). Zinc modulates PPARgamma signaling and activation of porcine endothelial cells. *J Nutr* 133, 3058-3064.

Mesika, A., Ben-Dor, S., Laviad, E.L., and Futerman, A.H. (2007). A new functional motif in Hox domain-containing ceramide synthases: identification of a novel region flanking the Hox and TLC domains essential for activity. *J Biol Chem* 282, 27366-27373.

Miele, L., Cordella-Miele, E., Xing, M., Frizzell, R., and Mukherjee, A.B. (1997). Cystic fibrosis gene mutation (Δ F508) is associated with an intrinsic abnormality in Ca^{2+} -induced arachidonic acid release by epithelial cells. *DNA Cell Biol* 16, 749-759.

Mimoun, M., Coste, T.C., Lebacqz, J., Lebecque, P., Wallemacq, P., Leal, T., and Armand, M. (2009). Increased tissue arachidonic acid and reduced linoleic acid in a mouse model of cystic fibrosis are reversed by supplemental glycerophospholipids enriched in docosahexaenoic acid. *J Nutr* 139, 2358-2364.

Mollinedo, F., and Gajate, C. (2015). Lipid rafts as major platforms for signaling regulation in cancer. *Adv Biol Regul* 57, 130-146.

Montes de Oca, M., Loeb, E., Torres, S.H., De Sanctis, J., Hernandez, N., and Talamo, C. (2008). Peripheral muscle alterations in non-COPD smokers. *Chest* 133, 13-18.

Montgomery, S.T., Mall, M.A., Kicic, A., Stick, S.M., and Arest, C.F. (2017). Hypoxia and sterile inflammation in cystic fibrosis airways: mechanisms and potential therapies. *Eur Respir J* 49.

Moore, T.C., Hartkamp, R., Iacovella, C.R., Bunge, A.L., and McCabe, C. (2018). Effect of Ceramide Tail Length on the Structure of Model Stratum Corneum Lipid Bilayers. *Biophys J* 114, 113-125.

Morin, C., Cantin, A.M., Rousseau, E., Sirois, M., Sirois, C., Rizcallah, E., and Fortin, S. (2015). Proresolving Action of Docosahexaenoic Acid Monoglyceride in Lung Inflammatory Models Related to Cystic Fibrosis. *Am J Respir Cell Mol Biol* 53, 574-583.

Moser, C., Jensen, P.O., Kobayashi, O., Hougen, H.P., Song, Z., Rygaard, J., Kharazmi, A., and N, H.b. (2002). Improved outcome of chronic *Pseudomonas aeruginosa* lung infection is

associated with induction of a Th1-dominated cytokine response. *Clin Exp Immunol* 127, 206-213.

Moss, R.B., Hsu, Y.P., and Olds, L. (2000). Cytokine dysregulation in activated cystic fibrosis (CF) peripheral lymphocytes. *Clin Exp Immunol* 120, 518-525.

Moyron-Quiroz, J.E., Rangel-Moreno, J., Kusser, K., Hartson, L., Sprague, F., Goodrich, S., Woodland, D.L., Lund, F.E., and Randall, T.D. (2004). Role of inducible bronchus associated lymphoid tissue (iBALT) in respiratory immunity. *Nat Med* 10, 927-934.

Muhlebach, M.S., Stewart, P.W., Leigh, M.W., and Noah, T.L. (1999). Quantitation of inflammatory responses to bacteria in young cystic fibrosis and control patients. *Am J Respir Crit Care Med* 160, 186-191.

Mukhopadhyay, A., Saddoughi, S.A., Song, P., Sultan, I., Ponnusamy, S., Senkal, C.E., Snook, C.F., Arnold, H.K., Sears, R.C., Hannun, Y.A., and Ogretmen, B. (2009). Direct interaction between the inhibitor 2 and ceramide via sphingolipid-protein binding is involved in the regulation of protein phosphatase 2A activity and signaling. *FASEB J* 23, 751-763.

Mullen, T.D., Hannun, Y.A., and Obeid, L.M. (2012). Ceramide synthases at the centre of sphingolipid metabolism and biology. *Biochem J* 441, 789-802.

Murakami, M., Taketomi, Y., Sato, H., and Yamamoto, K. (2011). Secreted phospholipase A2 revisited. *J Biochem* 150, 233-255.

Murakami, M., Yamamoto, K., Miki, Y., Murase, R., Sato, H., and Taketomi, Y. (2016). The Roles of the Secreted Phospholipase A2 Gene Family in Immunology. *Adv Immunol* 132, 91-134.

Murase, R., Sato, H., Yamamoto, K., Ushida, A., Nishito, Y., Ikeda, K., Kobayashi, T., Yamamoto, T., Taketomi, Y., and Murakami, M. (2016). Group X Secreted Phospholipase A2 Releases omega3 Polyunsaturated Fatty Acids, Suppresses Colitis, and Promotes Sperm Fertility. *J Biol Chem* 291, 6895-6911.

Mustafa, M.H., Khandekar, S., Tunney, M.M., Elborn, J.S., Kahl, B.C., Denis, O., Plesiat, P., Traore, H., Tulkens, P.M., Vanderbist, F., and Van Bambeke, F. (2017). Acquired resistance to macrolides in *Pseudomonas aeruginosa* from cystic fibrosis patients. *Eur Respir J* 49.

Nährlich, L., Mainz, J.G., Adams, C., Engel, C., Herrmann, G., Icheva, V., Lauer, J., Deppisch, C., Wirth, A., Unger, K., *et al.* (2013). Therapy of CF-patients with amitriptyline and placebo--a

randomised, double-blind, placebo-controlled phase IIb multicenter, cohort-study. *Cell Physiol Biochem* 31, 505-512.

Navarra, S.V., Guzman, R.M., Gallacher, A.E., Hall, S., Levy, R.A., Jimenez, R.E., Li, E.K., Thomas, M., Kim, H.Y., Leon, M.G., *et al.* (2011). Efficacy and safety of belimumab in patients with active systemic lupus erythematosus: a randomised, placebo-controlled, phase 3 trial. *Lancet* 377, 721-731.

Neill, D.R., Saint, G.L., Bricio-Moreno, L., Fothergill, J.L., Southern, K.W., Winstanley, C., Christmas, S.E., Slupsky, J.R., McNamara, P.S., Kadioglu, A., and Flanagan, B.F. (2014). The B lymphocyte differentiation factor (BAFF) is expressed in the airways of children with CF and in lungs of mice infected with *Pseudomonas aeruginosa*. *PLoS One* 9, e95892.

Nerlov, C., and Graf, T. (1998). PU.1 induces myeloid lineage commitment in multipotent hematopoietic progenitors. *Genes Dev* 12, 2403-2412.

Niehaus, W.G., Jr., and Samuelsson, B. (1968). Formation of malonaldehyde from phospholipid arachidonate during microsomal lipid peroxidation. *Eur J Biochem* 6, 126-130.

Niemela, P.S., Hyvonen, M.T., and Vattulainen, I. (2006). Influence of chain length and unsaturation on sphingomyelin bilayers. *Biophys J* 90, 851-863.

Nieuwenhuis, E.E., Matsumoto, T., Exley, M., Schleipman, R.A., Glickman, J., Bailey, D.T., Corazza, N., Colgan, S.P., Onderdonk, A.B., and Blumberg, R.S. (2002). CD1d-dependent macrophage-mediated clearance of *Pseudomonas aeruginosa* from lung. *Nat Med* 8, 588-593.

Nissen, S.E., and Wolski, K. (2007). Effect of rosiglitazone on the risk of myocardial infarction and death from cardiovascular causes. *N Engl J Med* 356, 2457-2471.

Njoroge, S.W., Laposata, M., Katrangi, W., and Seegmiller, A.C. (2012). DHA and EPA reverse cystic fibrosis-related FA abnormalities by suppressing FA desaturase expression and activity. *J Lipid Res* 53, 257-265.

Njoroge, S.W., Seegmiller, A.C., Katrangi, W., and Laposata, M. (2011). Increased Delta5- and Delta6-desaturase, cyclooxygenase-2, and lipoxygenase-5 expression and activity are associated with fatty acid and eicosanoid changes in cystic fibrosis. *Biochim Biophys Acta* 1811, 431-440.

Nutt, S.L., and Kee, B.L. (2007). The transcriptional regulation of B cell lineage commitment. *Immunity* 26, 715-725.

O'Sullivan, B.P., and Freedman, S.D. (2009). Cystic fibrosis. *Lancet* 373, 1891-1904.

Ogilvie, V., Passmore, M., Hyndman, L., Jones, L., Stevenson, B., Wilson, A., Davidson, H., Kitchen, R.R., Gray, R.D., Shah, P., *et al.* (2011). Differential global gene expression in cystic fibrosis nasal and bronchial epithelium. *Genomics* 98, 327-336.

Ohkawa, H., Ohishi, N., and Yagi, K. (1979). Assay for lipid peroxides in animal tissues by thiobarbituric acid reaction. *Anal Biochem* 95, 351-358.

Ollero, M., Junaidi, O., Zaman, M.M., Tzamelis, I., Ferrando, A.A., Andersson, C., Blanco, P.G., Bialecki, E., and Freedman, S.D. (2004). Decreased expression of peroxisome proliferator activated receptor gamma in *cftr*^{-/-} mice. *J Cell Physiol* 200, 235-244.

Osawa, Y., Uchinami, H., Bielawski, J., Schwabe, R.F., Hannun, Y.A., and Brenner, D.A. (2005). Roles for C16-ceramide and sphingosine 1-phosphate in regulating hepatocyte apoptosis in response to tumor necrosis factor-alpha. *J Biol Chem* 280, 27879-27887.

Ostedgaard, L.S., Moninger, T.O., McMenimen, J.D., Sawin, N.M., Parker, C.P., Thornell, I.M., Powers, L.S., Gansemer, N.D., Bouzek, D.C., Cook, D.P., *et al.* (2017). Gel-forming mucins form distinct morphologic structures in airways. *Proc Natl Acad Sci U S A* 114, 6842-6847.

Park, Y.B., Lee, S.K., Kim, D.S., Lee, J., Lee, C.H., and Song, C.H. (1998). Elevated interleukin-10 levels correlated with disease activity in systemic lupus erythematosus. *Clin Exp Rheumatol* 16, 283-288.

Park, Y.H., Jang, W.H., Seo, J.A., Park, M., Lee, T.R., Park, Y.H., Kim, D.K., and Lim, K.M. (2012). Decrease of ceramides with very long-chain fatty acids and downregulation of elongases in a murine atopic dermatitis model. *J Invest Dermatol* 132, 476-479.

Patke, A., Mecklenbrauker, I., Erdjument-Bromage, H., Tempst, P., and Tarakhovskiy, A. (2006). BAFF controls B cell metabolic fitness through a PKC beta- and Akt-dependent mechanism. *J Exp Med* 203, 2551-2562.

Pedersen, S.S., Espersen, F., Hoiby, N., and Jensen, T. (1990). Immunoglobulin A and immunoglobulin G antibody responses to alginates from *Pseudomonas aeruginosa* in patients with cystic fibrosis. *J Clin Microbiol* 28, 747-755.

Perez, A., van Heeckeren, A.M., Nichols, D., Gupta, S., Eastman, J.F., and Davis, P.B. (2008). Peroxisome proliferator-activated receptor-gamma in cystic fibrosis lung epithelium. *Am J Physiol Lung Cell Mol Physiol* 295, L303-313.

Petrache, I., Kamocki, K., Poirier, C., Pewzner-Jung, Y., Laviad, E.L., Schweitzer, K.S., Van Demark, M., Justice, M.J., Hubbard, W.C., and Futerman, A.H. (2013). Ceramide synthases

expression and role of ceramide synthase-2 in the lung: insight from human lung cells and mouse models. *PLoS One* 8, e62968.

Pewzner-Jung, Y., Brenner, O., Braun, S., Laviad, E.L., Ben-Dor, S., Feldmesser, E., Horn-Saban, S., Amann-Zalcenstein, D., Raanan, C., Berkutzki, T., *et al.* (2010a). A critical role for ceramide synthase 2 in liver homeostasis: II. insights into molecular changes leading to hepatopathy. *J Biol Chem* 285, 10911-10923.

Pewzner-Jung, Y., Park, H., Laviad, E.L., Silva, L.C., Lahiri, S., Stiban, J., Erez-Roman, R., Brugger, B., Sachsenheimer, T., Wieland, F., *et al.* (2010b). A critical role for ceramide synthase 2 in liver homeostasis: I. alterations in lipid metabolic pathways. *J Biol Chem* 285, 10902-10910.

Pewzner-Jung, Y., Tavakoli Tabazavareh, S., Grassme, H., Becker, K.A., Japtok, L., Steinmann, J., Joseph, T., Lang, S., Tuemmler, B., Schuchman, E.H., *et al.* (2014). Sphingoid long chain bases prevent lung infection by *Pseudomonas aeruginosa*. *EMBO Mol Med* 6, 1205-1214.

Poolman, E.M., and Galvani, A.P. (2007). Evaluating candidate agents of selective pressure for cystic fibrosis. *J R Soc Interface* 4, 91-98.

Portal, C., Gouyer, V., Leonard, R., Husson, M.O., Gottrand, F., and Desseyn, J.L. (2018). Long-term dietary (n-3) polyunsaturated fatty acids show benefits to the lungs of *Cftr* F508del mice. *PLoS One* 13, e0197808.

Pranke, I.M., Hatton, A., Simonin, J., Jais, J.P., Le Pimpec-Barthes, F., Carsin, A., Bonnette, P., Fayon, M., Stremmer-Le Bel, N., Grenet, D., *et al.* (2017). Correction of CFTR function in nasal epithelial cells from cystic fibrosis patients predicts improvement of respiratory function by CFTR modulators. *Sci Rep* 7, 7375.

Pullmannova, P., Pavlikova, L., Kovacik, A., Sochorova, M., Skolova, B., Slepicka, P., Maixner, J., Zbytovska, J., and Vavrova, K. (2017). Permeability and microstructure of model stratum corneum lipid membranes containing ceramides with long (C16) and very long (C24) acyl chains. *Biophys Chem* 224, 20-31.

Pynn, C.J., Henderson, N.G., Clark, H., Koster, G., Bernhard, W., and Postle, A.D. (2011). Specificity and rate of human and mouse liver and plasma phosphatidylcholine synthesis analyzed in vivo. *J Lipid Res* 52, 399-407.

Quan, J.M., Tiddens, H.A., Sy, J.P., McKenzie, S.G., Montgomery, M.D., Robinson, P.J., Wohl, M.E., Konstan, M.W., and Pulmozyme Early Intervention Trial Study, G. (2001). A two-year

randomized, placebo-controlled trial of dornase alfa in young patients with cystic fibrosis with mild lung function abnormalities. *J Pediatr* 139, 813-820.

Rabionet, M., Bayerle, A., Jennemann, R., Heid, H., Fuchser, J., Marsching, C., Porubsky, S., Bolenz, C., Guillou, F., Grone, H.J., *et al.* (2015). Male meiotic cytokinesis requires ceramide synthase 3-dependent sphingolipids with unique membrane anchors. *Hum Mol Genet* 24, 4792-4808.

Ramsey, B.W., Davies, J., McElvaney, N.G., Tullis, E., Bell, S.C., Drevinek, P., Griese, M., McKone, E.F., Wainwright, C.E., Konstan, M.W., *et al.* (2011). A CFTR potentiator in patients with cystic fibrosis and the G551D mutation. *N Engl J Med* 365, 1663-1672.

Randell, S.H., Fulcher, M.L., O'Neal, W., and Olsen, J.C. (2011). Primary epithelial cell models for cystic fibrosis research. In *Cystic Fibrosis (Methods in Molecular Biology)*, K.K. Amaral M., ed. (Springer), pp. 285-310.

Randell, S.H., Liu, J.Y., Ferriola, P.C., Kaartinen, L., Doherty, M.M., Davis, C.W., and Nettlesheim, P. (1996). Mucin production by SPOC1 cells--an immortalized rat tracheal epithelial cell line. *Am J Respir Cell Mol Biol* 14, 146-154.

Ranger, A.M., Hodge, M.R., Gravallesse, E.M., Oukka, M., Davidson, L., Alt, F.W., de la Brousse, F.C., Hoey, T., Grusby, M., and Glimcher, L.H. (1998). Delayed lymphoid repopulation with defects in IL-4-driven responses produced by inactivation of NF-ATc. *Immunity* 8, 125-134.

Rauch, M., Tussiwand, R., Bosco, N., and Rolink, A.G. (2009). Crucial role for BAFF-BAFF-R signaling in the survival and maintenance of mature B cells. *PLoS One* 4, e5456.

Ravirajan, C.T., Wang, Y., Matis, L.A., Papadaki, L., Griffiths, M.H., Latchman, D.S., and Isenberg, D.A. (2004). Effect of neutralizing antibodies to IL-10 and C5 on the renal damage caused by a pathogenic human anti-dsDNA antibody. *Rheumatology (Oxford)* 43, 442-447.

Reiterer, G., Toborek, M., and Hennig, B. (2004). Peroxisome proliferator activated receptors alpha and gamma require zinc for their anti-inflammatory properties in porcine vascular endothelial cells. *J Nutr* 134, 1711-1715.

Rink, L., and Gabriel, P. (2001). Extracellular and immunological actions of zinc. *Biometals* 14, 367-383.

Riordan, J.R., Rommens, J.M., Kerem, B., Alon, N., Rozmahel, R., Grzelczak, Z., Zielenski, J., Lok, S., Plavsic, N., Chou, J.L., and et al. (1989). Identification of the cystic fibrosis gene: cloning and characterization of complementary DNA. *Science* 245, 1066-1073.

Robinson, T.E., Goris, M.L., Zhu, H.J., Chen, X., Bhise, P., Sheikh, F., and Moss, R.B. (2005). Dornase alfa reduces air trapping in children with mild cystic fibrosis lung disease: a quantitative analysis. *Chest* 128, 2327-2335.

Rogan, M.P., Stoltz, D.A., and Hornick, D.B. (2011). Cystic fibrosis transmembrane conductance regulator intracellular processing, trafficking, and opportunities for mutation-specific treatment. *Chest* 139, 1480-1490.

Rogiers, V., Vercruyse, A., Dab, I., and Baran, D. (1983). Abnormal fatty acid pattern of the plasma cholesterol ester fraction in cystic fibrosis patients with and without pancreatic insufficiency. *Eur J Pediatr* 141, 39-42.

Roulet, M., Frascarolo, P., Rappaz, I., and Pilet, M. (1997). Essential fatty acid deficiency in well nourished young cystic fibrosis patients. *Eur J Pediatr* 156, 952-956.

Rouzer, C.A., and Marnett, L.J. (2009). Cyclooxygenases: structural and functional insights. *J Lipid Res* 50 Suppl, S29-34.

Roy, M.G., Livraghi-Butrico, A., Fletcher, A.A., McElwee, M.M., Evans, S.E., Boerner, R.M., Alexander, S.N., Bellinghausen, L.K., Song, A.S., Petrova, Y.M., et al. (2014). Muc5b is required for airway defence. *Nature* 505, 412-416.

Saddoughi, S.A., Gencer, S., Peterson, Y.K., Ward, K.E., Mukhopadhyay, A., Oaks, J., Bielawski, J., Szulc, Z.M., Thomas, R.J., Selvam, S.P., et al. (2013). Sphingosine analogue drug FTY720 targets I2PP2A/SET and mediates lung tumour suppression via activation of PP2A-RIPK1-dependent necroptosis. *EMBO Mol Med* 5, 105-121.

Saiman, L., Anstead, M., Mayer-Hamblett, N., Lands, L.C., Kloster, M., Hocevar-Trnka, J., Goss, C.H., Rose, L.M., Burns, J.L., Marshall, B.C., et al. (2010). Effect of azithromycin on pulmonary function in patients with cystic fibrosis uninfected with *Pseudomonas aeruginosa*: a randomized controlled trial. *JAMA* 303, 1707-1715.

Saiman, L., Mayer-Hamblett, N., Anstead, M., Lands, L.C., Kloster, M., Goss, C.H., Rose, L.M., Burns, J.L., Marshall, B.C., Ratjen, F., and Team, A.Z.M.S. (2012). Open-label, follow-on study of azithromycin in pediatric patients with CF uninfected with *Pseudomonas aeruginosa*. *Pediatr Pulmonol* 47, 641-648.

Saini, R.K., and Keum, Y.S. (2018). Omega-3 and omega-6 polyunsaturated fatty acids: Dietary sources, metabolism, and significance - A review. *Life Sci* 203, 255-267.

Salvi, S., and Holgate, S.T. (1999). Could the airway epithelium play an important role in mucosal immunoglobulin A production? *Clin Exp Allergy* 29, 1597-1605.

Samuelsson, B., Dahlen, S.E., Lindgren, J.A., Rouzer, C.A., and Serhan, C.N. (1987). Leukotrienes and lipoxins: structures, biosynthesis, and biological effects. *Science* 237, 1171-1176.

Saraiva, M., and O'Garra, A. (2010). The regulation of IL-10 production by immune cells. *Nat Rev Immunol* 10, 170-181.

Sassa, T., Suto, S., Okayasu, Y., and Kihara, A. (2012). A shift in sphingolipid composition from C24 to C16 increases susceptibility to apoptosis in HeLa cells. *Biochim Biophys Acta* 1821, 1031-1037.

Scalapino, K.J., Tang, Q., Bluestone, J.A., Bonyhadi, M.L., and Daikh, D.I. (2006). Suppression of disease in New Zealand Black/New Zealand White lupus-prone mice by adoptive transfer of ex vivo expanded regulatory T cells. *J Immunol* 177, 1451-1459.

Scapini, P., Bazzoni, F., and Cassatella, M.A. (2008). Regulation of B-cell-activating factor (BAFF)/B lymphocyte stimulator (BLyS) expression in human neutrophils. *Immunol Lett* 116, 1-6.

Schiemann, B., Gommerman, J.L., Vora, K., Cachero, T.G., Shulga-Morskaya, S., Dobles, M., Frew, E., and Scott, M.L. (2001). An essential role for BAFF in the normal development of B cells through a BCMA-independent pathway. *Science* 293, 2111-2114.

Schiffmann, S., Ziebell, S., Sandner, J., Birod, K., Deckmann, K., Hartmann, D., Rode, S., Schmidt, H., Angioni, C., Geisslinger, G., and Grosch, S. (2010). Activation of ceramide synthase 6 by celecoxib leads to a selective induction of C16:0-ceramide. *Biochem Pharmacol* 80, 1632-1640.

Schneider, P., MacKay, F., Steiner, V., Hofmann, K., Bodmer, J.L., Holler, N., Ambrose, C., Lawton, P., Bixler, S., Acha-Orbea, H., *et al.* (1999). BAFF, a novel ligand of the tumor necrosis factor family, stimulates B cell growth. *J Exp Med* 189, 1747-1756.

Scholz, J.L., Crowley, J.E., Tomayko, M.M., Steinel, N., O'Neill, P.J., Quinn, W.J., 3rd, Goenka, R., Miller, J.P., Cho, Y.H., Long, V., *et al.* (2008). BLyS inhibition eliminates primary B cells

but leaves natural and acquired humoral immunity intact. *Proc Natl Acad Sci U S A* *105*, 15517-15522.

Schuck, S., Honsho, M., Ekroos, K., Shevchenko, A., and Simons, K. (2003). Resistance of cell membranes to different detergents. *Proc Natl Acad Sci U S A* *100*, 5795-5800.

Schupp, M., Curtin, J.C., Kim, R.J., Billin, A.N., and Lazar, M.A. (2007). A widely used retinoic acid receptor antagonist induces peroxisome proliferator-activated receptor-gamma activity. *Mol Pharmacol* *71*, 1251-1257.

Scriver, C.R. (1995). *The metabolic and molecular bases of inherited disease*, 7th ed. edn (New York: McGraw-Hill, Health Professions Division).

Serhan, C.N., Hong, S., Gronert, K., Colgan, S.P., Devchand, P.R., Mirick, G., and Moussignac, R.L. (2002). Resolvins: a family of bioactive products of omega-3 fatty acid transformation circuits initiated by aspirin treatment that counter proinflammation signals. *J Exp Med* *196*, 1025-1037.

Serhan, C.N., and Ward, P.A. (1999). *Molecular and cellular basis of inflammation*. (Totowa, N.J., Humana Press).

Serhan, C.N., Yang, R., Martinod, K., Kasuga, K., Pillai, P.S., Porter, T.F., Oh, S.F., and Spite, M. (2009). Maresins: novel macrophage mediators with potent antiinflammatory and proresolving actions. *J Exp Med* *206*, 15-23.

Shi, Y. (2009). Serine/threonine phosphatases: mechanism through structure. *Cell* *139*, 468-484.

Shikano, M., Masuzawa, Y., Yazawa, K., Takayama, K., Kudo, I., and Inoue, K. (1994). Complete discrimination of docosahexaenoate from arachidonate by 85 kDa cytosolic phospholipase A2 during the hydrolysis of diacyl- and alkenylacylglycerophosphoethanolamine. *Biochim Biophys Acta* *1212*, 211-216.

Shimizu, T., Shimizu, S., Hattori, R., Gabazza, E.C., and Majima, Y. (2003). In vivo and in vitro effects of macrolide antibiotics on mucus secretion in airway epithelial cells. *Am J Respir Crit Care Med* *168*, 581-587.

Shishodia, S., Gutierrez, A.M., Lotan, R., and Aggarwal, B.B. (2005). N-(4-hydroxyphenyl)retinamide inhibits invasion, suppresses osteoclastogenesis, and potentiates apoptosis through down-regulation of I(kappa)B(alpha) kinase and nuclear factor-kappaB-regulated gene products. *Cancer Res* *65*, 9555-9565.

Silva, L.C., Ben David, O., Pewzner-Jung, Y., Laviad, E.L., Stiban, J., Bandyopadhyay, S., Merrill, A.H., Jr., Prieto, M., and Futerman, A.H. (2012). Ablation of ceramide synthase 2 strongly affects biophysical properties of membranes. *J Lipid Res* 53, 430-436.

Simons, K., and Ikonen, E. (1997). Functional rafts in cell membranes. *Nature* 387, 569-572.

Simons, K., and Toomre, D. (2000). Lipid rafts and signal transduction. *Nat Rev Mol Cell Biol* 1, 31-39.

Simopoulos, A.P. (1998). Overview of evolutionary aspects of omega 3 fatty acids in the diet. *World Rev Nutr Diet* 83, 1-11.

Singer, S.J., and Nicolson, G.L. (1972). The fluid mosaic model of the structure of cell membranes. *Science* 175, 720-731.

Siskind, L.J., Kolesnick, R.N., and Colombini, M. (2002). Ceramide channels increase the permeability of the mitochondrial outer membrane to small proteins. *J Biol Chem* 277, 26796-26803.

Skolova, B., Hudska, K., Pullmannova, P., Kovacik, A., Palat, K., Roh, J., Fleddermann, J., Estrela-Lopis, I., and Vavrova, K. (2014). Different phase behavior and packing of ceramides with long (C16) and very long (C24) acyls in model membranes: infrared spectroscopy using deuterated lipids. *J Phys Chem B* 118, 10460-10470.

Skotland, T., Sandvig, K., and Llorente, A. (2017). Lipids in exosomes: Current knowledge and the way forward. *Prog Lipid Res* 66, 30-41.

Smith, C., Winn, A., Seddon, P., and Ranganathan, S. (2012). A fat lot of good: balance and trends in fat intake in children with cystic fibrosis. *J Cyst Fibros* 11, 154-157.

Sociale, M., Wulf, A.L., Breiden, B., Klee, K., Thielisch, M., Eckardt, F., Sellin, J., Bulow, M.H., Lobbert, S., Weinstock, N., *et al.* (2018). Ceramide Synthase Schlank Is a Transcriptional Regulator Adapting Gene Expression to Energy Requirements. *Cell Rep* 22, 967-978.

Soltys, J., Bonfield, T., Chmiel, J., and Berger, M. (2002). Functional IL-10 deficiency in the lung of cystic fibrosis (cftr(-/-)) and IL-10 knockout mice causes increased expression and function of B7 costimulatory molecules on alveolar macrophages. *J Immunol* 168, 1903-1910.

Sorio, C., Montresor, A., Bolomini-Vittori, M., Caldres, S., Rossi, B., Dusi, S., Angiari, S., Johansson, J.E., Vezzalini, M., Leal, T., *et al.* (2016). Mutations of Cystic Fibrosis Transmembrane Conductance Regulator Gene Cause a Monocyte-Selective Adhesion Deficiency. *Am J Respir Crit Care Med* 193, 1123-1133.

Staubach, S., and Hanisch, F.G. (2011). Lipid rafts: signaling and sorting platforms of cells and their roles in cancer. *Expert Rev Proteomics* 8, 263-277.

Stiban, J., and Perera, M. (2015). Very long chain ceramides interfere with C16-ceramide-induced channel formation: A plausible mechanism for regulating the initiation of intrinsic apoptosis. *Biochim Biophys Acta* 1848, 561-567.

Strandvik, B., Gronowitz, E., Enlund, F., Martinsson, T., and Wahlstrom, J. (2001). Essential fatty acid deficiency in relation to genotype in patients with cystic fibrosis. *J Pediatr* 139, 650-655.

Strokin, M., Sergeeva, M., and Reiser, G. (2003). Docosahexaenoic acid and arachidonic acid release in rat brain astrocytes is mediated by two separate isoforms of phospholipase A2 and is differently regulated by cyclic AMP and Ca²⁺. *Br J Pharmacol* 139, 1014-1022.

Tabary, O., Corvol, H., Boncoeur, E., Chadelat, K., Fitting, C., Cavaillon, J.M., Clement, A., and Jacquot, J. (2006). Adherence of airway neutrophils and inflammatory response are increased in CF airway epithelial cell-neutrophil interactions. *Am J Physiol Lung Cell Mol Physiol* 290, L588-596.

Tabary, O., Escotte, S., Couetil, J.P., Hubert, D., Dusser, D., Puchelle, E., and Jacquot, J. (2001). Relationship between IkappaBalpha deficiency, NFkappaB activity and interleukin-8 production in CF human airway epithelial cells. *Pflugers Arch* 443 Suppl 1, S40-44.

Tang, X., Benesch, M.G., and Brindley, D.N. (2015). Lipid phosphate phosphatases and their roles in mammalian physiology and pathology. *J Lipid Res* 56, 2048-2060.

Teichgraber, V., Ulrich, M., Endlich, N., Riethmuller, J., Wilker, B., De Oliveira-Munding, C.C., van Heeckeren, A.M., Barr, M.L., von Kurthy, G., Schmid, K.W., *et al.* (2008). Ceramide accumulation mediates inflammation, cell death and infection susceptibility in cystic fibrosis. *Nat Med* 14, 382-391.

Tertilt, C., Joh, J., Krause, A., Chou, P., Schneeweiss, K., Crystal, R.G., and Worgall, S. (2009). Expression of B-cell activating factor enhances protective immunity of a vaccine against *Pseudomonas aeruginosa*. *Infect Immun* 77, 3044-3055.

Thomas, G.R., Costelloe, E.A., Lunn, D.P., Stacey, K.J., Delaney, S.J., Passey, R., McGlenn, E.C., McMorran, B.J., Ahadizadeh, A., Geczy, C.L., *et al.* (2000). G551D cystic fibrosis mice exhibit abnormal regulation of inflammation in lungs and macrophages. *J Immunol* 164, 3870-3877.

Thomas, R.L., Jr., Matsko, C.M., Lotze, M.T., and Amoscato, A.A. (1999). Mass spectrometric identification of increased C16 ceramide levels during apoptosis. *J Biol Chem* 274, 30580-30588.

Thompson, J.S., Bixler, S.A., Qian, F., Vora, K., Scott, M.L., Cachero, T.G., Hession, C., Schneider, P., Sizing, I.D., Mullen, C., *et al.* (2001). BAFF-R, a newly identified TNF receptor that specifically interacts with BAFF. *Science* 293, 2108-2111.

Thudichum, J.L.W. (1884). A treatise on the chemical constitution of the brain : based throughout upon original researches (London: Baillière, Tindall, and Cox).

Tidhar, R., Zelnik, I.D., Volpert, G., Ben-Dor, S., Kelly, S., Merrill, A.H., Jr., and Futerman, A.H. (2018). Eleven residues determine the acyl chain specificity of ceramide synthases. *J Biol Chem* 293, 9912-9921.

Toma, S., Emionite, L., Scaramuccia, A., Ravera, G., and Scarabelli, L. (2005). Retinoids and human breast cancer: in vivo effects of an antagonist for RAR-alpha. *Cancer Lett* 219, 27-31.

Turpin, S.M., Nicholls, H.T., Willmes, D.M., Mourier, A., Brodesser, S., Wunderlich, C.M., Mauer, J., Xu, E., Hammerschmidt, P., Bronneke, H.S., *et al.* (2014). Obesity-induced CerS6-dependent C16:0 ceramide production promotes weight gain and glucose intolerance. *Cell Metab* 20, 678-686.

Ulrich, M., Worlitzsch, D., Viglio, S., Siegmann, N., Iadarola, P., Shute, J.K., Geiser, M., Pier, G.B., Friedel, G., Barr, M.L., *et al.* (2010). Alveolar inflammation in cystic fibrosis. *J Cyst Fibros* 9, 217-227.

Underwood, B.A., Denning, C.R., and Navab, M. (1972). Polyunsaturated fatty acids and tocopherol levels in patients with cystic fibrosis. *Ann N Y Acad Sci* 203, 237-247.

Van Biervliet, S., Devos, M., Delhaye, T., Van Biervliet, J.P., Robberecht, E., and Christophe, A. (2008a). Oral DHA supplementation in DeltaF508 homozygous cystic fibrosis patients. *Prostaglandins Leukot Essent Fatty Acids* 78, 109-115.

Van Biervliet, S., Vande Velde, S., Van Biervliet, J.P., and Robberecht, E. (2008b). The effect of zinc supplements in cystic fibrosis patients. *Ann Nutr Metab* 52, 152-156.

van Blitterswijk, W.J., van der Luit, A.H., Veldman, R.J., Verheij, M., and Borst, J. (2003). Ceramide: second messenger or modulator of membrane structure and dynamics? *Biochem J* 369, 199-211.

Van Goor, F., Hadida, S., Grootenhuis, P.D., Burton, B., Cao, D., Neuberger, T., Turnbull, A., Singh, A., Joubran, J., Hazlewood, A., *et al.* (2009). Rescue of CF airway epithelial cell function in vitro by a CFTR potentiator, VX-770. *Proc Natl Acad Sci U S A* *106*, 18825-18830.

Van Goor, F., Hadida, S., Grootenhuis, P.D., Burton, B., Stack, J.H., Straley, K.S., Decker, C.J., Miller, M., McCartney, J., Olson, E.R., *et al.* (2011). Correction of the F508del-CFTR protein processing defect in vitro by the investigational drug VX-809. *Proc Natl Acad Sci U S A* *108*, 18843-18848.

Van Handel, E., and Zilversmit, D.B. (1957). Micromethod for the direct determination of serum triglycerides. *J Lab Clin Med* *50*, 152-157.

Varfolomeev, E., Kischkel, F., Martin, F., Seshasayee, D., Wang, H., Lawrence, D., Olsson, C., Tom, L., Erickson, S., French, D., *et al.* (2004). APRIL-deficient mice have normal immune system development. *Mol Cell Biol* *24*, 997-1006.

Varshney, P., Yadav, V., and Saini, N. (2016). Lipid rafts in immune signalling: current progress and future perspective. *Immunology* *149*, 13-24.

Veit, G., Avramescu, R.G., Perdomo, D., Phuan, P.W., Bagdany, M., Apaja, P.M., Borot, F., Szollosi, D., Wu, Y.S., Finkbeiner, W.E., *et al.* (2014). Some gating potentiators, including VX-770, diminish DeltaF508-CFTR functional expression. *Sci Transl Med* *6*, 246ra297.

Veit, G., Xu, H., Dreano, E., Avramescu, R.G., Bagdany, M., Beitel, L.K., Roldan, A., Hancock, M.A., Lay, C., Li, W., *et al.* (2018a). Structure-guided combination therapy to potently improve the function of mutant CFTRs. *Nat Med* *24*, 1732-1742.

Veit, G., Xu, H., Dreano, E., Avramescu, R.G., Bagdany, M., Beitel, L.K., Roldan, A., Hancock, M.A., Lay, C., Li, W., *et al.* (2018b). Structure-guided combination therapy to potently improve the function of mutant CFTRs. *Nat Med*.

Verhaeghe, C., Delbecq, K., de Leval, L., Oury, C., and Bours, V. (2007). Early inflammation in the airways of a cystic fibrosis foetus. *J Cyst Fibros* *6*, 304-308.

Veronesi, U., De Palo, G., Marubini, E., Costa, A., Formelli, F., Mariani, L., Decensi, A., Camerini, T., Del Turco, M.R., Di Mauro, M.G., *et al.* (1999). Randomized trial of fenretinide to prevent second breast malignancy in women with early breast cancer. *J Natl Cancer Inst* *91*, 1847-1856.

Veronesi, U., Mariani, L., Decensi, A., Formelli, F., Camerini, T., Miceli, R., Di Mauro, M.G., Costa, A., Marubini, E., Sporn, M.B., and De Palo, G. (2006). Fifteen-year results of a

randomized phase III trial of fenretinide to prevent second breast cancer. *Ann Oncol* 17, 1065-1071.

Voelzmann, A., and Bauer, R. (2010). Ceramide synthases in mammals, worms, and insects: emerging schemes. *Biomol Concepts* 1, 411-422.

Wainwright, C.E., Elborn, J.S., Ramsey, B.W., Marigowda, G., Huang, X., Cipolli, M., Colombo, C., Davies, J.C., De Boeck, K., Flume, P.A., *et al.* (2015). Lumacaftor-Ivacaftor in Patients with Cystic Fibrosis Homozygous for Phe508del CFTR. *N Engl J Med* 373, 220-231.

Walters, S., Webster, K.E., Sutherland, A., Gardam, S., Groom, J., Liuwantara, D., Marino, E., Thaxton, J., Weinberg, A., Mackay, F., *et al.* (2009). Increased CD4+Foxp3+ T cells in BAFF-transgenic mice suppress T cell effector responses. *J Immunol* 182, 793-801.

Wang, D., Wang, W., Duan, Y., Sun, Y., Wang, Y., and Huang, P. (2008). Functional coupling of Gs and CFTR is independent of their association with lipid rafts in epithelial cells. *Pflugers Arch* 456, 929-938.

Wang, G., Krishnamurthy, K., Umapathy, N.S., Verin, A.D., and Bieberich, E. (2009). The carboxyl-terminal domain of atypical protein kinase Czeta binds to ceramide and regulates junction formation in epithelial cells. *J Biol Chem* 284, 14469-14475.

Watkins, S.M., Zhu, X., and Zeisel, S.H. (2003). Phosphatidylethanolamine-N-methyltransferase activity and dietary choline regulate liver-plasma lipid flux and essential fatty acid metabolism in mice. *J Nutr* 133, 3386-3391.

Wilmott, R.W., Amin, R.S., Colin, A.A., DeVault, A., Dozor, A.J., Eigen, H., Johnson, C., Lester, L.A., McCoy, K., McKean, L.P., *et al.* (1996). Aerosolized recombinant human DNase in hospitalized cystic fibrosis patients with acute pulmonary exacerbations. *Am J Respir Crit Care Med* 153, 1914-1917.

Winter, E., and Ponting, C.P. (2002). TRAM, LAG1 and CLN8: members of a novel family of lipid-sensing domains? *Trends Biochem Sci* 27, 381-383.

Woodland, R.T., Fox, C.J., Schmidt, M.R., Hammerman, P.S., Opferman, J.T., Korsmeyer, S.J., Hilbert, D.M., and Thompson, C.B. (2008). Multiple signaling pathways promote B lymphocyte stimulator dependent B-cell growth and survival. *Blood* 111, 750-760.

Wu, C.J., Conze, D.B., Li, T., Srinivasula, S.M., and Ashwell, J.D. (2006). Sensing of Lys 63-linked polyubiquitination by NEMO is a key event in NF-kappaB activation [corrected]. *Nat Cell Biol* 8, 398-406.

Xiao, G., Harhaj, E.W., and Sun, S.C. (2001). NF-kappaB-inducing kinase regulates the processing of NF-kappaB2 p100. *Mol Cell* 7, 401-409.

Yadav, K., Singh, M., Angurana, S.K., Attri, S.V., Sharma, G., Tajeja, M., and Bhalla, A.K. (2014). Evaluation of micronutrient profile of North Indian children with cystic fibrosis: a case-control study. *Pediatr Res* 75, 762-766.

Yanagihara, K., Seki, M., and Cheng, P.W. (2001). Lipopolysaccharide Induces Mucus Cell Metaplasia in Mouse Lung. *Am J Respir Cell Mol Biol* 24, 66-73.

Yang, J., Eiserich, J.P., Cross, C.E., Morrissey, B.M., and Hammock, B.D. (2012). Metabolomic profiling of regulatory lipid mediators in sputum from adult cystic fibrosis patients. *Free Radic Biol Med* 53, 160-171.

Ye, Y.Z., Strong, M., Huang, Z.Q., and Beckman, J.S. (1996). Antibodies that recognize nitrotyrosine. *Methods Enzymol* 269, 201-209.

Yin, Z., Bahtiyar, G., Zhang, N., Liu, L., Zhu, P., Robert, M.E., McNiff, J., Madaio, M.P., and Craft, J. (2002). IL-10 regulates murine lupus. *J Immunol* 169, 2148-2155.

Yoshida, H., Nishina, H., Takimoto, H., Marengere, L.E., Wakeham, A.C., Bouchard, D., Kong, Y.Y., Ohteki, T., Shahinian, A., Bachmann, M., *et al.* (1998). The transcription factor NF-ATc1 regulates lymphocyte proliferation and Th2 cytokine production. *Immunity* 8, 115-124.

Zaidman, N.A., Panoskaltzis-Mortari, A., and O'Grady, S.M. (2016). Differentiation of human bronchial epithelial cells: role of hydrocortisone in development of ion transport pathways involved in mucociliary clearance. *Am J Physiol Cell Physiol* 311, C225-236.

Zemanick, E.T., and Hoffman, L.R. (2016). Cystic Fibrosis: Microbiology and Host Response. *Pediatr Clin North Am* 63, 617-636.

Zemanick, E.T., and Wainwright, C. (2016). Alterations of the Nasopharyngeal Microbiota in Infants with Cystic Fibrosis. Cystic Fibrosis Transmembrane Conductance Regulator and Antibiotic Effects. *Am J Respir Crit Care Med* 193, 473-474.

Zhao, L., Spassieva, S.D., Jucius, T.J., Shultz, L.D., Shick, H.E., Macklin, W.B., Hannun, Y.A., Obeid, L.M., and Ackerman, S.L. (2011). A deficiency of ceramide biosynthesis causes cerebellar purkinje cell neurodegeneration and lipofuscin accumulation. *PLoS Genet* 7, e1002063.

Zhou, L., Dey, C.R., Wert, S.E., DuVall, M.D., Frizzell, R.A., and Whitsett, J.A. (1994). Correction of lethal intestinal defect in a mouse model of cystic fibrosis by human CFTR. *Science* 266, 1705-1708.

Ziobro, R., Henry, B., Edwards, M.J., Lentsch, A.B., and Gulbins, E. (2013). Ceramide mediates lung fibrosis in cystic fibrosis. *Biochem Biophys Res Commun* 434, 705-709.

APPENDIX

A 1.0 Supplement

The mixture of 25 µl of brain lipid extract in chloroform (Avanti 131101C), subjected to thin-layer chromatography on the silica plate, and transferred to nytran membrane by diffusion. After separation on silica gel, standards were visualized after 30 min incubation in iodine vapor.

The **Figure 1.3.8B** illustrates comparison of the binding of polyclonal and monoclonal antibodies against ceramides mixture commercially available from Sigma and Glycobiotech to various species of ceramides. Commercially available standards of ceramide subspecies (C14:0, C16:0, C18:0, C18:1, C20:0, C24:0 and C24:1) and non-naturally occurring internal standards (C17:0 and C25:0ceramides) were obtained from AVANTI Polar Lipids Inc. (Alabaster, AL, purity > 99%). HPLC grade solvents were purchased from Fluka (Milwaukee, MO). All other chemicals, including Merck grade silica gel (9385, 230–400 mesh, 60 Å) were from Sigma-Aldrich (St. Louis, MO).

The stock solutions of ceramides were prepared at 1 mg/ml in chloroform. After dilution with ethanol, a working solution of C14:0, C16:0, C18, C18:1, C20:0, C24:0 and C24:1 mixture was prepared at 714 ng/ml for each ceramide species in one solution. This solution was divided into 0.5 ml fractions and saved at (−80°C) until analysis. A mixture of C17:0 and C25:0 solution in ethanol at concentrations of 1000 ng/ml and 2000 ng/ml, respectively, was prepared as an internal standard solution. Fifty microliters of internal standard solution corresponding to 50 ng of C17:0 and 100 ng of C25:0 was used for each analysis.

For the detection of lipid species by antibodies, nytran membrane was incubated with Bovine Serum Albumin (BSA) dissolved in PBS (1%) to block non-specific sites, and then with the primary antibodies: monoclonal anti-ceramide antibody clone 15B4 from Sigma (cat# C8104-50T ST) and polyclonal anti-ceramide antibody clone S58-9 from Glycobiotech (S58-9, Glycobiotech). After the incubation with the primary antibodies, nytran membrane was washed 5 times with PBS-Tween (0.1%) and subsequently incubated overnight with anti-mouse IgM diluted 1:250 (Sigma; M8644). Finally, the paper was washed 5 times and incubated with tetramethylbenzidine (Vector laboratories) to develop the color.

Table A1.0 *Fenretinide does not affect the levels of Cers1 and Cers4 mRNA*

	ACTN	Cers1	Cers4
WT-Ctrl	18.10	31.40	25.90
WT-Fen	18.85	31.95	26.25
CFTR-Ctrl	17.95	31.85	25.00
CFTR-Fen	17.70	31.35	24.60
	Fold Change	Cers1	Cers4
		1.148698	1.319508
		1.189207	1.109569

qPCR analysis (Ct values and fold changes)
of Cers1 and Cers4 in CFBE41o- cells